STUDIES ON OPTIMAL DESIGN AND OPERATION OF INTEGRATED DISTILLATION ARRANGEMENTS

by

Atle Christer Christiansen

A Thesis Submitted for the Degree of Dr. Ing.

Department of Chemical Engineering
Norwegian University of Science and Technology

Submitted December 1997

ABSTRACT

The scientific literature on distillation as a measure of separating a feed mixture into its constituents, probably dates back at least several hundred years. However, in spite of an exceedingly vast literature on this topic, there are still numerous tasks that at present remain unresolved. Among the features that perhaps have triggered most of the previous research, is the large energy requirements which in fact ranks distillation as one of the most energy consuming process operations on a world wide basis. The conventional approach towards increasing the efficiency has been towards heat integration between columns or between the column and other parts of the plant. However, due to the scrutiny from company policies and constraints passed on by environmental regulations, more recent research aims at designs that offer savings in both operational (energy) *and* capital costs.

This work puts emphasis on a certain class of integrated distillation arrangements. In particular we consider means for direct coupling of distillation columns, so as to use the underlying physics to facilitate more energy efficient separations. One such arrangement, the dividing wall column was proposed in a patent almost 50 years ago, and then analyzed on a thermodynamical basis by Petlyuk and coworkers in the 60's. Its use in industrial practice is however still very limited. It is therefore the intention of this work to increase the the understanding of such columns, in terms of (optimal) operation and design.

In order to analyze such columns one may resort to numerical simulations of conceptual models, which typically display highly nonlinear behavior. The conceptual models are commonly also very ill-conditioned, and in sum these features pose great challenges for any numerical method to be used in the analysis. The numerical methods discussed in this work are thus well suited to solve models of distillation columns. We propose a *tear and grid method* that to some extent exploits the sparsity, since the number of tear variables required for solving a distillation model usually is rather small. The parameter continuation method we discuss is furthermore well suited for ill-conditioned problems, since one always stays close to the feasible solutions. However we stress that the focus is put on simplicity and robustness, rather than complexity and ability to handle any pathological problem.

To extend the analysis of integrated columns beyond the scope of numerical simulations, we also put emphasis on analytical results which apply in certain limiting cases. In particular the limiting case of an infinitely long column is important, as it yields the overall minimum energy usage. Moreover, we consider the concept of the *preferred separation* which is of great importance for prefractionator arrangements. From this analysis we also obtain information of great importance for practical operation of such columns.

Finally we use the proposed numerical methods to optimize Petlyuk arrangements for separating ternary and quaternary mixtures. Results from this and other works indicate that such arrangements offer large potential savings in energy usage as well as capital costs, which should increase the interest in these arrangements both in academia and from industrial practitioners.

ACKNOWLEDGMENTS

As I now find myself contemplating on the years spent on the work displayed in this thesis, I sense the awkwardness and uneasiness of trying to give the readers an outline of the bits and peaces of close to four years of *living*. It is not really the fear that words may not convey the essence of memories and meanings. Rather it is the phlegmatic notion of coming to terms with an era at its inevitable end. The first thing that springs to mind, is to admit that I never believed this journey would take place as traveling smoothly and briskly, without encountering the occasional ups and downs. Having said this, I'm also struck by the complexity embedded in trying to draw a brief and consistent historical review of the essentials of my studies.

There are a lot of people who deserves credit for in some way or other helping me to actually finish up, and wrap this thesis together. Due to the immanent ambivalence between the impacts these people have had on my actual work, and the autonomy of solitary research, it may be difficult to give credit to *all* people to whom credit may be due. Still, I would like to mention some of those who have had the largest and most significant influence on me during these last four years.

I am in many ways indebted to my supervisor Sigurd Skogestad for having the courage and stamina required to stimulate and guide my research activities. Without his support and fruitful contributions this thesis would never have emerged. I thank you for having the patience to endure the times after my less succesful "Phlogiston" research, when chemical engineering by far seemed to me the most interesting scene of work. In this respect I am grateful for being allowed some space to pursue my interest in philosophy. I cheeringly recall the good times we've had at conferences and social gatherings, where focus on subjects beyond the reach of chemical engineering and control have prevailed. Unforgettable moments such as the attempt to promote the "reindeer dance" in Rhodes, the "belly dancers" in Antalya and the omnipotent phrase "we have sat the sats", are such that are not to be forgotten. Finally I express my gratitude for having sufficient belief in me, so as to offer me a position and to take me up as a student. I hope this thesis provides some pay-back on your investments.

Among my other past and present colleagues there is no lucid way in which I can fully acknowledge the help and support from John Morud. In some sense it is fair to say that his contributions and enthusiasm were among the most important reasons for me to stick on this path towards graduation. The support offered by his insights on almost any aspect touched upon in this thesis, is invaluable and cannot be expressed briefly. This is a view which I am sure many other people at our department would share. I am also grateful for the many discussions we shared on other issues of more philosophical significance.

My family, Cecilie and my closest friends deserve my most sincere empathy and thanks. My father, mother and Line for always having great confidence in me, although my outspoken doubts and apparent lack of perseverance must at times have made this somewhat difficult. The warmth and enthusiasm they have always given, and my experience of them always willingly trying to project themselves onto my workspace, comes as close as possible to my understanding of love. My mom is in fact

the person most directly to blame for me moving back to Trondheim to commence this work, and her supportive judgments and tender pragmatism are among the most important reasons for sticking out. To my father I owe the curiosity and surge for knowledge along with the ability to sustain the courage of my convictions. The latter has at times become somewhat of an immanent compulsion, and our fruitful conversations still bring out feelings of exaltation. Due to differences in age, which in younger years prevented wholesome conversations on common grounds, I have during the last few years been fortunate enough to experience the becoming of a "new" and dear friendship. To the dearest of all sisters, although I'm short of actually having more than one in a physical sense, I thank my lovely sister Line for frequent and ubiquitous conversations that always keep my alert in a most stimulating manner. Friendships in general do come hard, but some are fortunately enveloped by un–escapable connections.

Although Cecilie hardly can be made responsible for making me start this work, she most surely has provided me with very good reasons for finishing. Despite constraints imposed by the geographically suboptimal locations of Oslo and Trondheim, we have made our best to evoke and sustain enthusiasm in our relationship. The lack of opportunities to share hopes and doubts on a every-day-basis, should nevertheless provide excellent chances for us to receive the "stick-together-under-long-odds" award. I thank you for moments of euphoria, longings, laughter, your wit, Vietnam, Indigo Girls, infantile conversations in the spirit of "Hakke-bakke skogen", your dazzling eyes, phone bills, elated attractions and last but not the least, for your ability to make feel alive to the very fullness of the concept. For past times and time to come!

My friends have throughout these years provided an extremely stimulating and sociable environment, in which the ground has been laid for understanding of other and much more important aspects than those related to my thesis work. Given the scarcity of these pages I can sadly mention only but a few. Hans Petter and Kjetil are graciously thanked for their friendship, their humor, the sharing of ideas, their exuberance in ways of being and their sincere commitment in open hearted conversations. Thanks to Tina and Eyvind for many a night out toping, their "joie de vivre", their lust for life, the passionate late night talks and "nach-spiels". A special thank to Dag S. for many of the same reasons, but most of all for bringing back to me the delights and joys of reading. To Bjarne and Sune; thanks for reminding me that there is a place to be called home, where the luggage of enjoyable moments from the past finds a safe home. Thanks also for vivid and memorable visits to Trondheim. Erik S., Lars Brede and Jeppe are thanked for numerous and vibrant talks on subjects of mind as well as matter. On the less formal side, I thank Aschehoug and Gyldendahl for their reluctance, Morgenbladet and Dagbladet for their courtesy and 3B for their cheap beers. Finally I acknowledge The Norwegian Research Council for financial support during my visits to Berkeley, Fiji and Aachen.

"No names have been changed to protect the innocent,
since God Almighty protects the innocent
as a matter of Heavenly routine"
-Kurt Vonnegut-

Contents

List of Figures

List of Tables

Chapter 1

Introduction

1.1 Motivation

During the last decades there has been an ever growing concern in the chemical engineering environment, dedicated to the task of developing more cost and energy efficient process equipment. This need stems partly from the scrutiny of tighter operational constraints, but is on a higher level driven by the concern for developing an environmentally (ecologically) sound industry. During the last couple of decades it has for instance become evident that many of the threats to the global environment, such as the accumulation of green house gases and acid rains, are energy related issues. The global trend in industry and research is thus a twofold focus on energy, constituted by a stronger emphasis on energy efficiency *and* a move towards incorporating renewable energy technologies. A comprehensive discussion of aspects related to the energy issues, is given in a recent report from the United Nations Development Programme (Energy and Programme 1997). The following paragraph gives a short summary of the attitudes they put forward

> During the last decade, technological developments and operating experiences have made many technologies (particularly those utilizing renewable energy) more mature and competitive, creating many new opportunities. What is needed now is to identify existing and potential opportunities and to design policies and other measures to capture their benefits. To take advantage of these new opportunities the following activities are needed: conducting and promoting demonstration projects to illustrate the technologies' potential and cost-effectiveness, utilizing existing markets, and building up new markets... In addition, continued research and development is needed to improve some technologies still further.

In this work we put emphasis on measures for improving the *end-use energy efficiency* of separation systems. In terms of energy intensity we may mention that the amount of energy required for separations, ranks *distillation* as one of the largest energy consumers on a world wide basis, using about 3% of the *total* energy in the U.S. alone (Ognisty 1995). The objective of this work is thus partly to trigger future research

so as to facilitate implementations of more cost efficient (i.e. capital and energy) *separation* systems.

1.2 Energy Efficient Distillation Arrangements

In the present work we focus at large on energy efficient complex distillation arrangements for the separation of multicomponent mixtures. By complex we here understand arrangements that differs on a *structural* level from conventional ones with sequences of columns arranged in series. One distinguishing feature of such complex columns is that they utilize *direct* coupling between different column sections. This differs structurally from the common approach to integrating distillation columns, where *indirect coupling* is often used by heat integrating regular columns. An important issue to bear in mind is that we in this work we have chosen to compare the efficiency of complex distillation arrangements only with sequences of regular columns. We have thus omitted comparison with heat integrated schemes, for which the reason is twofold. Firstly, it is crucial to establish a *common ground* for comparing the efficiency of new arrangements for both the present and future works. Conventional arrangements of regular columns thus provide a natural basis, since these are the most common in industry and the (minimum) energy usage is easily obtained for such schemes. Secondly, since this work at large represents a conceptual study, we want to avoid complicating "second order" effects that usually should be taken into account in the analysis of heat integrated schemes. In the latter case it usually so that columns should be operated under different pressures, so that one should also consider detailed thermodynamics to address the influence of pressures on the vapor-liquid equilibria.

One class of such complex distillation arrangements is the "Petlyuk arrangements", for which we in this work propose a general definition to form a common basis for the present and future work. The analysis of such columns draws from previous works by Petlyuk and coworkers, e.g. Petlyuk and Platonov (1964), Petlyuk *et al.* (1965) and Petlyuk *et al.* (1966). The basis for these works was a thermodynamic analysis that aimed for a reversible distillation process. Since reversible distillation requires infinite columns *and* distribution of utility along the column, such columns are obviously not desirable neither from a practical nor economical point of view. However, one of the important results emerging from these works, is the emphasis on a certain optimal/easiest/preferred split sequence for the multicomponent separation. In this work we elaborate on the issue of finding the optimal split sequence, for which we obtain very useful *analytical* results. These results not only give explicit equations for the minimum energy usage for sharp and non-sharp separations, but in fact also enhances the understanding of how such columns may be operated. In particular we obtain two important parameters that define regions within which the minimum energy usage stays relatively constant, and within which optimal operation is relatively insensitive to changes in the operating parameters.

Although the potential for large energy and capital savings are well documented, the industries have so far been reluctant to use and carry out extensive research on such novel designs as the Petlyuk column. To account for this resistance, arguments have touched upon issues such as lack of knowledge and understanding, along with

(immanent) scepticism towards practical issues such as to how such columns may be controlled. However, more recent industrial practice and research indicates that some of these issues are soon to be resolved. For this reason our work aims to *extend* the scope of previously known complex columns. We will introduce complex *Petlyuk arrangements* for the separation of ternary and quaternary mixtures, that allows for implementations in single shells using dividing walls or vertical partitions. Such schemes inherently offer large savings in both capital and operational (energy) costs. We provide results showing that the energy savings typically are in the order of 40%, although even larger savings are possible.

1.3 Numerical Methods for System Analysis

It is well established in the literature that distillation models in general display highly nonlinear behavior and they are often ill-conditioned. The strongly non-linear behavior is well documented in recent works on dynamics and control by for example Skogestad (1987) and Jacobsen (1991). For complex distillation arrangements such as the Petlyuk column, we also face a strongly pronounced coupling between the system equations in the distillation model. This further complicates the system behavior and may give rise to nonlinear phenomena such as multiple steady states and even the occurrence of *holes* within certain operating regions (Wolff and Skogestad (1995) and Morud (1995)). Such inherent characteristics pose problems not only for issues of control and operation, but also for any numerical method used for simulation. A very important aspect in order to carry out detailed analysis is thus that of deriving reliable and efficient numerical methods for various purposes.

We have in this work focused primarily on numerical methods for *steady state* analysis, for which the general purpose is to find one or all solutions to a system of nonlinear algebraic equations (NAE's). Even though this is an area in which extensive research has been carried out the last decades, and for which a wide range of methods are available through various software packages, there are still problems for which special purpose algorithms may work better. All simulations presented in the present work has been carried out using Matlab, which is a *" high performance language for technical computing"* (The Mathworks 1995). However, Matlab is in its present state in general not very well suited for simulations of large systems. For this reason we have invested heavily in exploiting inherent model/system characteristics to obtain efficient algorithms. For instance we make extensive use of continuation methods for both simulation and optimization purposes. The advantage of using such methods is that information from previously obtained solutions is used in a systematic and expedient manner. Continuation methods are for instance helpful in the way that one may easily utilize search directions in which the model are relatively insensitive towards changes in the system parameters, so that convergence problems are avoided.

1.4 Thesis Overview

This thesis address various aspects related to optimal design and operation of (complex) energy efficient distillation arrangements. Each chapter is written in the form of a paper, and may thus be read independently, including the literature references which are given at the end of each paper. In order to give a comprehensive and lucid presentation, the thesis divides into three main parts. In *Part I* we consider methods for obtaining numerical ("exact") solutions to a system of equations representing for instance a complex distillation model. *Part II* consider approximate solutions to such process models using certain assumptions and some issues of importance for practical operation. In *Part III* we then propose several new structures for a particular class of integrated distillations columns, which we then solve using some of the the numerical methods discussed in *Part I*.

Part I : Numerical methods for steady state analysis

This part which comprises chapters 2 and 3, addresses general purpose numerical methods to be used for solving systems of nonlinear algebraic equations (NAE's). Some of these methods, such as the homotopy continuation methods and the *tear and grid* method, are in their present states only applicable to relatively small systems. The main parts are however dedicated to the issue of *continuation methods*, which are used also for simulations of larger systems such as the complex distillation arrangements discussed in the last part of the thesis. We discuss two different algorithms, based on a conventional predictor-corrector method and one in which we use a secant predictor to enable simultaneous solution of an augmented system of equations. We demonstrate how these methods may be used for parametric continuation in any hyper-space, meaning that one may consider the impact of variations in several parameters simultaneously. We also present a scheme for embedding steady state optimization in a continuation scheme, which proves useful in the optimization of highly nonlinear and coupled process models.

Part II : Shortcut methods to obtain V_{min} and the "preferred separation"

In chapters 4 and 5, we discuss aspects related to finding the minimum energy inputs (V_{min}) for multicomponent separations. Chapter 4 addresses a simplified shortcut method for calculating V_{min}, which allows one to derive *explicit* equations to be used for qualitative purposes. Although it is inherently an approximate method, due to an underlying assumption in the way we account for the distributing components, we demonstrate that explicit analytical equations may be derived. These expressions are shown to be exact in certain limiting cases, e.g. for large amounts of intermediate and for the so called *"preferred" separation*. We ask the reader to take this consideration into account, when we argue that the main purpose for using shortcut methods is to obtain insights that are otherwise difficult to derive from numerical simulations. Such information is not available through the use of other shortcut methods such as the well known Underwood method, which in general requires iterative solutions. Through numerical examples we display the regions in composition space in which our method provides good or poor estimates of the true V_{min}. In general we find that our method gives reasonably accurate results within the regions where the particular

distillation sequences (i.e. direct or indirect) are optimal.

In chapter 5 we examine in more detail the *preferred separation* for ternary mixtures and the separation corresponding to a *"balanced"* main column. Although the preferred separation in general refers to a certain distribution of the intermediate component, for which the absolute minimum energy input is required in an infinite column, it is of interest to examine its use also for other splits and column *sequences*. Based on observations from simulations of an "infinite" prefractionator column (large number of stages), we derive new analytical expressions that allows one to obtain the minimum energy usage for the prefractionator column for any distribution of the intermediate component assuming sharp splits between the light and heavy component. We then use this result to analyze whether the preferred separation is optimal also when the energy usage of downstream columns are taken into account. For sharp separations we find that the preferred separation is always optimal. We also briefly discuss the issue of the preferred separation for non-sharp separations between the key components. Finding the optimal split sequences is furthermore crucial when considering other complex distillation arrangements such as the Petlyuk arrangements to be discussed in the last part of the thesis.

Part III : Complex Distillation Arrangements

In part III consisting of chapters 6 and 7 we consider a particular class of complex distillation arrangements, namely the Petlyuk arrangements. In chapter 6 we give a conceptual analysis of such arrangements, for which we propose a general definition. We briefly discuss the aspect of sharp split arrangements, and issues related to reversibility of distillation processes. We then extend the *Petlyuk ideas* to consider partitioned distillation columns for the separation of quaternary mixtures. Based on superstructures proposed in the literature, we propose arrangements that allows for implementations in a single shell using only a single reboiler and a single condenser. We give a brief discussion of the large number of degrees of freedom that are available for such columns.

In chapter 7 we discuss the issues of optimal design and to some extent operation of the Petlyuk arrangements proposed in chapter 6. Based on simple yet detailed stage to stage models assuming constant molar flows and constant relative volatilities, we use the previously proposed optimization scheme to compute the minimum energy usage for these columns. The energy efficiency is then compared to conventional arrangements of regular columns in sequence. We find that the Petlyuk arrangements with a sufficiently large number of stages offer energy savings in the order of 40%. We also discuss some practical issues related to obtaining good initial guesses for the optimizations. Finally we illustrate how one may derive sensitivity functions for the objective function based on Taylor series expansions. These functions are then used to characterize the optimal solutions in terms of high and low gain directions for changes in the parameters, from which we conclude that feedback control is required to maintain optimal operation.

Finally, in chapter 8 we present a work on parametric sensitivity in batch distillation. This work in particular was motivated by previous findings for continuous columns, where steady state multiplicities and instabilities was reported (Jacobsen and Skogestad 1991). Based on a mathematical analysis of a general model, we show

that the same phenomena that caused such multiplicity carry over to batch columns where they cause the columns to exhibit *parametric sensitivity* (PS). We give a comprehensive analysis of PS for general dynamical systems, in which we also critically review criteria used in the literature on batch reactors. Using a linear analysis we then determine conditions that favor PS. Even though the mathematical analysis considers a simple model, in which we for instance neglect tray holdups, we show by numerical simulations that severe sensitivity may arise also for columns where these restrictive assumptions is not made. In order to address the impacts for practical operation we also consider the influence of different control configurations and operating strategies on PS.

References

Energy and Atmosphere Programme (1997). UNDP Initiative for Sustainable Energy. Technical report. United Nations Development Programme. Document is available on the Internet : http://www.undp.org/seed/energy/unise/.

Jacobsen, E. W. (1991). Studies on Dynamics and Control of Distillation Columns. PhD thesis. University of Trondheim, The Norwegian Institute of Technology.

Jacobsen, E. W. and S. Skogestad (1991). Multiple steady–states in ideal two–product distillation. *AIChE Journal* **37**(4), 499.

Morud, J. (1995). Studies on the Dynamics and Operation of Integrated Processes. PhD thesis. University of Trondheim. The Norwegian Institute of Technology. Norway.

Ognisty, T. P. (1995). Analyze Distillation Columns With Thermodynamics. *Chem. Eng. Prog.* pp. 40–46.

Petlyuk, F. B. and V. M. Platonov (1964). Thermodynamically Reversible Multicomponent Distillation. *Khim. Prom.* (10), 723.

Petlyuk, F. B., V. M. Platonov and D. M. Slavinskij (1965). Thermodynamically Optimal Method for Separating Multicomponent Mixtures. *Int. Chem. Eng.* **5**(3), 555–561.

Petlyuk, F. B., V. M. Platonov and V. S. Avetlyan (1966). Optimum Arrangements in the Fractionating Distillation of Multicomponent Mixtures. *Khim. Prom.* **42**(11), 865.

Skogestad, S. (1987). Studies on Robust Control of Distillation Columns. PhD thesis. California Instiutute of Technology.

The Mathworks, Inc. (1995). *MATLAB Reference Guide.*

Wolff, E. A. and S. Skogestad (1995). Operation of Integrated Three–Product (Petlyuk) Distillation Columns. *Ind. Chem. Eng. Res.* **34**(6), 2094–2103.

Chapter 2

Numerical Methods for Steady State Analysis. Part I : Obtaining Initial Solutions

Atle C. Christiansen, John Morud and Sigurd Skogestad*

Department of Chemical Engineering
Norwegian University of Science and Technology, NTNU
N–7034 Trondheim Norway

Revised version of paper presented at
SIMS'96, Trondheim, Norway, June 11-13 1996
Proceedings, p 217-230

Abstract

This paper considers numerical methods for finding initial solutions to systems of non–linear algebraic equations (NAE's). We briefly discuss the difference between methods belonging to the classes of local and global methods. Among the global methods, we consider *homotopy–continuation* methods and discuss inherent difficulties in using such methods. In particular we address inherent characteristics such as potential unboundedness of the homotopy path. To assure bounded paths we provide some insight into how appropriate *branch–jumping* techniques may be applied. We also present a novel *tear and grid method* based on conventional techniques of partitioning and precedence ordering. Finally we give a comparative analysis of the methods in terms of a few example problems.

*Author to whom correspondence should be addressed : Fax : +47 7359-4080, E-mail: skoge@chembio.ntnu.no

2.1 Introduction

During the last decades an extensive range of computer–aided methods for both steady state and dynamic simulation has evolved. Driven by an increase in both computer availability as well as computing power and efficiency, computer aided tools are now standard features in most aspects of chemical process engineering. A recent review of available numerical methods for process design, optimization and control with emphasis on non–linear analysis, is given by Seider *et al.* (1991). In this chapter we however limit ourselves to the study of numerical methods for *steady state analysis* of process models. Thus we consider procedures for finding one or all solutions to a system of non–linear algebraic equations (NAE's) which we here denote by

$$\begin{aligned} & f(\mathbf{x}, \lambda) \;=\; 0 \\ & f : \mathcal{R}^m \times \mathcal{R}^k \rightarrow \mathcal{R}^m, \quad \mathbf{x} \in \mathcal{R}^m, \quad \lambda \in \mathcal{R}^k \end{aligned} \tag{2.1}$$

where $\mathbf{x}$ is a m-dimensional vector of state variables and λ a k-dimensional vector of parameters. Sargent (1981) gives an excellent review of methods for solving NAE's that were available at the time the review was written, and claims that *"there is no method which clearly stands out from all the rest in terms of both reliability and efficiency"*. Even though the engineers now face a bewildering range of methods and proposals for new methods appear quite frequently in the literature, Sargent's analysis still seems to hold in the general sense. In the following discussion we ask the reader to bear in mind the important difference between *methods* (numerical techniques) and *codes* (algorithms). The importance of this distinction lies in the simple fact that numerical methods may be implemented according to different schemes according to different codes and programming languages. In this work we put emphasis on methods rather than codes, thus leaving out detailed analysis of for example computational efficiency or algorithmic aspects.

In the future it is to be expected that the engineer will require specific solution methods designed to deal with the particular problem at hand. Being able to choose the *optimal* solution method from a library of different algorithms, according to some predefined objective, is thus a great advantage. We argue that the objectives for choosing the appropriate numerical methods should be formulated based on the size, complexity and difficulty of the problem at hand, rather than rigor or ability to handle any pathological problem. A rule of thumb should be to avoid shooting sparrows with canons. In the literature it is common to distinguish between *local* and *global* methods, depending on the respective domains of attraction for convergence. We thus start by giving a brief discussion on the use of local versus global methods for finding initial solutions.

Local methods. Among the most common local methods used in solving chemical engineering problem are the Newton, Secant, Broyden and Deflation methods. In general such local methods display poor convergence properties, unless good starting guesses are provided due to dependency on the function evaluations at the particular point. Although methods exist for enlarging the domain of attraction, local methods often fail to converge. Venkataraman and Lucia (1988) argues that failure is "always due to some physical inconsistency in the model". However, to avoid these incon-

sistencies good starting points are required which may be difficult to obtain if little knowledge exist about the system. In this respect we suggest to use the tear and grid method to screen the solution space, in order to indicate in which regions solutions are likely to occur. Other and more accurate methods should then be used to obtain the "exact" solutions.

Another objection to using local methods is that they can at best find one solution for each given starting guess. Since most chemical engineering models contain non–linear equations, multiple solutions and other complex behavior arise quite frequently. Knowledge about what kind of behavior one may expect is invaluable in both process design and control, hence methods that are able to detect for example steady state multiplicity should be available to the engineer.

Global methods. Although there exist methods for finding all solutions of typical systems of equations arising in chemical engineering, e.g. branch and bound methods (Horst and Pardalos 1995), these methods require a computational effort that increases exponentially with the problem size. However, this applies asymptotically, and for many problems arising in conceptual design of distillation systems, it is possible to exploit sparsity to reduce them to medium size- or even small problems. In such cases the computational times may be reasonable, or even small. In this work we consider a *homotopy–continuation* scheme based on pseudo arc–length continuation. Although these methods have been used for quite some time in other disciplines, it is only during the last decade that successful applications to chemical engineering problems have been reported. We also introduce a much simpler *tear and grid method*, in which we utilize insights from conventional partitioning and precedence ordering techniques combined with gridding of variables. Both methods are used to find initial solutions and to explore solutions in the parameter space.

Exploiting Algebraic Structure. An important issue which is often neglected in the design of numerical methods is to exploit algebraic structure. For *large sparse problems* Sargent (1981) claims that it is always worth partitioning, but we show in this work that the pay-back may be considerable also for small problems. Partitioning addresses the task of decomposing the whole problem into smaller subsets which are then solved in turn. In a textbook by Westerberg *et al.* (1979) several approaches to exploiting the algebraic structure is considered. We use these standard techniques to derive a highly efficient solution strategy for finding one or all solutions to a system of NAE's.

Outline of paper. In section 2 we discuss a particular method to obtain *constrained* solutions, in which some of the variables x are specified and the task is to compute the required values for the corresponding parameters λ. In section 3 we give a brief review on classical approaches to formulation and numerical solution of various homotopy–continuation schemes. We also discuss some inherent difficulties in using available homotopies, and in particular we address the issue of potential unboundedness of the homotopy paths. To restrict the path to some finite domain we apply branch–jumping techniques which are based on variable transformations and symmetrical arguments. Such techniques have the advantage that no changes in the model equations are required. We then, in section 4, present a novel algorithm called *tear and grid method*

is introduced. The method is in principle based on conventional procedures for choosing a suitable set of tear or decision variables and reformulating the model equations by simple algebraic manipulations. The algebraic structure is exploited and in some cases the algorithm may yield *explicit* solution schemes, thus eliminating the need for costly iterations. Finally in section 7 we present a comparative analysis of the different methods with emphasis on aspects such as simplicity, flexibility and computational efficiency.

2.2 Constrained Solutions by Feedback Control

In order to find at least one solution to the system NAE's given by (2.1), we stress that one should distinguish between finding *unconstrained* and *constrained* solutions. Note that we here use the term constrained with respect to the system (output) variables. In the former case, all degrees of freedom (e.g the values of *all* parameters λ) are fixed and the task is to solve a *square* system of NAE's given by

$$f(\mathbf{x}) = 0, \quad \lambda = \lambda_0 \tag{2.2}$$

As previously discussed, one may in principle apply any local or global method to find the desired solution(s). However, we also note that when we consider chemical engineering problems, the system of NAE's often resembles a steady state solution of a general dynamic model, which typically is constituted by mass and energy balances as well as thermodynamic and equilibrium relations. Provided there is a stable steady state, the solution is quite easily obtained by solving the original dynamic model to a steady state using some numerical integration scheme, e.g. Runge Kutta methods or BDF–formulas.

This special feature is utilized as we now turn to the issue of finding constrained solutions, in which case we want to be able to specify some of the (output) variables. This is the typical situation in design, in which some of the outputs are specified and the corresponding inputs needs to be obtained. These solutions may of course be obtained in the same manner as for the unconstrained case, simply by adding additional equations for the equality constraints and augmenting the vector of variables correspondingly. This is the situation commonly encountered in flowsheeting simulation, where for instance "recycle" (tear) variables (Westerberg *et al.* 1979) are used to solve the flowsheet in a hierarchical manner. However, if we instead have a dynamic model available, we will next illustrate an alternative approach for computing *constrained solutions* using feedback control. As a minor comment one may also argue that solving the general dynamic model to a steady state using dynamic simulation, is a more "consistent" and intuitive way of obtaining such a solution.

If we then denote the outputs by y, the state variables by x and the inputs by λ, the system of ordinary differential equations (ODE's) is given by

$$\dot{\mathbf{x}} = g(x, y, \lambda) \tag{2.3}$$

Our task is now to find a steady state solution by integrating the system of ODE's (2.3), subject to some variables (outputs) being constrained. The desired solution is

thus found by solving the following problem

$$\begin{aligned} & g(x, y, \lambda) = 0 \\ \text{subject to} \quad & \\ & y = y_s \end{aligned} \tag{2.4}$$

where y_s are the constraints (set points). In order to find the corresponding (input) parameters λ, we simply consider the dynamic model as a *feedback control* system and compute λ using a simple feedback law

$$\lambda = K\,(y - y_s) \tag{2.5}$$

in which K is the controller given by a simple single-input-single-output (SISO) controller or any kind of multivariable (MIMO) controller. The requirement is naturally that the particular controller yields a stable closed loop system. Finally, one may consider the problem constituted of (2.3)–(2.5) as that of solving a differential algebraic system of equations (DAE) which we denote by

$$f(\dot{x}, x, y, \lambda) = 0$$

In figure 2.1 we give an example in which feedback control was applied to obtain desired product purities $y_{S,i}$ for a separation process of a quaternary mixture. The objective is simply to achieve certain purities for the products of each of the components A, B, C and D. The column is a complex distillation arrangement previously

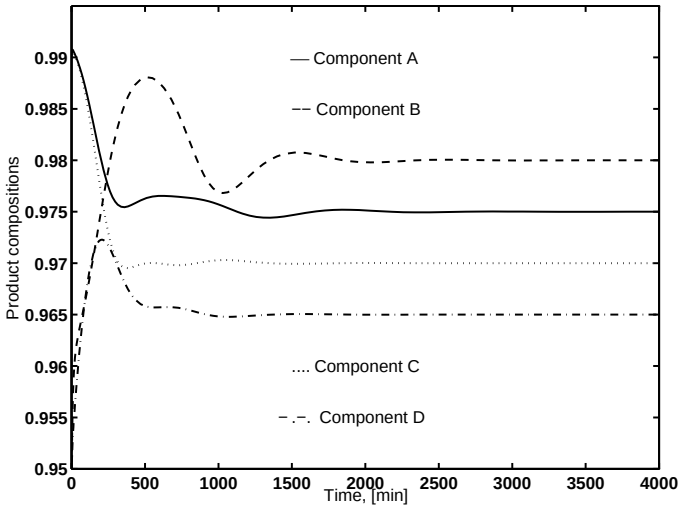

Figure 2.1: Closed loop simulation of a complex distillation column using a steady state decoupler to obtain constrained steady state solutions

presented by Christiansen *et al.* (1997), for which it was difficult to find constrained solutions using steady state solvers. For the controller we used a simple stationary

decoupler, and as demonstrated in the figure the simulation converges to the desired steady state solutions. The initial values corresponds to an unconstrained (open loop) steady state solution in which case the values for the system parameters λ were specified. From the Figure we observe that the new constrained solutions are located by dynamic simulation until the steady state is reached. We should also note here that a very important issue is that of deriving a *stable* controller. This is however not an issue dealt with in this work. Next, we consider methods belonging to the class of homotopy–continuation methods.

2.3 Homotopy–Continuation Methods

Due to the lack of global convergence properties for most conventional Newton or quasi–Newton methods, *homotopy–continuation methods* were introduced in solving chemical engineering problems during the late 70's and early 80's. The ideas of continuation methods are however not new, and were according to Ortega and Rheinboldt (1970) introduced in the literature in the 1930's to solve a single non–linear equation. The homotopy function may be solved by discretizing the homotopy path and applying a local method such as Newton's method at each point of discretization. However the computation effort may be reduced substantially by reformulating the homotopy function to an initial value problem (IVP) as suggested by Davidenko (1953). The IVP can be solved by any numerical integration routine, but most algorithms use some predictor–corrector scheme, e.g. Euler predictor and Newton corrector step. Homotopy–continuation schemes have proven to be very effective, though computationally inefficient, and have been used extensively the last decade. A comprehensive survey of the use of homotopy continuation in computer aided design is given in a recent article by Wayburn and Seader (1987). The continuation algorithm used in this work deviates somewhat from the classical approach in that we use theory from linear algebra in an explicit manner to find search directions. Using such information we avoid increasing the dimensionality of the problem by introducing an additional parameter such as the arc–length. Our algorithm is based on the principles described in a work by Morud (1995), where continuation methods are used to explain complex behavior displayed by a integrated distillation column known as the Petlyuk column, previously observed by Wolf (1994). Among other applications of homotopy–continuation methods within chemical engineering we mention a few important works. Multiple solutions of interlinked distillation columns were also computed from different starting guesses by Chavez *et al.* (1986) and from homotopy continuation Lin *et al.* (1987). Kovach and Seider (1987) applied an algorithm with particular emphasis on avoiding limit points for the simulation of an industrial heterogeneous azeotropic distillation tower. A similar approach was used by Chang and Seader (1988) to show how certain design parameters affect a continuous reactive–distillation system. Fidkowski *et al.* (1991) use continuation methods to demonstrate how elementary bifurcation theory may be used in the design of nonideal multicomponent distillation. For reviews on methods and other applications we refer to the works of Seider *et al.* (1991), Wayburn and Seader (1987) or Allgower and Georg (1993). The mathematical principles of the continuation algorithm is thoroughly described in

several textbooks (see e.g. Seydel (1988) or Kubiček and Marek (1983)). There also exist some semi–commercial applications, e.g. AUTO (Doedel n.d.) or HOMPACK (Watson *et al.* 1987)). Among the more recent works we acknowledge the works of Paloschi (1995) and Paloschi (1997), in which a new class of *bounded* homotopies are introduced to restrict the homotopy paths to prescribed domains.

2.3.1 Formulating the Homotopy Functions

The underlying idea of homotopy continuation is to embed the function $f(x)$ in a *blending* function $H(x,t)$ forming the linear homotopy function

$$H(x,t) = tf(x) + (1-t)\,g(x) = 0 \tag{2.6}$$

where $f(x)$ denotes the model equations, x the model variables, t the homotopy parameter and $g(x)$ a system of equations for which a solution is known or easily obtained. The latter is a key point in understanding the proficiency of using homotopy functions, since we may ease the task of solving a difficult problem $f(x)$ by using as a starting point a solution to $g(x)$ which is easily solved or in fact known *a priori*. The homotopy path is defined by the locus of all solutions found by tracking equation (2.6) starting from $t = 0$ with a known or easily obtained initial solution $x = x_0$, and ending at $t = 1$ for which $f(x) = 0$. From equation (2.6) wee see that

$$H(x,0) = g(x) = 0 \tag{2.7}$$

$$H(x,1) = f(x) = 0 \tag{2.8}$$

thus the desired solution to $f(x) = 0$ is obtained if and only if the homotopy path is tracked up to the point where $t = 1$. Under certain assumptions $H(x,t)$ is continuous such that the path containing $(x,0)$ also contains $(x,1)$ (see Ortega and Rheinboldt (1970)). Under these conditions one may also find several solutions, by allowing the path to extend beyond these limits. However this is often not the case, and obstacles that may prevent successful tracking is discussed in the next section. Several choices exist for $g(x)$ each yielding a different homotopy with different behavior. Alternative homotopies are :

Fixed point homotopy	$H(x,t) = tf(x) + (1-t)(x - x_0)$	(2.9)
Newton homotopy	$H(x,t) = f(x) - (1-t)f(x_0)$	(2.10)
Affine homotopy	$H(x,t) = tf(x) + (1-t)A(x - x_0)$	(2.11)

where A denotes a proper weighting matrix to avoid scaling problems, typically chosen as $f'(x_0)$. Yet another alternative is to choose $g(x)$ as a problem which is easier to solve than $f(x)$, for example in solving a distillation problem with non–ideal thermodynamics starting with a solution for the ideal case as shown by Vickery and Taylor (1986). In this work we show how solutions to a model of a *reactive* distillation column $f(x)$ may be obtained by choosing $g(x)$ as a model of an *ordinary* distillation column, for which a solution is more easily obtained. These different homotopies are then said to form a convex linear homotopy (Kovach and Seider 1987), so that the residuals

f_i decay linearly from the initial values given by x_0. The advantage with the fixed point homotopy is, besides its simplicity, that any additional multiplicities introduced by adding further *functions* is avoided. Other homotopies may have more appealing numerical properties, but in general there are no definite guidelines for choosing the optimal one. Problem caused by undesired multiplicities and other difficulties which may cause failure is treated in the next section.

Solving the Homotopy function

The *classical* solution method involves discretization of the homotopy path, in which a local method (e.g. Newton's method or Broyden) may be applied at each point of discretization. However, as was suggested by Davidenko (1953), computational efficiency may be greatly improved by reformulating the homotopy function 2.6 to an *initial value problem* (IVP). By differentiating the homotopy function (2.6) with respect to t we derive

$$\begin{aligned} \frac{dH(x,t)}{dt} &= \frac{\partial H}{\partial x}\frac{dx}{dt} + \frac{\partial H}{\partial t} = 0 \\ \Rightarrow \frac{dx}{dt} &= -\left(\frac{\partial H}{\partial x}\right)^{-1}\frac{\partial H}{\partial t} \end{aligned} \tag{2.12}$$

Given an initial solution, x_0, equation (2.12) constitutes an IVP which may be integrated by any numerical integration scheme, e.g. Runge Kutta or Gear's method. Most continuation methods use some predictor–corrector scheme, typically an Euler predictor and Newton corrector. If the homotopy path is connected, it is obtained by tracking (2.12) from $t = 0$ with $x = x_0$, and ending at $t = 1$ for which $f(x) = 0$. However, tracking the homotopy path may fail in some cases, if proper precautions are not taken in the path following procedure.

Unboundedness and non–uniqueness of homotopy paths

A detailed analysis of situations under which homotopy–continuation methods may fail is presented in a work of Wayburn and Seader (1987). We will here give a brief discussion of the most common causes of failure, of which one is that

i) The Jacobian $\partial H/px$ becomes singular at turning points

To avoid problems in tracking the solution curve across turning points, most algorithms proposed in the literature introduce the *arc–length* to define the search directions along the path. We have use a slightly modified approach in which orthogonal search directions are found from linear algebra as described in a work by Morud (1995). In addition to difficulties in crossing turning points, problems also arise when

ii) The homotopy path becomes unbounded

Since the homotopy path needs to be finite in order to be trackable, some kind of branch jumping technique or variable transformation must be introduced if unboundedness is displayed. Seader *et al.* (1990) suggested to use mapped continuation methods, called *toroidal* and *boomerang* mapping, in which variables that extend to $\pm\infty$ are kept bounded through a proper transformation. The authors conjecture that *all* solutions may be traced from any starting point using a fixed point homotopy and

allowing all variables to take complex values. Sufficient proof of such global convergence properties does however not exist, and whether or not all solutions may be found from *one* starting point is still an open question. Taylor *et al.* (1996) also exploit the potential for carrying out distillation calculations in the complex domain. They argue that allowing for complex solutions in the iteration procedure enhances convergence in cases where methods operating only in the real domain failed. One objection to the latter approach is that using complex arithmetics considerably increases the computational efforts, as is also noted by Taylor *et al.* (1996). In a recent work Paloschi (1995) introduced new bounded homotopies that on one hand avoids tracking complex paths, and at the same time guarantees solution paths to remain inside a prescribed region. Since these bounded homotopies produce dense Jacobians, even when the original problem is sparse, Paloschi (1997) later proposed homotopies which retain the sparsity patterns of the original problem. The author, however, recognized the need for more work on theoretical aspects of these proposed homotopies.

iii) Multiple solutions may exist for $g(x) = 0$

If the added function $g(x)$ has multiple solutions, the homotopy path may return to a second solution of this simpler problem without passing through the desired solutions to $f(x) = 0$. Wayburn and Seader (1987) use the concept of *topological degree* to indicate when multiple solutions of $g(x)$ may cause failure in using for example the Newton homotopy. This problem is however easily avoided by using the fixed point homotopy since the residuals $x - x_0$ is simply a vector of scalars. In order to avoid undesired scaling problems with the fixed point method one may resort to the Affine homotopy which is scale invariant.

iv) Variables may exceed the domain on which they are defined

on negative values at some point along the path. Since thermodynamic functions often involve logarithms or square roots they become undefined when substituting negative values. Wayburn and Seader (1987) suggests to use the absolute value functions to resolve such problems. However, this problem is conveniently handled using a new class of bounded homotopies (Paloschi 1995, Paloschi 1997).

v) Occurrence of *isolated* solutions along the homotopy path

There is at present date no method which rigorously deals with problems of isolas as noted also by Seader *et al.* (1990), and we pose this problem as a great challenge for future work.

As an alternative to the approaches suggested by Seader *et al.* (1990) and Paloschi (1995), we will in the next section focus on some simple *branch–jumping* techniques in order to overcome the problems of unbounded paths. By using the simple *inverse mapping* function, we show how arguments of symmetry may be used to predict where solution branches connect across asymptotes. In cases of single and linear asymptotes we found that the inverse mapping works satisfactorily. However, in situations where for example several asymptotes lie arbitrarily close in the variable space (as for the CSTR example to be discussed later), or in cases of non–linear asymptotes, the situation is not that simple and the algorithm displayed poor convergence characteristics.

Further work needs to be done on both theoretical and numerical aspects of this issue. Before going into detail on the mathematical issues of continuation and branch jumping, we illustrate the usefulness of applying branch jumping techniques by considering a simple scalar example function previously studied by Lin *et al.* (1987) and Seader *et al.* (1990).

Introductory Example : Scalar Function. To illustrate the usefulness of applying branch jumping techniques we consider the simple scalar example function previously studied by Lin *et al.* (1987) and Seader *et al.* (1990). The function is given by

$$f(x) = x^2 - 3x + 2 \tag{2.13}$$

for which the analytical solutions $x = \{1, 2\}$ are easily obtained. We applied the fixed point homotopy $H(x,t) = t\left(x^2 - 3x + 2\right) + (1-t)(x - x_0)$ and figure 2.2 shows the homotopy paths and the two solutions to $f(x) = 0$ denoted I and II at $t = 1$. The path consists of three branches and is traversed in the direction indicated by arrows. Starting at the arbitrary initial point $x_0 = 1.5$ on branch 1, we find *both* solutions by allowing the homotopy path to extend beyond the interval $0 \leq t \leq 1$. We see that the path goes to infinity at the connection points $(t, x) = \{(0, \pm\infty), (\pm\infty, 1.2929), (\pm\infty, 2.7071)\}$. In spite of its unboundedness the homotopy curve is successfully tracked numerically by applying a simple *inverse mapping function* which imposes a jump of finite length in the mapped variable space. We now give an outline of how the branch–jumping illustrated by this example is

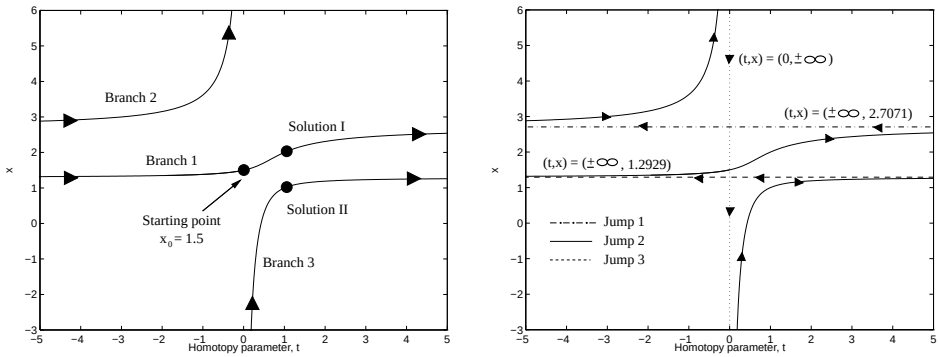

Figure 2.2: Homotopy paths for $H(x) = x^2 - 3x + 2 + (1-t)(x - x_0)$.

obtained.

2.3.2 Branch–jumping Techinques

Since the homotopy path needs to be of finite length we need some method to jump across the asymptotes, and in order to enable such branch–jumping, a direction for the jump in the solution space needs to be defined. We demonstrate how such directions

may be found based on theory from linear algebra and simple arguments of symmetry. In the preceeding discussion the term *branch* is used to denote a curve or surface reflecting the solutions in a branching diagram, i.e. a diagram depicting for example x versus t where (x,t) solves the homotopy functions (2.6). We now outline the general principles of the methods, but the detailed mathematical issues are described in Appendix A.

Method 1: Aligned Asymptotes This first method is particularly simple in that we utilize arguments of symmetry in a way which requires that the asymptotes are aligned with the coordinate axis of the original variable space. The underlying idea of the method is to impose a finite step in the transformed variable y which is mapped according to the *inverse mapping function*

$$y = \frac{1}{x_i} \tag{2.14}$$

where x_i denotes the variable for which asymptotes arise, i.e. the homotopy path connects at $\pm\infty$ for some value of x_i. The reader should note that we do not distinguish between variables x or the homotopy parameter t, since both variables may go to infinity along the path. The issue of finding a point on the connecting solution branch also involves a predictor–corrector scheme. In the predictor step we try to find the required direction of the jump in a similar fashion as described for the general Euler predictor. A step in the direction of the null-space of the Jacobian matrix of the original variable space x_i, and the corresponding step in the mapped variable $1/x_i$ is illustrated in figure 2.3. The Jacobian matrix J is given by

$$J_{ij} = \frac{\partial f_i}{\partial x_j} \tag{2.15}$$

where f as before denotes the system of equations constituted by the variables x.
As illustrated in figure 2.3 we thus wish to find a step such that

$$\frac{1}{x_{new}} = \frac{1}{x_{old}} + \Delta\left(\frac{1}{x}\right) \tag{2.16}$$

Using these symmetric arguments requires that inverse has a continuous first derivative through origo. If not the mapped curve has a break point and symmetric arguments does not apply. The method may also fail in cases where *several* variables become large simultaneously, or the asymptotes are not aligned with the orthogonal coordinate axes of the original variable space. In such cases we wish to define a subspace in which only *one* of the variables is large. Finding such a subspace requires some way of rotating the coordinate axes, an issue that is dealt with in the next section.

Method 2 : Skew Asymptotes One way of finding the desired subspace in case of skew asymptotes is to align one of the coordinate axes in the rotated space with the direction of the asymptote of one variable. In order to use arguments of symmetry as described in the last section we aim to find a subset of coordinate axes which are orthogonal to the direction of the asymptote. A basis for such a rotated variable space

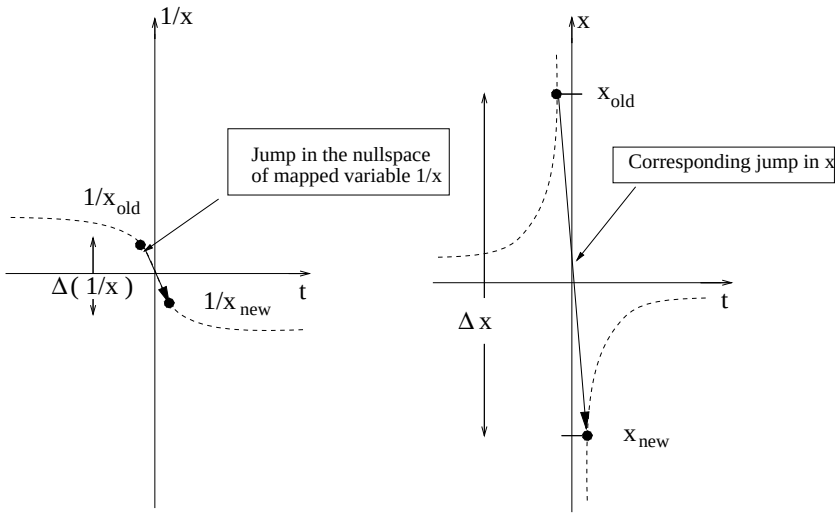

Figure 2.3: Schematic demonstrating branch–jumping across asymptotes using simple variable transformation and symmetry

is formed by a matrix, say T, whose column space is spanned by the bases for the left null-space $\mathcal{N}(J^T)$ and the column space $\mathcal{R}(J)$ of the Jacobian matrix J defined by equation (2.15). From linear algebra we know that for a n–dimensional vector $x \in \mathcal{R}^m$, this matrix T spans the whole of $\mathcal{R}^m$. If we denote the new variables by the vector ζ, we have that

$$x = T\zeta \tag{2.17}$$

thus x is in the column space of T (linear combination of the columns). We then wish to find the direction of the jump in the rotated variable space, $\Delta\zeta$, which we previously defined to be in the direction of null–space, $\mathcal{N}(\zeta)$. Hence we have

$$J\Delta x = JT\Delta\zeta = 0 \tag{2.18}$$

where the matrix product JT defines the Jacobian of the rotated function space, $f(\zeta(\lambda), \zeta)$. We wish to make a small step in $1/\zeta$ in the direction of the null space and thus follow the same steps as demonstrated for *Method 1* to eventually obtain $\Delta x = T\Delta\zeta$. We have applied this method to some simple example problems, and it occurs that there still are some difficulties that arise in situations where several variables display asymptotic behavior simultaneously. In order to make a jump one needs to make certain assumptions with respect to where the branches connect. For the simplest case of linear asymptotes we may use arguments based on symmetry in the prediction of new values for the variables. However when the asymptotes are non–linear, symmetrical considerations are not at all that obvious. Finding robust solution methods that deal with such situations represents a challenge that should be dealt with in future works. In the next section we outline the features of the alternative *tear and grid approach*.

2.4 Methods Exploiting Algebraic Structure

The approach proposed here is a method which uses information of algebraic structure to decompose the system of NAE's into smaller subproblems, called partitions. The irreducible partitions obtained in the first sequence may be decomposed even further by guessing some of the variables occurring in the subset, a method known as tearing. In this work the tear variables are found by inspection, but in the general case the directed graph is not very helpful and an algorithm is required to obtain the optimal set of tear variables. When finding initial solutions to $f(x) = 0$ each subset includes an equal number of equations and variables, hence tearing leaves one residual for each tear variable. If possible one should choose the number of tear variables so that the system of NAE's may be reduced to a sequence of single–variable equations by simple algebraic manipulations. If such an explicit solution scheme is obtained, costly iterations are avoided. However, conventional tearing methods still involve some iterative scheme since the residuals must be adjusted until the desired solution is found. The procedure proposed here suggests instead to use a grid of the tear variables and calculate the residuals for each point in the grid. Solutions may then be obtained either by visual inspection of the solution surfaces or by numerical interpolation between the points in the grid, depending on the accuracy required. The method is also well suited for exploring solutions in the parameter space. Bifurcation diagrams are easily obtained by using the bifurcation parameters as the grid variables. In the next section we illustrate in terms of a simple example how the method may be used.

2.4.1 Conventional Design of Decomposition Methods

Decomposition methods aim at finding smaller subsets, or partitions, of the system of NAE's that are easy to solve. Partitioning involves the assignment of which *output* variables to be solved by each of the equations. This choice is not arbitrary since a partition of a system is unique (see e.g. Sargent (1981)). Precedence ordering on the other hand involves finding the order in which the equations are to be solved. These ideas can be illustrated by the following simple example. We display the occurrence (incidence) matrix where each row corresponds to an equation f_i and each column to a variable x_i. Entries denoted by 1's in row i and column j thus indicate that variable x_j appears explicitly in equation f_i.

$$\begin{array}{c|ccccc} & x_1 & x_2 & x_3 & x_4 & x_5 \\ f_1 & 1 & & & 1 & 1 \\ f_2 & 1 & 1 & 1 & & 1 \\ f_3 & 1 & 1 & 1 & & \\ f_4 & 1 & 1 & & 1 & \\ f_5 & & & 1 & 1 & 1 \end{array} \tag{2.19}$$

As suggested by Westerberg *et al.* (1979) the best way to obtain the partitioning and precedence ordering is probably to use a *directed graph* where an arrow pointing from node f_i to f_j if and only if the assigned output variable for f_i appears in f_j. By assigning each variable x_i to the corresponding equation f_i, we obtain the directed

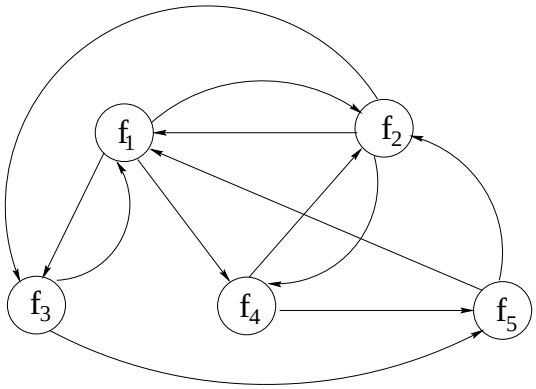

Figure 2.4: Directed graph for example (2.19)

graph shown in figure 2.4. By making an appropriate choice of *tear variables* we may then find a completely decomposed partition. By inspection of the directed graph in figure 2.4 one finds that if x_1 and x_2 are assigned as tear–variables, leaving f_1 and f_2 for calculation of the residuals, x_3, x_4 and x_5 may be calculated sequentially from equations f_3–f_5. Depending on the form of equations f_3–f_5 one may in some cases compute x_3, x_4 and x_5 explicitly, but in the general case iterative schemes must be used. Figure 2.5 shows the directed graph that results after choosing the tear variables, i.e. deleting objects 1 and 2 and the corresponding arrows in figure 2.4. A

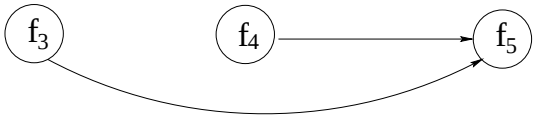

Figure 2.5: Reduced graph obtained by tearing

conventional solution procedure based on this proposed scheme typically involves the following steps

(1) Guess values for x_1 and x_2 (*tearing*)

(2) Calculate x_3 and x_4 directly from f_3 and f_4

(3) Calculate x_5 from f_5 using x_3 and x_4 from step (2)

(4) Calculate the residuals from equations f_1 and f_2

(5) Iterate until sufficient accuracy is obtained for the residuals

As conventional tearing commonly yields an iterative scheme, we show in the next section that by choosing a proper set of tear variables and making a grid of these, iterations *may* be avoided. Note however that the solution scheme depends strongly on the form of the equations, and that explicit schemes arise only in particular cases.

2.4.2 Tear and Grid Method

We may now outline the features of the tear and grid method. The first steps follows th standard methods outlined in the previous section, i.e. partitioning, precedence ordering and tearing. One should note that finding *all* solutions requires that the non–teared functions yield unique solutions. For this purpose it is sufficient to find a linear subset of equations. The principles of the method are conveniently described by considering the system (2.19) discussed in the last section, since solutions may be visualized in 3 dimensional plots.

Finding initial solutions. After assigning the tear variables we find the appropriate partitioning and precedence ordering which yield a completely decomposed subset. We then make a grid of the chosen tear variables, in this case x_1 and x_2 which yields two residuals Res_1 and Res_2. We then calculate x_3–x_5 from equations f_3–f_5. A very important issue is then that of making sure that unique solutions are found for the variables. In the general case one should test the equations for uniqueness since uniqueness is *not* a general feature of nonlinear equations. Then we obtain the residuals for the two teared functions f_1 and f_2 for each point in the grid. We thus obtain a solution *surface* for Res_1 and $Res2$ respectively, when displayed as functions of the tear variables. Since we require that both residuals must be zero, the solutions are then found in a plane denoted the *0 contour*, where $Res_1(x_1, x_2)$ and $Res_2(x_1, x_2)$ are zero. Finally we locate the solutions at the intersections of the residual surfaces and the *0 contour*. We illustrate by some example problems given in the next section that solution surfaces are quite conveniently visualized. We also apply the homotopy–continuation method, and eventually we give an evaluation of the two methods according to measures such as computational efficiency, implementation effort and graphical visualization.

Coarseness of grid. In order to find either an initial solution or solutions in parameter space one needs to specify the number of points in the grid. Depending on the accuracy required for the solutions, the coarseness of the grid may be chosen for convenience. One may for instance apply the grid method to obtain an initial *screening* of the solution surface in order to find in which regions solutions may be found. By reducing the domain of the grid variables step by step and thereby narrowing in the solutions, one may reduce the computation time considerably compared to making a fine grid of the *whole* solution space. This is of special importance when little information exist about the process, i.e. in the design of new processes.

Interpolation methods An important issue when displaying the solution surfaces obtained from the grid method, is the accuracy provided by the numerical interpo-

lation routines. The solutions found by inspection are usually approximate, and if higher accuracy is required one should either resort to interpolation between neighboring points or use the grid points as initial guesses for some Newton–based method. Most available algorithms for interpolation use some polynomial approximation, i.e. Lagrange polynomial or inverse interpolation. The interpolation polynomial aims to connect the computed data points by selecting a polynomial of appropriate order depending on the number of grid points. Potential problems with this approach are that one may fail to find some solutions if the grid is too coarse, or one may also introduce additional solutions due to over-fitting. For some of the examples we found that transformation of some variables may be required prior to computing the solution surfaces.

2.5 Numerical Results

We present in this section numerical results obtained with the proposed methods for three example problems representing simplified models of physical processes, i.e. (1) two CTSR's in series; (2) a coupled cell reaction and (3) a reactive distillation process. The example problems are chosen partly because they conveniently demonstrate problems related to complex behavior of the homotopy path. For the CSTR's we show that convergence problems arise if several variables become unbounded simultaneously, since it is difficult to obtain a suitable direction for the branch jump. For the coupled cell example we illustrate that isolas may occur along the homotopy path, thus preventing successful tracking. The final reactive distillation example is motivated also by the desire to find out whether multiple solutions exist for simple one stage columns. For all examples we show that multiple solutions are easily obtained without difficulties by applying the *tear and grid method.*

Example 1 : Two CSTR's in series

We here consider a model of two CSTR's in series (see e.g. Kubiček and Marek (1983) or Seydel (1988) for details regarding the model). The steady state model is comprised by a system of *four* coupled non–linear equations

$$(1-\Lambda)\,x_2 + Da_1\,(1-x_1)\,exp\left(\frac{\theta_1}{1+\theta_1/\gamma}\right) = 0 \quad (2.20)$$

$$(1-\Lambda)\,\theta_2 - \theta_1 + Da_1 B\,(1-x_1)\,exp\left(\frac{\theta_1}{1+\theta_1/\gamma}\right) - \beta_1\,(\theta_1-\theta_{c1}) = 0 \quad (2.21)$$

$$x_1 - x_2 + Da_2\,(1-x_2)\,exp\left(\frac{\theta_2}{1+\theta_2/\gamma}\right) = 0 \quad (2.22)$$

$$\theta_1 - \theta_2 + Da_2 B\,(1-x_2)\,exp\left(\frac{\theta_2}{1+\theta_2/\gamma}\right) - \beta_2\,(\theta_2-\theta_{c2}) = 0 \quad (2.23)$$

Homotopy–continuation. We applied both fixed point and Newton homotopies in order to find a solution with the parameter values fixed as given in figure 2.6 (a) and (b). As demonstrated in figure 2.6 the homotopy function displays rather complex behavior, and great problems was experienced in the correction step due to

difficulties in finding a proper direction of the *branch jump*. Numerical instability, in the sense of unstable oscillations in the correction step, was encountered due to the Jacobian matrix becoming close to singular in the vicinity of the asymptotic points. This example illustrates one of the problems often encountered when using *branch–jumping* techniques based on arguments of symmetry, namely that a suitable upper limit on the size (norm) of x needs to be chosen *a priori* for when the jump is to be taken. If the specified upper bound is chosen such that the direction of the null–space vector for the mapped variable, evaluated at $1/x$, does not pass through or rather closely to $-1/x_i$, convergence problems in the corrector step are to be expected. Convergence properties thus relies heavily on the *inverse* being sufficiently close to zero. If not, it becomes difficult to predict at which point the branches connect beyond the asymptote. For the example considered here it may be preferable to apply either *bounded homotopies* as suggested by Paloschi (1995) or allowing continuation in the complex domain (Seader *et al.* 1990). However, there are no proofs that guarantee convergence for either of these methods. Using complex arithmetics also increases the size of the problem, hence computational issues are in general unfavorable for such methods.

Other forms of complex behavior may also occur that may prevent successful tracking. Situations where the homotopy path extends towards large values for some value of x or t and returns without displaying asymptotic behavior, or situations where the asymptotes are non–linear are examples of such behavior for which no rigorous methods appear to exist. For the specific problem at hand, the homotopy path was eventually tracked by applying continuation up to a point in the vicinity of the second (vertical) asymptote. The remaining solution branches was then found by discretizing the homotopy function in t and solving the system of equations by a Newton–method.

Tear and grid approach. Although the homotopy–continuation algorithm exhibited poor convergence properties, initial solutions were quite easily obtained by the grid approach. We consider the example corresponding to the parameter values given in Figure 2.6 (a). In Figure 2.7 (a) and (b) we give the residual–surfaces Res_1 and Res_2 respectively displayed as functions of the tear variables. The initial solution for θ_1 and θ_2 are finally located by the intersection of the residuals in the 0–contour as shown in Figure (d). We see that the solutions correspond to what was found using the homotopy–continuation method, but in this case solutions were obtained with considerably less effort. In the next example we illustrate that the homotopy functions may display isolas along the homotopy path, thus introducing additional difficulties with respect to branch jumping.

Example 2 : Coupled Cell Reaction

Consider the following system describing a model of a trimolecular reaction (see Seydel (1988) for details concerning the model)

$$\begin{aligned} 2 - 7x_1 + x_1^2 x_2 + \lambda(x_3 - x_1) &= 0 \\ 6x_1 - x_1^2 x_2 + 10\lambda(x_4 - x_2) &= 0 \\ 2 - 7x_3 + x_3^2 x_4 + \lambda(x_1 + x_5 - 2x_3) &= 0 \\ 6x_3 - x_3^2 x_4 + 10\lambda(x_2 + x_6 - 2x_4) &= 0 \end{aligned} \tag{2.24}$$

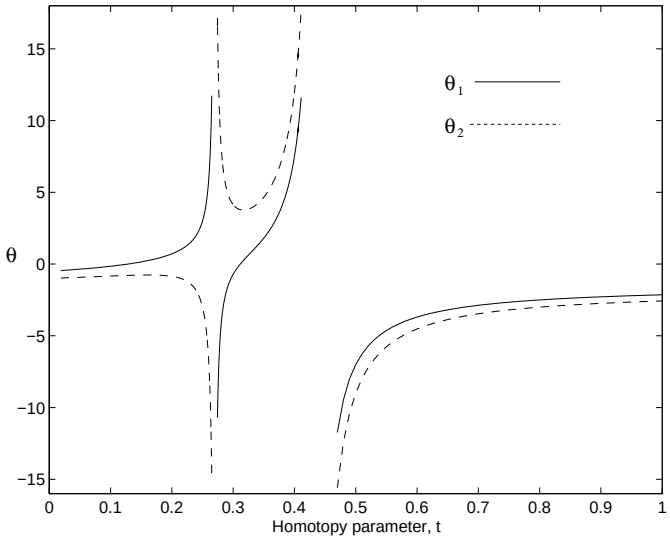

(a) $\lambda = .5,\ \beta_1 = \beta_2 = 1,\ B = 22,\ \gamma = 1000,\ \theta_{c1} = \theta_{c2} = -3,\ Da_1 = Da_2 = 0.5$

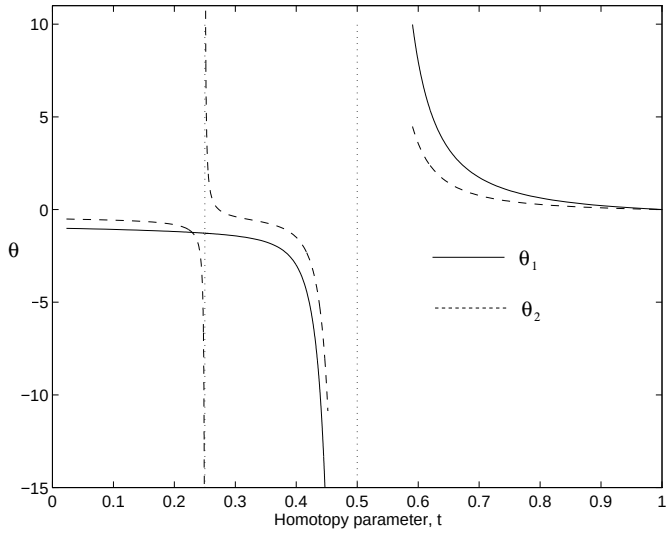

(b) $\lambda = .5,\ \beta_1 = \beta_2 = 1,\ B = 15,\ \gamma = 1000,\ \theta_{c1} = \theta_{c2} = -3,\ Da_1 = Da_2 = 0.5$

Figure 2.6: Fixed point homotopy paths for example of two CSTR's in series

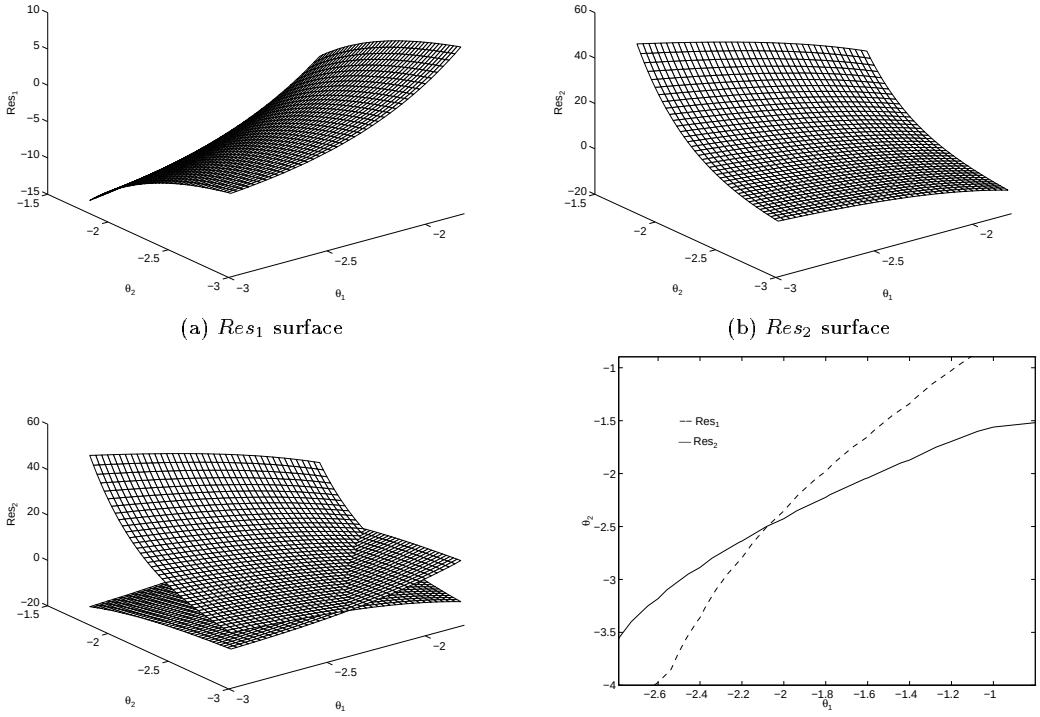

(a) Res_1 surface

(b) Res_2 surface

(c) Intersection of residual surfaces

(d) 0 contour

Figure 2.7: Visualization of solutions to $f(x) = 0$ for CSTR example

$$2 - 7x_5 + x_5^2 x_6 + \lambda(x_3 - x_5) = 0$$
$$6x_5 - x_5^2 x_6 + 10\lambda(x_4 - x_6) = 0$$

where the coupling coefficient λ is chosen as the branching parameter.

Homotopy–continuation. We applied a fixed point homotopy function to the model and found (incidentally) that isolated solution branches appear along the homotopy path. Isolas were obtained for a wide selection of starting guesses, and in each case prevented successful tracking of the homotopy path. In order to escape from the closed solution manifold (isola), we would have to keep track of previous solutions and then use some criteria to enable a jump in the parameter space. However, there are at present date no rigorous way of predicting where the branches connect beyond the isolas. For some homotopies it is however possible to guarantee that isolated solutions will not arise (Paloschi 1995), but this is not an issue dealt with in this work. We should note that the isolated solution branches were obtained after a branch jump was imposed, due to some variable(s) displaying asymptotic behavior. In this case we assigned an upper limit of $x_i(t) = 20$ for the variables, so that when this bound is exceeded a branch jump is to take place. Note also that the problem is multidimensional ($x \in \mathcal{R}^6$), and the curves in Figure 2.8 are thus projected onto the 2-dimensional (t, x_i) space.

Tear and Grid approach. From the occurrence matrix displayed in (2.25) we find that an explicit solution scheme is obtained by choosing for example x_1 and x_2 as tear variables. We note that other sets of tear variables also yield explicit schemes. Deleting the rows for x_1 and x_2 yields the assignment of output variables as indicated by encircled occurrences in (2.26), which leaves f_5 and f_6 for calculation of the residuals.

	x_1	x_2	x_3	x_4	x_5	x_6
f_1	1	1	1			
f_2	1	1		1		
f_3	1		1	1	1	
f_4		1	1	1		1
f_5			1		1	1
f_6				1	1	1

(2.25)

	x_3	x_4	x_5	x_6
f_1	①			
f_2		①		
f_3	1	1	①	
f_4	1	1		①
f_5	1		1	1
f_6		1	1	1

(2.26)

Unique solutions are guaranteed since the assigned variables appear as linear terms in the unteared functions. The residual surfaces and solutions are displayed in figure 2.9, and as shown in d) there are in fact 6 solutions denoted (I)–(VI) for x_1 and x_2 within the prescribed grid for $\lambda = 1.3$. Our results are in excellent agreement with

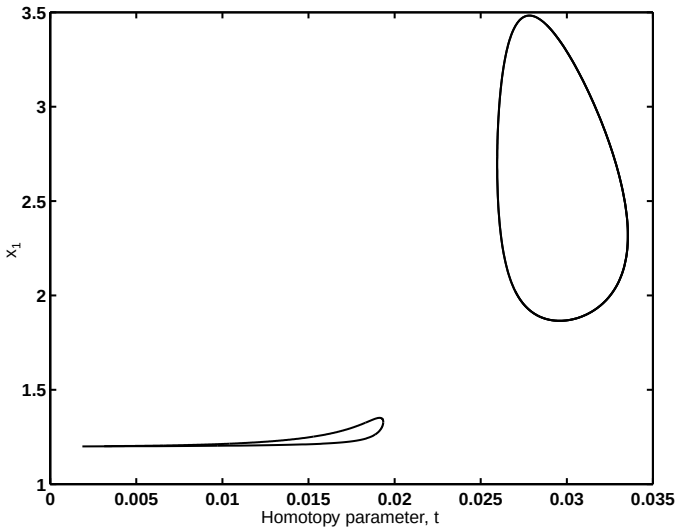

(a) x_1 as a function of t

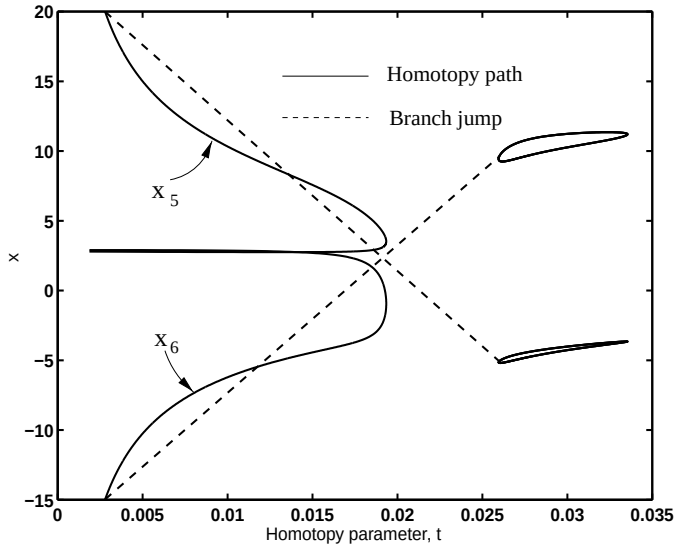

(b) Branch jumps

Figure 2.8: Occurrence of isolas along the homotopy path for coupled cell reaction example. Figure (b) illustrates branch jumps due to asymptotic behavior for variables x_5 and x_6.

results given by Seydel (1988), who applied continuation to explore solutions for a range of λ–values.

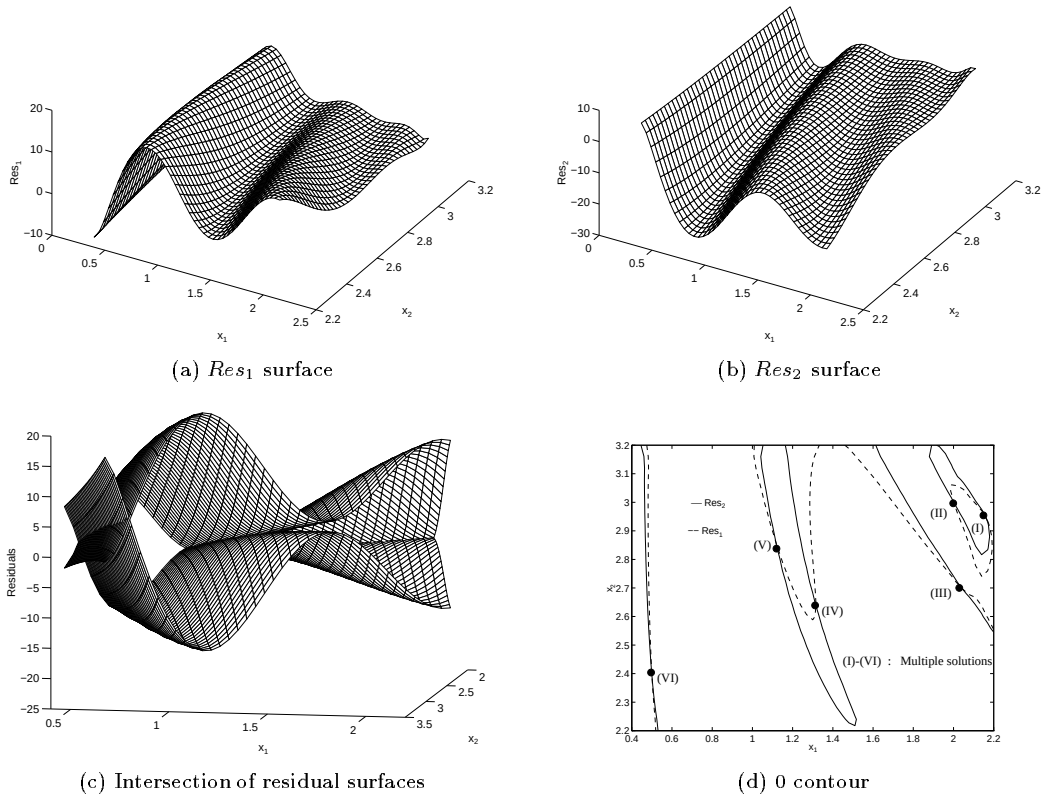

(a) Res_1 surface

(b) Res_2 surface

(c) Intersection of residual surfaces

(d) 0 contour

Figure 2.9: Visualization of solutions to $f(x) = 0$ for coupled cell reaction example

Example 3 : One Stage Reactive Distillation Column
Consider the following model for a one tray reactive distillation column of a ternary mixture, where the following reversible second order reaction occurs.

$$2C \quad \Leftrightarrow \quad A + B$$

The following common assumptions are made for the model

- Ideal trays
- Constant molar flows
- Total condenser
- Negligible heat of reaction

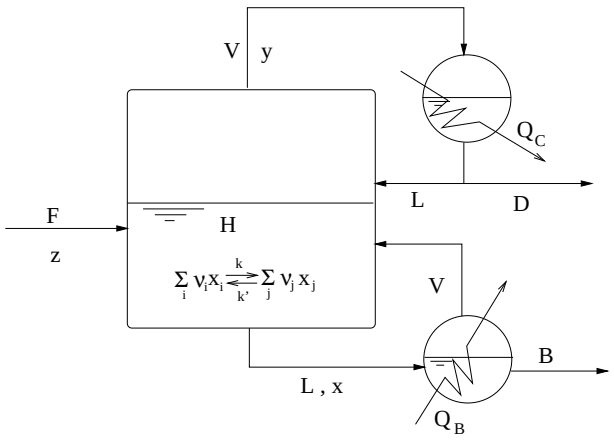

Figure 2.10: Schematic of one stage reactive distillation column

A schematic of the column is given in figure 2.10

Steady State Model. Using the notation given in figure 2.10 we obtain the following steady state model

$$Fz_A - (V-L)y_A - (F+L-V)x_A + \nu_A r_A = 0 \quad (2.27)$$

$$Fz_B - (V-L)y_B - (F+L-V)x_B + \nu_B r_B = 0 \quad (2.28)$$

$$y_A - \frac{\alpha_1 x_A}{(\alpha_1-1)x_A + (\alpha_2-1)x_B + 1} = 0 \quad (2.29)$$

$$y_B - \frac{\alpha_2 x_B}{(\alpha_1-1)x_A + (\alpha_2-1)x_B + 1} = 0 \quad (2.30)$$

$$L\left((M_A - M_C)y_A + (M_B - M_C)y_B + M_C\right) - L_w = 0 \quad (2.31)$$

The reaction rate for a second order reaction is typically given as

$$r_A = r_B = -\frac{r_C}{2} = k_f H\left(x_C^2 - \frac{x_A x_B}{K}\right) \quad (2.32)$$

where k_f is the reaction rate constant, H is the tray holdup and K is the equilibrium constant respectively. One should note that the model represented by equations (1)–(5) has been somewhat simplified by substituting for the total material balance $F = D+B$, the distillate split $V = D+L$ and the sum of mole fractions $\sum_j x_j = \sum_j y_j = 1$. We further stress that we have not made the common assumption of molar inputs, and thus consider a column where the reflux L_w is given on a *mass* rate basis, i.e. $[kg/min]$. When specifying the feed conditions and the *mass* reflux (L_w) the reduced system of equations thus exist of 5 variables (x_A, x_B, y_A, y_B and L) and 5 (non–linear) functions, $f(x) = 0$. Process data for the reactive distillation example is given in table 1. We introduce the dimensionless Damkohler number, $Da = k_f H/F$, by dividing equations (29) and (30) with the feed ratio F A point of interest, besides using the example to validate the numerical methods, is to examine whether multiple steady

Table 2.1: Process data for nominal case of reactive distillation column

Relative volatility :	$\alpha_1 = 10$
Relative volatility:	$\alpha_2 = 1/3$
Damkohler number:	$Da = 5$
Molar boilup :	$V = 5.5\ [kmol/min]$
Mass reflux :	$L_w = 440\ [kg/min]$
Feed flow :	$F = 1.0\ [kmol/min]$
Equilibrium Constant :	$K = 0.5$
Column holdup :	$H = 1.0\ [kmol]$
Molar weight of light component :	$M_A = 78\ [kg/kmol]$
Molar weight of intermediate component :	$M_B = 116\ [kg/kmol]$
Molar weight of heavy component :	$M_C = 97\ [kg/kmol]$
Feed composition :	$z_A = 1/3$
Feed composition :	$z_B = 1/3$

states exist for the simple example model. The example is motivated by a work on multiplicities in ideal binary ordinary distillation columns by Jacobsen and Skogestad (1991).

Homotopy–continuation method. In figure 2.11 (a) we show the homotopy path obtained from *one* run of the homotopy–continuation algorithm for the nominal case given in Table 2.1. The Figure demonstrates that *multiple steady state solutions* are displayed by the model of the reactive distillation column. The steady state solutions denoted (I)–(IV) are found as solutions for a value of the homotopy parameter $t = 1$. We used a Newton–like homotopy $H(x,t) = tf(x) + (1-t)\,g(x)$, where we chose for $g(x)$ a model of the corresponding *non–reactive* distillation column. The solution to $g(x) = 0$ is quite easily obtained by a simple Newton Raphson method. Figure 2.11 (a) also demonstrates that the solution branches becomes unbounded for some values of t. The branch–jumping is obtained by applying the inverse mapping function described as method 1. When an initial solution is obtained from the homotopy continuation scheme, we may apply continuation in some other parameter to explore the solution space as for example the mass reflux is varied. The bifurcation diagram of L vs. L_w is shown in figure 2.11 (b), and demonstrates that multiple solutions exist for some interval of L_w. The cause of multiplicity is due to a singularity in the input transformation between molar (L) and mass reflux (L_w), which has previously been shown for ordinary distillation columns by Jacobsen and Skogestad (1991). Note that solution (IV) obtained from the homotopy continuation corresponds to a non–physical solution, since the mole fractions become larger than one. We were however not able to obtain this solution from continuation in L_w, which suggests that the branching diagrams for the variables as a function of L_w is not continuous through the solutions (I)–(IV).

Grid–approach. Note in the following that we have plotted the surfaces for $Res_1 + Res_2$ and $Res_1 - Res_2$, since the surfaces for Res_1 and Res_2 were hard to distinguish

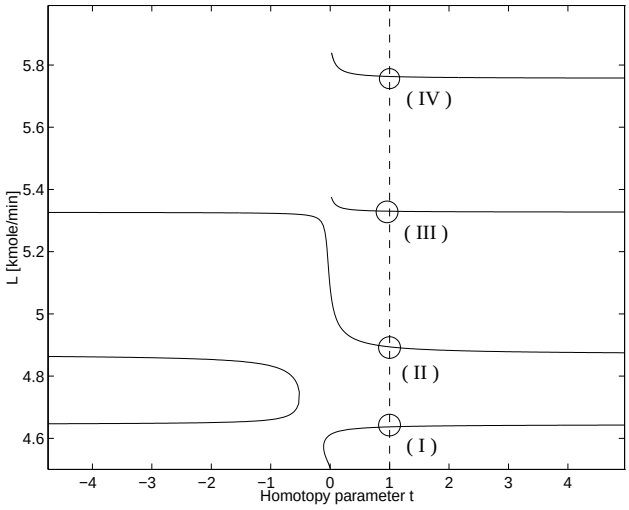

(a) Homotopy path for L

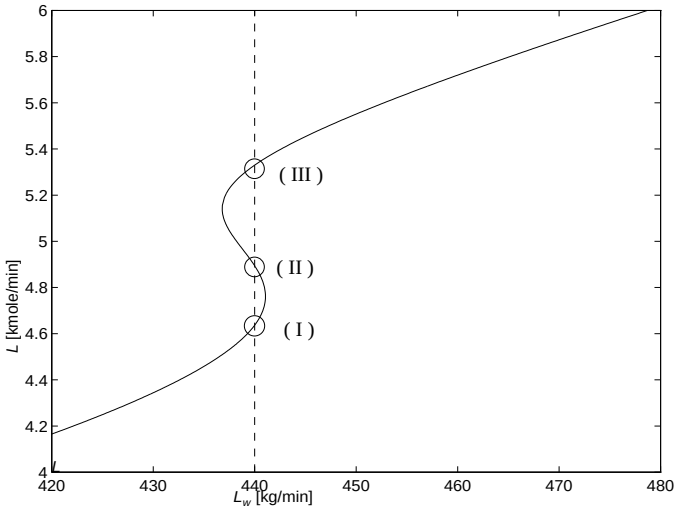

(b) Bifurcation diagram for L vs. L_w

Figure 2.11: Homotopy path illustrating multiple solutions for L (a), and bifurcation diagram displaying L versus L_w (b) for reactive distillation example

by visual inspection. In figure 2.12 we illustrate the shape of the residual–surfaces and show that the model display multiple solutions for the given value of L_w.

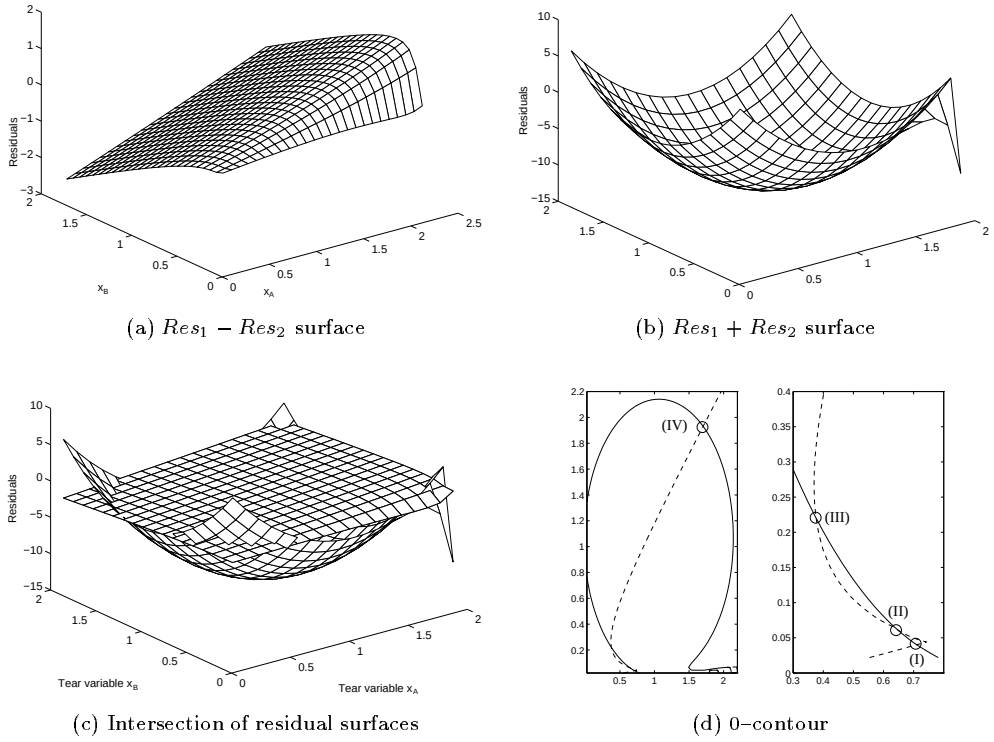

(a) $Res_1 - Res_2$ surface

(b) $Res_1 + Res_2$ surface

(c) Intersection of residual surfaces

(d) 0–contour

Figure 2.12: Visualization of steady state solutions for reactive distillation example

2.6 Discussion and Conclusions

In this paper we have addressed two alternative numerical methods for solving systems of nonlinear algebraic equations (NAE's). We first considered a homotopy continuation scheme, which usually requires substantial effort in terms of both implementation (code) and computing time. However, for a small class of example problems, all solutions were successfully obtained using a globally convergent fixed point or Newton homotopy. The only exception was an example of a coupled cell reaction, where isolated solution branches occurred along the homotopy path. We also discussed other situations under which the homotopy-continuation method may fail, due to potential unboundedness of the homotopy path. To resolve problems arising when variables extend to infinity, we applied two simple *branch jumping* techniques. By using a simple *inverse mapping* functions we show how search directions for a predictor–corrector

scheme may be found by utilizing theory from linear algebra and arguments of symmetry. However, in all cases, also when the homotopy continuation method failed, we showed that a novel *tear and grid* method found all solutions.

The *tear and grid method* possesses some appealing properties compared to other methods proposed in the literature. Among these features we first emphasize that such methods are straightforward to implement in a high level language such as Matlab The Mathworks (1995). However, the perhaps most appealing feature is the convenient visualization of solution surfaces, which applies to finding initial solutions as well as exploring solution in the parameter space. Among the drawbacks we recognize that the method may become infeasible for large problems, due to increasing *computational complexity*. For large systems, where a large number of tear variables is required, the computational effort may thus become excessive. Typically one finds that the computation time increases exponentially with the size of the problems to be solved. This is the same situation as for global optimization problems, where so called NP–hard problems are often encountered.

Thus, one may argue that the method in general is suitable only for relatively small problems. However, it is also important to recognize that problems such as the conceptual design of distillation processes, commonly yields *sparse* systems of equations. Since the number of tear variables for such problems may not be very large, we argue that the method is still useful for a large number of practical problems. Furthermore, in process analysis one is frequently set to analyze simplified models of the more complex chemical engineering plant, in order to obtain important information regarding process behavior. The proof of multiple steady states in ideal binary distillation (Jacobsen and Skogestad 1991), explanation of *holes* in some operating regions for integrated distillation columns (Morud 1995) or exhaustive analysis of dynamic behavior displayed by CSTR's (e.g. van Heerden (1953) and Uppal *et al.* (1974)) are all examples of important discoveries obtained from analysis of simplified problems. For somewhat large problems one may also consider using *partial* tearing. Even though iterations are required in this case in the solution of smaller subproblems, considerable savings may result since simultaneous solution of the whole problem is avoided. Furthermore there are algorithms for choosing a convenient set of tear variables. Finally we stress that depending on the size, complexity and difficulty of the problem at hand, one should in any case consider the grid approach as a worthy candidate for solving systems of NAE's frequently occurring within chemical engineering, along with the spectra of solution methods that already exist.

Nomenclature

Note that we give here only the nomenclature used in the main body of the paper. For the examples we have defined the variables and parameters explicitly.

A – Weighting factor for Affine homotopy
J – Jacobian matrix
f_i – Equation number i
H – Homotopy function

K – Controller in feedback law
T – Basis matrix for rotated variable space
t – Homotopy parameter
$\mathbf{x}$ – Vector of (state) variables
x_i – Variable number i
y – Vector of output variables
z – Augmented vector of variables and parameters
z_i – Mole fraction of component i in feed

Greek letters

Δ – Deviation variable
λ – Vector of parameters
∂ – Derivatives
ζ – Vector of variables in rotated variable space

Subscripts

s – Set-point
new – Solution after branch-jump
old – Solution from which branch-jump is taken

Calligraphic

$\mathcal{N}$ – Basis for nullspace
$\mathcal{R}^m$ – Vector space of dimension m

References

Allgower, E. and K. Georg (1993). Continuation and Path Following. *Acta Numerica* pp. 1–64.

Chang, Y. A. and J. D. Seader (1988). Simulation of Continuous Reactive Distillation by a Homotopy–Continuation Method. *Comp. Chem. Eng.* **12**(12), 1243–1255.

Chavez, C. R., J. D. Seader and T. L. Wayburn (1986). Multiple Steady–State Solutions for Interlinked Separation Systems. *Ind. Eng. Chem* **25**, 566–576.

Christiansen, A. C., S. Skogestad and K. Lien (1997). Partitioned Petlyuk Arrangements for Quaternary Separations. In: *Distillation and Absorption '97* (R. Darton, Ed.). Vol. 2. IChemE. pp. 745–746.

Davidenko, D. (1953). On a New method of Numerically Integrating a System of Nonlinear Equations. *Dokl. Akad. Nauk USSR* **88**, 601.

Doedel, E. J. (n.d.). AUTO: Software for Continuation and Bifurcation Problems in Ordinary Differential Equations. Technical report.

Fidkowski, Z. T., M. F. Malone and M. F. Doherty (1991). Nonideal Multicomponent Distillation : Use of Bifurcation Theory for Design. *AIChE Journal* **37**(12), 1761–1779.

Horst, R. and P. M. Pardalos (1995). *Handbook of Global optimization*. Kluwer Academic.

Jacobsen, E. W. and S. Skogestad (1991). Multiple Steady–States in Ideal Two–Product Distillation. *AIChE Journal* **37**(4), 499.

Kovach, J. W. and W.D. Seider (1987). Heterogenous Azeotropic Distillation – Homotopy–Continuation Methods. *Comp. Chem. Eng.* **11**(6), 593–605.

Kubiček, M. and M. Marek (1983). *Computational Methods in Bifurcation Theory and Dissipative Structures.* Springer Series in Computational Physics. Springer–Verlag New York Inc.

Lin, W. J., J. D. Seader and T. L. Wayburn (1987). Computing Multiple Solutions to Systems of Interlinked Separation Columns. *AIChE Journal* **33**(6), 886–897.

Morud, J. (1995). Studies on the dynamics and operation of integrated plants. PhD thesis. University of Trondheim, The Norwegian Institute of Technology.

Ortega, J. M. and W. C. Rheinboldt (1970). *Iterative Solutions of Nonlinear Equations in Several Variables.* Academic Press. New York.

Paloschi, J. R. (1995). Bounded Homotopies to Solve Systems of Algebraic Nonlinear Equations. *Comp. Chem. Eng.* **19**(12), 1243–1254.

Paloschi, J. R. (1997). Bounded Homotopies to Solve Systems of Sparse Algebraic Nonlinear Equations. *Comp. Chem. Eng.* **21**(5), 531–541.

Sargent, R. W. H. (1981). A Review of Methods for Solving Nonlinear Algebraic Equations. In: *Foundations of Computer-aided Process Design* (R. S. H. Mah and W. D. Seider, Eds.). Engineering Foundation. New York.

Seader, J. D., M. Kuno, W. J. Lin, S. A. Johnson, K. Unsworth and J. Wiskin (1990). Mapped Continuation Methods for Computing All Solutions to General Systems of Nonlinear Equations. *Comp. Chem. Eng.* **14**(1), 71.

Seider, W. D., D. B. Brengel and S. Widago (1991). Nonlinear Analysis in Process Design. *AIChE Journal* **37**(1), 1–37.

Seydel, R. (1988). *From Equilibrium to Chaos, Practical Bifurcation and Stability Analysis.* Elsevier Science Publishing Co., Inc.

Taylor, R., K. Achuthan and A. Lucia (1996). Complex Domain Distillation Calculations. *Comp. Chem. Engng.* **20**(1), 93–111.

The Mathworks, Inc. (1995). *MATLAB Reference Guide.*

Uppal, A., W. H. ray and A. B. Poore (1974). On the Dynamic Behaviour of Continuous Stirred Tank Reactors. *Chem. Eng. Sci.* **29**, 967–985.

van Heerden, C. (1953). Autothermic Processes. *Ind. Eng. Chem.* **45**(6), 1242–1247.

Venkataraman, S. and A. Lucia (1988). Solving Distillation Problems by Newton–like Methods. *Comp. Chem. Eng.* **12**(1), 55–69.

Vickery, D. J. and R. Taylor (1986). Path-following Approaches to the Solution of Multicomponent, Multistage Separation Process Problems. *AIChE Journal.*

Watson, L.T., S. C. Billups and A. P. Morgan (1987). Algorithm 652, HOMPACK : A Suite of Codes for Globally Convergent Homotopy Algorithms. *ACM Trans. Math. Software* **11**, 281.

Wayburn, T. L. and J. Seader (1987). Homotopy Continuation Methods for Computer Aided Process Design. *Comp. Chem. Eng.* **11**, 7–25.

Westerberg, A. W., H. P. Hutcison, R. L. Motard and P. Winter (1979). *Process Flowsheeting.* Cambridge University Press.

Wolf, E. A. (1994). Studies on Control of Integrated Plants. PhD thesis. University of Trondheim, The Norwegian Institute of Technology.

Appendix A Search directions for inverse mapping function

We here show how one may find the step of a desired length in the null–space of the *mapped variable space* which we may denote

$$x' = (x_1, \ldots, \ y, \ldots, \ x_n) \, , \in \mathcal{R}^m \tag{2.33}$$

where y denotes the simple inverse mapping $y = 1/x$ of the variable(s) for which the homotopy path becomes unbounded. The elements in the Jacobian matrix for the mapped variable space may be written

$$J' = \frac{\partial f}{\partial x'} = (f_{x_1} | \ldots | f_y | \ldots | f_{x_n}) \tag{2.34}$$

By partial differentiation of the inverse mapping function we obtain

$$f_y = \frac{\partial f}{\partial x} \cdot \frac{\partial x}{\partial y} = -x_i^2 f_{x_i} \tag{2.35}$$

To avoid introducing the mapped variables explicitly in the system of equations, we simply multiply the column of the original Jacobian by minus the square of x_i, evaluated at the point from which the jump is to be taken. The direction of the jump in the mapped variable space is then

$$n = (n_1, \ldots, n_y, \ldots, n_n) \, , \quad \in \mathcal{N}(\mathcal{J}') \tag{2.36}$$

In cases of vertical or linear asymptotes, we may use arguments of symmetry in order to predict new values of the variables beyond the asymptote. For the inverse mapping function we wish to make a finite jump from $1/x_{old}$ to $1/x_{new}$. Due to symmetry around origo in the mapped variable space we assume that $1/x_{new} = -1/x_{old}$. The desired step $\Delta(1/x)$ must satisfy the condition

$$\frac{1}{x_{new}} = \frac{1}{x_{old}} + \Delta\left(\frac{1}{x}\right) \tag{2.37}$$

Substituting $(1/x_{new})$ by $-(1/x_{old})$ in (2.37) yields the desired step

$$\Delta\left(\frac{1}{x}\right) = -\frac{2}{x_{old}} \tag{2.38}$$

In order to obtain a jump of desired length we normalize the vector spanning the null–space by the scaling

$$n' = -\frac{2}{x_i \cdot n_y} n \tag{2.39}$$

Finally we substitute the n_y element in the null–space vector (2.36) by $-2x_i$, thus mapping the variable space back to the original $x \in \mathcal{R}^m$. Since the curve for the inverse only rarely is *absolutely* symmetrical around origo for the point from which the jump is taken, we need to apply a Newton corrector in order to find a converged solution. Total symmetry is only found for jumps in the vicinity of origo (see figure 2.3, thus we have to make sure that x is sufficiently large before imposing the step. This method therefore works satisfactorily only in cases where the homotopy path is symmetric around the asymptote.

Chapter 3

Numerical Methods for Steady State Analysis. Part II : Exploring Solutions in Parameter Space

Atle C. Christiansen, John Morud and Sigurd Skogestad*

Department of Chemical Engineering
Norwegian University of Science and Technology, NTNU
N–7034 Trondheim Norway

Unpublished

Abstract

This paper considers numerical methods for steady state analysis of underdetermined (non-square) systems of non–linear algebraic equations (NAE's). The focus is thus on methods for exploring solutions in parameter space, i.e. obtaining solutions to the system of NAE's for a range of parameter values. We first address the use of one– and multidimensional continuation methods, after which we demonstrate some features of a novel *tear and grid method*, previously proposed by the authors. The latter method draws its characteristics from conventional techniques of partitioning and precedence ordering, with the addition of using a grid of the desired subset of variables. Both methods may be used to obtain initial solutions as well as finding solutions in the parameter space. Finally we consider a slightly modified gradient projection method embedded in a continuation scheme for optimization purposes. The applicability of the methods is illustrated in terms of a few example problems.

*Author to whom correspondence should be addressed : Fax : +47 7359-4080, E-mail: skoge@chembio.ntnu.no

3.1 Introduction

In the previous chapter we considered numerical methods for finding one or all *initial solutions* to a system of non–linear algebraic equations, which we denote by

$$\begin{array}{l} f(\mathbf{x},\lambda) \;=\; 0 \\ f : \mathcal{R}^m \times \mathcal{R}^k \rightarrow \mathcal{R}^m, \quad \mathbf{x} \in \mathcal{R}^m, \quad \lambda \in \mathcal{R}^k \end{array} \tag{3.1}$$

where $\mathbf{x}$ is a m-dimensional vector of state variables and λ a k-dimensional vector of parameters. By initial we mean solutions of the variables $\mathbf{x}$ for specified values of the parameters λ, In this chapter we extend the analysis to also obtain solutions in the parameter space, i.e. we aim to find solutions for the system variables $\mathbf{x}$ for a range of parameter values λ. Tracing solutions in parameter space is of special importance in order to obtain information of non–linear phenomena. Examining the impact of nonlinearities is essential in process design, where the engineers commonly apply only local methods. An excellent review of methods for nonlinear analysis is given by Seider *et al.* (1991). In a concluding remark the authors argue that the development of new tools for analyzing complex nonlinear behavior *" are enabling engineers to prepare more economical designs that operate closer to or within these regimes"*. Among the different tools that have proven useful are mathematical concepts such as bifurcation analysis (catastrophe theory) and singularity theory. The applications in chemical engineering are widespread, and in particular for analysis of chemical reactor systems where there is an exhaustive literature due to the early theoretical works of van Heerden (1953) and Bilous and Amundson (1955). Although bifurcation analysis also involves the study of complex *dynamic* phenomena such as limit cycles and even chaos, we in this work limit ourselves to steady state behavior.

The results from bifurcation analysis are typically displayed in bifurcation or *branching* diagrams, in which the number (multiplicity) of solutions within the different branches are depicted. In order to compute these diagrams one commonly uses continuation methods, in which the solutions are traced along the path spanned by the bifurcation parameter(s). Excellent books within this area are Golubitsky and Schaeffer (1985) and Seydel (1988), in which the latter is somewhat less rigorous in the use of mathematical proofs and formalism. For computational and numerical issues we also advise the reader to confer the textbook by Kubiček and Marek (1983).

One might pose critical questions as to why there should be a need for additional methods, as there indisputably exist a wide range of methods in the literature. However, the methods discussed in this paper have some apparent advantages. Firstly the methods are easy to implement in a high level programming language such as Matlab (The Mathworks 1995), which is used for all simulations in this work. Another advantage is that the methods ensure that one always stay close to the feasible solutions, so that they are well suited for ill–conditioned problems such as distillation columns, which are studied extensively later in the thesis. The methods furthermore require relatively little "book–keeping", in the sense that we do not distinguish between parameters and (state) variables. We simply use an augmented vector which includes both variables and parameters. This again make the methods easy to implement. Finally, the methods are not intended to solve any pathological problem, but

are rather based on a "cut and try" philosophy. It is easy to check a posteriori if a feasible solution in fact has been obtained. To sum up, we emphasize that the general approach taken in this work is to put emphasis on simplicity rather than rigor; the methods are easily implemented but they are still robust.

As a simple alternative to using continuation methods, we also consider a scheme in which we make a grid of the parameters within the prescribed range. Hence we have at each point a square system, for which any local numerical method may be applied. Such schemes become infeasible if the number of grid variables is large and one needs to solve a large number of equations. However, instead of solving the whole *square* system, one may reduce the computational effort considerably by exploiting the underlying structure of the equations. Initiated by the decomposition strategies in early works of Sargent and Westerberg (1964) and later by Westerberg *et al.* (1979), efficient solution procedures have been proposed which utilizes the *sparsity* of many chemical engineering models. Such methods are now standard features in most available modeling and simulation software, such as SPEEDUP and gPROMS from Imperial College, ASCEND from Carnegie Mellon and ASPEN developed at MIT. A core element within such systems are strategies for exploiting sparsity. In this work we consider a particular algorithm in which tearing and algebraic manipulations are combined with gridding of a subset of the variables. We show that in some cases this approach allows for *explicit* solution schemes, for which the computation time is reduced by orders of magnitude due to elimination of costly iterative schemes.

Outline of paper. In section 2.2 we introduce the reader to the use of *continuation* methods, for which the solution space is traced by path following. We consider two approaches for identifying the search directions in a predictor–corrector scheme, in which both are based on augmenting the vector of variables according to the number of bifurcation parameters. In the first case we use an Euler predictor in the null space of an augmented Jacobian and corrector steps in the row space, whereas we in the second use a secant predictor and *simultaneous solution* of the augmented system using Broyden's method. We also demonstrate in section 2.3 how a certain class of steady state optimization methods may be embedded into a continuation scheme. In section 2.4 we show how one may use the previously proposed tear and grid method to explore solutions in the parameter space. Finally, in section 2.5 we demonstrate the applicability of the proposed methods in terms of a few numerical examples.

3.2 Continuation Methods

In order to keep the following outline simple, we here consider a system with a single parameter λ. Extending this to include several parameters is however straightforward. Given an initial solution to the system of NAE's in (3.1), say (x_0, λ_0), the purpose of *continuation* is to obtain a family of successive solutions, e.g.

$$(x_1, \lambda_1),\ (x_2, \lambda_2), \ldots,\ (x_n, \lambda_n) \tag{3.2}$$

until one reaches a desired target point, say (x_n, λ_n). The *classical* solution method involves discretization of the continuation path, in which a local method (e.g. Newton's method or Broyden) may be applied at each point of discretization. However,

as was suggested by Davidenko (1953), computational efficiency may be greatly improved by reformulating the algebraic system (3.1) to an *initial value problem* (IVP). By differentiating the function with respect to the continuation parameter λ we derive

$$\frac{df(x,\lambda)}{d\lambda} = \frac{\partial f}{\partial x}\frac{dx}{d\lambda} + \frac{\partial f}{\partial \lambda} = 0 \tag{3.3}$$

and by rearranging we obtain

$$\frac{dx}{d\lambda} = -\left(\frac{\partial f}{\partial x}\right)^{-1}\frac{\partial f}{\partial \lambda} \tag{3.4}$$

Given an initial solution, (x_0, λ_0), equation (3.4) constitutes an IVP for $dx/d\lambda$ which may be integrated by any numerical integration scheme. Most continuation methods use some predictor–corrector scheme, typically an Euler predictor and Newton corrector. The solution path is thus obtained by tracking the IVP (3.4) from $\lambda = \lambda_0$ with $x = x_0$ until the desired λ_n.

An important issue in process analysis is to examine nonlinear phenomenon such as steady state multiplicity, for which bifurcation theory provides the mathematical foundation. A *bifurcation point* (x^*, λ^*) is said to occur if the number of solutions to (3.1) changes as the path traverses through (x^*, λ^*). The well known *turning points* and *pitchfork bifurcations* belong to this class. However, from a computational point of view, bifurcation points impose difficulties for path following since the Jacobian $\partial f/\partial x^*$ becomes singular, i.e. the tangent is not defined. To avoid problems in tracking the solution curve at turning points, most methods proposed in the literature introduce the *arc–length* to define search directions along the path.

Search directions in predictor–corrector schemes. To compute the successive solutions, most continuation algorithms apply some predictor–corrector scheme, typically an Euler predictor and Newton corrector. In this work we consider two slightly modified approaches, in which we avoid introducing the arc–length parameter explicitly in the solution scheme. The first method uses simple linear algebra to obtain *orthogonal* search directions in a predictor–corrector scheme. Choosing orthogonal search directions is a means for speeding up the convergence as advocated by Haselgrove (1961). However, for large systems, this approach is computationally expensive due to the generation of large matrices at each continuation point. Using sparse matrix techniques to avoid operations on the full matrices may of course reduce the computational effort. Instead, in order to avoid recomputing matrices at each step, we also consider an alternative method. Here we use a secant predictor as proposed by Seydel (1988), and solve the predictor and corrector steps *simultaneously* as an an augmented system of equations at each continuation point. The augmented system constitutes the original system of NAE's and additional equation resembling the requirement of orthogonal corrector steps. If we then use Broyden's (Broyden 1965) method for this augmented system, we may in fact use only rank one updates of the Jacobian matrix along the continuation path, and recompute only when the estimates are *poor* so that convergence problems are encountered. For the examples we have considered, the advantage of using an updating scheme for the Jacobian matrix offers

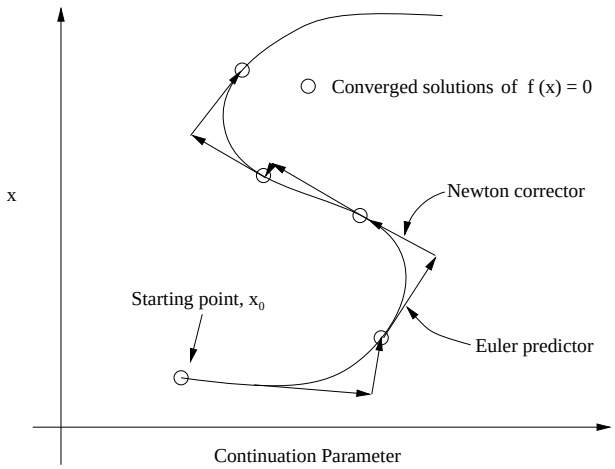

Figure 3.1: Continuation using predictor corrector scheme for solving IVP

reductions in computation time by almost two orders of magnitude compared to the previous scheme.

3.2.1 Solving IVP Using Tangent Predictor

An important element in our algorithm, which distinguishes it somewhat from most other methods found in the literature, is that we directly augment the vector of state variables so that we now operate on the vector $\hat{x} = [\ x \mid \lambda\ ]^T$. We are thus to solve an under-determined system of equations given by

$$f\,(\hat{x}) = 0, \quad \hat{x} \in \mathcal{R}^{m+k} \tag{3.5}$$

Using the augmented $\hat{x}$ allows us to find the search directions for the predictor and corrector step in a simple and straightforward manner. For reasons of simplicity we will in the rest of the presentation treat x also as the augmented vector (slight abuse of notation). A simple solution procedure is to use an Euler predictor and a Newton corrector to trace the family of solutions (3.2) as described in the next sections.

Euler predictor. In figure 3.1 we illustrate how the stepwise procedure is used to find a family of solutions, corresponding to different values of the parameter λ. In the predictor step we start at a known point in the solution space, x_k, and make a finite step in a hyperplane tangential to the curve. For convenience we illustrate this only for the 2-dimensional case. By linearizing the augmented function $f(x)$ around a solution point x_k, for which $f(x_k) = 0$ we get

$$f(x_{k+1}) \approx f(x_k) + \frac{\partial f}{\partial x_k^T}\,(x_{k+1} - x_k) = f(x_k) + J\delta x \tag{3.6}$$

We recognize here the matrix of partial derivatives $J = \partial f/\partial x^T$ as the augmented Jacobian matrix, where the last column is the derivative of f with respect to the con-

tinuation parameter λ. The Jacobian is typically generated numerically using central differences, although analytical derivatives may of course also be used if available. Since the objective is to find the solution for which $f(x_{k+1}) = 0$, so that equation (3.6) reduces to $J\delta x = 0$, we find that the Euler predictor step δx *along* the path will be in the *null space* of the augmented Jacobian, $\mathcal{N}(J)$. The Euler step thus becomes

$$x_{k+1} = x_k + h\delta x \tag{3.7}$$

where h is the step-length in the direction of the nullspace–vector $\delta x \in \mathcal{N}(J)$.

Newton Corrector. In the corrector step we apply a Newton Raphson like scheme in order to iterate towards a converged solution for $f(x_{k+1}) = 0$. By choice we require that the corrector steps should be taken in a direction *orthogonal* to the predictor step. From linear algebra we know that the subspace orthogonal to the null–space is the *row space* $\mathcal{R}(J^T)$. Since we also have that the pseudo–inverse $J^\dagger$ always provides solutions in the row space, we thus iterate in the row space in which $J^\dagger$ is evaluated at the previous solution point x_k. Using mathematical formulation the corrector steps are thus given by

$$x_{k+1}^{n+1} = x_{k+1}^{n} - J^\dagger f\left(x_{k+1}^{n}\right), \quad n = 0, 1, \ldots, \infty \tag{3.8}$$

in which n denotes iteration count. The corrector step is repeated until the error norm is reduced beyond a given tolerance ϵ^{tol}, say until $\|f(x_{k+1}^{n+1})\| \leq \epsilon^{tol}$.

If convergence problems are encountered, which often is the case, there are several measures to be taken in order to increase the accuracy during iteration. A common remedy is to update the Jacobian matrix, using for example a *rank one update* at each new iteration step (see e.g. Westerberg *et al.* (1979)) or if necessary recompute the Jacobian. Another crucial aspect is to use efficient algorithms for step–length control, for which several suggestions have occurred in the literature. In this work we have however used a very simple approach in which we assign a certain upper limit on the number of iterations. If this limit is exceeded we reduce the step–length successively until convergence.

When using the proposed method we have to compute both the Jacobian, the null–space and the pseudo inverse at each step, which becomes computationally expensive for *large* systems. A more efficient scheme is to apply a secant predictor, and solve an augmented system of equations which includes an additional equation for the corrector step, as illustrated in the next section.

3.2.2 Simultaneous Solution Using Secant Predictor

Instead of taking the predictor step in a tangential hyperplane, for which we have to compute the Null space, we may use a secant predictor for which two initial solutions are required. As illustrated in figure 3.2 (a), the direction for the predictor step is simply found by linear extrapolation from two previous solutions, say x_{k-1} and x_k. The predictor step is thus given by

$$x_{pred} = x_k + \underbrace{\frac{x_k - x_{k-1}}{\|x_k - x_{k-1}\|_2}}_{\|\eta\|}\delta \tag{3.9}$$

where for computational reasons we apply a *normalized* secant step of a chosen length δ. If we denote the converged solution by x_{k+1} and require that the corrector step should be taken in a hyperplane *orthogonal* to the predictor step as illustrated in figure 3.2 (b) the following equation applies

$$\eta^T (x_{pred} - x_{k+1}) = 0 \tag{3.10}$$

If we return to the original model description, constituted by variables x and the

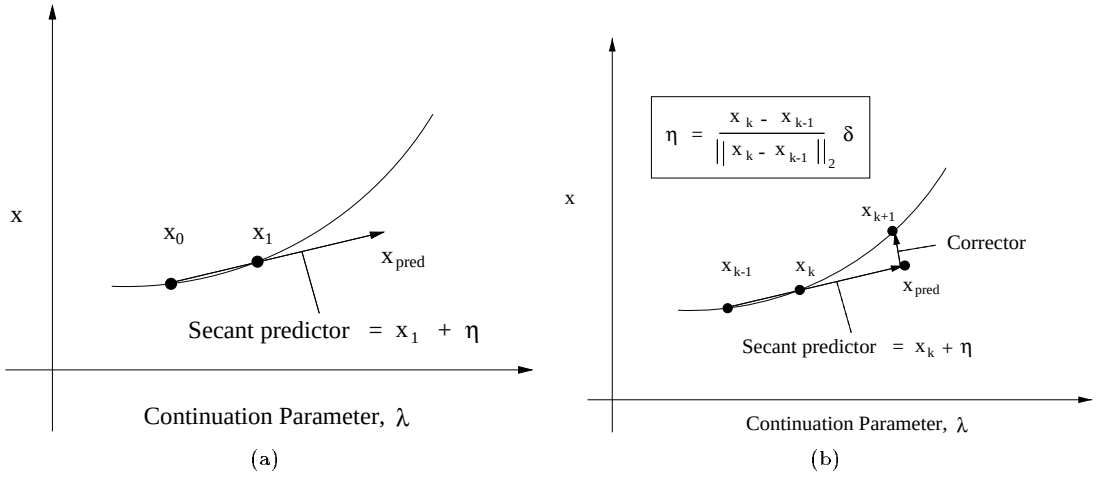

Figure 3.2: Continuation using secant predictor (a) and orthogonal corrector (b)

continuation parameter λ, we note that if we augment the system of equations (3.5) with the equation giving the direction for the corrector step (3.10), we in fact have a *square* system to be solved by any of the previously mentioned methods. However, the perhaps most important feature is that by using a scheme such as Broyden's method, we may use a *rank one update* of the Jacobian instead of recomputing it for each consecutive continuation point. Furthermore, since the proposed method avoids computations of the null and row spaces, the computational effort is reduced considerably. The continuation method thus reduces to that of applying Broyden's method successively to the following system

$$\hat{f}(\hat{x}) \quad = \left\{ \begin{array}{c} f(\hat{x}) \\ \eta^T (\hat{x}_{pred} - \hat{x}) \end{array} \right\} = 0, \quad \hat{x} = [x, \lambda]$$

in which the initial direction is defined according to either increasing or decreasing values of λ.

However, due to potential convergence problems, one needs to provide criteria for when the Jacobian matrix ($J = \partial \hat{f} / \partial \hat{x}$) should be updated. In appendix A we discuss briefly a procedure for updating J based on a Broyden updates and a simple back-tracking algorithm, for which J is recomputed if the norm of $f(x)$ is not

reduced after a certain number of back trackings. We also demonstrate that using Broyden updates may actually degrade numerical performance, compared to omitting the Broyden updates and simply use a constant Jacobian during continuation. However, our experience is that there are few general guidelines regarding the *optimal* approach on how to update the Jacobian during path following.

So far we have only considered continuation in one dimension, but we may in fact do continuation in *any* subset of the parameter space, i.e. hyperspace.

3.2.3 Parametric Continuation in Hyperspace

The method to be described here, is an extension of a method previously described in a work by Morud (1995). We first illustrate the method by considering the simplest case of a system with two degrees of freedom, say λ_1 and λ_2. Our objective is thus to compute all solutions to the system within a prescribed region of λ_1 and λ_2. The solution manifold will thus in this case consist of a two dimensional family of solutions, i.e. a *two–dimensional solution surface*. One way of computing this surface is to consider one *primary* continuation parameter, say λ_1, and one *secondary* parameter.

Since we now consider an under-determined system with two degrees of freedom, we need two additional equations in order to obtain a nonsingular solution. From the previous section we recall that requiring orthogonal search directions for the predictor and corrector step yields one additional specification (equation). The choice of this additional specification is almost arbitrary, but we may for instance choose a certain ratio between the two continuation variables, e.g.

$$\lambda_2 = \lambda_2^0 + \phi \left(\lambda_1 - \lambda_1^0 \right) \tag{3.11}$$

where λ_1^0 and λ_2^0 are initial solutions, and ϕ is the ratio between λ_1 and λ_2. We then repeat the continuation for a set of ϕ, each time starting at the initial solution x_0. We then trace a set of "rays" in the parameter space, and the two-dimensional surface $f(x, \lambda_1, \lambda_2)$ is finally spanned by interpolation between the rays for the desired range of ϕ.

Wee see that this procedure may easily be generalized to continuation in any hyperspace, simply by adding equations for the relation between the primary and the set of secondary continuation parameters. For the simultaneous solution procedure presented in the last section, the task is thus to trace the solution path for the following problem by continuation within a prescribed region of the parameters λ_i

$$\hat{f}(\hat{x}) = \left\{ \begin{array}{c} f(\hat{x}) \\ \eta^T \left(\hat{x}_{pred} - \hat{x_0} \right) \\ \lambda_2 = \lambda_2^0 + \phi_1 \left(\lambda_1 - \lambda_1^0 \right) \\ \vdots \\ \lambda_n = \lambda_n^0 + \phi_{n-1} \left(\lambda_{n-1} - \lambda_{n-1}^0 \right) \end{array} \right\} = 0, \quad \hat{x} = [x \mid \lambda_1 \mid \cdots \mid \lambda_n] \tag{3.12}$$

The ratios ϕ_i may be set arbitrarily, or one may for simplicity use the same value for all additional specifications. At each continuation step we may then use for example Broyden's method to solve the square system of equations in (3.12), which allows

us to use Broyden updates of the Jacobian for successive continuation points. The procedure is then repeated for a set of angles ϕ, giving a solution manifold in the $n-dimensional$ parameter space. Having addressed the use of continuation methods for exploring solutions in parameter space, we demonstrate in the next section how such methods may be embedded in (steady state) optimization schemes.

3.3 Using Continuation Methods for Optimization

The motivation for using continuation methods in steady state optimization, is that one often faces steady state models that are highly non–linear and *ill–conditioned*. In such cases the task of finding even an initial, and possibly sub–optimal solution, may be very difficult. Thus it may be useful to approach the optimum in a step-wise procedure, starting from an initial solution and at each successive point utilize information from the previous solution to define the search directions. The method we discuss here is due to an unpublished work of Morud (1996), and may be considered a special case of the more general class of gradient projection methods (see e.g. Luenberger (1984)). Before discussing the method in detail we comment on two important aspects. Firstly we stress that the method proposed here in general requires a feasible starting point to avoid convergence problems, i.e. a steady state solution of the system of NAE's. Secondly we note that all (intermediate) solutions on the path towards the optimum are feasible, so that the algorithm falls within the class of *primal* methods (e.g Luenberger (1984)). We thus avoid problems of for instance negative mole fractions, which is a common source of numerical failure when using thermodynamics that uses logarithmic functions.

For the steady state optimization problem we thus consider a model at steady state given by a system of NAE's

$$g(x, y, u) = 0 \tag{3.13}$$

where x are the states, y the outputs and u a set of variables which we are free to specify, i.e. control variables (inputs) and system parameters. Our task is now to minimize some objective function Φ with respect to the input variables u. Using mathematical formulation, we thus pose the optimization problem as

$$\min_u \Phi_1(x, y, u) \tag{3.14}$$

subject to the constraints given by the process model (3.13) and set points for the outputs. Since a subset of the manipulated variables are used to control the outputs y, we may reformulate the problem as

$$\min_\lambda \Phi_2(x, y_s, \lambda) \tag{3.15}$$

where y_s are the set points and λ the set of parameters left for optimization purposes.

The rationale behind the proposed method is to project the gradient onto the working surface in order to define the search direction towards the optimum. By recalling the discussion from section 2.2, in which we used search directions in the

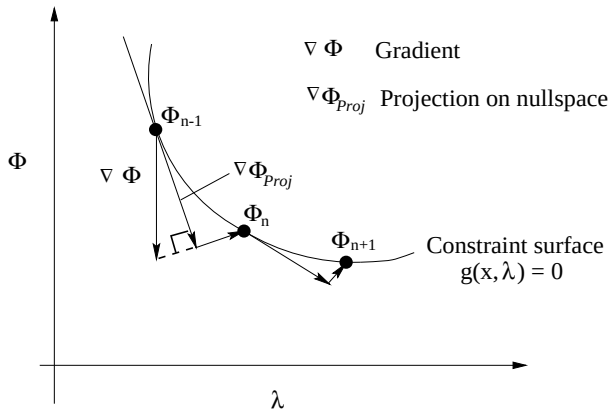

Figure 3.3: Path following in optimization by continuation

null and row space, we see that there is ample scope for using gradient projection methods in a continuation scheme. For ill–conditioned problems, where convergence problems are often encountered, it is profitable to look for search directions, so that movements in this direction impose relatively small changes in $g(x, y, u)$. One such direction is the nullspace of the Jacobian, and we thus seek a projection of the gradient $\nabla\Phi$ onto this subspace. If $\mathcal{N}$ denotes a basis for the nullspace of the Jacobian, we know from linear algebra (Strang 1988) that a least squares approximation to this problem is given by orthogonal projection, which yields

$$\nabla\Phi_{Proj} = \mathcal{N}\left(\mathcal{N}^T\mathcal{N}\right)^{-1}\mathcal{N}^T\nabla\Phi \tag{3.16}$$

An illustration of the proposed scheme is given in figure 3.3. If we furthermore choose an orthonormal basis for $\mathcal{N}$, so that $\mathcal{N}^T\mathcal{N} = I$ the identity matrix, the predictor step is thus given by

$$\nabla\Phi_{Proj} = \epsilon\mathcal{N}\mathcal{N}^T\nabla\Phi \tag{3.17}$$

where ϵ is the step-length. In the corrector step we may simply apply Newton Raphson like iterations in the row space as given previously by (3.8) to obtain a feasible point.

3.3.1 Active Set Approach for Inequality Constraints

We have now presented a procedure which embeds optimization in a continuation scheme, in order to optimize an objective function subject to a steady state model and a set of *equality* constraints. If we also include *inequality* constraints, some modifications must be made in the continuation procedure. The underlying principles of the method used here are similar to the class *active set methods* (see e.g. Luenberger (1984)).

Since we consider only small steps, we may allow ourselves to neglect the inequality constraints in the predictor step. Hence the predictor is taken in the nullspace

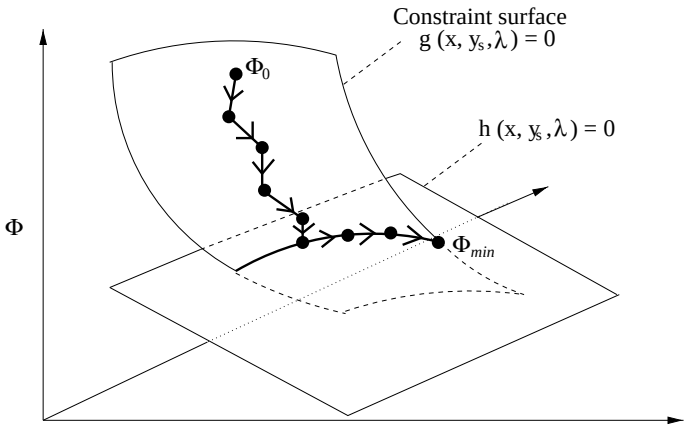

Figure 3.4: Adding constraint by active set approach

of the Jacobian corresponding only to the steady state model $f(x, \lambda)$ (equality constraints). In the corrector steps we then for each iteration check against the *active* set of constraints, so that we may discard any *inactive* constraints and include only the constraints that are active during the iterations. We note that the active set of course always includes the steady state model constituted of mass and heat balances, thermodynamics etc. In figure 3.4 we illustrate the details of the method by displaying a continuation path towards an optimum. For the first few steps we see that the inequalities are inactive, thus we need only consider the constraints represented by the steady state model $g(x, y_s, \lambda)$ when computing the search directions. However, as the first predictor step takes the solution outside the feasible region, the inequality constraint(s) $h(x, y_s, \lambda)$ becomes active and the feasible solution is recovered in the corrector step. The path to the optimum is then traversed along the intersection of the constrained surfaces.

In the next section we return to the issue of exploring solutions in parameter space using a *tear and grid approach*.

3.4 Exploit Structure Using Tear and Grid Method

In the previous chapter we outlined the general features of the *tear and grid method*, which was used to obtain initial solutions for a system of NAE's. We now extend the scope for using this method, and demonstrate that it may also prove useful for exploring solutions in parameter space. Thus, if the system of equations is *non square*, one needs to specify either a parameter or a variable for each degree of freedom (DOF) in order to provide nonsingular initial solutions. However, using the grid approach one may instead make a grid in the parameters or a convenient subset of the variables, and solve the *square* set of equations at each grid point. Hence by assigning "tear" (grid) variables corresponding to the number of DOF's, one may solve an under-determined set of equations to obtain (all) solutions in the parameter space.

By making a proper choice of grid variables and appropriate algebraic manipulations of the model equations, one may in some cases derive *explicit* solution schemes. This in case eliminates the need for time consuming iterative calculations, which typically involves *Newton-Raphson* like schemes. However, one central issue regarding explicit solution schemes needs some elaboration. If we want to obtain *all* solutions for the chosen set of grid variables, it is *sufficient* that the remaining system of equations yield *unique* solutions for the non–teared variables. One situation for which this condition is satisfied, is the special case where the non-teared functions yield a *linear* subset. However, non–uniqueness often occurs if we consider for example strongly coupled or highly nonlinear systems, where complex behavior such as *steady state multiplicity* or *isolas* is often encountered. We emphasize that the tear and grid method may be used for any number of tear variables, although it is difficult to visualize the solutions when more than two tear variables are needed. It is however still possible to locate the solutions (numerically) by interpolation.

The rationale behind the method was described in the previous chapter. The basic features are thus standard methods such as partitioning, precedence ordering and tearing. The details of the method are conveniently described by considering the example of a reactive distillation column, introduced in the previous chapter. The motivation for choosing this example is twofold. Firstly we find that the system may be completely decomposed, which allows for *explicit* solutions of the remaining equations. Secondly, we have that solution surfaces may be conveniently visualized in 3 dimensional plots since there are only two DOF's.

The detailed model is given in the section for numerical results, and consists of 7 variables in 5 equations, which we for simplicity denote by x_1–x_7 and f_1–f_5. We may display the occurrence (incidence) matrix to expose the underlying structure of the equations, . Each row in the matrix corresponds to an equation f_i and each column to a variable x_i. Entries appearing as 1's in row i and column j thus indicate that variable x_j appears explicitly in equation f_i.

	x_1	x_2	x_3	x_4	x_5	x_6	x_7
f_1	1	1	1		1	1	
f_2	1	1		1	1	1	
f_3	1	1	1				
f_4	1	1		1			
f_5			1	1	1		1

(3.18)

When using the tear and grid method we aim at decomposing the system of NAE's into a subset which may allow for an *explicit* solution scheme. This is guaranteed if a decomposition leads to a *linear* subset. By inspection of (3.18) we find that a convenient set of tear variables is x_1 (x_A) and x_2 (x_B). The reduced occurrence matrix now becomes

$$
\begin{array}{c|ccccc}
 & x_3 & x_4 & x_5 & x_6 & x_7 \\
f_1 & 1 & & 1 & 1 & \\
f_2 & & 1 & 1 & 1 & \\
f_3 & \textcircled{1} & & & & \\
f_4 & & \textcircled{1} & & & \\
f_5 & 1 & 1 & 1 & & 1
\end{array}
\tag{3.19}
$$

$$
\begin{array}{c|ccc}
 & x_5 & x_6 & x_7 \\
f_1 & 1 & 1 & \\
f_2 & 1 & 1 & \\
f_5 & & 1 & 1
\end{array}
\tag{3.20}
$$

As indicated by (3.19) the chosen assignment allows in this case for sequential solutions of x_3 from f_3 and x_4 from f_4. By a thorough analysis of the model equations we also find that the solutions may be obtained explicitly. The remaining reduced system in (3.20), consisting of variables x_5, x_6, x_7 and equations f_1, f_2, f_5, apparently needs to be solved iteratively. However, by inspection find that all variables appear linearly in the remaining equations, assuring unique relations between the variables. Simple algebraic manipulations thus yields a *complete decomposition*, hence costly iterative schemes are avoided. The task of obtaining vital information about the form of the equations, in order to determine the solution strategy (e.g. iterative or explicit), is not an issue which is easily dealt with. Some steps towards this have been taken by Ramirez (1989), although this problem by far is solved.

3.5 Numerical Results

We present in this section numerical results obtained with the proposed methods. The reactive distillation example is motivated also by the desire to find out whether multiple solutions exist for simple one stage columns. We show that multiplicity does arise, and the solutions are easily obtained using the *tear and grid method*.

Example 1 : Complex Distillation Arrangements.

The example column ($\vdash$) considered here was introduced by (Christiansen *et al.* 1997) and will be discussed in a later chapter, hence detailed information regarding the model is not given here. However, we mention that the task is to separate a four component mixture into product streams enriched in the respective constituents. The model consists of 213 variables and 6 parameters (DOFs) λ, out of which 4 DOF's are used to fix (control) the purities of the product streams. Since we then have two 2 DOFs left, we may compute the solution manifold by continuation in two dimensions as described previously. In figure 3.5 we give results from numerical simulations in which we display solutions for a range of the parameter values in (λ_1, λ_2) space. Figure 3.5 (a) illustrates the rays corresponding to different angles ϕ_i as defined in equation (3.11). In figure 3.5 (b) we show the same rays in 3 dimensional space for some variable X. As previously mentioned, the solution manifold is in this case a two dimensional surface. Such a surface is then computed using some interpolation method, typically based on minimizing the mean square error between the vectors. Figure 3.6 displays the surface corresponding to figure 3.5 (b).

Example 2 : Reactive Distillation Column.

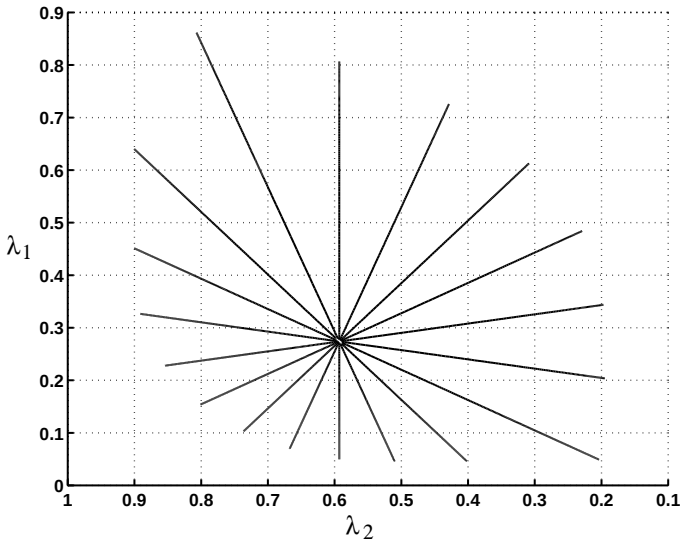

(a)

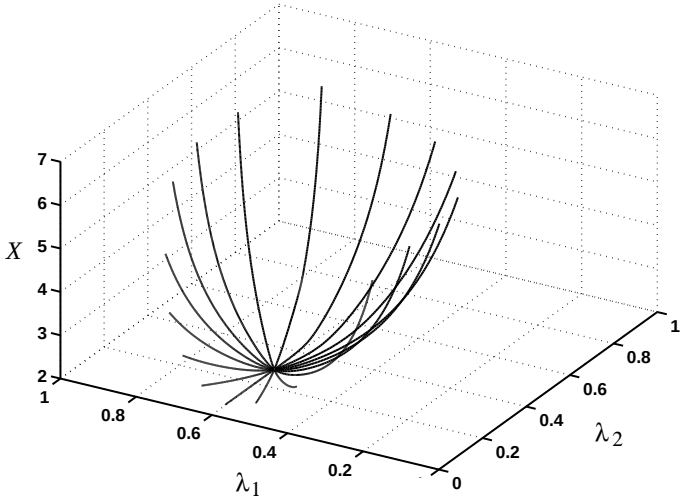

(b)

Figure 3.5: Two parameter continuation where Figure (a) illustrates "rays" corresponding to different ratios between the continuation parameters λ_1 and λ_2. Figure (b) shows the corresponding solutions for the model parameter X

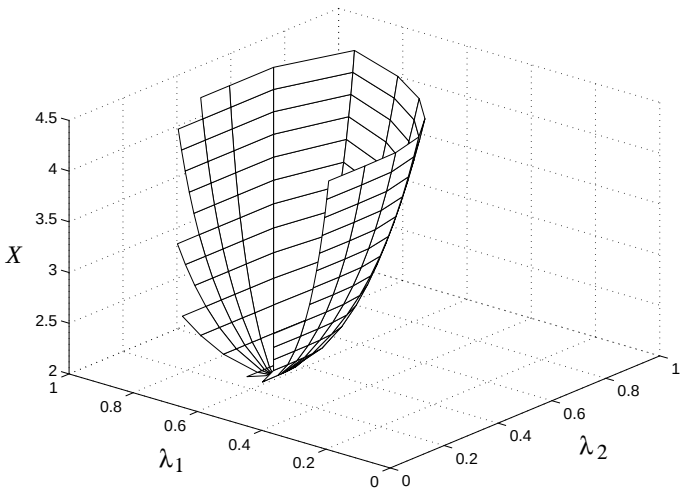

Figure 3.6: Solution surface computed by interpolation displaying X as a function of λ_1 and λ_2

The model for the column was given in the last chapter, but for simplicity we rewrite the model equations here where we have used that $x_C = 1 - x_A - x_B$ and introduced the Damkohler number $Da = k_f H/F$. The resulting model is given by

$$Fz_A - (V-L)y_A - (F+L-V)x_A + FDa\left(1 - x_A - x_B - \frac{x_A x_B}{K^{eq}}\right) = 0 \quad (3.21)$$

$$Fz_B - (V-L)y_B - (F+L-V)x_B + +FDa\left(1 - x_A - x_B - \frac{x_A x_B}{K^{eq}}\right) = 0 \quad (3.22)$$

$$y_A - \frac{\alpha_1 x_A}{(\alpha_1 - 1)x_A + (\alpha_2 - 1)x_B + 1} = 0 \quad (3.23)$$

$$y_B - \frac{\alpha_2 x_B}{(\alpha_1 - 1)x_A + (\alpha_2 - 1)x_B + 1} = 0 \quad (3.24)$$

$$L\left((M_A - M_C)y_A + (M_B - M_C)y_B + M_C\right) - L_w = 0 \quad (3.25)$$

When specifying the feed conditions, D and V we are left with two degrees of freedom since we are free to vary the mass reflux L_w and the Damkohler number Da. In order to explore solutions in parameter space we are allowed to specify *any two* variables or parameters and solve the remaining square system of equations. In order to find all solutions it is required that the remaining equations are unique in the assigned variables. The under-determined system of NAE's thus consist of 7 variables and parameters and 5 non–linear functions. The variables are $x_A, x_B, y_A, y_B, L, Da, L_w$ which we denote x_1–x_7. Process data for the reactive distillation example was given in table 2.1 in chapter 1. A point of interest, besides using the example to validate the numerical methods, is to examine whether multiple steady states exist for the simple example model. The example is motivated by a work on multiplicities in ideal

binary ordinary distillation columns by Jacobsen and Skogestad (1991).

As discussed previously, by making an appropriate grid of x_1 and x_2, we are thus able to compute the whole solution space for *all* combinations of x_1 and x_2. Solutions computed at some points in the grid may off course be infeasible, for example negative flows or mole fractions, but this is easily checked by back calculations. In figure 3.7 a) we show a 3 dimensional solution surface in (y_2, L, L_w) space and in b) we illustrate shapes of typical contours for constant L_w. We note that the branching diagrams in fact display multiple solutions for given L_w.

Example 3 : Constrained optimization.

We here illustrate the features of the proposed optimization procedure in terms of a simple *mathematical* example. The example is chosen for convenience so as to illustrate that the procedure adequately deals with equality and inequality constraints. The optimization problem we consider is given by

$$\begin{array}{lll} \text{Minimize} & f(x,y) & = x^2 + y^2 \\ \text{Subject to} & h(x,y) & = 0.25 - xy = 0 \\ & g_1(x) & = |x| \geq 1 \\ & g_2(y) & = |y| \geq 1 \end{array} \tag{3.26}$$

The results from the optimization is shown in figure 3.8, where the stapled lines illustrate different contours for the objective function, and the solid line the equality constraint. The circles show the continuation path towards the optimum, starting from two feasible initial points of $(x, y) = \{(-.25, -1), (0.25, 1)\}$ from which the optimum is located in a finite number of steps. The optimum is found to be $\phi = 0.5$ corresponding to $x = y = \pm 0.5$, which is easily confirmed analytically (e.g. substitute y from $h(x, y)$ and solve for the first order conditions). We also note that by starting from a feasible initial point, none of the converged solutions lie outside the feasible region.

3.6 Discussion and Conclusions

In this paper we have considered two methods for exploring solutions in the parameter space of a system of nonlinear algebraic equations (NAE's), i.e. parameter continuation schemes and a *tear and grid* method. We proposed two implementations of a parameter continuation algorithm, where one is based on a conventional predictor-corrector scheme. The other implementation, which is found to be much more efficient, is based on solving an augmented system of equations using Broyden's method for each continuation step. The increased efficiency owes to using rank one updates (Broyden) of the Jacobian, so that expensive re–evaluations of this matrix is avoided. We also demonstrated how one may embed steady state optimization within such a continuation scheme. We also extended the scope of a previously proposed *tear and grid* method, so as to solve also under-determined (non–square) NAE's.

A common feature of the methods presented here is that we at large put emphasis on simplicity, so as to make it easy to implement them in a high level programming language. Among the main advantages with the continuation schemes, we firstly

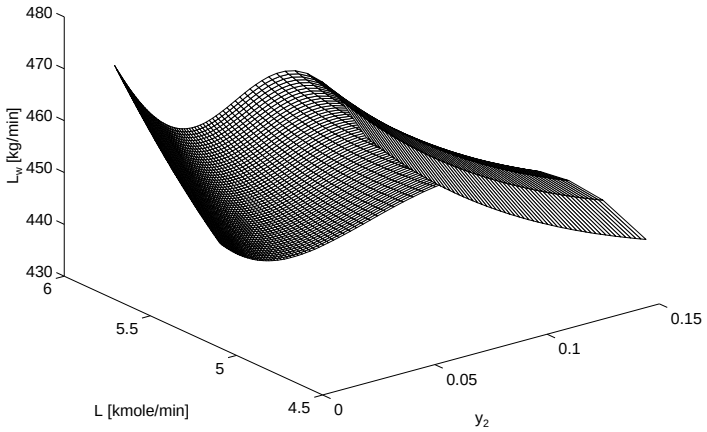

(a) Solution surface in (y_2, L, L_w) space

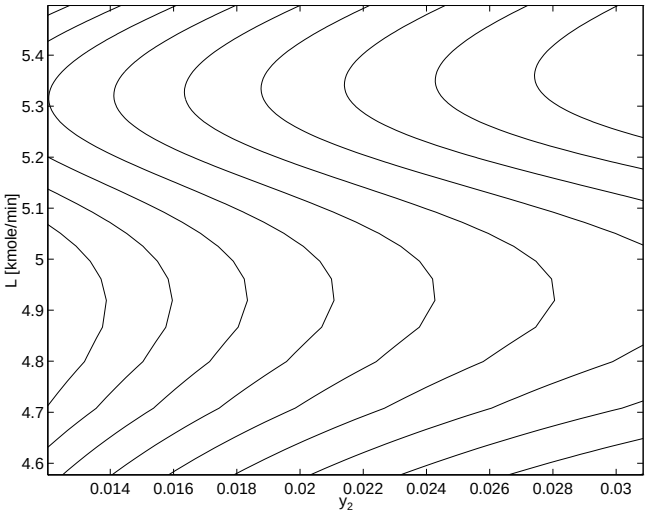

(b) L_w contours

Figure 3.7: Branching diagrams for reactive distillation example

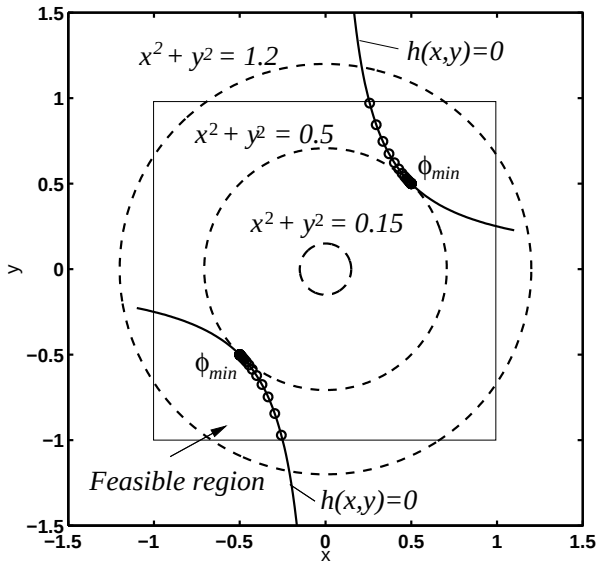

Figure 3.8: Constrained optimization by continuation

recognize that one always stays close to a feasible solution. This is particularly favorable for ill–conditioned processes, where convergence problems are often encountered. Secondly, the methods are favored by small extent of book keeping. Since we use an augmented vector, which includes both (state) variables and parameters, we do not distinguish between those in the solution procedure. This again facilitates ease of implementation.

Finally we should comment some on the important aspect of computational complexity. As explained in the introduction of chapter 2, methods for finding all solutions to a set of nonlinear equations tend to increase exponentially with the problem size, and this is the case for the tear and grid method as well as simultaneous continuation in many variables. However, many problems arising in practice are not that large, and we have nevertheless found these methods to be very useful for many practical problems in conceptual design of distillation systems. In this chapter we successfully applied the methods to a few example problems of different complexity.

Nomenclature

Note that we give here only the nomenclature used in the main body of the paper. For the examples we have defined the variables and parameters explicitly.

J – Jacobian matrix
f_i – Equation number i
Da – Damkohler number

F – Feed flowrate [kmol/min]
K^{eq} – Equilibrium constant
L – Reflux flowrate [kmol/min]
M_i – Molar weight of component i [kg/kmol]
u – Vector of inputs or control variables
V – Vapor flow rate [kmol/min]
$\mathbf{x}$ – Vector of (state) variables
$\hat{x}$ – Augmented vector of variables and parameters
x_i – Variable number i
$x_{A,B,C}$ – Liquid mole fraction of components A, B and C
y – Vector of output variables
$y_{A,BC}$ – Vapor mole fraction of components A, B and C
z_i – Mole fraction of component i in feed

Greek letters

α_i – Relative volatility of components i
δ – Step in variable space
ϵ – Step size
ϵ^{tol} – Tolerance for norm
η – Normalized secant step
λ – Vector of parameters
λ_i – Parameter number i
∇ – Gradient of objective function
∂ – Derivatives
Φ – Objective function to be minimized
ϕ_i – Ratio between continuation parameters
ζ – Vector of variables in rotated variable space

Subscripts

A, B, C – Chemical species A, B and C
$pred$ – Predictor step
$Proj$ – Orthogonal projection
s – Set-point
w – Mass flow in (kg/min)

Calligraphic

$\mathcal{N}$ – Basis for nullspace
$\mathcal{R}^m$ – Vector space of dimension m

References

Bilous, O. and N. R. Amundson (1955). Chemical Reactor Stability and Sensitivity. *A.I.C.h.E Journal* **1**, 513–521.

Broyden, C. G. (1965). A Class of Methods for Solving Simultaneous Nonlinear Equations. *Math. Comp.* **19**, 577–593.

Christiansen, A. C., S. Skogestad and K. Lien (1997). Partitioned Petlyuk Arrangements for Quaternary Separations. In: *Distillation and Absorption '97* (R. Darton, Ed.). Vol. 2. IChemE. pp. 745–746.

Davidenko, D. (1953). On a New method of Numerically Integrating a System of Nonlinear Equations. *Dokl. Akad. Nauk USSR* **88**, 601.

Golubitsky, M. and D. G. Schaeffer (1985). *Singularities and Groups in Bifurcation Theory.* Vol. I of *Applied Mathematical Sciences.* Springer–Verlag New York Inc.

Haselgrove, C. B. (1961). The solution of nonlinear equations and of differential equations with two–point boundary conditions. *Comp. J.* **4**, 255–259.

Jacobsen, E. W. and S. Skogestad (1991). Multiple Steady–States in Ideal Two–Product Distillation. *AIChE Journal* **37**(4), 499.

Kubiček, M. and M. Marek (1983). *Computational Methods in Bifurcation Theory and Dissipative Structures.* Springer Series in Computational Physics. Springer–Verlag New York Inc.

Luenberger, D. G. (1984). *Linear and Nonlinear Programming.* 2 ed.. Addison-Wesley Publishing Company. Reading, Massachusetts.

Morud, J. (1995). Studies on the dynamics and operation of integrated plants. PhD thesis. University of Trondheim, The Norwegian Institute of Technology.

Morud, J. (1996). Private communication.

Press, W. H., S. A. Teulkosky, W. T. Vetterling and B. P. Flannery (1992). *Numerical Recipies in Fortran.* 2 ed.. Cambridge University Press.

Ramirez, W. F. (1989). *Computational Methods for Process Simulation.* Butterworth series in chemical engineering. Butterworth Publishers.

Sargent, W. H. and A. Westerberg (1964). "Speedup" in Chemical Engineering Design. *Trans. Inst. Chem. Eng.* **42**, T190–T197.

Seider, W. D., D. B. Brengel and S. Widago (1991). Nonlinear Analysis in Process Design. *AIChE Journal* **37**(1), 1–37.

Seydel, R. (1988). *From Equilibrium to Chaos, Practical Bifurcation and Stability Analysis.* Elsevier Science Publishing Co., Inc.

Strang, G. (1988). *Linear Algebra and its Applications.* Harcourt Brace Jovanovich, Inc.

The Mathworks, Inc. (1995). *MATLAB Reference Guide.*

van Heerden, C. (1953). Autothermic Processes. *Ind. Eng. Chem.* **45**(6), 1242–1247.

Westerberg, A. W., H. P. Hutcison, R. L. Motard and P. Winter (1979). *Process Flowsheeting.* Cambridge University Press.

Appendix A Practical Issues on Implementation

We here discuss some practical issues related to efficient implementation of the numerical methods presented in this chapter. For a comprehensive review on computational issues we refer to any standard book on numerical methods, e.g. Press *et al.* (1992). We first address the use of back-tracking for iterative schemes, after which we discuss some aspects related to updates of the Jacobian matrix.

A.1 Back tracking

Conventional Newton Raphson schemes commonly display poor convergence properties if appropriate measures are not taken during the course of iteration. A simple, yet reliable and efficient remedy for avoiding convergence problems, is to apply *back tracking* (Press *et al.* 1992). Back tracking is used to ensure that the norm of the residuals decrease at each step during the iterations. We thus consider a scheme of successive iterations given by

$$\Delta x = -\epsilon J^{-1} f \tag{3.27}$$

where ϵ is the step-size, f the vector of residuals and J the Jacobian matrix. If we consider small steps ϵ, we may use a linear approximation for the *reduction* in the squared norm of f, which yields

$$\Delta ||f||_2 = \Delta \left(f^T f \right) \approx 2 f^T f_x \Delta x = 2 f^T J \Delta x \tag{3.28}$$

By substituting for Δx from (3.27) we finally obtain

$$\Delta ||f||_2 \approx -2\epsilon f^T f = -2\epsilon ||f||_2 \ < \ 0 \tag{3.29}$$

This demonstrates that $||f||_2$ decreases provided we choose a sufficiently small iteration step. Hence if the norm increases during the course of iteration, we simply use backtracking to reduce ϵ until the norm decreases. Reducing ϵ is a simple strategy, and a common approach is instead to make a line search to actually minimize $||f||_2$ in the chosen search direction. In our method we simply half ϵ until the norm is reduced, again to facilitate simple implementation. We may note that Press *et al.* (1992) suggests to always try a full Newton step first.

A.2 Updating the Jacobian matrix

. Evaluating the Jacobian matrix is commonly one of the most expensive operations during numerical simulations. Since analytical solutions are difficult to derive, estimates are normally computed using finite differences. In order to improve the approximations of the Jacobian, various schemes are proposed in the literature. Here we consider a particular case, namely *rank one updates* using Broyden's method (Broyden 1965). We will not go into details regarding implementation issues, for which we refer to any standard textbook on numerical methods.

When using Broyden's method to obtain a single root of a system of NAE's, there is an underlying assumption of orthogonality between the prediction error and the current step. However, in the continuation scheme described in section 3.2.2 we use Broyden updates when traversing from one solution to the next on the continuation path. Hence, the orthogonality assumption may or may not apply. It is perforce difficult to judge how this will affect the approximate Jacobian, and thus the impact on numerical efficiency. In figure 3.9 we illustrate the required CPU–time along the continuation path for the complex distillation example discussed in the previous section. The solid line corresponds to the CPU–time when we use Broyden updates of

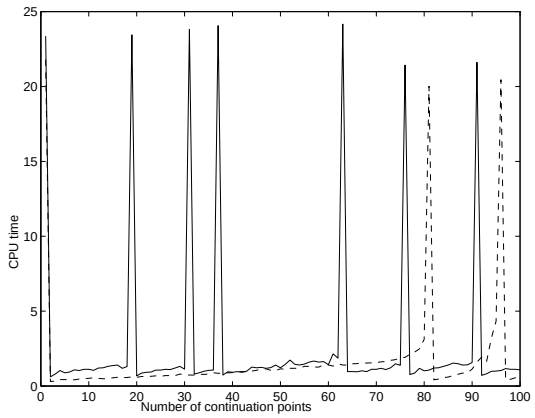

Figure 3.9: CPU time for continuation using Broyden's method

J, whereas the dashed line corresponds to using a constant J. The peaks arise due to recomputing the Jacobian, which we require if the norm is not reduced after 4 attempts of back–tracking. The figure quite surprisingly illustrates that using the Broyden update may make the prediction worse than keeping J constant, in the sense that re-computation of J is required more frequently. The total CPU time increases from 160 to 270 CPU's when using the Broyden update. However, we strongly emphasize that this result by no means must be taken as a general confirmation. We also found cases where the situation was reversed. We pose the question of analyzing under what circumstances Broyden updates may or may not be used for continuation methods, as an interesting problem for future works on numerical methods.

Chapter 4

Explicit Shortcut Method for Minimum Energy Calculations in Multicomponent Distillation

Atle C. Christiansen and Sigurd Skogestad*

Department of Chemical Engineering
Norwegian University of Science and Technology, NTNU
N–7034 Trondheim Norway

Unpublished

Abstract

In this paper we propose an explicit shortcut method to calculate the minimum energy requirements for sequences of regular distillation columns. The theoretical base for the procedure draws on previous results from the literature, but distinguishes itself from these methods by using physical insight for additional simplifying assumptions. The major contribution from the proposed method is besides its simplicity, the usefulness for screening purposes. The method may be used for analytical purposes to determine for what mixtures complex columns such as prefractionator arrangements should offer the largest savings compared to conventional arrangements. Furthermore we discuss optimality conditions for different conventional arrangements in terms of feed compositions and relative volatilities. In particular we discuss the importance of using partial condensers for upstream columns, since total condensers and thus liquid feeds to downstream columns seems to be taken for granted in many works in the literature.

*Author to whom correspondence should be addressed : Fax : +47 7359-4080, E-mail: skoge@chembio.ntnu.no

4.1 Introduction

Due to the importance of energy optimizations, an exhaustive amount of works has evolved in the literature during the last decades on simple methods to calculate the minimum reflux and/or boilup for sequences of regular distillation columns. Some works have also extended the analysis to complex columns such as sidestream columns, prefractionator arrangements and the Petlyuk column. In order to avoid extensive literature reviews, we simply refer to the comprehensive review article on minimum energy calculations by Köhler *et al.* (1995).

Most of the works in the literature are to some extent based on Underwood's method, which is an exact and reliable method for solving the stage-by-stage material balance equations that results upon assuming constant relative volatilities and constant molar flows. Another important advantage with this method is that one can easily obtain solutions for the limiting cases with an infinite number of stages (i.e. minimum reflux) and with infinite refluxes (i.e. minimum number of stages). However, when using this class of methods one must in the general case still resort to numerical computations since the solutions can only be found iteratively.

There are two important shortcomings with Underwood's method. Firstly it does not apply to many industrial (real) mixtures with complex thermodynamics, but for this case we may of course find the exact solutions numerically. Secondly, and more importantly for our purposes, Underwood's method is not suited to obtain *qualitative* information in the form of analytical *explicit* equations. Such information is crucial for obtaining insight into the "optimal" distillation arrangement for the separation of a particular mixture (feed compositions, relative volatility). Although there are a few works that address this issue, the results are generally restricted to a certain class of separation schemes (e.g. direct or indirect splits). In this work we will thus not elaborate further on the use of Underwood's method, but instead put emphasis on simple methods that offers insight in terms of simple analytical and *explicit* equations. The principal motivation for this work is thus to obtain explicit equations that allows for a quick *paper and pencil* analysis to obtain qualitative insight. To validate the behavior of the real process model one should thereafter turn to rigorous numerical simulations for which reliable and efficient software is now available. Using the method proposed in this work we in fact find that it provides accurate results in the regions of the composition space for within which the different conventional arrangements are optimal, e.g. use direct split for large amounts of light component or indirect split for large amounts of heavy.

When comparing for instance the performance of Petlyuk or other complex columns to conventional schemes, the most common choices are the direct and indirect split schemes. In the literature (e.g. Glinos and Malone (1988) and Douglas (1988)) it is reported that the direct split requires the lowest energy input for the majority of separations, i.e. feed compositions and relative volatilities. However, as we will demonstrate, this is correct only if one considers column sequences where all feeds to downstream columns are taken as saturated liquid, i.e. total condensers are used for the overhead (distillate). In the case of indirect split schemes this is clearly undesirable if the objective is to minimize the total boilup. Also, since there seems to be a

general agreement in the literature to use the total vapor requirement as a measure of the total cost of distillation columns, we here consider the more favorable case of partial condensation of the distillate flow in the *upstream columns*. The method proposed here is a simple analogy to a minimum reflux formula previously proposed by King (1971). The outline and results of this paper is to some extent analogous to a previous work by Glinos and Malone (1988). However, the results of Glinos and Malone (1988) are based on certain approximations using Underwood's equation. Although the approach used here draws form the same theoretical foundations, there is a notable difference in the underlying simplicity, which in our case allows one to derive explicit equations without having to resort to calculus. For the particular case when the *preferred* separation is carried out as the first split, we find that our method provides useful (and accurate) explicit equations for limiting cases (e.g. mole fraction of intermediate $B \to 1$). These are cases in which the maximum savings occur for a (directly coupled) prefractionator relative to the direct and indirect split. Before proceeding with our analysis, we stress that *all* expressions derived in this paper are based on the assumptions of constant molar flows and constant relative volatilities (i.e. ideal mixtures).

4.2 Analytical Equations for Minimum Boilup

In addition to the class of Underwood methods, there are also other *group methods* available in the literature. For binary mixtures King (1971) proposed the following formula to compute the minimum reflux for a *saturated liquid feed*

$$\left(\frac{L}{F}\right)_{min} = \frac{\phi_L^D - \alpha_{LH}\phi_H^D}{\alpha_{LH} - 1} \tag{4.1}$$

where L is the reflux, F the feed, α_{LH} the relative volatility between light (L) and heavy (H) component. ϕ_i^D denotes the recoveries of each component where superscript D refers to the distillate and the subscripts to the light (L) and heavy keys (H) respectively. By a simple mass balance (steady state) around the condenser we thus obtain the equation for the minimum boilup (V_{min})

$$V_{min} = \frac{\phi_{LK}^D - \alpha_{LH}\phi_{HK}^D}{\alpha_{LH} - 1} F + D \tag{4.2}$$

For the special case of *sharp separations*, in which the recoveries are close to one, equation (4.1) becomes

$$\left(\frac{L}{F}\right)_{min} = \frac{1}{\alpha_{LH} - 1} \tag{4.3}$$

and equation (4.2) becomes

$$\left(\frac{V}{F}\right)_{min} = \frac{1}{\alpha_{LH} - 1} + \frac{D}{F} \tag{4.4}$$

The corresponding minimum for the sharp separation of a *saturated vapor feed* is

$$\left(\frac{V}{F}\right)_{min} = \frac{1}{\alpha_{LH} - 1} \tag{4.5}$$

These formulas may under certain assumptions apply also to multicomponent mixtures, for which King (1971) provides a comprehensive discussion. However for the multicomponent case, we will show later that (4.2) gives the actual V_{min} only in the particular case of what is called the *"preferred separation"* (Stichlmair 1988).

In a later work Stichlmair (1988) presents a very useful graphical visualization of Underwood's method. For the special case of ternary mixtures he shows how one may derive exact analytical formulas for the conventional direct and indirect sequence. However, for our purpose, the formulas by Stichlmair (1988) are not as useful for the direct and indirect splits, since numerical computations are required in these cases. Recall that our objective is to derive *explicit* methods to be used for screening purposes, and more importantly to indicate for which mixtures the different sequences are favorable. Still, the significant contribution of Stichlmair (1988) which has been exploited in the present work, is the analysis of the particular case where the *preferred* separation is carried out.

More recently Porter and Momoh (1991) proposed a simple and approximate method for minimum vapor calculations for sharp separations of a saturated liquid feed. If R_F denotes the ratio between the actual and minimum reflux ratio, the following equation was proposed to compute V_{min} for a mixture of NC components

$$V_{min} = \underbrace{\sum_{i=1}^{LK} F_i}_{\text{distillate term}} + \underbrace{\left(\sum_{i=1}^{NC} F_i\right) \frac{R_F}{\alpha_{LH} - 1}}_{\text{feed term}} \tag{4.6}$$

For sharp separations and binary mixtures, (4.6) is identical to (4.4) if we set $R_F = 1$. As shown in the paper, the minimum vapor for a sequence of columns is obtained by summation of equation (4.6) for all columns. However, there are two important aspects that the authors do not recognize. Firstly, as also stated by King (1971) (which is not acknowledged by the authors), it is easily shown that the proposed formula (4.6) always provide an upper bound for V_{min}. Thus, it is in general conservative to include all components in the "feed term". Secondly, the authors do not appreciate that for the indirect sequence, the feed to subsequent columns may be taken as vapor, for which the "distillate term" in equation (4.6) evaporates. For this reason, this method always assign an undue penalty to the indirect scheme. Taking these arguments into account, formula (4.6) will usually provide a rather conservative estimate for the minimum boilup, which is also confirmed in the textbook by Smith (1995). We therefore propose an alternative approach based on the approach of King and additional "physical" insight. We show that this "new" formula in some cases gives a *lower* bound for the minimum heat for direct split sequence.

4.2.1 Approximate Solution - Explicit Equation for V_{min}

What we propose here is a simple extension of the method proposed by King (1971) to the case of multicomponent separations. In order to do so, we first make the simplifying assumption that for each pseudo-binary mixture we only take into account the *distributing* components when computing the minimum boilup. To put this more clearly, we base our results on the general assumption that any *non–distributing* components in general will not strongly influence the pseudo-binary separation, and may thus be discarded from the "feed term" in equation (4.6). For any pseudo-binary separation we thus substitute the feed F in equation (4.1) with the feed of distributing components. We here denote the low boiling component by A, and the remaining sequence of NC components are ranked in terms of their volatility. Thus, substituting the feed term in equation (4.2) by the feed of distributing components, we obtain the following equation for a single column with a saturated liquid feed

$$V_{min} = \frac{\phi^D_{LK} - \alpha_{LH}\phi^D_{HK}}{\alpha_{LH} - 1} \sum_{i=LK}^{HK} F_i + D \tag{4.7}$$

and similarly for a saturated vapor feed

$$V_{min} = \frac{\phi^B_{HK} - \alpha_{LH}\phi^B_{LK}}{\alpha_{LH} - 1} \sum_{i=LK}^{HK} F_i \tag{4.8}$$

where superscript B denotes the bottom product and F_i refers to the molar feed of distributing components. Note that for a *sharp* separation we have for the distillate flow

$$D = \sum_{i=1}^{LK} D_i \tag{4.9}$$

Hence we propose the following explicit formula to calculate V_{min} for multicomponent separations, carried out as a sequence of pseudo-binary splits in $NC - 1$ regular columns

$$V_{min} = \sum_{i=1}^{NC-1} \left(\underbrace{\frac{\phi^D_{LK} - \alpha_{LH}\phi^D_{HK}}{\alpha_{LH} - 1} \sum_{j=LK}^{HK} F_j}_{\text{feed term}} + \underbrace{(1 - q_i)\, D_i}_{\text{distillate term}} \right) \tag{4.10}$$

where q_i is introduced to account for the feed quality for each column, i.e. $q_i = 1$ for saturated vapor and $q_i = 0$ for a saturated liquid. For partly saturated feeds q_i is simply given as the vapor fraction. We thus stress that the distillate term is only to be considered for saturated or partly saturated liquid feeds. For the limiting case of pure products ($\phi^D_{LK} = 1, \phi^D_{HK} = 0$) and a saturated liquid feed, equation (4.10) becomes

$$V_{min} = \sum_{i=1}^{NC-1} \left(\sum_{j=LK}^{HK} \frac{F_j}{\alpha_{LH} - 1} + (1 - q_i)\, D_i \right) \tag{4.11}$$

Hence we have a simple and explicit equation for the boilup which takes as arguments only the relative volatilities and the feed compositions. As previously mentioned, the purpose for using this analogy is that it offers a simple means for comparing the minimum energy inputs for the direct and indirect split schemes with that of a prefractionator. The latter is of great import since the prefractionator is the first stage towards utilizing direct coupling of columns, which is the essential feature for the Petlyuk arrangements.

4.3 Analytical Treatment for Ternary Mixtures

In this section we present a comparative analysis for the direct and indirect schemes and the prefractionator arrangement based on our proposed method. We emphasize that the expressions are approximate, and therefore to be used primarily for qualitative and screening purposes. To quantify the errors embedded within the method we provide numerical results in the next section for the errors compared to exact methods (e.g. Underwood's method). The objective of this part is thus to compare these arrangements in terms of total boilup requirements, and also to indicate under which conditions the different arrangements are favorable.

All the results in this section apply to a saturated liquid feed of components A, B and C with relative volatilities given by α_{AC}, α_{AB} and α_{BC}. For notational simplicity we will use A, B and C to represent the feed rates of the components, i.e. $A = Fz_A$, $B = Fz_A$ and $C = Fz_C$ where z_i is the feed composition.

4.3.1 "Pseudo-binary" method for ternary separations

As shown in Figure 4.1 there are three alternative separations for *sharp* splits of a ternary mixture in a single column. Case (i) corresponds to a sharp A/B split, case

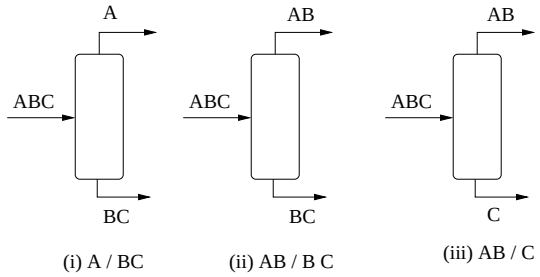

Figure 4.1: First column in sharp split sequences for ternary mixtures

(ii) to a sharp A/C split and case (iii) to a sharp B/C split. For saturated liquid feeds we use the proposed equation (4.11), and obtain the following explicit expressions for the minimum reboil for the single column

$$V_{min}^{A/B} = \frac{A+B}{\alpha_{AB}-1} + A \tag{4.12}$$

$$V_{min}^{A/C} = \frac{F}{\alpha_{AC}-1} + A + \phi_B^D B \tag{4.13}$$

$$V_{min}^{B/C} = \frac{B+C}{\alpha_{BC}-1} + A + B \tag{4.14}$$

where ϕ_B^D denotes the fraction of intermediate B in the distillate, i.e. $(1-\phi_B^D)B$ in the bottoms. Note here that for the A/C split, the minimum boilup occurs for a particular value of ϕ_B^D which is uniquely determined by the so called preferred separation, i.e.

$$\phi_B^D = \frac{\alpha_{BC}-1}{\alpha_{AC}-1} \tag{4.15}$$

The preferred separation refers to the energetically favorable split which may be shown to yield the absolute minimum boilup for a ternary separation in an infinite regular column. We will elaborate on this issue later. For saturated vapor feeds the distillate terms are omitted, and we thus obtain

$$V_{min}^{A/B} = \frac{A+B}{\alpha_{AB}-1} \tag{4.16}$$

$$V_{min}^{A/C} = \frac{F}{\alpha_{AC}-1} \tag{4.17}$$

$$V_{min}^{B/C} = \frac{B+C}{\alpha_{BC}-1} \tag{4.18}$$

In Figure 4.2 we show the mass balance lines which indicates the compositions of the top and bottoms products for the three cases. Here small letters b and d refer to the

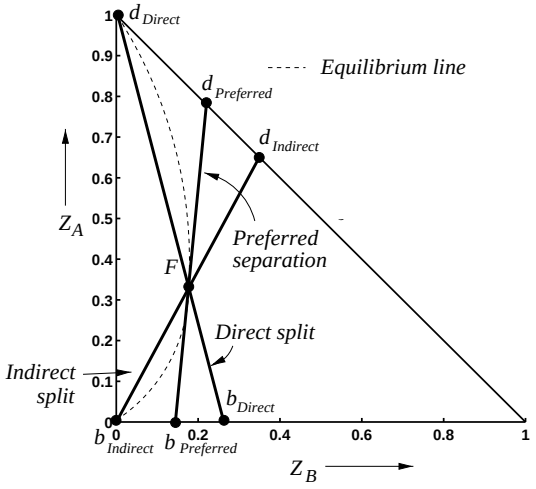

Figure 4.2: Mass balance lines for sharp splits of a ternary mixture in a single column

bottoms and distillate products respectively. We ask the reader to note that for the *preferred separation*, the distillation lines and the equilibrium lines are colinear in the

feed point. This is used by Stichlmair (1988) to derive explicit equations for the minimum boilup. When separating a ternary mixture into its constituents, the three cases above corresponds to the first stage in the separation sequences commonly referred to as the direct split (A/BC), the indirect split (AB/C) and the *preferred separation* (AB/BC). We now demonstrate how to derive the approximate expressions for V_{min} for these three separations.

4.3.2 Direct split sequence

If we denote the consecutive columns in the direct split sequence by $C1$ and $C2$ as shown in figure 4.3 and assume sharp separations in each column, we obtain for a saturated liquid feed $(F = 1)$

$$V_{min}^{C1} = \frac{A+B}{\alpha_{AB}-1} + A \tag{4.19}$$

$$V_{min}^{C2} = \frac{B+C}{\alpha_{BC}-1} + B \tag{4.20}$$

Hence the total boilup requirement becomes

$$V_{min}^{D} = \frac{A+B}{\alpha_{AB}-1} + \frac{B+C}{\alpha_{BC}-1} + A + B \tag{4.21}$$

where superscript D denotes the direct split. If we compare this result with the

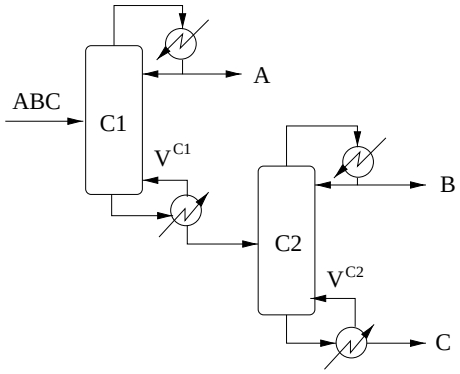

Figure 4.3: Direct split sequence for ternary separations

method proposed by Porter and Momoh (1991), we find that there is a difference equal to $C/(\alpha_{AB}-1)$. This additional term arise since the authors take into account *all* components in the feed term, whereas we only consider the distributing components.

Among other approximate formulas proposed in the literature, we may compare our formula to the one given by Glinos and Malone (1984) which gives

$$V_{min}^{D} = \frac{A+B}{f\,(\alpha_{AB}-1)} + \frac{C}{f\,(\alpha_{AC}-1)}A + B, \quad f = 1 + \frac{B}{F \cdot 100} \tag{4.22}$$

According to the authors this expression is generally less than 4% in error. Taking the difference between equations (4.21) and (4.22) we obtain

$$\Delta V_{min}^{D} = \frac{(1-f)(A+B)}{f(\alpha_{AB}-1)} + \frac{C}{f(\alpha_{AC}-1)} \tag{4.23}$$

Since f is close to one ($f_{max} = 1$ for $B = 1$), we find that the difference is small when C is small and/or α_{BC} is large. Conversely, if C is large the difference becomes large. However we also emphasize that if C is large one should not use the direct split scheme, and we may therefore use our formula at least for qualitative purposes due to its simplicity.

An important finding is that the minimum boilup given by (4.21) in fact yields a *lower bound* for the actual V_{min}^{D}. Hence, it generally yields an optimistic prediction of V_{min} for any feed mixture. The fact that it yields a lower bound is explained by considering the underlying assumptions of our simplified method. Our assumption is that the presence of any high boiling component should not be considered for the separation in the first column, in which pure A is withdrawn. For small amounts of the high boiler C and a large α_{AB} relative to α_{BC}, this is essentially correct, since the small amounts of C in the vapor will not affect the separation of A/B. However, as the amount of C increases and α_{AB} decreases relative to α_{BC}, the presence of heavy component C in both vapor and liquid phase will become more pronounced, and will make the A/B separation more difficult. To achieve the desired sharp splits this means that both reflux and boilup needs to be increased, hence (4.21) yields a lower bound. We elaborate on this issue later, where we also provide a "graphical interpretation" to account for this lower bound.

4.3.3 Indirect split sequence

For the indirect split scheme one should distinguish between two cases depending on the feed quality for the second column shown in figure 4.4. We first consider the case

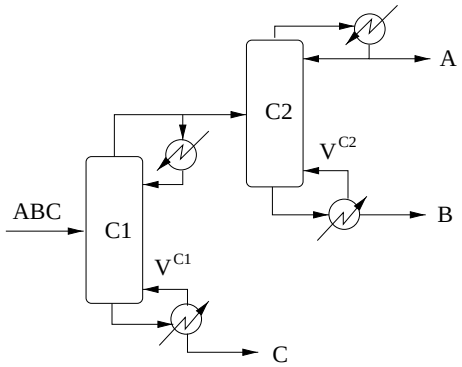

Figure 4.4: Indirect split sequence for ternary separations

of a total condenser, in which case the feed to column $C2$ is saturated liquid. The

minimum boilup for the first column is

$$V_{min}^{C1} = \frac{B+C}{\alpha_{BC}-1} + A + B \tag{4.24}$$

This approximate expression applies to both a partial and a total condenser.

(i) Total condenser.
If we use a total condenser which gives a saturated liquid feed to $C2$, we must include the distillate term also for column $C2$, so that we find

$$V_{min}^{C2} = \frac{A+B}{\alpha_{AB}-1} + A \tag{4.25}$$

Adding the boilups in (4.24) and (4.25) for the two columns we obtain for the indirect sequence

$$V_{min}^{I} = \frac{A+B}{\alpha_{AB}-1} + \frac{B+C}{\alpha_{BC}-1} + 2A + B \tag{4.26}$$

Compared to the direct scheme, our simplified analysis thus suggest that the indirect scheme with a total condenser "always" requires a larger boilup. This is obviously not correct, and the "error" is due to the assumptions of distributing components. For the indirect split we acknowledge that equation (4.26) should be modified so as to take into account the influence of non–distributing components. Before going into detailed discussions on this matter, we first consider the more preferable case in which we use a partial condenser for the distillate from $C1$, i.e. use a vapor feed to $C2$.

(ii) Partial condenser. If we on the other hand use a *partial* condenser, we may eliminate the distillate term for $C2$ and thus obtain a lower value for V_{min}^{C2}

$$V_{min}^{C2} = \frac{A+B}{\alpha_{AB}-1} \tag{4.27}$$

The total boilup requirement thus becomes

$$V_{min}^{I} = \frac{A+B}{\alpha_{AB}-1} + \frac{B+C}{\alpha_{BC}-1} + A + B \tag{4.28}$$

which in fact is the same equation as for the direct sequence given by (4.21). Compared to the method of Porter and Momoh (1991), there is a difference equal to the terms $A/(\alpha_{BC}-1)+A$. This deviation is again due to the authors including all components in the "feed term" $(A/(\alpha_{BC}-1))$ and not considering vapor feed (A). The approximate expression proposed by Glinos and Malone (1984) for the indirect split with a partial condenser is

$$V_{min}^{I} = \left(\frac{A}{\alpha_{AC}-1} + \frac{B+C}{\alpha_{BC}-1}\right)\frac{1}{1+z_A z_C} + A + B \tag{4.29}$$

By inspection of equations (4.28) and (4.29) we find that the difference is small if z_C and the ratio α_{AB}/α_{BC} are large, which as we will show are cases where the indirect split is favorable.

By comparing equations (4.28) and (4.21) one may conclude from our simplistic analysis that the direct and indirect scheme with partial condenser should require the same boilup. However, as stated in the previous section, there is a crucial aspect which explains why the indirect scheme in many cases will require a lower boilup than that given by equation (4.28). We present the argument in a stepwise manner, in order to clarify the impact caused by the presence of non–key components.

(I) Heavy non–key in *liquid* feed

If we increase the fraction of heavy non–key in the feed, this will in general have no substantial isolated effect on the separation, except that the temperature levels must increase. The latter assumes that α for the key components remains constant (independent of temperature). This corresponds to increasing the amount of C in the feed for the direct split scheme.

(II) Light non–key in *vapor* feed

If we instead consider an increase in the fraction of light non-key in a vapor feed, we also find that the effect is small on the separation of the key components. This simply corresponds to decreasing the pressure in the top section of the column, the same as increasing the fraction of A in the vapor feed for the indirect split.

However, there is one situation in which the presence of non–keys have a large impact;

(III) Light non–key in *liquid* feed

The effect of increasing the fraction of light non–key relative to the key components, will in this case have two main effects

(a) A larger fraction of the light non–key traverses to the top section of the column. This in itself has no effect on the separation, but to keep the vapor flow of the key components in the top section unchanged we would need to increase the boilup relative to the binary separation.

(b) However, this increase of boilup would benefit the separation in the bottom section, so that the overall effect is not easy to predict.

As a remark we note that a similar large effect as in case (III) above would be expected for a heavy non-key in a *vapor* feed, but this case does not occur for the separations studied in this paper since we consider saturated liquid feeds to the first column. To compensate in the approximate expressions, we may propose the following formula for the indirect sequence;

$$V_{min}^{C1} = \frac{B+C}{\alpha_{BC}-1} + B + \beta A, \quad \beta \in [0,1] \tag{4.30}$$

and

$$V_{min}^{I} = \frac{A+B}{\alpha_{AB}-1} + \frac{B+C}{\alpha_{BC}-1} + B + \beta A, \quad \beta \in [0,1] \tag{4.31}$$

It is not straightforward to determine under what conditions one should use the lower bound corresponding to $\beta = 0$, or the upper bound of $\beta = 1$. However, if we use $\beta = 0$, equation (4.31) will always give a lower bound for V^I_{min} for the indirect split. This is however an optimistic prediction, and will provide relatively large deviations for instance when A is large. For consistency we will however use $\beta = 1$ in the following analysis.

4.3.4 Error analysis for direct and indirect sequence

Since the proposed method is based on certain simplifying assumptions regarding the effect of non-distributing components, it is of great import to provide measures of the degree of accuracy. For the ternary case it is in fact relatively straightforward to give a graphical visualization of the relative errors compared to the exact solutions (Underwood). One way of doing this is to consider the distillation lines for the separation of the light key (direct split) in the first "ternary" column. The argument is of course similar for the indirect split. We also emphasize that it is only the ternary separation that is of interest, since the proposed method is exact in the binary case. The issue of distillation paths is conveniently described in the literature (e.g. Stichlmair (1988)), so we give here only a brief overview. In Figure 4.5 we give a typical representation of the separation paths for the direct split. In order to use the

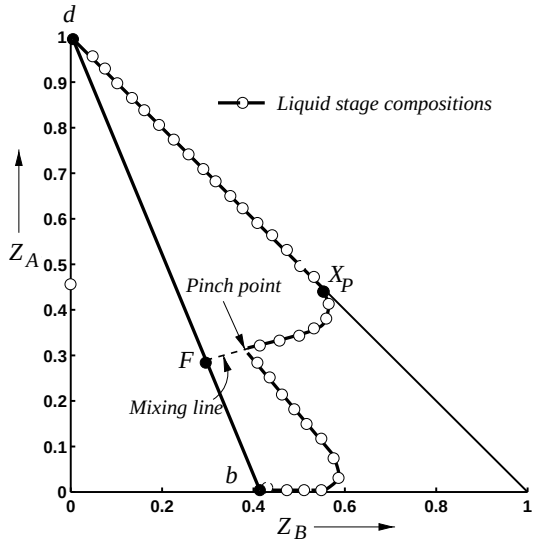

Figure 4.5: Separation of light component from a ternary mixture at minimum reflux

exact methods for computing the minimum reboil, based on Underwood's method or the approach used by King (1971) or Stichlmair (1988), one needs to compute the mapping of the pinch point composition x_P on the AB apex. Note that the pinch point actually occurs at the feed point as illustrated in Figure 4.5, whereas x_P denotes the "mapped" pinch composition onto the binary AB. Finding x_P for

ternary mixtures requires the solution of a quadratic equation, which does not serve our purpose since we aim for an *explicit* analytic equation. Hence, in order to obtain such explicit answers to be used for *qualitative* and *analytical* purposes (we again stress this issue which is the focal point of our work), there are in fact two ways to obtain an approximation of this pinch composition. The alternative proposed in this work is to take the pseudo-binary composition along the secant from $C = 1$ through the feed point z_F. This corresponds to approximating x_P by

$$x_A^* = \frac{z_A}{z_A + z_B} \tag{4.32}$$

where z_i denotes the feed compositions. Alternatively we may take the composition along the line of constant z_A, for which $z_B = 1 - z_A$. These cases are illustrated in Figure 4.6. The real pinch point x_P lies between the two approximate compositions. Using this analogy we may show that our method always give a lower bound for the minimum reboil for the direct split.

From the literature (Stichlmair 1988) we know that the minimum reflux ratio $R = L/D$ may be taken as the ratio of the relative lengths of the vectors given by

$$R_{min} = \frac{x_{Di} - y_{Fi}}{y_{Fi} - z_i} \tag{4.33}$$

where x_{Di} denotes the distillate composition, whereas z_i and y_{Fi} are feed compositions (related by the equilibrium) of component i. Note that the ratio in equation (4.33) is the same for ternary and binary mixtures, and applies to each component i. However, equation (4.33) only applies to the particular case where the distillation and the equilibrium lines are colinear at the feed (pinch) point, i.e. for binary separations and the preferred separation. Thus when separating either the low boiler (direct split) or the high boiler (indirect), the pinch point will move away from the feed point. In these cases one cannot use equation (4.33), and instead one must compute the real pinch composition x_P. For the direct split, the minimum reflux R_{min}^D can then be determined from

$$R_{min}^D = \frac{1}{(\alpha_{AB} - 1)\, x_P} \tag{4.34}$$

Since we aim for explicit equations we thus use the approximation for the pinch composition x_A^* instead of the real x_P. As demonstrated in Figure 4.6 x_A^* is in fact always closer to the distillate composition (higher) than the real x_P. Our method will thus always yield a lower bound for the minimum reboil for the *direct split*, since using x_A^* involves dividing by a larger number in equation (4.34). Conversely, an "upper bound" is obtained if we instead take the pinch composition along the constant $x_A^* = A$. We note that the relative error will increase as we approach the vertex $C = 1$, and in fact will become negligible as we approach the vertex $B = 1$. The error also depends on the relative volatilities since they determine the direction of the distillation and equilibrium vectors, i.e. the "angle" between the lines extending from the feed point towards the real pinch x_P and the pseudo binary composition x_A^* respectively. In general, we thus find that the error also increases with decreasing α_{AB}.

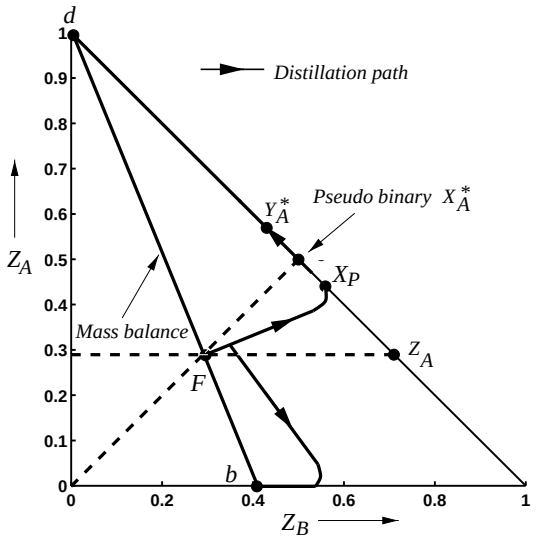

Figure 4.6: Illustration of minimum reflux computations for direct split

4.3.5 3–column Prefractionator Arrangement

The idea of using a prefractionator is to reduce the exergy losses caused by process irreversibilities, in the sense that it allows for potentially *reversible splits* (e.g. Petlyuk *et al.* (1965), King (1971)). We first consider the simplest case, in which we need three regular columns for the ternary separation as demonstrated in figure 4.7. In order to use our method we also need to specify the split fraction ϕ_B^D of the intermediate component B which is taken over the top (distillate). Note here that the light (A) and heavy (C) keys are not adjacent in volatilities, so that we must include the non-key (B) in the "feed term". Assuming sharp separations we obtain from (4.2)

$$V_{min}^{C1} = \frac{F}{\alpha_{AC}-1} + A + \phi_B^D B \tag{4.35}$$

$$V_{min}^{C2} = \frac{A+\phi_B^D B}{\alpha_{AB}-1} \tag{4.36}$$

$$V_{min}^{C3} = \frac{\left(1-\phi_B^D\right) B + C}{\alpha_{BC}-1} + \left(1-\phi_B^D\right) B \tag{4.37}$$

where (4.36) and (4.37) are exact, whereas (4.35) is exact only for the "preferred" value given by Stichlmair (1988) $\phi^{pref} = (\alpha_{BC}-1)/(\alpha_{AC}-1)$. In the following analytical treatment we will only consider this preferred separation for the 3–column arrangement. (Note that a comprehensive discussion of this "preferred" separation will also be given in chapter 5 of this thesis.) Also note that the expression assumes a vapor feed to column $C2$. For liquid feed (total condenser), one must add an extra term A for the distillate term (D in equation (4.11)). Adding the terms in (4.37) we thus obtain the minimum overall boilup for the 3–column prefractionator arrangement

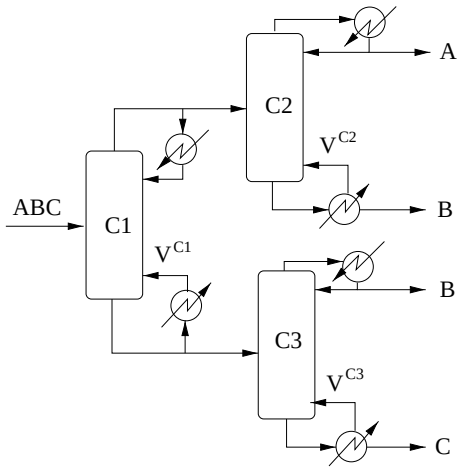

Figure 4.7: 3–column prefractionator arrangement for ternary separations

(V_{min}^{P3}) with a vapor feed to column $C2$.

$$V_{min}^{P3} = \frac{F}{\alpha_{AC}-1} + \frac{A+\phi_B^D B}{\alpha_{AB}-1} + \frac{\left(1-\phi_B^D\right)B+C}{\alpha_{BC}-1} + A + B \tag{4.38}$$

We have here used the simple fact that $A+B+C=F$. We here denote the prefractionator arrangement with three columns by $P3$, in order to distinguish it from the directly coupled Prefractionator to be introduced in the next section which has only two columns (i.e. $P2$).

The preferred separation. As previously mentioned, Stichlmair (1988) derived a simple explicit equation for the minimum boilup for the *preferred separation*. For the prefractionator $C1$ Stichlmair (1988) gives

$$V_{min}^{C1} = \frac{F}{\alpha_{AC}-1} + A + \frac{\alpha_{BC}-1}{\alpha_{AC}-1}B \tag{4.39}$$

If we then compare equation (4.39) with equation (4.37) derived from our method, we see that the equations are equal if the fraction of intermediate (ϕ_B^D) taken overhead is given by

$$\phi^{pref} = \frac{\alpha_{BC}-1}{\alpha_{AC}-1} \tag{4.40}$$

This is commonly used in the literature to denote the fractional recovery of B in the distillate requiring the minimum boilup (see e.g. Fidkowski and Krolikowski (1986)), without referring to this particular case as the preferred separation.

Fractional savings for 3–column prefractionator arrangement. In order to investigate the potential savings for the prefractionator arrangement relative to the

direct split, we may simply examine the difference between equation (4.38) and equation (4.21). Note that using equation (4.21) also for the indirect split sequence corresponds to choosing $\beta = 1$ in equation (4.31). Equating the difference between the direct sequence and the 3–column prefractionator arrangement, we obtain

$$\Delta V_{min} = V_{min}^{D} - V_{min}^{P3} = \frac{\left(1-\phi_B^D\right) B}{\alpha_{AB}-1} + \frac{\phi_B^D B}{\alpha_{BC}-1} - \frac{F}{\alpha_{AC}-1} \tag{4.41}$$

where superscript D denotes the direct split. Using equation (4.41) we may thus derive the following approximate expression for under what conditions the 3–column prefractionator arrangement requires a lower boilup

$$\Delta V_{min} > 0 \text{ iff } \frac{\phi_B^D B}{\alpha_{AB}-1} + \frac{\left(1-\phi_B^D\right) B}{\alpha_{BC}-1} > \frac{F}{\alpha_{AC}-1} \tag{4.42}$$

Hence, we find that the potential decrease in boilup does *not* depend on the amounts of A or C, but is a strict function of the relative volatilities and the amount of B. Before analyzing particular cases in terms of compositions and relative volatilities, we may give the "general" equation for the fractional savings for the prefractionator scheme relative to the direct scheme (and for the indirect split scheme with $\beta = 1$)

$$\frac{\Delta V_{min}}{V_{min}^{D}} = \frac{\frac{\left(1-\phi_B^D\right)B}{\alpha_{AB}-1} + \frac{\phi_B^D B}{\alpha_{BC}-1} - \frac{F}{\alpha_{AC}-1}}{\frac{A+B}{\alpha_{AB}-1} + \frac{B+C}{\alpha_{BC}-1} + A + B} \tag{4.43}$$

To obtain the fractional savings, we first obtain the difference between the "prefractionator" and the conventional direct (and indirect) split. By substituting for $\phi_B^D = \phi^{pref}$ from (4.40) in equation (4.41), we find after some algebra the following explicit condition for $\Delta V_{min} = V_{min}^{D} - V_{min}^{P3}$

$$\Delta V_{min} = \frac{B\left(\alpha_{AC} + \alpha_{AB} - \alpha_{BC} - 1\right) - F\left(\alpha_{AB} - 1\right)}{\left(\alpha_{AB}-1\right)\left(\alpha_{AC}-1\right)} \tag{4.44}$$

Hence we find a simple explicit equation in terms of the feed composition of intermediate B and the volatilities for when $\Delta V_{min} > 0$

$$\Delta V_{min} > 0 \quad \text{iff} \quad B > \frac{\alpha_{AB}-1}{\alpha_{AC} + \alpha_{AB} - \alpha_{BC} - 1} F \tag{4.45}$$

In order to obtain even simpler expressions we may first consider the situation in which the relative volatilities between the adjacent components are equal, i.e. $\alpha_{AB} = \alpha_{BC} = \alpha$. From equation (4.45) we thus obtain the following condition under which the prefractionator offer savings relative to the direct scheme

$$\begin{aligned} B &> \frac{\alpha-1}{\alpha^2-1} F = \frac{\alpha-1}{\left(\alpha-1\right)\left(\alpha+1\right)} F \\ \Leftrightarrow \quad B &> \frac{1}{\alpha+1} F \end{aligned} \tag{4.46}$$

where we have used the simple fact that $\alpha_{AC} = \alpha_{AB}\alpha_{BC} = \alpha^2$. For this particular case we thus find that the prefractionator arrangement allows savings only if the feed contains more than a certain lower amount of intermediate. For the fractional savings we obtain from equation (4.43) after some simple algebra

$$\frac{\Delta V_{min}}{V_{min}^{D}} = \frac{B\,(\alpha+1) - F}{(\alpha+1)\,[F + \alpha B + A\,(\alpha-1)]} \tag{4.47}$$

Hence we find that the fractional savings increase with the amount of intermediate B in the feed, and for the limiting case in which $B \to F$ we find that

$$\frac{\Delta V_{min}}{V_{min}^{D}} = \frac{\alpha}{(\alpha+1)^2} \tag{4.48}$$

Hence, the maximum savings of 25 % occur for close boiling mixtures where we have that $\alpha \approx 1$.

4.3.6 Directly Coupled Prefractionator

For the prefractionator arrangement considered in the last section, one needs $2(NC-1)$ condensers and reboilers. If we instead merge columns $C2$ and $C3$ via *direct coupling* as illustrated in Figure 4.8, we eliminate one condenser and one reboiler. Eliminating utilities thus in itself allows for additional reductions in the total energy requirement. Note in the following that we consider a partial condenser for the prefractionator column $C1$, and thus a vapor feed to $C2$ since this always is favorable in terms of the energy usage (e.g. Fidkowski and Krolikowski (1990)). One should also note that the energy "cost" may not decrease for practical (industrial) operation, since the heat requirement for the *main* column is added at the highest temperature and the cooling takes place at the lowest temperature. Thus, if the upper feed controls ($V^{C2} > V^{C3}$), all the heat to the main column is supplied at the highest temperature whereas for the 3–column arrangement only a portion of the heat (V^{C3}) is added here. This again refers the important distinction between exergy (levels) and energy (loads), since the reduction in energy loads comes at the expense of increasing the temperature levels at which the energy is supplied. However, we strongly emphasize that if the lower feed controls, there is *no* additional cost involved with the direct coupling, and that the directly coupled of course always have the smallest energy load. Before we proceed, there is an aspect that should be made clear since it is of great import for the analysis. For the directly coupled prefractionator arrangement there are two fortunate "coincidents". The first is that the simplified expression for the energy usage of the prefractionator is in fact exact when the preferred separation is carried out, and secondly that the preferred separation yields the overall minimum energy usage for the arrangement (Stichlmair 1988).

For the prefractionator arrangement in Figure 4.7, we have that the required boilup for column $C2$ is equal to the maximum for columns $C2$ and $C3$ (e.g. Stichlmair (1988) and Fidkowski and Krolikowski (1990)), which gives for the overall boilup V_{min}^{P2}

$$V_{min}^{P2} = V_{min}^{C1} + max\{V_{min}^{C2}, V_{min}^{C3}\} \tag{4.49}$$

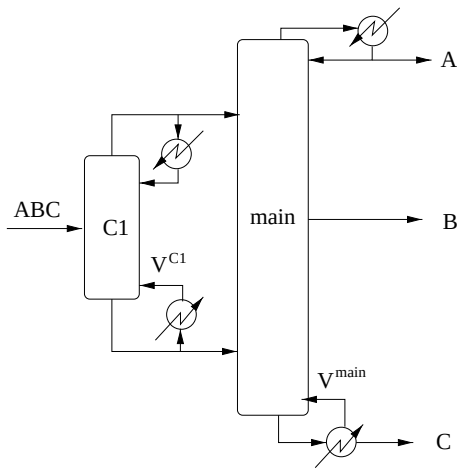

Figure 4.8: Prefractionator with direct coupling for ternary separations

where $V_{min}^{C1}, V_{min}^{C2}$ and V_{min}^{C3} are given by equations (4.35)–(4.37). We here use superscript $P2$ to denote that we use only two (coupled) columns as opposed to the previous 3–column arrangement ($P3$). Note that taking the maximum of either V_{min}^{C2} or V_{min}^{C3} in general applies only to the case of sharp separations, for which the main column undertakes the two binary separations A/B and B/C. To use the analytical equations for the prefractionator we thus need to determine under what conditions V_{min}^{C2} or V_{min}^{C3} will be the larger. In the literature this analysis is referred to as determining whether the upper feed (V^U) or lower feed controls (V^L). For this purpose one may thus simply equate the difference between V_{min}^{C2} and V_{min}^{C3} in equation (4.37). The condition for when the main column is balanced (i.e. $V_{min}^{C2} = V_{min}^{C3}$, may thus be written in terms of the fractional recovery of B

$$\phi^{bal} = \frac{(F-A)(\alpha_{AB}-1) + B(\alpha_{AB}-1)(\alpha_{BC}-1) - A(\alpha_{BC}-1)}{B((\alpha_{BC}-1) + (\alpha_{AB}-1) + (\alpha_{AB}-1)(\alpha_{BC}-1))} \tag{4.50}$$

where superscript *bal* denotes a balanced main column.

In order to find the minimum boilup for the directly coupled Prefractionator, we thus need to consider two distinct cases, for which either the upper or lower feed controls. As will be shown in chapter 5, the preferred separation is always optimal for the prefractionator column, so that the lower feed controls at the optimum if $\phi^{bal} > \phi^{pref}$, and the upper feed controls at the optimum if $\phi^{bal} < \phi^{pref}$. The equations for the minimum boilup are thus derived using equations (4.35)–(4.37)

(i) Upper feed controls, i.e. $\phi^{bal} < \phi^{pref}$

$$V_{min}^{P2U} = \frac{F}{\alpha_{AC}-1} + \frac{A+\phi^{pref}B}{\alpha_{AB}-1} + A + \phi^{pref}B \tag{4.51}$$

(ii) Lower feed controls, i.e. $\phi^{bal} > \phi^{pref}$

$$V_{min}^{P2L} = \frac{F}{\alpha_{AC}-1} + \frac{C + \left(1-\phi^{pref}\right) B}{\alpha_{BC}-1} + A + B \tag{4.52}$$

Fractional savings for directly coupled Prefractionator. Assume that $\phi_B^D = \phi^{pref}$ the expressions for the prefractionator arrangement are exact. Using the expression for direct split as a datum ($\beta = 1$ for the indirect split), we derive from equations (4.21) and (4.52) the following expression for the potential savings when the lower feed controls

$$\Delta V_{min}^{L} = V_{min}^{D} - V_{min}^{P2L} = \frac{A+B}{\alpha_{AB}-1} + \frac{B-F}{\alpha_{AC}-1} \tag{4.53}$$

Since $A + B \leq F$ we see from equation (4.53) that the largest savings arise for close boiling mixtures mixtures (i.e. small relative volatilities) with a large fraction of the intermediate component. Similarly, we find for the case when the upper feed controls

$$\Delta V_{min}^{U} = V_{min}^{D} - V_{min}^{P2U} = \frac{B\alpha_{AC}-F}{\alpha_{AC}-1} + \frac{B+C}{\alpha_{BC}-1} \tag{4.54}$$

By inspection we again find that the savings are largest for $B = F$ and small α_{ij}.

We thus consider in some more detail the limiting case with $B \to F$. Glinos and Malone (1988) report that the maximum savings in this case are 50%. We will here support these findings in terms of analytical equations derived from our method. As shown in Appendix A1, we find for the preferred separation that the lower feed controls in this case if and only if[1]

$$\alpha_{BC} < \frac{\alpha_{AC}+1}{2} \tag{4.55}$$

As also shown in the Appendix, we derive the following explicit equations for the fractional savings of the directly coupled Prefractionator relative to the conventional sequences

$$\frac{\Delta V_{min}^{U}}{V_{min}^{D}} = \frac{\alpha_{AC}-\alpha_{BC}}{\alpha_{AC}-1} \tag{4.56}$$

$$\frac{\Delta V_{min}^{L}}{V_{min}^{D}} = \frac{\alpha_{BC}-1}{\alpha_{AC}-1} \tag{4.57}$$

The maximum fractional savings were in both cases shown to be 50%, which occurs for

$$\alpha_{BC} = \frac{\alpha_{AC}+1}{2} \tag{4.58}$$

[1] Note that the simplified expressions for the direct and indirect splits are exact when $B \to F$

Furthermore, if we consider the case for which $\alpha_{AB} = \alpha_{BC} = \alpha$, we find from (4.55) that the lower feed controls always since the following condition always applies

$$\alpha < \frac{\alpha^2 + 1}{2} \quad \Leftrightarrow \alpha > 1 \tag{4.59}$$

In this case the fractional savings are

$$\frac{\Delta V^L_{min}}{V^D_{min}} = \frac{\alpha - 1}{\alpha^2 - 1} = \frac{1}{\alpha + 1} \tag{4.60}$$

The maximum fractional savings are thus 50%, which in this case occur for close boiling mixtures, i.e. $\alpha \to 1$. The expressions derived here are also important for the Petlyuk column, since its analogy to the prefractionator arrangement is close. We may therefore expect that the results derived here carry over also to the Petlyuk column, and when $\alpha_{ij} \to 1$ Fidkowski and Krolikowski (1986) in fact report that the savings approach 50% as for the prefractionator.

4.4 Optimal Column Arrangements for Ternary Separations

In this section we present numerical results which illustrate the optimality regions in composition space for the different distillation arrangements considered in the previous sections. We stress that all results are obtained from exact solutions using Underwood's method or the analytical equations proposed by Stichlmair (1988). For the prefractionator arrangement we use the results derived in the previous section, since they are exact for the preferred separation. In section 4.5 we then give results that quantify the errors when using the approximate method used in the previous analytical treatment.

4.4.1 Optimality Regions for Direct and Indirect Splits

The task of determining the optimal sequence for ternary splits is a very well known problem, and there is an exhaustive literature within this area. However, there still seems to be some ambiguity with respect to on what "basis" one should obtain the optimality regions for the different sequences. In the works by Glinos and Malone (1988) and Fidkowski and Krolikowski (1986) for instance, it seems to be taken for granted that the feeds to the downstream columns are in liquid phase. For the indirect split scheme this is as previously discussed suboptimal, since one may instead use a partial condenser and thus a vapor feed to the downstream column. The optimality regions presented in Glinos and Malone (1988) thus indicate that there is only a very small region within the composition space for which the indirect sequence is optimal. This applies to all three cases of "qualitatively" different separation, i.e. (1) separations for which the A/B split is as difficult as the B/C split ($\alpha_{AB} = \alpha_{BC}$), (2) separations where the A/B split is easier ($\alpha_{AB} > \alpha_{BC}$) and (3) separations where the A/B split is more difficult ($\alpha_{AB} < \alpha_{BC}$). However, we will demonstrate that this

situation is practically reversed if we consider indirect splits with partial condensers and thus vapor feed to subsequent columns.

$\alpha_{AB} = \alpha_{BC}$. We first consider the case for which the difficulty of separation is the same for the A/B and B/C splits. As shown in figure 4.9 we find that if we use a partial condenser and vapor feed, there is a considerably larger region of optimality for which the indirect split is the superior. The contours in Figure 4.9 (b) illustrates

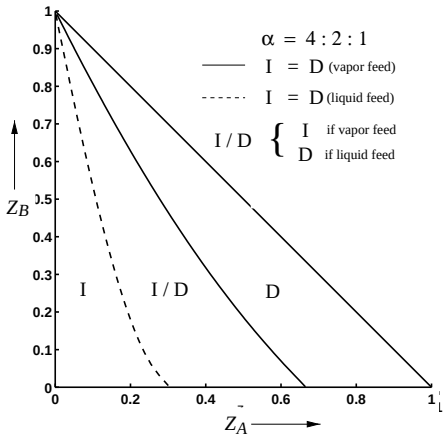

(a) Optimality regions

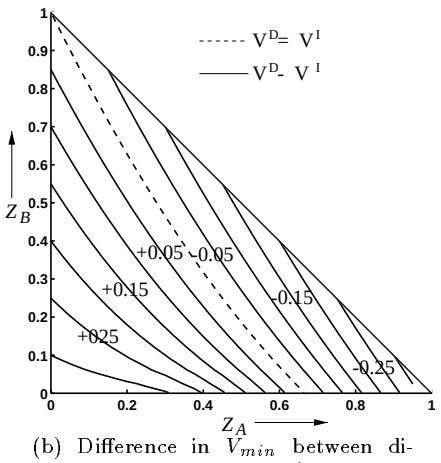

(b) Difference in V_{min} between direct and indirect sequence (partial condenser)

Figure 4.9: Optimality regions (a) and contour plots of difference in V_{min} (b) for indirect and direct split sequence for $\alpha = 4 : 2 : 1$. I and D denotes the regions where the indirect and direct sequences are optimal. A vapor (liquid) feed corresponds to using a partial (total) condenser in the first column for the indirect split.

the difference in molar boilups between the two schemes (i.e. $V^D_{min} - V^I_{min}$), from which we note that there is a certain symmetry along lines of constant C. Compared to the results of Glinos and Malone (1988) we thus find that considering only total condensers for the indirect split (i.e. liquid feeds) does not give a reasonable picture of the optimality regions. It is *always* favorable to use vapor feeds, irrespective of direct or indirect splits, as also stressed by King (1971) and Stichlmair (1988). In order to examine how the optimality regions are affected by the difficulty of the binary separations, we also investigate two complementary cases for which the A/B split is easier than the B/C split ($\alpha_{AB} > \alpha_{BC}$) and more difficult ($\alpha_{AB} < \alpha_{BC}$).

$\alpha_{AB} > \alpha_{BC}$. In Figure 4.10 we illustrate that the region in which the indirect split is favorable is enlarged if the A/B split becomes easier relative to the B/C split. From the contour plots we also find that the difference becomes large for almost equimolar mixtures of A and B with small amounts of B. These findings thus contradicts the common heuristic "do the easiest split first" (e.g.Douglas (1988)), in which the direct

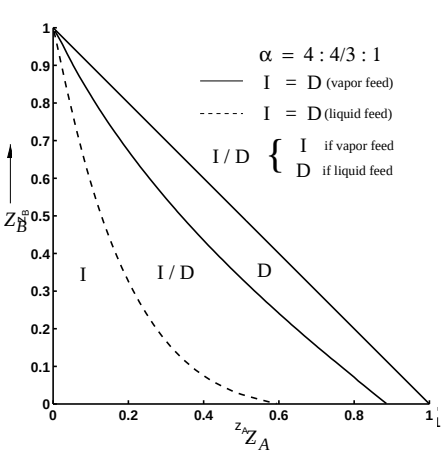

(a) Optimality regions

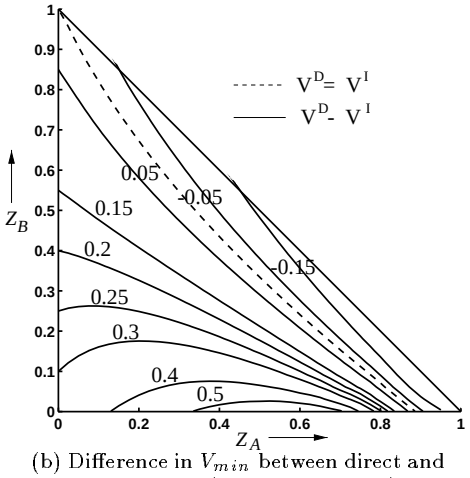

(b) Difference in V_{min} between direct and indirect sequence (partial condenser)

Figure 4.10: Optimality regions (a) and contour plots for difference in V_{min} (b) for indirect and direct split sequence for $\alpha = 4 : 4/3 : 1$

split in this case should be preferred since $\alpha_{AB} > \alpha_{BC}$. Our results support the previous findings by Glinos and Malone (1988).

$\alpha_{AB} < \alpha_{BC}$. In Figure 4.11 we give the optimality regions in the case where the B/C split is easier than the A/B split. By comparing Figures 4.11 and 4.9 we find that the region of optimality for the indirect split decreases as α_{AB} decreases relative to α_{AC}, again opposing the heuristic of performing the easiest split first.

4.4.2 3–column prefractionator arrangement

As indicated in the previous analytical treatment, there may be cases where the 3–column prefractionator arrangement requires lower energy usage than the indirect or direct split schemes. We may note that the 3–column arrangement in most cases is not likely to be used in practice. Its significance lies however in that is useful in understanding the stepwise procedure towards the directly coupled prefractionator. In figures 4.12 4.13 and 4.14 we illustrate the optimality regions for the 3–column arrangement versus the conventional schemes, and contour plots for the relative savings in energy usage. In the contour plots we have compared the energy usage of the 3–column arrangement to the best (V_{opt}) of the direct and indirect split schemes respectively, i.e.

$$\frac{\Delta V_{min}}{V_{opt}} = \frac{Max\{V^D_{min}, V^I_{min}\} - V^{P3}_{min}}{Max\{V^D_{min}, V^I_{min}\}} \cdot 100\% \tag{4.61}$$

where V^{P3}_{min} s given by equation (4.38) and V_{min} for the direct and indirect schemes are computed iteratively from the *exact* analytical equations presented by Stichlmair

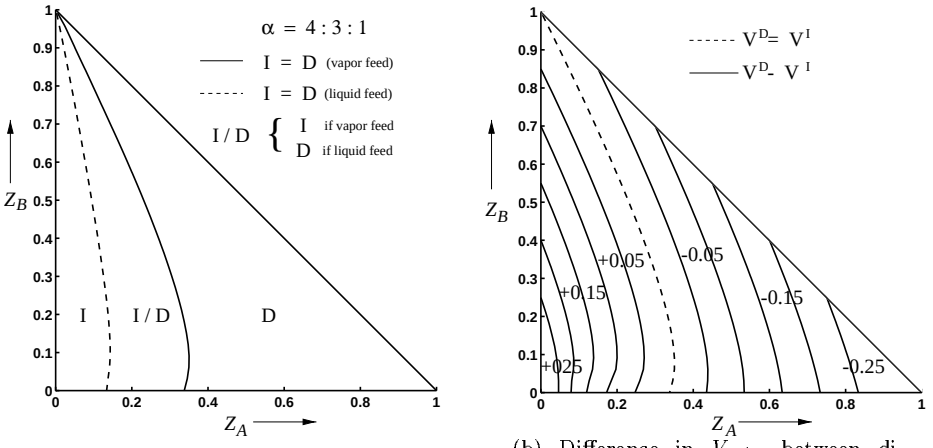

(a) Optimality regions

(b) Difference in V_{min} between direct and indirect sequence (partial condenser)

Figure 4.11: Optimality regions (a) and contour plots for difference in V_{min} (b) for indirect and direct split sequence for $\alpha = 4 : 3 : 1$

(1988). From the previous analytical treatment, we found in the special case when $\alpha_{AB} = \alpha_{BC}$, that the maximum savings should occur when $B \to F$. From equation (4.48) the maximum savings are

$$\frac{\Delta V_{min}}{V^D_{min}} = \frac{\alpha}{(\alpha+1)^2} \tag{4.62}$$

Substituting $\alpha = 2$ yields maximum savings of 22.2% which indeed is verified in Figure 4.12 (b). Computations also show that the savings approach 25% as $\alpha_{ij} \to 1$ (not shown here).

For the other two mixtures illustrated in Figures 4.13 and 4.14, we also find as expected that the optimality regions depend strongly on the relative volatilities. It is interesting to note that the region where the 3–column arrangement is optimal, is largest when the A/B split is the most difficult. This is due to using a partial condenser for the prefractionator column, which as previously shown reduces the energy consumption of column $C2$ with a term equal proportional feed rate of A. Recall that when the A/B split is most difficult, column $C2$ will usually dominate the energy usage.

4.4.3 Directly Coupled Prefractionator

Finally we consider the directly coupled Prefractionator, which should display the highest energy efficiency compared to the previous schemes. From our analytical results we showed that the largest savings amount to 50%, which occurs in the limiting

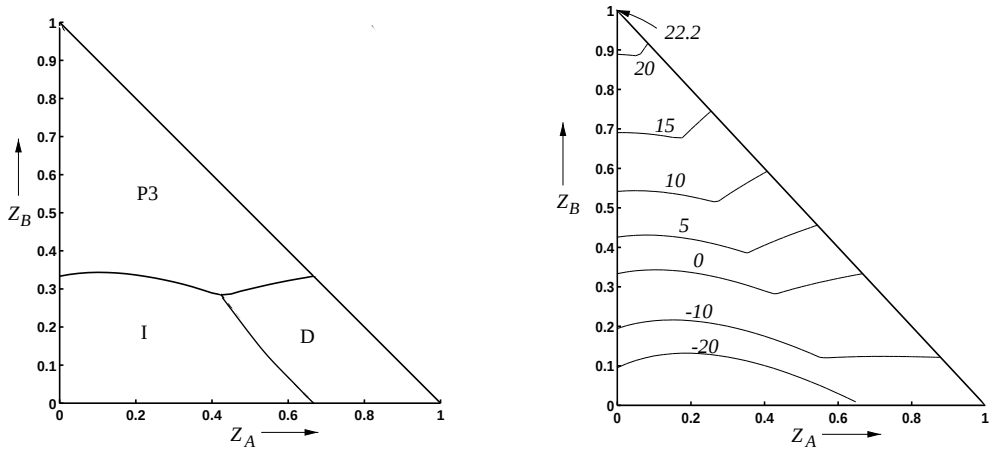

(a) Optimality regions (b) Contour plots of $\Delta V_{min}/V_{opt}$

Figure 4.12: Optimality regions for ternary separations (a) and contour plots (b) of relative savings for 3–column prefractionator arrangement with $\alpha = 4 : 2 : 1$

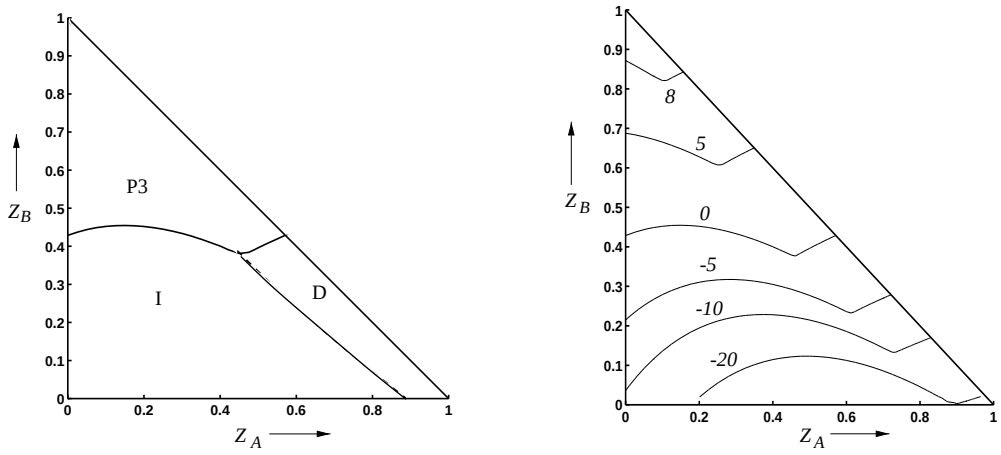

(a) Optimality regions (b) Contour plots of $\Delta V_{min}/V_{opt}$

Figure 4.13: Optimality regions for ternary separations (a) and contour plots (b) of relative savings for 3–column prefractionator arrangement with $\alpha = 4 : 4/3 : 1$

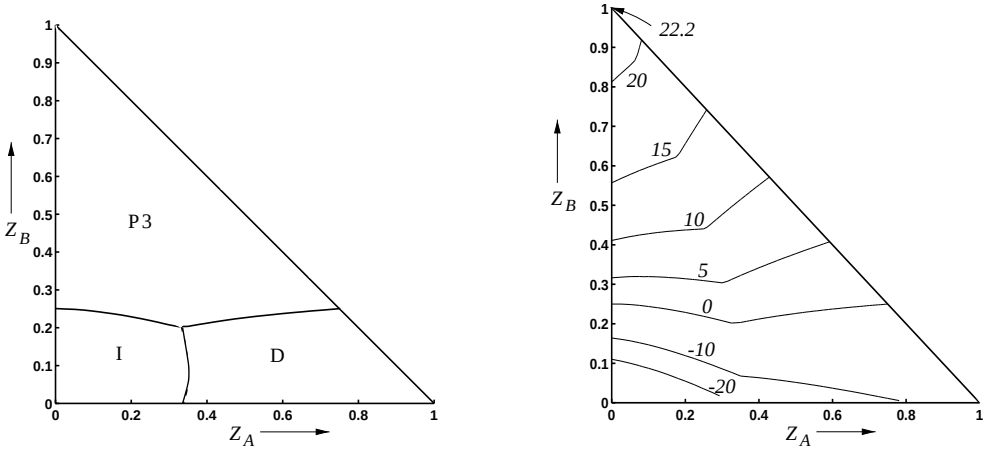

(a) Optimality regions (b) Contour plots of $\Delta V_{min}/V_{opt}$

Figure 4.14: Optimality regions for ternary separations (a) and contour plots (b) of relative savings for 3–column prefractionator arrangement with $\alpha = 4:3:1$

case when $B \to F$ and in cases where $\alpha_{ij} \to 1$ and when the relative volatilities satisfies $\alpha_{BC} = (\alpha_{AC} + 1)/2$. In order to compare the numerical results with the findings from the analytical treatment, we consider here three different cases. Note again that the relative savings are obtained using V_{min}^{P2} from equation (4.49) in equation (4.61) and *exact* solutions for the indirect and direct schemes.

(i) $\alpha_{AB} = \alpha_{BC} = \alpha$

In Figure 4.15 we give results for the optimality regions and the relative savings for an example where $\alpha = 2$. The numerical computations show that the largest fractional savings amounts to 33% when $B \to 1$. For this case we have that the lower feed controls, and the numerical results thus confirm the analytical results given by equation (4.57), i.e.

$$\frac{\Delta V_{min}^{L}}{V_{min}^{D}} = \frac{\alpha_{BC} - 1}{\alpha_{AC} - 1} = 33\% \tag{4.63}$$

(ii) $\alpha_{BC} = \frac{\alpha_{AC}+1}{2}$

Numerical results for such a case, where we chose $\alpha_{AB} = 1.6$ and $\alpha_{BC} = 2.5$, are shown in Figure 4.16. From Figure 4.16 (a) we find that there are only very small regions in the composition space where the indirect or direct split schemes require a smaller energy usage. The only cases where the prefractionator arrangement is suboptimal, is as expected when the feed mixture contains mostly light or heavy component. From the analytical results we found as given in equation (4.58), that

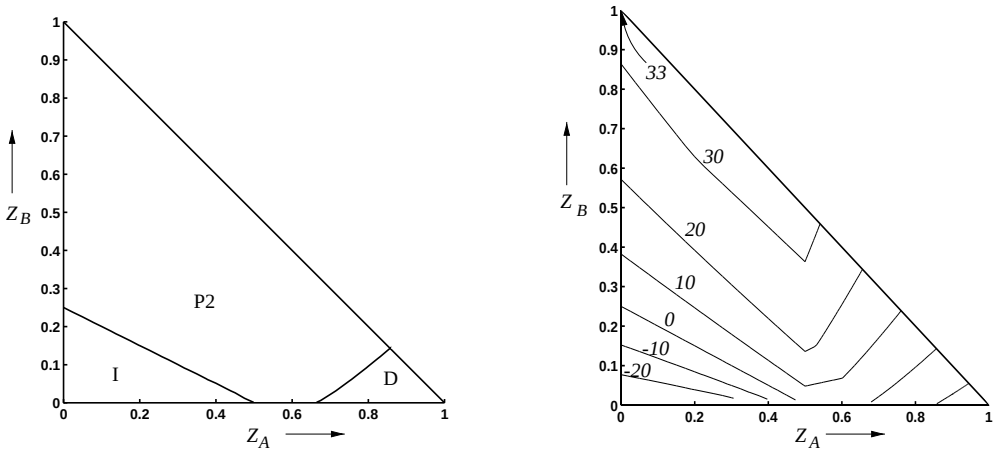

(a) Optimality regions (b) Contour plots of $\Delta V_{min}/V_{opt}$

Figure 4.15: Optimality regions for ternary separations (a) and contour plots (b) of relative savings for directly coupled Prefractionator with $\alpha = 4 : 2 : 1$

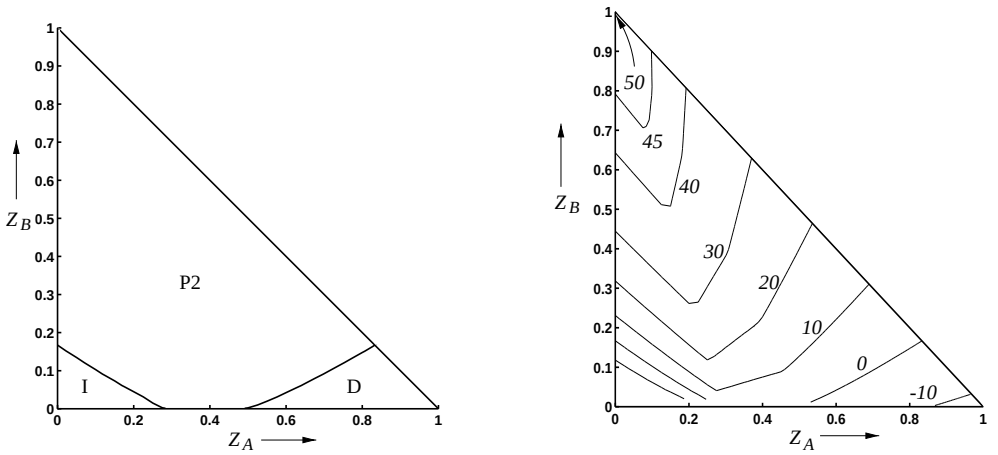

(a) Optimality regions (b) Contour plots of $\Delta V_{min}/V_{opt}$

Figure 4.16: Optimality regions for ternary separations (a) and contour plots (b) of relative savings for directly coupled Prefractionator with $\alpha = 4 : 2.5 : 1$

this particular set of relative volatilities, for which the main column is "balanced", should give the largest fractional savings when $B \to F$, i.e.

$$\frac{\Delta V_{min}}{V^D_{min}} = \frac{\alpha_{BC} - 1}{\alpha_{AC} - 1} = 50\% \tag{4.64}$$

The results for the relative savings in Figure 4.16 (b) thus confirms the analytical results.

(iii) $\alpha_{ij} \to 1$

Finally we consider the limiting case of close boiling mixtures, where $\alpha_{ij} \to 1$. As indicated by equation (4.60), the maximum savings should also in this case approach 50% when $B \to 1$. In Figure 4.17 (a) we give the optimality regions in a case where $\alpha_{AB} = \alpha_{BC} = 1.1$. In fact, we find that the optimality region decreases somewhat compare to the previous two cases. As shown in Figure 4.17 (b), the relative savings approach 50% when $B \to F$.

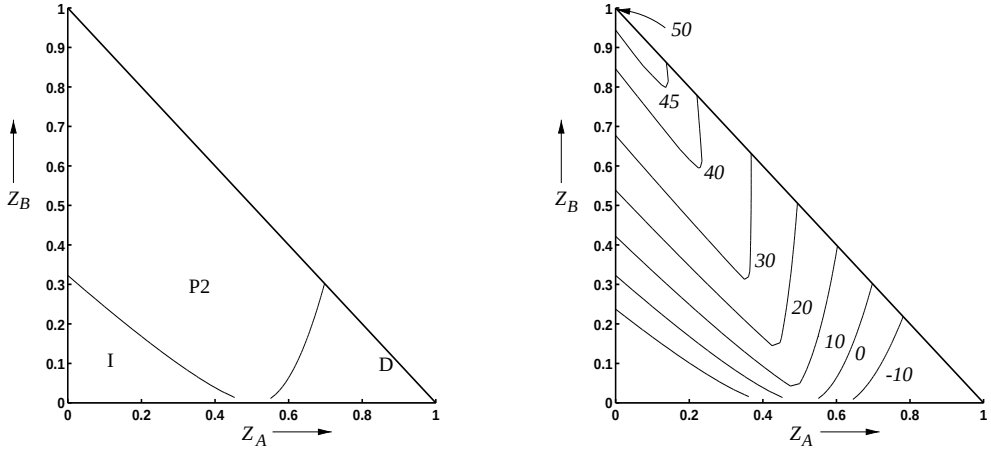

(a) Optimality regions (b) Contour plots of $\Delta V_{min}/V_{opt}$

Figure 4.17: Optimality regions for ternary separations (a) and contour plots (b) of relative savings for directly coupled Prefractionator with $\alpha = 1.21 : 1.1 : 1$

4.5 Error Analysis for Proposed Shortcut Method

In this section we give numerical results to quantify the errors associated with the proposed shortcut method. We previously argued that the most important asset of the method, was to obtain qualitative information that is otherwise not available from exact methods such as Underwood's method. Nevertheless, in order to analyze the goodness of the analytical results it is still of importance to quantify the errors relative

to the exact methods. We furthermore showed that the most important application of the method, is to indicate the relative savings for the directly coupled prefractionator. The reason for the latter is as previously mentioned twofold: (*i*) the expressions are exact for the preferred separation and (*ii*) the preferred separation is always optimal for this arrangement. Hence, the errors are expected to be small in this case.

Since the equations are exact for the prefractionator, the errors in the relative savings are only due to the expressions for the indirect and direct sequences. In Figure 4.18 we compare the approximate results with exact solutions for the relative savings of the prefractionator arrangement. As seen in the Figure we find that the approximate equations give reasonably accurate predictions within the whole region where the directly coupled prefractionator is optimal, and not only in certain limiting cases such as $B \rightarrow F$.

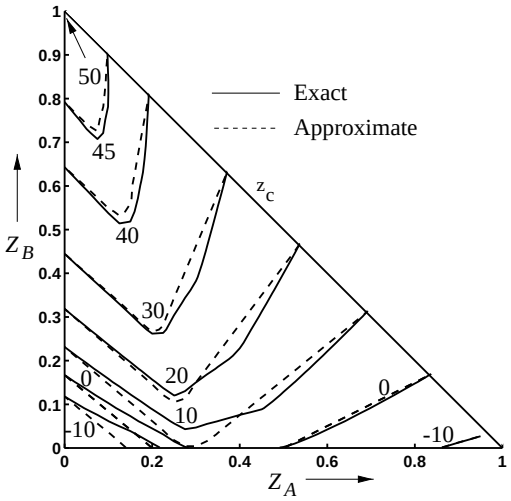

Figure 4.18: Comparison of exact and approximate solutions for directly coupled prefractionator arrangement. The contour plots are obtained for $\alpha = 4 : 2.5 : 1$.

However, even though the errors usually are small when we use the method to predict the savings for the prefractionator *arrangement*, the errors may become large in certain regions of the composition space when we use the method only for the conventional arrangements. As previously discussed the shortcut method provides a lower bound for the *direct split*. For the indirect split, the situation is somewhat more complex and it is difficult to predict the "sign" of the errors. As was illustrated graphically in a previous section, the error is due assuming that the mapped pinch composition of the binary mixture leaving the first column is equal to the relative feed composition. The error will thus depend on the locus of the ternary feed mixture in composition space. Furthermore, the magnitude depends on whether one considers the error for the *sequence* of two columns, or only for the first column. The latter case is the "formally" correct, since the analytical results for the binary columns are exact, i.e. the error is solely due to the simplified equation for V_{min}^{D} in the first column ($C1$).

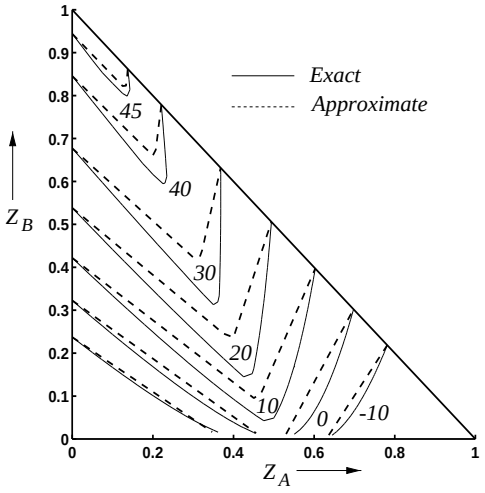

Figure 4.19: Comparison of exact and approximate solutions for directly coupled prefractionator arrangement. The contour plots are obtained for $\alpha = 1.21 : 1.1 : 1$.

However, we again stress that our objective is to give a simple analytical method for the minimum reboil, to enable a quick and analytical comparison of different column *arrangements*. Hence, for the sake of argument we may claim that the relative errors for single regular columns are of less importance than the overall error for the arrangement. Numerical results for the error analysis of the conventional schemes are given in Appendix B.

4.6 Conclusions

In this paper we have proposed an *explicit* shortcut method to compute the minimum energy usage for multicomponent separations. The method is only approximate, although in certain limiting cases it yields exact results. The most important feature of this method, is that it may easily be used to provide qualitative information which is difficult to obtain from exact methods such as Underwood's method. In this paper we use the shortcut method to illustrate the optimality regions of different distillation arrangements. For ternary separations we provided a comprehensive analysis, in which we obtained analytical expressions for the relative differences between the different arrangements. For instance, we derived simple expressions that indicate for which mixtures the largest relative savings are obtained for a prefractionator arrangement, relative to conventional schemes. These findings are then verified by exact numerical solutions of the set of Underwood equations, or from analytical solutions of these found in the literature. We also demonstrate the importance of using partial condensers for downstream columns, since the use of only total condensers is often assumed in the literature. For the direct and indirect schemes, we show that taking this into account increases the optimality regions for the indirect scheme considerably. We

however emphasize that caution must be used when applying the proposed method. In terms of an error analysis we demonstrate that in certain cases the relative errors may become large.

Nomenclature

A, B, C – Feed rate of chemical species [kmol/min]
D – Distillate flow rate [kmol/min]
D_i – Distillate flow rate of component i [kmol/min]
f – Parameter in minimum reflux expression, i.e. $f = 1 + B/(F \cdot 100)$
F – Feed flow rate [kmol/min]
F_i – Feed flow rate of component i [kmol/min]
HK – Heavy key
L – Reflux flow rate [kmol/min]
LK – Light key
NC – Number of components
q – Feed enthalpy
R – External reflux ratio, i.e. L/D
R_F – Ratio between minimum and actual reflux
S – Separation factor
V – Boilup from reboiler [kmol/min]
x_i – Liquid mole fraction of component i
x_{Di} – Liquid mole fraction of component i in distillate
x_P – Mapped liquid mole fraction at pinch point
y_i – Vapor mole fraction of component i
y_{Fi} – Liquid mole fraction of component i in feed
z_i – Liquid mole fraction of component i in feed

Greek letters

α_{ij} – Relative volatility between components i and j
Δ – Deviation variable
ϕ^{pref} – Fractional recovery of component B for the preferred separation
ϕ^{bal} – Fractional recovery of component B for a balanced main column
ϕ_i^B – Fractional recovery of component i in bottom flow
ϕ_i^D – Fractional recovery of component i in distillate flow

Sub– and superscripts

bal – Balanced main (sidestream) column
D – Direct split
I – Indirect split
min – Minimum flow conditions for infinite number of stages
$pref$ – Preferred separation

References

Douglas, J. M. (1988). *Conceptual Design of Chemical Processes.* McGraw–Hill Book Company.

Fidkowski, Z. and L. Krolikowski (1986). Thermally Coupled system of Distillation Columns: Optimization Procedure. *AIChE Journal* **32**(4), 537–546.

Fidkowski, Z. and L. Krolikowski (1990). Energy Requirements of Nonconventional Distillation Systems. *AIChE Journal* **36**(8), 1275–1278.

Glinos, K. and M.F. Malone (1984). Minimum Reflux, Product Distribution, and Lumping Rules for Multicomponent Distillation. *Ind. Eng. Chem. Process Des. Dev.* pp. 764–768.

Glinos, K. and M.F. Malone (1988). Optimality Regions for Complex Column Alternatives in Distillation Systems. *Chem. Eng. Res. Des.* **66**(3), 229–240.

King, C. J. (1971). *Separation Processes.* McGraw-Hill Chemical Engineering Series. McGraw-Hill Book Company.

Köhler, J., P. Poelmann and E. Blass (1995). A Review on Minimum Energy Calculations for Ideal and Nonideal Distillations. *Ind. Eng. Chem. Res.* **34**(4), 1003–1020.

Petlyuk, F. B., V. M. Platonov and D. M. Slavinskij (1965). Thermodynamically Optimal Method for Separating Multicomponent Mixtures. *Int. Chem. Eng.* **5**(3), 555–561.

Porter, K. E. and S. O. Momoh (1991). Finding the Optimum Sequence of Distillation columns - an Equation to Replace the "Rules of Thumb" (Heuristics). *Chem. Eng. Journal* **46**, 97–108.

Smith, R. (1995). *Chemical Process Design.* Wiley.

Stichlmair, J. (1988). Distillation and Rectification. *Ullmann's Encyclopedia of Industrial Chemistry* **B3**, 4–1 – 4–94.

Appendix A Analytical Results for "Preferred Separation"

As previously mentioned there are two distinguished operating regions for the Prefractionator, for which either the upper ($V^{C2} > V^{C3}$) or lower feed ($V^{C3} > V^{C2}$) controls. In this section we are thus concerned with the fractional savings between the direct sequence (and indirect with $\beta = 1$) and the Prefractionator for these two cases. From the previous analysis we find the following equations for when the upper feed controls ($V^U_{min} = V^{C1} + V^{C2}$),

$$V^U_{min} = \frac{F}{\alpha_{AC} - 1} + \frac{A + \phi^D_B B}{\alpha_{AB} - 1} + A + \phi^D_B \; B \tag{4.65}$$

and when the lower feed controls ($V^L_{min} = V^{C1} + V^{C3}$)

$$V^L_{min} = \frac{F}{\alpha_{AC} - 1} + \frac{\left(1 - \phi^D_B\right) B + C}{\alpha_{BC} - 1} + A + B \tag{4.66}$$

In order to obtain the maximum fractional savings we consider the limiting case in which $B \to F$. We thus need to determine under what conditions the upper and the lower feed controls respectively. From equations (4.65) and (4.66) we thus obtain

$$V^L_{min} - V^U_{min} = F\left(\left(1-\phi^D_B\right) + \frac{\left(1-\phi^D_B\right)}{\alpha_{BC}-1} - \frac{\phi^D_B}{\alpha_{AB}-1}\right) \tag{4.67}$$

After expanding the right hand side, we find that the lower feed controls if the following condition is satisfied

$$\left(1-\phi^D_B\right)\left(\alpha_{BC}-1\right)\left(\alpha_{AB}-1\right) + \left(1-\phi^D_B\right)\left(\alpha_{AB}-1\right) - \phi^D_B\left(\alpha_{BC}-1\right) > 0 \tag{4.68}$$

After some algebra this expression simplifies to

$$V^L_{min} > V^U_{min} \quad \text{iff} \quad \phi^D_B < \frac{\alpha_{AC}-\alpha_{BC}}{\alpha_{AC}-1} \tag{4.69}$$

Substituting for ϕ^D_B from expression (4.40) for the preferred separation, we thus find

$$V^L_{min} > V^U_{min} \quad \text{iff} \quad \alpha_{BC} < \frac{\alpha_{AC}+1}{2} \tag{4.70}$$

We should comment that this is of course exactly the same as examining the difference between columns V^{C2} and V^{C3} for the 3–column prefractionator arrangement. It is also reasonable that the lower feed controls when the B/C split is difficult relative to the A/B split, i.e. when α_{BC} is small relative to α_{AB}.

A.1 Upper feed controls : $\alpha_{BC} > \frac{\alpha_{AC}+1}{2}$

For the limiting case when $B \to F$ we obtain from equation (4.21) for the direct sequence

$$\left(\frac{V^D}{F}\right)_{min} = 1 + \frac{1}{\alpha_{AB}-1} + \frac{1}{\alpha_{BC}-1} \tag{4.71}$$

Again expanding the fractions we may rewrite this to

$$\left(\frac{V^D}{F}\right)_{min} = \frac{\left(\alpha_{AB}-1\right)\left(\alpha_{BC}-1\right) + \left(\alpha_{AB}-1\right) + \left(\alpha_{BC}-1\right)}{\left(\alpha_{AB}-1\right)\left(\alpha_{BC}-1\right)} \tag{4.72}$$

$$= \frac{\alpha_{AC}-1}{\left(\alpha_{AB}-1\right)\left(\alpha_{BC}-1\right)} \tag{4.73}$$

$$= \frac{1}{\phi^{pref}\left(\alpha_{AB}-1\right)} \tag{4.74}$$

For the Prefractionator we find from equation (4.65)

$$\left(\frac{V^U}{F}\right)_{min} = \frac{1}{\alpha_{AC}-1} + \frac{\phi^{pref}}{\alpha_{AB}-1} + \phi^{pref} \tag{4.75}$$

We may simplify this expression by substituting for ϕ^{pref} from equation (4.40) which gives

$$\left(\frac{V^U}{F}\right)_{min} = \frac{(\alpha_{AB}-1)+(\alpha_{BC}-1)+(\alpha_{AB}-1)(\alpha_{BC}-1)}{(\alpha_{AC}-1)(\alpha_{AB}-1)} \quad (4.76)$$

$$= \frac{\alpha_{AC}-1}{(\alpha_{AC}-1)(\alpha_{AB}-1)} \quad (4.77)$$

$$= \frac{1}{\alpha_{AB}-1} \quad (4.78)$$

Equating the difference between the Prefractionator and the direct split in equations (4.74) and (4.78) we derive

$$\left(\frac{\Delta V^U}{F}\right)_{min} = \frac{1-\phi^{pref}}{\phi^{pref}(\alpha_{AB}-1)} \quad (4.79)$$

Using equations (4.74) and (4.79) we find the relative difference between the direct split and Prefractionator, which is simply given by

$$\frac{\Delta V^U_{min}}{V^D_{min}} = 1-\phi^{pref} \quad (4.80)$$

$$= \frac{\alpha_{AC}-\alpha_{BC}}{\alpha_{AC}-1} \quad (4.81)$$

Hence, to obtain the largest savings we want ϕ^{pref} to be as small as possible. From equation (4.81) we thus find that the largest savings correspond to choosing $\alpha_{BC}=1$. However, as previously shown, there are lower bounds on ϕ^{pref} and thus α_{BC}, as given by conditions (4.69) and (4.70). The maximum fractional savings savings are thus obtained when $\alpha_{BC}=(\alpha_{AC}+1)/2$. Substituting this in equation (4.81) we thus obtain

$$\left(\frac{\Delta V^U_{min}}{V^D_{min}}\right)_{Max} = \frac{\alpha_{AC}-\frac{\alpha_{AC}-1}{2}}{\alpha_{AC}-1} = 50\% \quad (4.82)$$

A.2 Lower feed controls : $\alpha_{BC} < \frac{\alpha_{AC}+1}{2}$

Again for the limiting case when $B \to F$, we use the following formula for the direct split

$$\left(\frac{V^D}{F}\right)_{min} = \frac{1}{\alpha_{AC}-1} + \frac{1}{\alpha_{BC}-1} + 1 \quad (4.83)$$

For the prefractionator equation (4.66) gives

$$\left(\frac{V^L}{F}\right)_{min} = \frac{1}{\alpha_{AC}-1} + \frac{1-\phi^D_B}{\alpha_{BC}-1} + 1 \quad (4.84)$$

Taking the difference between equations (4.83) and (4.84) and substituting for ϕ_B^D gives

$$\left(\frac{\Delta V^L}{F}\right)_{min} = \frac{1}{\alpha_{AB}-1} + \frac{\phi_B^D}{\alpha_{BC}-1} - \frac{1}{\alpha_{AC}-1} \tag{4.85}$$

$$= \frac{1}{\alpha_{AB}-1} \tag{4.86}$$

And finally, using equations (4.86) and (4.74) we find the following simple equation for the fractional savings

$$\frac{\Delta V_{min}^L}{V_{min}^D} = \phi_B^D \tag{4.87}$$

$$= \frac{\alpha_{BC}-1}{\alpha_{AC}-1} \tag{4.88}$$

Thus in this case we want ϕ_B^D to be as large as possible to obtain the largest savings. However, there is in this case an *upper* bound on ϕ_B^D as given by (4.69). Hence the largest savings arise when both ϕ_B^D and thus also α_{BC} are equal to their respective upper bounds. Substitution then gives

$$\left(\frac{\Delta V_{min}^L}{V_{min}^D}\right)_{Max} = \frac{\frac{\alpha_{AC}+1}{2}-1}{\alpha_{AC}-1} = \underline{50}\% \tag{4.89}$$

Appendix B Error Analysis for Conventional Arrangements

In this section we provide numerical results for the relative errors when using the proposed shortcut method to estimate V_{min} for the conventional direct and indirect sequences.

B.1 Relative Error for Direct Sequence

We first consider the relative errors for the direct sequence, for which we will confirm that the proposed method always gives a lower bound for V_{min}^D. The relative error is for all cases computed by

$$\text{Error} = \frac{V^{exact} - V^{approx}}{V^{exact}} * 100 \tag{4.90}$$

(i) $\alpha_{AB} = \alpha_{BC}$

If we only consider the relative error for column $C1$, we find from the simulations that the relative error approaches 100%. This apparently "large" difference follows since the approximate V_{min}^{C1} approaches zero as the mole fraction of heavy component $z_C \to 1$. However, if we on the other hand consider the upper bound for V_{min} proposed

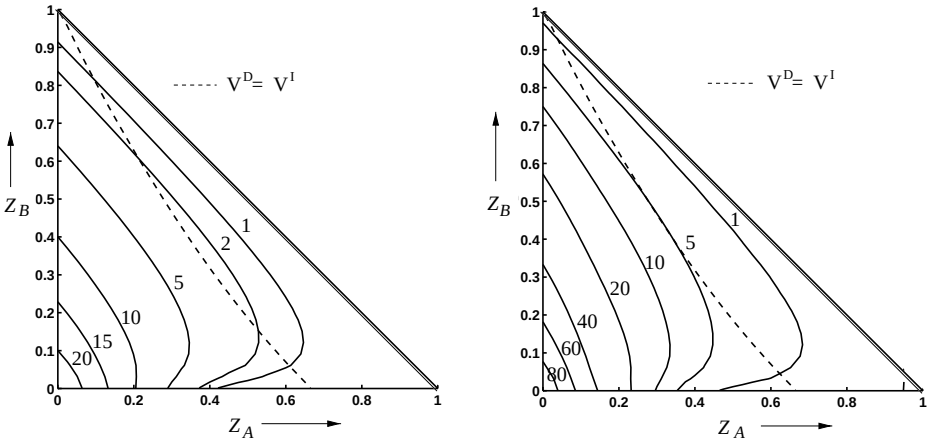

(a) Sequence, i.e. $C1 + C2$ (b) Column $C1$

Figure 4.20: Contour plots of relative error in V_{min} for direct split sequence with $\alpha = 4 : 2 : 1$

by King (1971) and Porter and Momoh (1991), the error is in fact as large as 300%. Furthermore, we make the interesting observation that the error is in fact very small within the region where the direct split is optimal. If we consider the contour plots of the relative error shown in Figure 4.20 (a), the maximum error within the region of optimality for the direct split is only 2.5%. We also note that the error is much smaller for the sequence compared to the binary column. This owes solely to the fact that our proposed method is exact for binary splits. Also note that the relative error is always grater than zero, which confirms that our method gives a lower bound on V^D_{min}.

(ii) $\alpha_{AB} \neq \alpha_{BC}$

In Figure 4.21 we give the relative errors for the cases of $\alpha_{AB} < \alpha_{BC}$ (a) and $\alpha_{AB} > \alpha_{BC}$ (b). Interestingly we find in the latter case that the errors for the sequence are small within the whole of the composition space, and the maximum error within the region where the direct split is optimal is only 1.5%.

B.2 Relative Error for Indirect Sequence

For the direct split, we found that the proposed method for obtaining the minimum reboil in fact yields a lower bound for V^D_{min}. However, for the indirect split the picture is not that simple. In this case one also needs to determine the fraction of the low boiler to be added in the "distillate term" (β in equation (4.31)). If we use $\beta = 0$ the proposed method will always give a lower bound. However, the prediction will then in most cases be very optimistic. Given the ambiguity with respect to β, it might be of interest to give an interpretation of $\beta = f(A, B, C)$, to indicate the appropriate value to be used within the different regions of the composition space. However, for

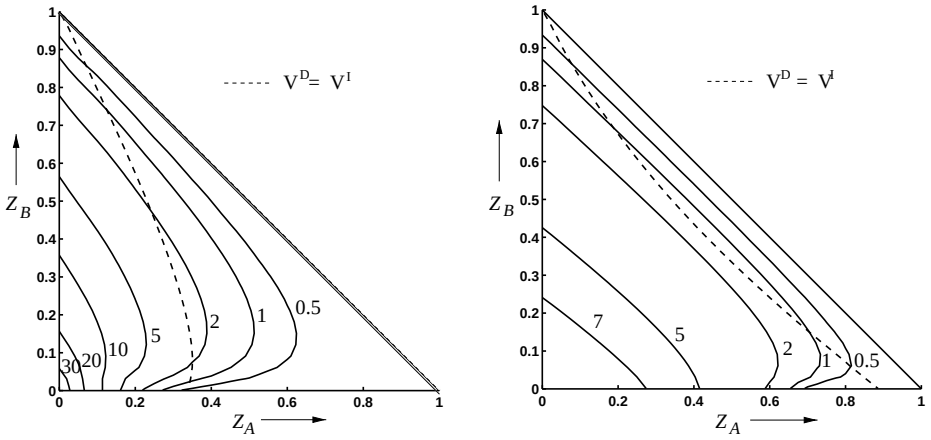

(a) $\alpha = 4:3:1$ (b) $\alpha = 4:4/3:1$

Figure 4.21: Contour plots of relative error in V_{min} for direct split sequence

the sake of consistency and simplicity, we have chosen to use $\beta = 1$ for the numerical results. In contrast to the situation for the direct split, it is difficult to predict the sign (lower or upper bound) of the relative error compared to the exact results due to the impact of β.

$\boldsymbol{\alpha_{AB} = \alpha_{BC}}$ In Figure 4.22 we find that the relative error is zero along the BC apex (binary split) and along a given line within the ternary region. The relative error then increases to a maximum of -20% along the binary edge of AC. As expected we find that using $\beta = 1$ gives neither a lower or upper bound.

$\boldsymbol{\alpha_{AB} \neq \alpha_{BC}}$ Relative errors for the two other qualitatively different separations are displayed in Figure 4.23. From the results we find that the magnitude of the (maximum) errors decrease as the region of optimality for the indirect split decreases. The maximum errors are still within 20%.

B.3 Relative Error Compared to Optimal sequence

When comparing the relative errors in the approximate equations for the direct and indirect splits, we found that the errors may be quite large outside the regions in composition space where the particular sequence (direct/indirect) is optimal. It is therefore of interest to compute the relative errors for the proposed method compared to the *optimal sequence* within each region. The results for $\alpha_{AB} = \alpha_{BC}$ are displayed in Figure 4.24. As seen in the Figure we find that within the region where the direct split sequence is optimal, the relative error is very small, i.e. approximately. 1-2 % depending on the relative volatilities. However, for the indirect split sequence we still face the problem of determining the fraction β as previously discussed. Results for other relative volatilities are displayed in Figures 4.25.

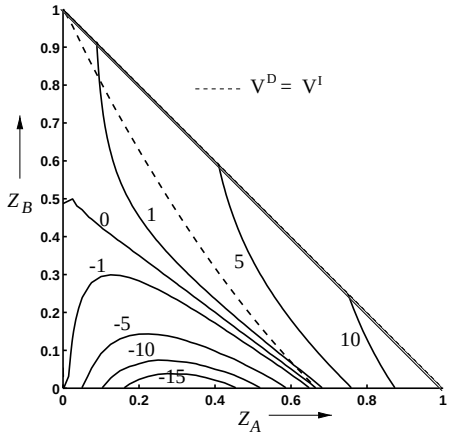

Figure 4.22: Contour plot of relative error in V_{min} for indirect split sequence with $\alpha = 4 : 2 : 1$

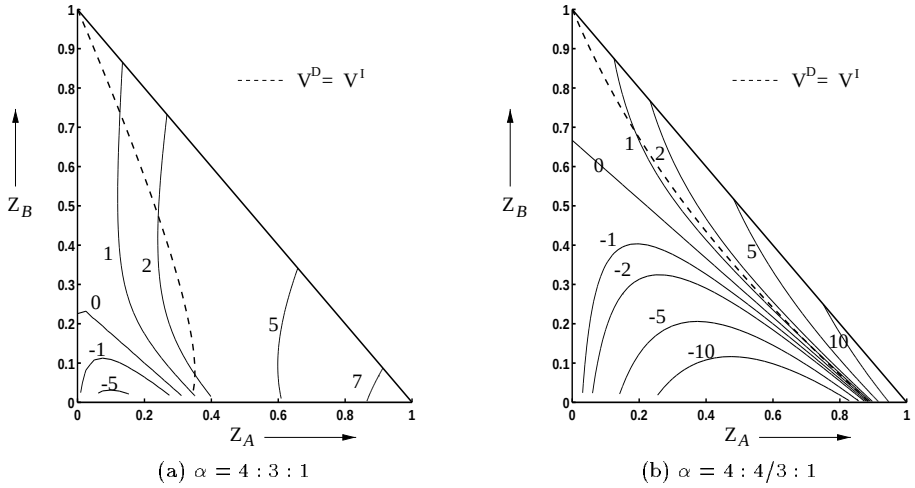

(a) $\alpha = 4 : 3 : 1$ (b) $\alpha = 4 : 4/3 : 1$

Figure 4.23: Contour plots of relative error for indirect split sequence

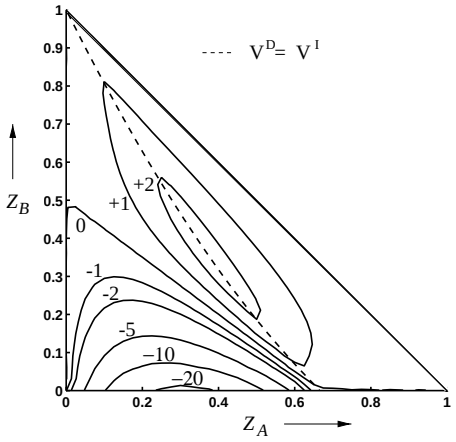

Figure 4.24: Relative error for approximate V_{min} compared to optimal sequence with $\alpha = 4:2:1$

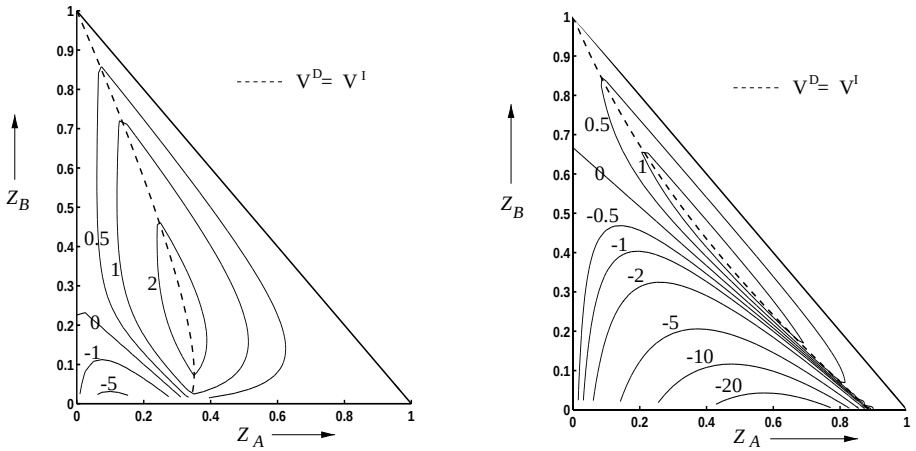

(a) $\alpha = 4:3:1$ (b) $\alpha = 4:4/3:1$

Figure 4.25: Relative errors for approximate V_{min} compared to optimal sequence.

Chapter 5

The Preferred Separation for Prefractionator Arrangements

Atle C. Christiansen and Sigurd Skogestad*

Department of Chemical Engineering
Norwegian University of Science and Technology, NTNU
N–7034 Trondheim Norway

A preliminary version was presented at
AIChE annual meeting Los Angeles, Nov. 1997, Paper 199d

Abstract

Prefractionator arrangements are often preferred from an energy point of view when separating ternary mixtures. The prefractionator performs a separation between the heaviest and lightest component, whereas the intermediate component distributes to both products. The energy usage in the prefractionator itself has a very sharp minimum for a particular distribution, which is the "preferred separation" of Stichlmair (1988). On the other hand, the energy usage in the downstream main column has a minimum when the two parts of the column, above and below the side stream, are "balanced". In the paper we derive simple analytic expression for the total energy usage of the two-column sequence as a function of the separation in the prefractionator. We find that although the preferred separation is optimal, at least for sharp splits in infinite columns, the energy usage is almost the same for any separation between the "preferred" and the "balanced". The same results are shown numerically to hold for columns with finite number of stages and non-sharp separation, as well as when the prefractionator and main column are directly coupled, as in the Petlyuk arrangement. Finally, some implications for the operation and control of such columns are discussed.

*Author to whom correspondence should be addressed : Fax : +47 7359-4080, E-mail: skoge@chembio.ntnu.no

5.1 Introduction

The task of finding the minimum energy input for multicomponent separations has received considerable interest in the literature. No doubt the most well known methods are those due to Underwood (e.g. Underwood (1948)), for which minimum flows are obtained through an exact (iterative) solution of the material balance equations corresponding to infinite columns. In order to enhance the understanding of minimum energy conditions beyond that of numerical computations, Petlyuk and coworkers dedicated a series of papers (e.g. Petlyuk and Platonov (1964), Petlyuk *et al.* (1965) and Petlyuk *et al.* (1966)) to the task of selecting the *thermodynamically* optimal distillation scheme. Based on the concept of reversible distillation, the authors argue that one of the optimality conditions, is that in each bisectional column only the components with extreme volatilities should be separated. For the ternary case this implies that to ensure reversible mixing of streams, the first split is taken between the light and heavy component, so that the intermediate component distributes between the bottoms and top products. Any other split between adjacent components will inherently introduce additional exergy loss and thus increase the energy usage. However, we strongly emphasize that the concept of reversibility also requires uniform distribution of utility (condensing and boilup) along the column, which is not realized in columns with one reboiler and one condenser. Thus, although arguments based on reversibility may provide expedient guidelines, one needs a more detailed analysis to provide conclusions for real columns.

The issue of minimum energy usage under the presence of distributing components was also examined by King (1971). The author introduced a shortcut (group) method to compute the minimum energy, but until present it remains somewhat unclear as to under which conditions the results of King (1971) apply. Stichlmair (1988) coined the phrase *preferred separation*, to denote the separation in the prefractionator that requires the minimum energy input. This particular split occurs when all components have a pinch at the feed location, and the author demonstrates that the optimality of this particular split is due to colinearity between the distillation and equilibrium lines at the feed point. However, the author does not elaborate on whether carrying out the preferred separation as the first split should give the *overall* minimum energy input for a sequence of columns, although is is stated that it *"usually"* is so.

In this paper we consider separating ternary mixtures in the prefractionator arrangements shown in Figure 5.1. This includes a "conventional" prefractionator (a) as well as the Petlyuk column (b), where the prefractionator and main columns are directly coupled so that the prefractionator has no heater or cooler. Both of these arrangements are interesting alternatives for industrial implementations. The task for the prefractionator is to split the heavy and light components, whereas the intermediate component distributes to both products. The downstream main column is a side-stream column where the three components may be recovered as pure products.

Several authors have considered methods to obtain the minimum energy usage for the Petlyuk column (see e.g. Cerda and Wersterberg (1981), Fidkowski and Krolikowski (1986), Nikolaides and Malone (1988), Glinos and Malone (1988) and Carlberg and Westerberg (1989)). Without going into detailed discussions of these

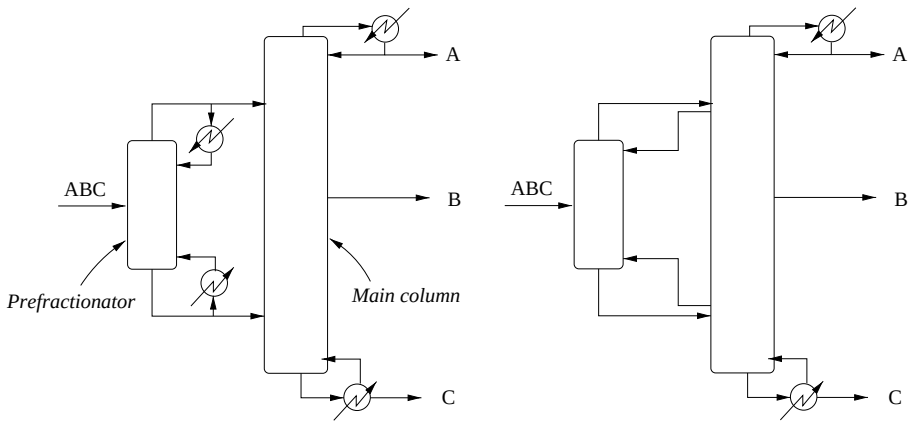

(a) Prefractionator (b) Petlyuk column

Figure 5.1: Prefractionator arrangements for separation of ternary mixtures

previous works, we put emphasis on the important finding by Fidkowski and Krolikowski (1986). Using a comprehensive analysis of the Underwood equations, the authors showed that that there is a *region* for the recovery of the intermediate component in which the minimum energy usage in fact is *constant*. According to Glinos and Malone (1988) the formulas presented by Fidkowski and Krolikowski (1986) was previously derived in a thesis of Stupin (1970). In this work we give results from numerical simulations which demonstrate that the results of Fidkowski and Krolikowski (1986) carry over also to columns with a finite number of stages. The results are obtained from numerical simulations of columns with a sufficiently large number of stages, assuming constant molar flows and constant relative volatilities. In this paper we provide results also for the prefractionator arrangement in Figure 5.1 (a). In particular, whereas the previous works consider exact solutions using Underwood's method, we in this work propose approximate *explicit* expressions that proves useful in the analysis of the prefractionator arrangement. By first considering the prefractionator arrangement, we also obtain physical insight related to the regions of constant energy usage (Fidkowski and Krolikowski 1986) for the Petlyuk column.

For the prefractionator arrangement, we demonstrate that there is a similar "flat" region where the energy usage remains relatively constant. We show analytically and numerically that this region is characterized by recoveries of the intermediate component corresponding to the *preferred* separation and a *balanced* main column. We then elaborate on an important issue that has not been given appropriate attention by the previous authors. This refers to the importance that this "flat" or constant region has for practical operation. In terms of practical operation, we find for both column arrangements that one may control the composition only at one end in the prefractionator and "overpurify" the other column end ("one–point control") without significant increases in the energy usage. Which end to control depends on whether the preferred or a balanced separation requires the largest recovery of intermediate

component in the prefractionator.

We also consider briefly the issue of *non–sharp* separations, for which we present results from numerical simulations where the product purity of the intermediate component is decreased relative to a pure product. The results show that the minimum energy usage moves away from the preferred separation for *sharp splits*, which in itself is hardly surprising. We give an account for the results by considering the distribution of the light and heavy components in the prefractionator for non-sharp separations.

Finally we stress that for ideal mixtures it is always optimal in terms of boilup to use a vapor feed when possible. This was also addressed in the previous chapter, where we found that taking this into account has a strong impact on previous results in the literature (e.g. the optimality regions for the direct and indirect split schemes presented by Glinos and Malone (1988)). Hence we consider prefractionator arrangements in which *partial condensers* are used for upstream columns, providing vapor feeds to downstream columns. In order to analyze such prefractionator arrangements we "decompose" the task, so that we first consider the prefractionator column and then the main column. Knowledge from these findings are then combined to understand the behavior when we consider the column *sequence*. In total we hope to provide a lucid and comprehensive overview of the literature, that may clear up some apparent misunderstandings.

5.2 Degrees of Freedom Analysis

One of the important aspects to be addressed in this paper, is how one should utilize the degrees of freedom (DOFs) for the prefractionator arrangements in Figure 5.1 in a "optimal" manner. For both arrangements we have after stabilization of levels and pressure five DOFs available for operation. Three of these are then consumed if we specify one purity in each product. The objective of this paper is then partly to indicate how one should treat the remaining two DOFs. In a sense, they are both related to the prefractionator column, even though the DOFs in a strict sense apply to the column *arrangement*.

For the Petlyuk column in Figure 5.1 (b), one might imagine that one of the remaining DOFs could be used to control one of the impurities in the sidestream product. The last DOF is then used to minimize the energy usage. However, due to the coupling between the upper and lower parts of the main column, it is in practice not possible to control two purities in the sidestream. Wolff and Skogestad (1995) showed that "holes" may appear in certain operating regions in this case. A detailed explanation for this behavior was later given by Morud (1995). The conclusion is that one should control only one composition in each product for the Petlyuk column. In this work we show that for "optimal" operation one in practice needs to use one DOF to stay within a certain operating region where the energy usage in fact remains relatively constant.

5.3 The Prefractionator Column

In this section we present expressions for the minimum energy usage V_{min} for ternary separations in a prefractionator column, using a group method previously introduced by King (1971). The feed is assumed to be saturated liquid (in Appendix A we also give the formulas that apply for *saturated vapor feeds*). Note that we in the following use subscript *min* to denote a column with an infinite number of stages, and that we use lowercase letters to denote the distillate (d) and bottom (b) flow rates to avoid confusion with the components (B) and the superscripts for the direct split scheme (e.g. V^D).

5.3.1 V_{min} and the preferred separation

Our starting point is the "binary equation" for the minimum reflux in a column with an infinite number of stages and a *saturated liquid feed* (King 1971)

$$\left(\frac{L}{F}\right)_{min} = \frac{\phi_L^d - \alpha_{LH}\phi_H^d}{\alpha_{LH} - 1} \tag{5.1}$$

Here L denotes the reflux, F the feed, ϕ_i^d the fractional recoveries of light and heavy components in the distillate d and α_{LH} the relative volatility between the two components. More precisely, the fractional recoveries are given by

$$\phi_i^d = \frac{dx_i^d}{Fz_i} \tag{5.2}$$

where z_i denotes the feed composition of component i. Actually, equation (5.1) applies to any two components in a multicomponent mixture if we assume that all components pinch at the feed stage, and King (1971) states that (5.1) applies if all *non-key* components distribute. In practice this means that the non-key components must be intermediate relative to the two (key) components.

If we then consider the separation of a ternary mixture ABC, for which we want to obtain a top product depleted in the high boiler (C) and a bottoms product depleted in the low boiler (A), equation (5.1) is valid if B has a pinch at the feed location. This is the *"preferred"* separation of Stichlmair (1988), and the corresponding preferred recovery of B is denoted ϕ^{pref}. For the separation between components A and C equation (5.1) gives

$$\left(\frac{L}{F}\right)_{min}^{pref} = \frac{\phi_A^d - \alpha_{AC}\phi_C^d}{\alpha_{AC} - 1} \tag{5.3}$$

where we use the superscript $pref$ to make clear that it only applies to the case of the preferred separation where all components have a pinch at the feed stage. The corresponding minimum boilup is

$$\left(\frac{V}{F}\right)_{min}^{pref} = \left(\frac{L}{F}\right)_{min}^{pref} + \left(\frac{d}{F}\right)^{pref} \tag{5.4}$$

In this case equation (5.1) applies also to the (non–sharp) separation between components A and B, i.e.

$$\left(\frac{L}{F}\right)_{min} = \frac{\phi_A^d - \alpha_{AB}\phi_B^d}{\alpha_{AB} - 1} \tag{5.5}$$

By equating (5.3) and (5.5) for given values of ϕ_A^d and ϕ_C^d, and solving with respect to ϕ_B^d, we obtain the "preferred" recovery of B in the distillate

$$\phi^{pref} \equiv \left(\phi_B^d\right)^{pref} = \frac{\phi_A^d\left(\alpha_{BC} - 1\right) + \alpha_{BC}\phi_C^d\left(\alpha_{AB} - 1\right)}{\alpha_{AC} - 1} \tag{5.6}$$

The distillate flow is then

$$\frac{d^{pref}}{F} = \phi_A^d z_A + \phi^{pref} z_B + \phi_C^d z_C \tag{5.7}$$

and we derive the desired expression for V_{min}

$$\left(\frac{V}{F}\right)_{min}^{pref} = \frac{\phi_A^d - \alpha_{AC}\phi_C^d}{\alpha_{AC} - 1} + \phi_A^d z_A + \phi^{pref} z_B + \phi_C^d z_C \tag{5.8}$$

For the special case of a sharp split between A and C ($\phi_A^d = 1$, $\phi_C^d = 0$) we get

$$\phi^{pref} = \frac{\alpha_{BC} - 1}{\alpha_{AC} - 1}, \quad \frac{d^{pref}}{F} = z_A + \frac{\alpha_{BC} - 1}{\alpha_{AC} - 1} z_B \tag{5.9}$$

and for the boilup

$$\left(\frac{V}{F}\right)_{min}^{pref} = \frac{1}{\alpha_{AC} - 1} + z_A + \frac{\alpha_{BC} - 1}{\alpha_{AC} - 1} z_B \tag{5.10}$$

This is the same expression as was previously presented by Stichlmair (1988) for the preferred separation.

However, the question remains as to how V_{min} changes if ϕ_B^d differs from the particular value ϕ^{pref}, and what is the additional cost? This is the central question to be addressed in the next section.

5.3.2 V_{min} for splits other than the preferred separation

In the following we want to derive an expression for V_{min} for sharp splits between A and C that applies to *any* recovery of the intermediate component, i.e. for all $\phi_B^d \in [0, 1]$.

Introductory example.
In order to address this issue, we first consider an introductory example for the separation of an equimolar saturated liquid feed with data given in Table 5.1. For the simulations we specify that the composition of light component A in the bottom, and the composition of heavy C in the top, should be equal to or less than a given upper

Table 5.1: Data for ternary separation in an "infinite" column

Number of stages	$N = 100$ $(N_F = 50)$
Feed compositions	$z_F = [1/3, 1/3, 1/3]$
Molar feed	$F = 1$ [kmol/min]
Relative volatility	$\alpha = 4 : 2 : 1$
Impurity spec.'s	$x_A^b \leq \epsilon$
	$y_C^d \leq \epsilon$

bound, i.e. $x_A^b \leq \epsilon$ and $y_C^d \leq \epsilon$. Note that for a sharp split $\epsilon \to 0$, but in the numerical calculations we mostly use $\epsilon = 10^{-4}$ (we should also mention that we used a finite number of stages $N = 100$, but exact calculation with the Underwood equations for infinite columns give almost identical results for V_{min}). The purpose of this numerical example is to compute V_{min} as a function of the distillate flow d with $\phi_B^d \in [0, 1]$.

By specifying d we fix one degree of freedom, and since we have only two degrees of freedom for a single column at steady state, we will find that only one of the impurity specifications (i.e. $x_A^b \leq \epsilon$ or $y_C^d \leq \epsilon$) will be active as an equality. Numerically we thus obtained two solution curves where we selected $x_A^b = \epsilon = 10^{-4}$ and $y_C^d = \epsilon = 10^{-4}$. The curves were computed using the continuation scheme presented in chapter 3, and are shown in Figure 5.2. As seen from the Figure we find that there is a sharp

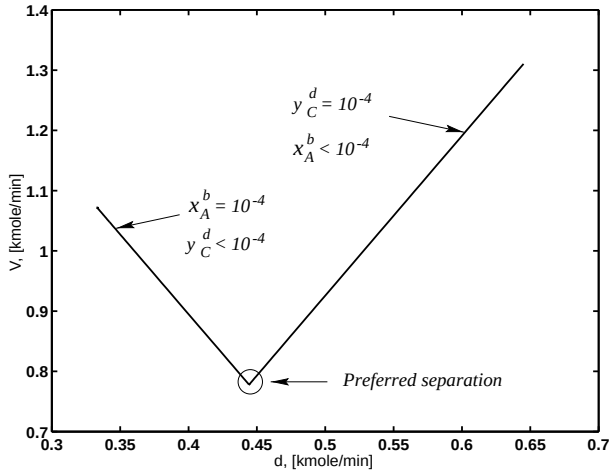

Figure 5.2: V_{min} as a function of distillate flow d for sharp A/C split, i.e. $\epsilon = 10^{-4}$.

minimum located at the intersection, which is the point corresponding to the preferred separation. Along the curves extending from this point we have that both purity specifications are satisfied, one as an equality the other as an inequality (see Figure 5.4). The only point where both appear as equalities ($x_A^b = y_C^d = \epsilon$) is at the intersection, which as mentioned is at the preferred separation.

Figure 5.3 which gives V_{min} for other values of ϵ, illustrates that selecting $\epsilon = 10^{-4}$ indeed gives the limiting value of V_{min} corresponding to a sharp separation. For example, the curves for purities of $\epsilon = 10^{-3}$ and $\epsilon = 10^{-4}$ are as shown in Figure 5.3 practically indistinguishable. One may also note that there is a well defined minimum

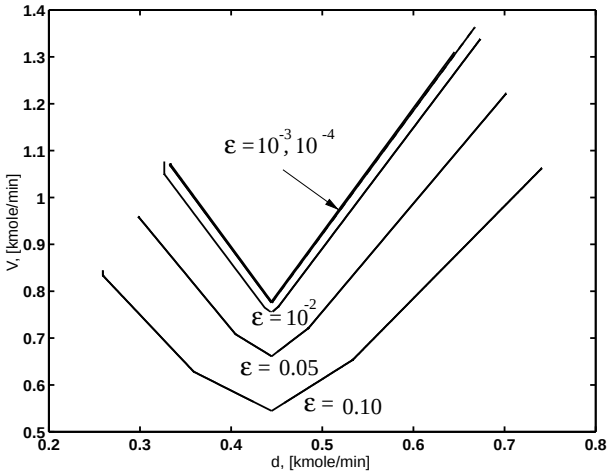

Figure 5.3: V_{min} as a function of distillate flow d for non-sharp separations with $\epsilon \in [10^{-4}, 10^{-1}]$.

also for non-sharp separations, an issue to be discussed later. In Figure 5.4 we have plotted on a semi-log scale the corresponding impurities at the column ends which is purer than required. We see that the impurities are satisfied as inequalities for all values of d, except for the preferred separation where they are both satisfied as equalities. Similar observations were also made by Carlberg and Westerberg (1989), in a detailed analysis of the Underwood equations for a simple non-sharp column. The authors showed that minimum reflux behavior (infinite column) divides into four distinct regions depending on the recovery of intermediate. Each region is then characterized by the recoveries of light and heavy in the distillate being either at their lower bound, upper bound or intermediate. Note that we have instead assigned bounds on the *mole fractions* of heavy key in the top and light key in the bottom, whereas Carlberg and Westerberg (1989) consider the recoveries of light and and heavy in the top. Using either mole fractions or recoveries is however somewhat complementary from a mathematical point of view, since the recoveries depend linearly on the mole fractions. In practice, the mole fractions will however have more of a physical significance. We will later demonstrate that these observations are of great importance for practical operation of prefractionator arrangements and the Petlyuk column.

To further verify the numerical results, we compute from equation (5.10) the minimum vapor flow for a sharp split (with data from Table 5.1)

$$V_{min}^{pref} = 0.778 \tag{5.11}$$

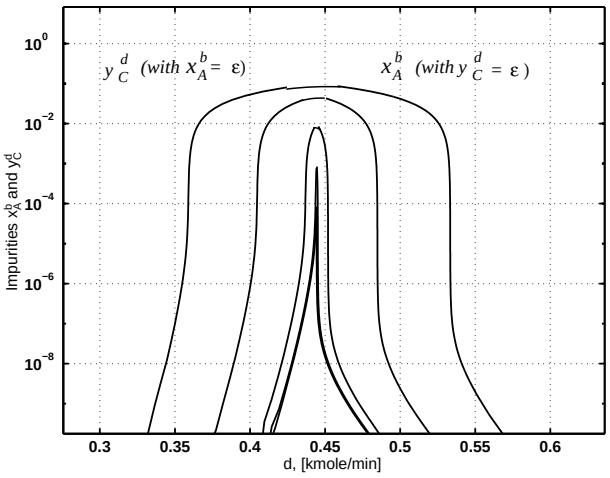

Figure 5.4: Impurities at column end which is purer than required for $\epsilon = 0.1, 0.05, 10^{-2}, 10^{-3}, 10^{-4}$. The left branches give $y_C^d < \epsilon$ when $x_A^b = \epsilon$ is kept constant, and the right branches give $x_A^b < \epsilon$ for constant $y_C^d = \epsilon$.

and the corresponding distillate flow using equation (5.7) is

$$d^{pref} = 0.444 \tag{5.12}$$

which agrees with our numerical simulations.

5.3.3 Analytical Results

In this section we will derive approximate analytical expressions for V_{min} as a function of the distillate flow d for the prefractionator arrangement. The reader may note that we here choose to use d as the independent variable, since it represents a variable of grater physical significance than for instance the recovery ϕ_B^d. From King (1971) we have the following exact expression for the minimum boilup

$$\left(\frac{V}{F}\right)_{min} = \frac{\alpha_{AC}\phi_A^d}{\alpha_{AC} - \theta_i} + \frac{\alpha_{AB}\phi_B^d}{\alpha_{BC} - \theta_i} + \frac{\phi_C^d}{1 - \theta_i} \tag{5.13}$$

where θ_i is the appropriate solution of the following 2nd order Underwood equation

$$\frac{\alpha_{AC} z_A}{\alpha_{AC} - \theta_i} + \frac{\alpha_{BC} z_B}{\alpha_{BC} - \theta_i} + \frac{z_C}{1 - \theta_i} - F(1 - q) = 0 \tag{5.14}$$

Here q is the feed enthalpy and $q = 1$ for saturated liquid feeds. For a sharp split between A and C ($\phi_A^d = 1$, $\phi_C^d = 0$) we get

$$\left(\frac{V}{F}\right)_{min} = \frac{\alpha_{AC}}{\alpha_{AC} - \theta} + \frac{\alpha_{AB}\phi_B^d}{\alpha_{BC} - \theta} \tag{5.15}$$

This proves that the relationship between V and ϕ_B^d, and thus between V and $d = Fz_A + F\phi^{pref}z_B$, is given by straight lines. This was already observed from the numerical results in Figures 5.2 and 5.3. The break in the straight lines at the preferred separation corresponds to a switch of Underwood root θ_i. As illustrated in Figure 5.2, the straight lines extend from the preferred separation to the two end points. The left end point is where all intermediate B leaves in the bottom, i.e. the direct A/BC split. Here $d = d^D$ and $V_{min} = V_{min}^D$. The right end point is where all B is taken over the top, i.e. the indirect AB/C split. Here $d = d^I$ and $V_{min} = V_{min}^I$. This is further illustrated graphically in Figure 5.5.

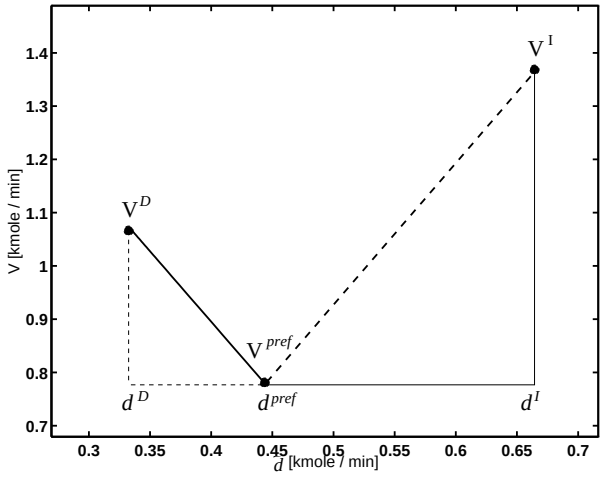

(a) $\alpha = 4 : 2 : 1$

Figure 5.5: Boilup V for sharp A/C split as a function of the distillate flow d. The results are shown for an equimolar feed mixture with $\alpha_{AB} = \alpha_{BC} = 2$

Since the relation between V_{min} and d yields a straight line for sharp splits and infinite columns, we thus find from Figure 5.5 the desired relationships

$$V_{min}^{C1} = V^{pref} + \frac{V_{min}^D - V^{pref}}{d^{pref} - d^D}\left(d^{pref} - d\right), \quad d < d^{pref} \tag{5.16}$$

$$V_{min}^{C1} = V^{pref} + \frac{V_{min}^I - V^{pref}}{d^I - d^{pref}}\left(d - d^{pref}\right), \quad d > d^{pref} \tag{5.17}$$

(We write V_{min}^{C1} with superscript $C1$ to make clear that these relationships apply only to the prefractionator column $C1$.) For sharp splits we have

$$\frac{d^D}{F} = z_A, \quad \frac{d^{pref}}{F} = z_A + \frac{\alpha_{BC} - 1}{\alpha_{AC} - 1}z_B, \quad \frac{d^I}{F} = z_A + z_B \tag{5.18}$$

Furthermore, Glinos and Malone (1984) derived reasonably accurate analytical ex-

pressions for V^D_{min} and V^I_{min} for sharp splits

$$\left(\frac{V^I}{F}\right)_{min} = \left(\frac{z_B + z_C}{\alpha_{BC} - 1} + \frac{z_A}{\alpha_{AC} - 1}\right) \frac{1}{1 + z_A z_C} + z_A + z_B \tag{5.19}$$

and

$$\left(\frac{V^D}{F}\right)_{min} = \frac{z_A + z_B}{f\,(\alpha_{AB} - 1)} + \frac{z_C}{f\,(\alpha_{AC} - 1)} + z_A \tag{5.20}$$

where $f = 1 + z_B/100$. The authors claim that these equations yield average errors in the order of 4% compared to exact methods (i.e. Underwood) and thus serve our purpose well. From (5.8) and (5.18)–(5.20) we derive the following expressions for the slopes in Figure 5.5

$$\frac{V^D_{min} - V^{pref}}{d^{pref} - d^D} = \frac{(\alpha_{AC} - 1)\,(z_A + z_B)}{f z_B\,(\alpha_{AB} - 1)\,(\alpha_{BC} - 1)} + \frac{z_C - 1}{f z_B\,(\alpha_{BC} - 1)} - 1 \tag{5.21}$$

$$\frac{V^I_{min} - V^{pref}}{d^I - d^{pref}} = \frac{z_A - (1 + z_A z_C)}{z_B\,(\alpha_{AC} - \alpha_{BC})\,(1 + z_A z_C)} + \frac{(z_B + z_C)\,(\alpha_{AC} - 1)}{z_B\,(\alpha_{AC} - \alpha_{BC})\,(1 + z_A z_C)\,(\alpha_{BC} - 1)} + 1 \tag{5.22}$$

As one will expect we find that the slopes of the curves extending from the minimum (preferred separation) towards the direct and indirect splits, depend on the difficulty of the separation, i.e. on the ratio α_{AB}/α_{BC}. In the next section we use expressions (5.17)–(5.21) to determine (analytically) whether it is always optimal to produce the preferred separation as the first split for the Prefractionator arrangement in Figure 5.1 (a).

5.4 The Main Sidestream Column

We here consider the energy usage (V_{min}) in the main column with sharp separations between components A, B and C. To derive the desired expression we first consider the 3–column arrangement in Figure 5.6 (b), where the prefractionator is denoted $C1$ whereas the downstream columns are $C2$ and $C3$. Note that a partial condenser is used for the prefractionator column $C1$, since using a *total* condenser increases the energy usage in $C2$ by a term proportional to the feed of light key (Fz_A). For minimum reflux calculations we can represent the main column of the Prefractionator in Figure 5.6 (a) as a special case of Figure 5.6 (b), and we then refer to columns $C2$ and $C3$ in order to distinguish between cases when the *upper* or *lower* feed controls for the main column. The required energy usage in the main column is thus

$$V^{main}_{min} = max\left(V^{C2}_{min}, V^{C3}_{min}\right) \tag{5.23}$$

depending on whether the lower feed (V^{C3}) or upper feed V^{C2} controls, i.e. is the larger. To compute V^{C2}_{min} and V^{C3}_{min} we make use of the following exact expressions for a sharp separation of a binary mixture:

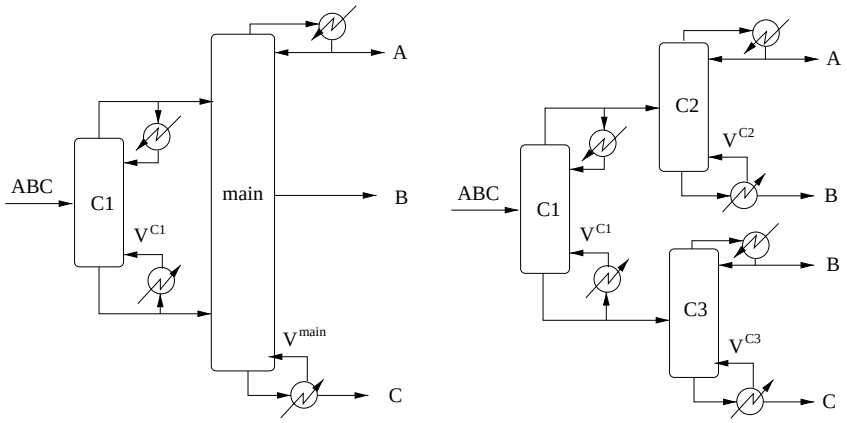

(a) Prefractionator (b) 3–column arrangement

Figure 5.6: Prefractionator arrangements for separation of ternary mixtures

The feed to column $C3$ is *saturated liquid*, and for a sharp split between A and B we have from (5.1)

$$V_{min}^{C3} = \frac{F^{C3}}{\alpha_{BC}-1} + d^{C3} \tag{5.24}$$

where $d^{C3} = F\left(1-\phi_B^d\right) z_B$ is the distillate flow and $F^{C3} = F\left(1-\phi_B^d\right) z_B + F z_C$ is the feed to column $C3$. F is as before the overall feed to the prefractionator $C1$, and ϕ_B^d is the fractional recovery of the intermediate component B in the distillate of the prefractionator. We then get for column $C3$

$$\left(\frac{V}{F}\right)_{min}^{C3} = \frac{\left(1-\phi_B^d\right) z_B + z_C}{\alpha_{BC}-1} + \left(1-\phi_B^d\right) z_B \tag{5.25}$$

The feed to column $C2$ is a saturated vapor, and a similar derivation for a sharp split between B and C yields

$$\left(\frac{V}{F}\right)_{min}^{C2} = \frac{F^{C2}}{\alpha_{AB}-1} = \frac{z_A + \phi_B^d z_B}{\alpha_{BC}-1} + \left(1-\phi_B^d\right) z_B \tag{5.26}$$

To compute V_{min}^{main} need to determine when the lower and upper feed controls respectively, for different mixtures and different values of ϕ_B^d. The "switch–over" value for ϕ_B^d occur when the main column is "balanced (i.e. $V_{min}^{C3} = V_{min}^{C2}$), and by equating (5.25) and (5.26) we find

$$\phi^{bal} = \frac{(1-z_A)(\alpha_{AB}-1) + z_B(\alpha_{AB}-1)(\alpha_{BC}-1) - z_A(\alpha_{BC}-1)}{z_B(\alpha_{BC}-1) + z_B(\alpha_{AB}-1) + z_B(\alpha_{AB}-1)(\alpha_{BC}-1)} \tag{5.27}$$

We thus have the following three operating regimes for the main sidestream column

(i)	$\phi_B^d < \phi^{bal}$	Lower feed controls,	i.e. $V_{min}^{main} = V_{min}^{C3}$
(ii)	$\phi_B^d = \phi^{bal}$	Balanced column,	i.e. $V_{min}^{main} = V_{min}^{C2} = V_{min}^{C3}$
(iii)	$\phi_B^d > \phi^{bal}$	Upper feed controls,	i.e. $V_{min}^{main} = V_{min}^{C2}$

Since V_{min}^{C3} decreases as we increase ϕ_B^d, and since V_{min}^{C2} increases as we increase ϕ_B^d, we find for the main (sidestream) column that

$$\min_{\phi_B^d} V_{min}^{main} \tag{5.28}$$

is obtained for $\phi_B^d = \phi^{bal}$. Thus when we consider only the energy consumption in the main column, then the best choice is to operate the prefractionator such that $\phi_B^d = \phi^{bal}$. This is illustrated in Figure 5.7. Before proceeding we mention that if

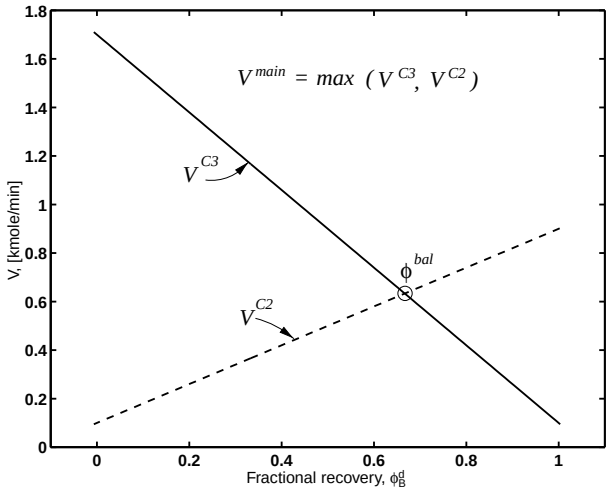

Figure 5.7: Minimum energy usage V_{min} for the main sidestream column as a function of the fractional recovery of intermediate ϕ_B^d for $\alpha = 4:2:1$ and $z_F = [1/3, 1/3, 1/3]$. The Figure illustrates that the overall V_{min} corresponds to a balanced column and occurs for $\phi_B^d = \phi^{bal}$.

we instead use a total condenser for the prefractionator so that the feed to $C2$ is a saturated liquid, then V_{min}^{C2} will increase and the value for ϕ^{bal} decreases.

5.5 Is the Preferred Separation Optimal for the Column Sequence?

In the previous sections we found that the minimum energy usage in a *prefractionator column* usually displays a very sharp minimum at the fractional recovery of intermediate component corresponding to the preferred separation (ϕ^{pref}), whereas the *main column* displays a similar sharp minimum for a balanced column (ϕ^{bal}). The question

should then be posed: Which of these values, if any, is best when considering the overall energy consumption in the two columns.

Using the expressions derived in section 5.2 and 5.3 we will in this section derive approximate analytical equations for the optimality conditions for the prefractionator arrangement in Figure 5.1 (a) with an infinite number of stages and sharp splits. Based on these expressions we show that the preferred separation is indeed optimal for all cases, but the overall optimum is quite "flat" for values of ϕ_B^d in the range between ϕ^{pref} and ϕ^{bal}.

The overall energy consumption

$$V_{min} = V_{min}^{C1} + V_{min}^{main} \tag{5.29}$$

can be easily computed as a function of ϕ_B^d using the analytical expressions for V_{min}^{C1} in (5.17) and (5.16), and for V_{min}^{main} in (5.23). Note that we can alternatively use the distillate flow leaving the prefractionator as our independent variable, since there is a unique (linear) mapping from ϕ_B^d to d:

$$d = F \sum_{i=1}^{n} \phi_i^d z_{fi} = F \left(\phi_A^d z_A + \phi_B^d z_B + \phi_C^d z_C \right) \tag{5.30}$$

Note in particular that for sharp splits the differentials are related by

$$\partial d = z_B \cdot \partial \phi_B^d \tag{5.31}$$

since the amount of A and C are constant in the distillate, i.e. $\phi_A^d = 1$ and $\phi_C^d = 0$.

5.5.1 Introductory example

In order to give further motivation for analyzing the optimality conditions of the preferred separation, we first consider an introductory example. The objective of this example is to compute V_{min} as a function of the fractional recovery ϕ_B^d, and compare the results with the prefractionator V_{min}^{C1} and the main column V_{min}^{main}. We here consider a mixture with a large amount of intermediate B. Figure 5.8 shows V_{min} as a function of the recovery ϕ_B^d for the example with relative volatilities of $\alpha = 4:2:1$ and feed compositions $z_F = [0.1, 0.8, 0.1]$. We find for this example that V_{min} for the sequence of two columns indeed corresponds to using the preferred separation as the initial split. However, as mentioned we find that there is a relatively large region in which the energy usage is almost constant, independent of the recovery, i.e. the decrease in $V^{main} = V^{C3}$ is approximately equal to the increase in V^{C1}. This region covers all intermediate recoveries between ϕ^{pref} and ϕ^{bal}. Note that $\phi^{pref} < \phi^{bal}$ in this case, but for other cases we may have $\phi^{pref} > \phi^{bal}$, as shown in Figure 5.9. In this case the region with approximately constant V_{min} is between ϕ^{bal} and ϕ^{pref}.

5.5.2 Analytical results

We here use the previously derived analytical expressions to show that for sharp splits it is always optimal to use $\phi_B^d = \phi^{pref}$ in the prefractionator, i.e. $d = d^{pref}$. We do

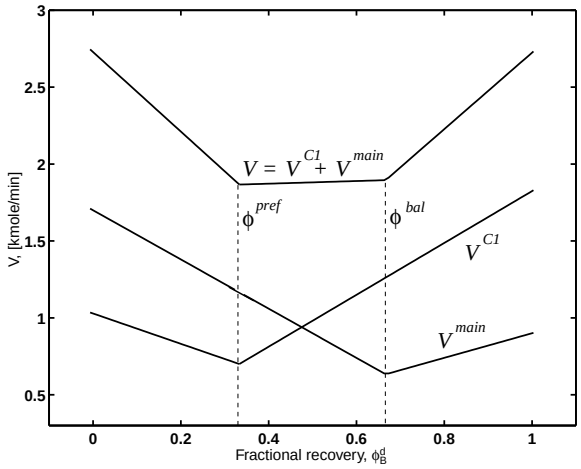

Figure 5.8: Minimum boilup V as a function of the fractional recovery of intermediate ϕ_B^d for $\alpha = 4:2:1$ and $z_F = [0.1, 0.8, 0.1]$. The Figure illustrates that there is a large region enveloped by ϕ^{pref} and ϕ^{bal}, in which V remains close to the overall minimum.

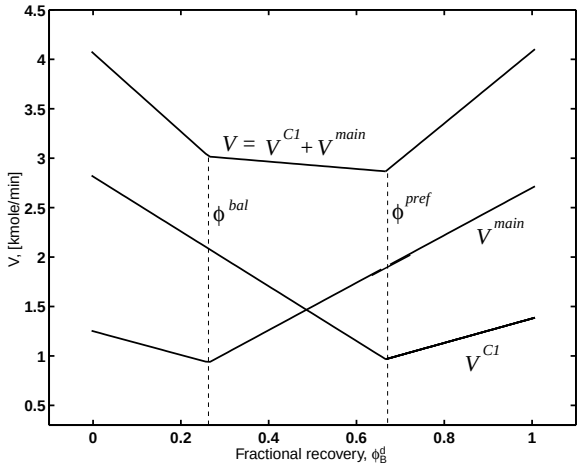

Figure 5.9: Minimum boilup V as a function of the fractional recovery of intermediate ϕ_B^d for $\alpha = 4:3:1$ and $z_F = [0.1, 0.8, 0.1]$. The Figure illustrates that there is a large region enveloped by ϕ^{pref} and ϕ^{bal}, in which V remains close to the overall minimum.

this by comparing the slopes (i.e. derivatives) for the prefractionator and the main column with respect to the distillate flow, i.e. $\partial V^{C1}/\partial d$ and $\partial V^{main}/\partial d$.

First consider the prefractionator $C1$. Using equations (5.17) and (5.22) we thus obtain for $d > d^{pref}$, (i.e. $\phi_B^d > \phi^{pref}$

$$\begin{aligned}\frac{\partial V^{C1}}{\partial d} &= \frac{V^I - V^{pref}}{d^I - d^{pref}} \\ &= \frac{z_A - (1 + z_A z_C)}{z_B (\alpha_{AC} - \alpha_{BC})(1 + z_A z_C)} \\ &\quad + \frac{(z_B + z_C)(\alpha_{AC} - 1)}{z_B (\alpha_{AC} - \alpha_{BC})(1 + z_A z_C)(\alpha_{BC} - 1)} + 1, \ (d > d^{pref}) \quad (5.32)\end{aligned}$$

Conversely we obtain using equations (5.16) and (5.21) for $d < d^{pref}$ (i.e. $\phi_B^d < \phi^{pref}$)

$$\begin{aligned}\frac{\partial V^{C1}}{\partial d} &= \frac{V^D - V^{pref}}{d^{pref} - d^D} \\ &= \frac{(\alpha_{AC} - 1)(z_A + z_B)}{f z_B (\alpha_{AB} - 1)(\alpha_{BC} - 1)} + \frac{z_C - 1}{f z_B (\alpha_{BC} - 1)} - 1, \ (d < d^{pref}) \quad (5.33)\end{aligned}$$

Next consider the main column, for which we obtain from (5.25) and (5.26)

$$\frac{\partial V^{main}}{\partial d} = \frac{\partial V^{C3}}{\partial d} = -\frac{\alpha_{BC}}{\alpha_{BC} - 1}, \ (d < d^{bal}) \quad (5.34)$$

and

$$\frac{\partial V^{main}}{\partial d} = \frac{\partial V^{C2}}{\partial d} = \frac{1}{\alpha_{AB} - 1}, \ (d > d^{bal}) \quad (5.35)$$

Note that these derivatives are *exact* for sharp splits and binary mixtures, since the minimum energy usage for the main column is equal to the *binary* separation requiring the largest energy. Our objective is now to determine whether the preferred separation is always optimal for the directly coupled Prefractionator. A simple analysis shows that we must consider the slope in the "flat" region for the two cases of

(1) $d^{pref} > d^{bal}$

and

(2) $d^{pref} < d^{bal}$

Case 1 : $d^{pref} > d^{bal}$ (Figure 5.10)
In this case the upper feed controls in the "flat" region and the preferred separation is *not* optimal if for $d^{bal} < d < d^{pref}$ we have $\partial V/\partial d$ positive, i.e. the overall energy usage (V) is smaller for some value of d than for d^{pref}. From (5.32) and (5.35) this is the case if and only if

$$\frac{1}{\alpha_{AB} - 1} > \frac{(\alpha_{AC} - 1)(z_A + z_B)}{f z_B (\alpha_{AB} - 1)(\alpha_{BC} - 1)} + \frac{z_C - 1}{f z_B (\alpha_{BC} - 1)} - 1 \quad (5.36)$$

After substituting for $\alpha_{AC} = \alpha_{AB}\alpha_{BC}$ and $z_C = 1 - (z_A + z_B)$ and some algebra, we find that the condition is equivalent to

$$\frac{(z_A + z_B)(\alpha_{AC} - 1 - \alpha_{AB} + 1) - f z_B (\alpha_{BC} - 1)(\alpha_{AB} - 1 + 1)}{f z_B (\alpha_{AB} - 1)(\alpha_{BC} - 1)} < 0 \quad (5.37)$$

$$\Downarrow$$

$$\frac{\alpha_{AB}(z_A + z_B)(\alpha_{BC} - 1) - \alpha_{AB} f z_B (\alpha_{BC} - 1)}{f z_B (\alpha_{AB} - 1)(\alpha_{BC} - 1)} < 0 \quad (5.38)$$

$$\Downarrow$$

$$\frac{\alpha_{AB}(z_A + (1 - f) z_B)}{f z_B (\alpha_{AB} - 1)} < 0 \quad (5.39)$$

Since the nominator is always larger than zero, we consider only the denominator. After substituting for $f = 1 + B/100$ we derive

$$\frac{\partial V}{\partial d} > 0 \quad \text{iff} \quad z_A < (f - 1) z_B = \frac{z_B^2}{100} \quad (5.40)$$

which is satisfied only when z_A is very small. From this result we see that the preferred separation is optimal in almost all cases, but we are lead to believe that there may exist some limiting cases with z_A small where the preferred separation is not optimal for the column sequence. However, it should be noted that (5.40) is based on the analytical expressions of Glinos and Malone (1988) which are are not quite exact. In order provide the *exact* optimality conditions for the preferred separation, one will have to use exact methods such as Underwood's method as shown by Fidkowski and Krolikowski (1986).

To verify the optimality condition (5.40) we give in Figure 5.10 numerical results for an example where we also applied Underwood's method to compute V^D and V^I used in equations (5.17) and (5.16). According to condition (5.40) we have that for this case ($z_A < z_B^2/100$), the true V_{min} should not correspond to the preferred separation. However, using Underwood's method instead of the approximate expressions by Glinos and Malone (1984), we find that the preferred separation indeed gives the true V_{min}. Thus it is for all separations, at least for sharp splits, optimal to use the *preferred separation* in the prefractionator. More importantly, the Figure also illustrates that there is a large region of recoveries enveloped by ϕ^{pref} and ϕ^{bal}, in which V remains close to the overall minimum. This is not stressed in any of the previous works, and is of great import for practical operation to be discussed later.

Case 2 : $\phi^{bal} > \phi^{pref}$ (Figure 5.11)
In this case the lower feed controls in the "flat" region between ϕ^{pref} and ϕ^{bal}, and From (5.33) and (5.34) the preferred split is *not* optimal if and only if

$$\frac{\alpha_{BC}}{\alpha_{BC} - 1} > \frac{z_A - (1 + z_A z_C)}{z_B (\alpha_{AC} - \alpha_{BC})(1 + z_A z_C)} + \frac{(z_B + z_C)(\alpha_{AC} - 1)}{z_B (\alpha_{AC} - \alpha_{BC})(1 + z_A z_C)(\alpha_{BC} - 1)} + 1 \quad (5.41)$$

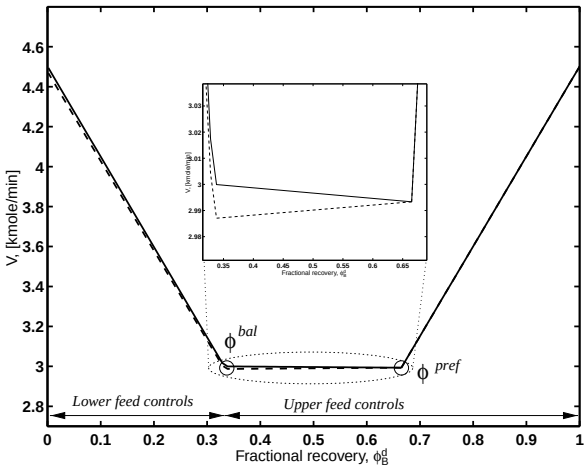

Figure 5.10: Analytical results for boilup V as a function of the fractional recovery of intermediate ϕ_B^d for $\alpha = 4:3:1$ and $z_F = [0.005, 0.99, 0.005]$. The Figure shows that the overall V_{min} corresponds to using the preferred separation (ϕ_{pref}) as the initial split. The dashed line is obtained using the approximate equations by Glinos and Malone (1984), and the solid line gives the exact solution obtained from Underwood's method.

In this case it becomes somewhat difficult to extract simple algebraic conditions as was the case for upper feed control, i.e. equation (5.40). However, after considering numerically a large range of mixtures, we have in fact not found any case for which condition (5.41) is satisfied. Nevertheless, we find as shown in Figure 5.11 that for low values of α_{BC} for which ϕ^{bal} is large, there may be very large regions in which V_{min} is relatively constant. Note that we in this case did not find any significant differences between the approximate equations and Underwood's method. One may note, although hardly surprising, that as $\alpha_{BC} \to 1$ we have that $\phi^{bal} \to 1$ and $\phi_{pref} \to 0$, hence the lower feed controls for all recoveries.

Case 3 : $d^{pref} = d^{bal}$ (Figure 5.12)
A special limiting case is when $\phi^{pref} = \phi^{bal}$. Such cases are obtained by equating expressions (5.9) and (5.27). It becomes somewhat complicated to derive simple conditions for when this may occur in the general case. However, for cases where the A/B split and B/C split are equally difficult so that $\alpha_{AB} = \alpha_{BC}$ we derive after some algebra that $\phi^{pref} = \phi^{bal}$ if and only if

$$z_A = \frac{1 + z_B\,(\alpha - 2)}{2} \tag{5.42}$$

Note that equation (5.42) may not apply for all compositions z_B, since we must require $z_A \leq 1$. For the particular case where $\alpha = 2$ the equality $\phi^{pref} = \phi^{bal}$ occurs always for $z_A = 0.5$. Figure 5.12 illustrates one such case with a sharp minimum where $\phi^{pref} = \phi^{bal}$. Finally we also recognize that the "flat" regions become smaller if a

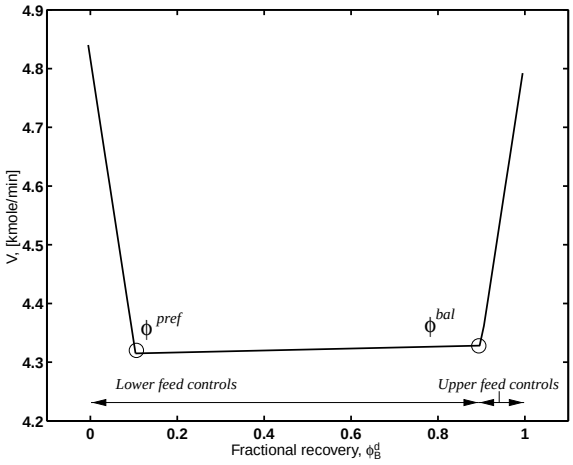

Figure 5.11: Analytical results for V_{min} as a function of the fractional recovery of intermediate ϕ_B^d for $\alpha = 4 : 1.3 : 1$ and $z_F = [0.005, 0.99, 0.005]$. The Figure illustrates a large region enveloped by ϕ^{pref} and ϕ^{bal} where V_{min} stays relatively constant.

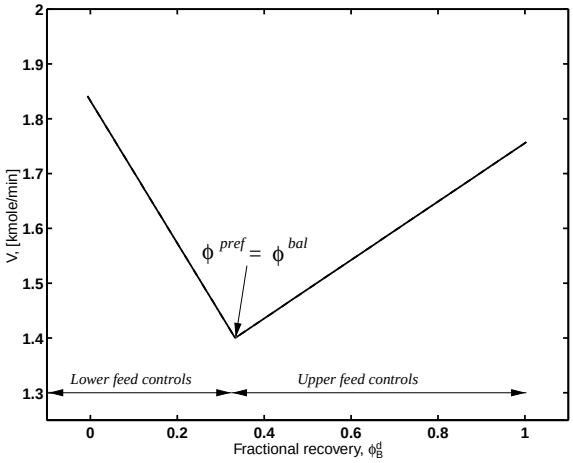

Figure 5.12: Analytical results for boilup V as a function of the fractional recovery of intermediate ϕ_B^d for $\alpha = 4 : 2 : 1$ and $z_F = [0.5, 0.1, 0.4]$. The Figure shows that there is a sharp minimum V_{min} where $\phi^{pref} = \phi^{bal}$.

total condenser is used in the prefractionator ($C1$), since ϕ^{bal} moves closer to ϕ^{pref}. This is because the region in which the upper feed controls becomes larger so that ϕ^{bal} is decreased, i.e. V^{C2} increases with a term proportional to Fz_A.

5.6 Implications for Operation

We have so far shown in terms of analytical and numerical results that for sharp splits it is optimal to use the preferred separation as the initial split. This preferred separation corresponds to a certain fractional recovery of the intermediate in the distillate from the prefractionator. However, we have also shown that there usually is a range of recoveries between ϕ^{pref} and ϕ^{bal} for which the energy usage (boilup) remains close to the minimum. For practical operation we want to maintain operation in this "flat" region. Again we have three cases

$\phi^{pref} < \phi^{bal}$ In this case we want to maintain $\phi_B^d \geq \phi^{pref}$ ($d \geq d^{pref}$). With reference to Figure 5.2 we see that to achieve this in the prefractionator, we want to keep the top product (y_C^d) at a given composition, and *overpurify* in the bottoms, i.e. a bottoms product almost completely depleted in the low boiler A. This means that it may be sufficient to use only one point control in the *top* of the prefractionator (i.e. use reflux for control) and set the the boilup in the bottoms at a value which is equal to or higher than the optimum value corresponding to $d = d^{pref}$.

$\phi^{pref} > \phi^{bal}$ This is the reversed case, for which we want to maintain $\phi_B^d \leq \phi^{pref}$ ($d \leq d^{pref}$). This may be achieved by controlling the bottom composition (x_A^b) and *overpurify* in the top of the prefractionator, i.e. a distillate product almost completely depleted in the high boiler C. In this case one may use one point control in the *bottoms* of the prefractionator, e.g. use reflux for control and set the boilup in the bottoms at a value which is equal to or higher than its optimal value corresponding to $d = d^{pref}$.

$\phi^{pref} = \phi^{bal}$ In this case V_{min} has a sharp minimum, so there is no "flat" region in which we can operate the column. This case may pose great difficulties for practical operation if one wants to achieve the minimum energy usage. Tight control is most likely needed in both ends of the prefractionator, i.e. use both reflux and boilup for control purposes.

Similar results are expected to hold also for the Petlyuk column, but there the vapor split (R_V) takes the role of the boilup to the prefractionator. These results show the importance of knowing whether ϕ^{pref} is smaller or larger than ϕ^{bal}.

5.7 Optimal Splits for the Petlyuk Column

As shown in Figure 5.1 (b) the Petlyuk columns shows a strong resemblance with the prefractionator arrangement studied above. Thus, one may expect that there is a

region of recoveries of the intermediate component, approximately between ϕ^{bal} and ϕ^{pref}, for which V_{min} remains almost constant. Indeed, this is the case, and for sharp separations we have in fact a region in which V_{min} is exactly constant. This is shown in the insightful analysis of Fidkowski and Krolikowski (1986).

To complete the foregoing analysis of the prefractionator column we here present the main results from this work. Through a careful analysis of the Underwood equations, Fidkowski and Krolikowski (1986) show that the minimum reflux for a sharp split between components A, B and C is given by

$$\left(\frac{L}{F}\right)_{min} = max\{\frac{z_A\theta_1}{\alpha_{AC}-\theta_1}, \frac{z_A\theta_2}{\alpha_{AC}-\theta_2} + \frac{\alpha_{BC}z_B}{\alpha_{BC}-\theta_2}\} \tag{5.43}$$

and corresponding for the minimum boilup

$$\left(\frac{V}{F}\right)_{min} = max\{\frac{\alpha_{AC}z_A}{\alpha_{AC}-\theta_1}, \frac{\alpha_{AC}z_A}{\alpha_{AC}-\theta_2} + \frac{\alpha_{BC}z_B}{\alpha_{BC}-\theta_2}\} \tag{5.44}$$

where θ_1 and θ_2 are the solutions of the Underwood equation (5.14). These roots may be computed for the *absolute* minimum solution for the prefractionator, which as previously discussed corresponds to the preferred separation. They then carry over to the solutions for the upper and lower part of the main sidestream column. The authors further show that V_{min} is constant between the fractional recoveries ϕ^{pref} given in equation (5.9) and the recovery ϕ^R given by

$$\phi^R = \frac{L_{min}\left(\alpha_{AC}-\alpha_{BC}\right) - Fz_A\alpha_{BC}}{L_{min}\alpha_{AC} - \left(L_{min} + Fz_A + Fz_C\right)} \tag{5.45}$$

As noted by Carlberg and Westerberg (1989) this constant minimum reflux *region* is constituted by 4 different sets of specifications for the recoveries and Underwood roots. We thus have that for Petlyuk columns with a sufficiently large number of stages, one may operate that column at any value between ϕ^{pref} and ϕ^R without any increase in the energy usage. For completeness, we also note that Carlberg and Westerberg (1989) extended the analysis for the Petlyuk column also to multicomponent mixtures with an arbitrary number of components.

We may further comment that ϕ^R for the Petlyuk column has the same significance as ϕ^{bal} for the prefractionator arrangement. However we stress that for the latter we found that the minimum energy usage is always smaller for ϕ^{pref} (although only slightly in many cases). We may compare the extent of the "flat" regions in the prefractionator arrangement and the "constant" region of the Petlyuk column. The difference between these depend only on the recoveries of ϕ^{bal} and ϕ^R, since the other limiting value is that of ϕ^{pref} which is the same for both columns. In Table 5.2 we give values of ϕ^{bal} and ϕ^R obtained from equations (5.27) and (5.45) for a feed composition of $z_F = [0.1, 0.8, 0.1]$ and different volatilities. We also give V_{min} for the two column arrangements.

Table 5.2: Comparison of prefractionator arrangement and Petlyuk column for sharp separations of a ternary mixture with $z_F = [0.1, 0.8, 0.1]$

Volatilities	ϕ^R	ϕ^{bal}	ϕ^{pref}	$V_{min}^{petlyuk}$	$V_{min}^{prefrac}$
$\alpha = 4:2:1$	0.6535	0.6667	0.3333	1.828	1.867
$\alpha = 4:3:1$	0.2691	0.2639	0.6667	2.830	2.867
$\alpha = 4:1.3:1$	0.9038	0.9740	0.1000	3.924	3.967

5.8 Preferred Separation in Real Columns Using a Finite Number of Stages

The analytical results presented in the previous sections apply to the special case of sharp splits and infinite columns. To verify the analytical results, and to examine the impact of "finite" columns, we now consider numerical simulations for simple, but detailed stage by stage models of distillation columns. Our objective is thus to establish whether using the preferred separation yields the minimum energy inputs for complex columns with a finite number of trays and finite purities. Results are presented both for the prefractionator arrangement and the Petlyuk column in Figure 5.1.

5.8.1 Optimal split-sequence for sharp splits

In this section we present numerical results from nonlinear simulations of staged columns assuming constant molar flows and constant relative volatilities. The process data for the simulations are given in Table 5.3. Here $N_i = 30$ denotes the number

Table 5.3: Data for ternary separations in real ("finite") column

Number of stages	$Ni = 30$
Feed compositions	$z_F = [0.1, 0.8, 0.1]$
Molar feed	$F = 1$ [kmol/min]
Relative volatility	$\alpha = 4:2:1$
Purity spec.'s	$x_i^P = 99.8\%$
	$x_A^b \leq 10^{-3}$
	$y_C^d \leq 10^{-3}$

of stages in each of the six column sections, giving a total of 180 stages for all arrangements. The product purities are given by $x_i^P = 99.8\%$ whereas x_A^b and y_C^d denote the purities of A and C in the bottoms and distillate flows from the prefractionator ($C1$), for which we for sharp splits chose the value of $\epsilon = 10^{-3}$. Note that we for all cases plot the boilup versus the distillate flow. This has however no practical implications since there is a unique (linear) mapping from the recoveries to the distillate given by equation (5.30).

For the arrangements in Figure 5.1 we have 5 DOFs at steady state. Since three of these are consumed in order to keep the product purities at the respective set

points, there is only one DOF left if we are to vary d freely. This last DOF is here used to keep either the purity of A in the bottoms (x_A^b) or C in the distillate (y_C^d) at their set-points of $\epsilon = 10^{-3}$. The procedure for obtaining the desired numerical results can then be outlined as follows. We first compute the minimum boilup using the gradient projection method discussed in chapter 3 for which we optimize with respect to the two remaining DOFs. Using this optimum as an initial point we then obtained the uniquely defined solution corresponding to $x_A^b = y_C^d = 10^{-3}$, for which all the DOFs are consumed. To determine whether the optimum corresponds to the preferred separation also for (real) columns with a finite number of stages, we then obtained solutions for different values of d by continuation along lines of constant x_A^b and y_C^d. We thus use the value of d corresponding to $x_A^b = y_C^d = 10^{-3}$ in order to switch between the solutions branches. Note also that as for the initial example in Figure 5.4, the impurity specifications are satisfied as inequalities for all other values of d.

5.8.2 Prefractionator arrangement

In Figure 5.13 we give numerical results for the prefractionator arrangement in Figure 5.1, using the data in Table 5.3. Figure 5.13 (a) illustrates an important feature with respect to practical operation. We find that the energy usage stays relatively constant in a region where we keep the composition in the top constant, i.e. $y_C^d = 10^{-3}$. As shown in Figure 5.13 (b), this region corresponds roughly to the region between the preferred separation (d^{pref}) and the balanced main column (d^{bal}). Figure 5.13 (b) also illustrates the comparison between the numerical results and the analytical results shown in Figure 5.8. The difference owes mainly to the fact that the simulations correspond to a column with a finite number of stages. An important issue to bear in mind, is that by introducing direct coupling between columns $C2$ and $C3$, we have that only a certain fraction of the impurities that enter from the distillate (C) or bottoms (A) of the prefractionator $C1$ will appear as impurities in the sidestream product B. This situation is different from a prefractionator arrangement with three columns, in which case any impurity either in the top or bottoms from the prefractionator leaves in the intermediate product streams. The impact of this direct coupling becomes even more pronounced as we decrease the *product* purity of the intermediate, and hence allow a larger fraction of impurities to enter from the top and/or bottoms of $C1$. This is treated later when considering non-sharp splits. We now proceed to give results for the Petlyuk column.

5.8.3 The Petlyuk column

As previously discussed one may use the Underwood equations to obtain exact analytical solutions for the minimum reflux conditions in Petlyuk columns (Fidkowski and Krolikowski 1986). However, we have not derived any *explicit* analytical results in this paper for the Petlyuk column, although its analogy to the prefractionator is close. We thus expect that the main results for the prefractionator carry over to the Petlyuk column. Note that for the Petlyuk column the *net* distillate flow and

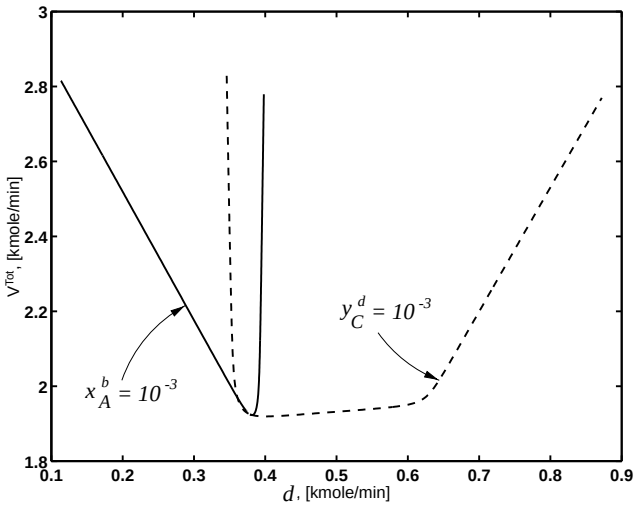

(a) Constant y_C^d, x_A^b

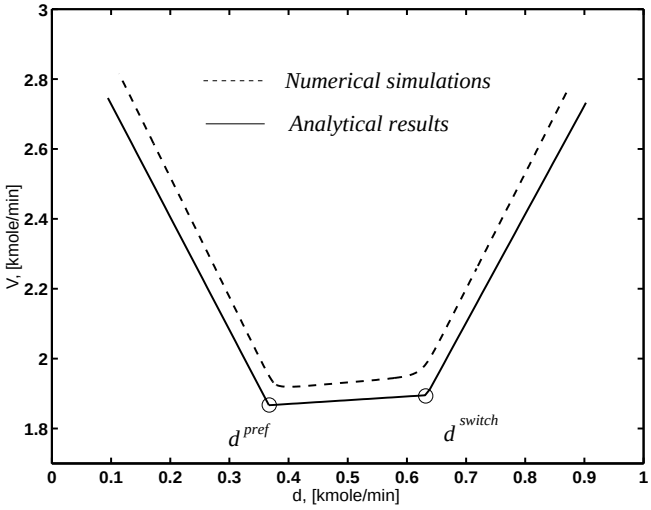

(b) Analytical vs. numerical results

Figure 5.13: Boilup for prefractionator arrangement in Figure 5.1 as a function of the intermediate distillate flow d with $\alpha = 4 : 2 : 1$ and $z_F = [0.1, 0.8, 0.1]$. The solid line in Figure (a) corresponds to $x_A^b = 10^{-3}$ and the dashed line to $y_C^d = 10^{-3}$. Figure (b) gives comparison between numerical and analytical results.

fractional recovery are given by

$$d = R_V V - R_L L \tag{5.46}$$

and

$$\phi_B^d = \frac{R_V V y_B^d - R_L L x_B^{d'}}{F z_B} \tag{5.47}$$

Here R_V and R_L denote the vapor and liquid split ratio from the main column to the prefractionator, y_B^d the vapor composition of B leaving the prefractionator and $x_B^{d'}$ the liquid composition entering in the top of the prefractionator. We should comment that ϕ_B^d in this case may extend outside the range $[0, 1]$ and that the (net) distillate flow may become negative. In Figure 5.14 (a) we show the energy usage V versus d for the Petlyuk column, when using the remaining DOF to fix either the impurity of light in the bottoms (solid line) or heavy in the top (dashed line).

We recognize that instead of consuming the last DOF for purity control, we may of course also use it for optimization purposes. To obtain the "true" optimal solutions for each value of d, we may optimize using for instance the values along constant x_A^b and y_C^d as initial guesses. The optimized curve is given in Figure 5.14 (b). The results indicate that the overall minimum boilup is constant within a large region of distillate flows, and for this example close to the curve given by $y_C^d = 10^{-3}$. According to the discussion in section 5.6 this is as expected, since $\phi^R > \phi^{pref}$ so that the lower feed controls. These results thus confirm that the findings of Fidkowski and Krolikowski (1986) carry over also to columns with a finite number of stages. We furthermore expect that the opposite situation applies to mixtures for which the upper feed controls. Hence if the upper feed controls, the boilup V should be relatively insensitive to changes in d along the line of constant x_A^b.

Comparison with results from the literature

We may now compare the results to the analytical results by Fidkowski and Krolikowski (1986). According to the authors V is constant (at least for infinite number of stages) in the region between ϕ^{pref} and ϕ^R. Computing ϕ^{pref} and ϕ^R from equations (5.9) and (5.45) we find for a sharp A/C split that they correspond to distillate flows of $d^{pref} = 0.3934$ and $d^R = 0.6228$. Comparing these to the optimized curve in Figure 5.14, we find good agreement which confirms the applicability of the analytical results also to columns with a finite number of stages. Note also that from equation (5.44) we obtain $V_{min} = 1.83$ and from the simulations we computed $V_{min} = 1.86$.

Furthermore we recognize that the regions plotted for constant x_A^b and y_C^d correspond to the qualitatively different regions characterized by Carlberg and Westerberg (1989). For instance we have that the left part in Figure 5.14, where the light component is kept constant at the upper bound $x_A^b = 10^{-3}$, and the distillate is practically depleted in the heavy component (i.e. $y_C^d \leq 10^{-3}$), corresponds to what Carlberg and Westerberg (1989) denote as region I. Note that keeping x_A^b at the upper bound, implies that the recovery of A in the top is at its lower bound. The other regions correspond to where y_C^d increases and finally reaches its upper bound of $y_C^d = 10^{-3}$.

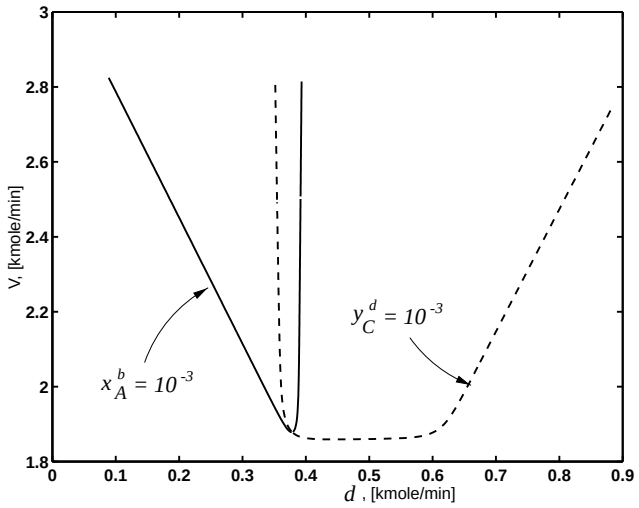

(a) Constant x_A^b, y_C^d

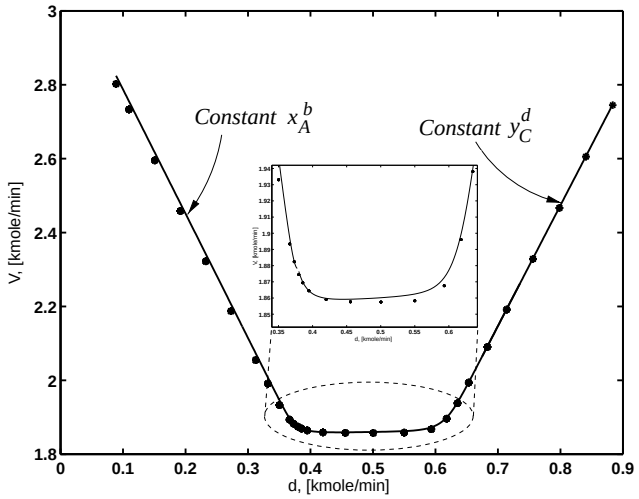

(b) Optimized V

Figure 5.14: Boilup for Petlyuk column as a function of the net distillate flow d. The solid line in (a) corresponds to $x_A^b = 10^{-3}$ and the dashed line to $y_C^d = 10^{-3}$. The solid line in (b) represents lines for constant x_A^b and y_C^d and the circles the optimized (minimized) solutions.

Implications for operation

The implications for operation of the Petlyuk column are in general the same as for the prefractionator arrangements in section 5.5. Furthermore, since there is a region in which V_{min} is constant, one may in fact choose any of the operating points within this region without increasing the energy usage compared to the overall minimum. The Petlyuk column thus proves to be a rather flexible arrangement, in that optimal operation is rather insensitive to changes and disturbances (at least for sharp splits). Although it may appear obvious, we should emphasize that the minimum energy usage is not independent of both DOFs in the prefractionator. Hence it is still required to use (at least) one point control in the prefractionator to maintain operation in the vicinity of the optimum. Furthermore, we acknowledge some important differences between the prefractionator and the Petlyuk column, owing to the direct coupling between the prefractionator and the main (sidestream) column. From a practical point of view it is most likely difficult to use on–line control of the vapor split R_V, so that one may in practice choose to design the column so that R_V during operation is within the optimal region.

Since some means for control in the prefractionator is needed, one may use the liquid split R_L for control. The probably easiest situation in terms of on–line operation, is thus when the lower feed controls, for which one can use R_L to control the impurity of the light component in the top (and overpurify in the bottoms by having R_V sufficiently large). If the upper feed controls, it is somewhat more difficult to control the prefractionator, since one must use the liquid split in the top to control the bottoms composition.

5.8.4 Optimal split-sequence for non-sharp splits

To investigate the impact of non-sharp separations on the optimal split–sequence, we present in this section numerical results for cases when we decrease the *product* purity of the intermediate component B. Thus, we examine the impact of the separation in the downstream (main) column on the optimal split for the prefractionator. This is in general a problem that does not have a unique solution, since we have two DOFs for the prefractionator and may specify any two of the six recoveries (i.e. top and bottom for all three components).

For the numerical examples we use the column data given in Table 5.3, but now we decrease the product purity of intermediate to $x_B^P = 98\%$. In Figure 5.15 we show that reducing x_B^P moves the optimum away from the preferred separation. In fact, the overall minimum energy usage does not correspond to using a sharp A/C split in the prefractionator. This is hardly surprising, since reducing the product purity of B allows for a certain amount of impurity to enter over the top and bottom of the prefractionator. It is thus possible to carry out a non-sharp separation in the prefractionator which reduces the required energy input. Importantly, we see that for the Petlyuk column that there is a "constant" region also for non-sharp separations, which is about as large as for the sharp split case. For this example, where the lower feed controls, one may in practice fix the vapor split at the optimal value and use one-point control in the top where the liquid split controls the top composition.

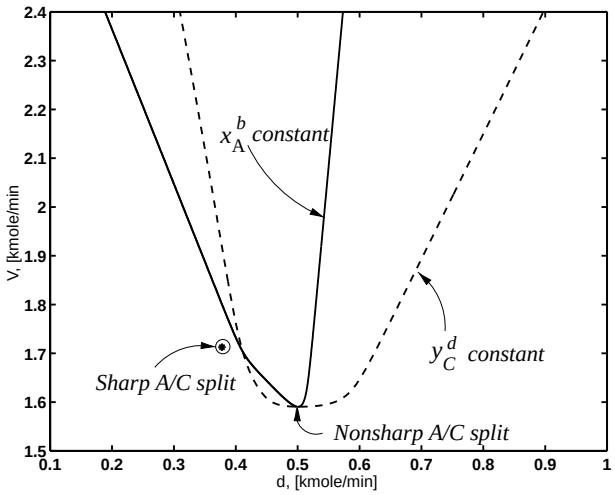

(a) Prefractionator

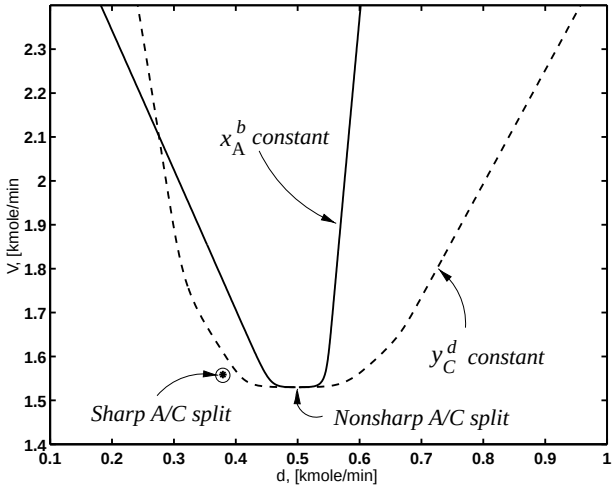

(b) Petlyuk column

Figure 5.15: Boilup for prefractionator arrangement (a) and Petlyuk column (b) as a function of the intermediate distillate flow d for non-sharp A/C split and intermediate product purity of $x_B^P = 98\%$. The solid lines correspond to $x_A^b = 2 \cdot 10^{-4}$ in Figure (a) and $x_A^b = 2 \cdot 10^{-5}$ in Figure (b). The dashed lines correspond to $y_C^d = 3 \cdot 10^{-2}$ in Figure (a) and $y_C^d = 1.4 \cdot 10^{-2}$ in Figure (b).

In figure 5.16 we compare the operating lines for constant y_C^d with the optimized curve, i.e. using the last DOF to minimize V for each value of d.

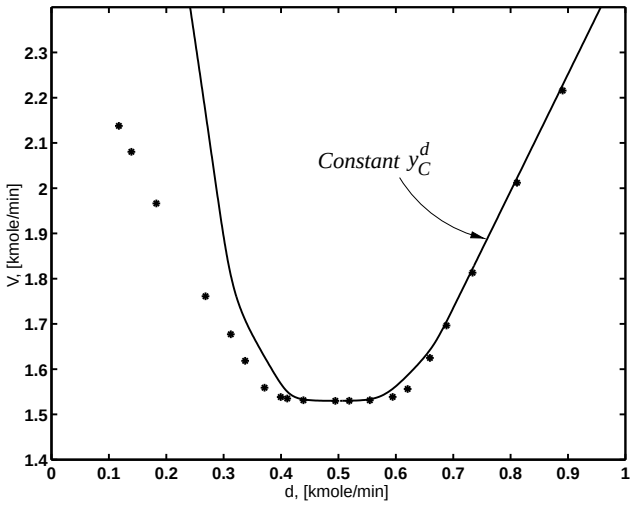

Figure 5.16: Boilup for Petlyuk column as a function of the intermediate distillate flow d for non-sharp A/C split. The solid line corresponds to controlling the composition in the top(i.e. $y_C^d = 1.4 \cdot 10^{-2}$) whereas the circles illustrate the optimized V for each value of d .

In Table 5.4 we give results from numerical optimizations using the data in Table 5.3, where minimum energy inputs are given for different column arrangements and intermediate purities x_B^P. In the table we have in terms of rigor also included data for a heat integrated implementation of a three–column prefractionator arrangement. It is interesting to observe that the savings for the Petlyuk column relative to the

Table 5.4: Minimum energy usage for prefractionator arrangements and Petlyuk column for different intermediate product purities

	$x_i^P = 99.8\%$	$x_B^P = 98\%$	$x_B^P = 95\%$
Heat integrated	$V_{min} = 1.92$	$V_{min} = 1.64$	$V_{min} = 1.25$
Prefractionator	$V_{min} = 1.91$	$V_{min} = 1.59$	$V_{min} = 1.20$
Petlyuk column	$V_{min} = 1.86$	$V_{min} = 1.53$	$V_{min} = 1.08$

prefractionator arrangements increase as the intermediate purity x_B^P is decreased. For $x_B^P = 95\%$ the additional savings are as large as 10%. One may also note that conventional arrangements such as the direct or indirect schemes require, a minimum energy usage of $V_{min} = 2.73$ for *sharp separations* of the given mixture in an infinite column. This value is easily obtained from Underwood's method.

A useful feature of the optimization procedure is that we may obtain the sensitivities for the energy usage with respect to the product purities, by computing the Lagrangian multipliers at the optimal solutions. This is an issue to be dealt with in chapter 7, so that the details of the calculation procedure is not given here. In table

5.5 we give Lagrangian multipliers for two product purities for the Petlyuk column. Using the information contained in these multipliers proves very useful, although we

Table 5.5: Lagrangian multipliers for the intermediate product purity

$x_i^P = 99.8\%$	$V_{min} = 1.86$	$\lambda = 43$
$x_B^P = 98\%$	$V_{min} = 1.53$	$\lambda = 15$

should emphasize that the results in general apply only locally since it is based on approximating the optimal surface as a quadrature. For instance we find that for $x_B^P = 0.98$ $\lambda = 15$. Hence if x_B^P is reduced to $x_B^P = 0.95$, we have that the *predicted* reduction in the energy usage is $\Delta V = 15 \cdot (0.98 - 0.95) = 0.45$. Compared to the results in table 5.4 we thus find excellent agreement since $\Delta V = 1.53 - 1.08 = 0.45$! For the sharp split case, the results are however not that accurate. This is is however as expected since there is a large *relative* decrease from $x_B^P = 0.998$ $x_B^P = 0.98$. Thus it is only correct for smaller reductions in x_B^P.

5.9 Prefractionator or Petlyuk Column?

We have in this paper discussed some important features of the prefractionator arrangements and the Petlyuk column, which proves useful for both operation and design. We may summarize these findings by comparing certain advantages and drawbacks for the two designs.

(1) The Petlyuk column always give a lower V_{min} as shown by Fidkowski and Krolikowski (1990), although the difference is usually small. The lower energy usage owes to supplying all heat (boilup) in the bottoms of the Petlyuk column, and all cooling (reflux) in the top, so that one in fact increases the internal flows in *all sections*. For the prefractionator arrangement a given part of the energy input is "only" used in the prefractionator column.

(2) The Petlyuk column has a region between certain recoveries for the intermediate component, given by $\phi_B^d \in [\phi^{pref} \phi^R]$, where V_{min} is constant. The prefractionator on the other hand displays a "flat" region where V_{min} may increase only little for changes in the recoveries in the region $\phi_B^d \in [\phi^{pref} \phi^{bal}]$ where V_{min}. This has important implications for operation, since one may use control in only one end of the prefractionator column and "overpurify" in the other end. The Petlyuk column thus have a slight advantages in terms of flexibility, since one may allow for operation within a certain range of recoveries, without paying a penalty of increased energy input.

(3) For operation and control it is also important to recognize that it is probably easier to control *external* flows (i.e. reflux and boilup) rather than manipulating the internal splits (vapor R_V and liquid R_L). For the prefractionator arrangement it thus proves useful to have an external condenser and reboiler compared to the directly coupled flows in the Petlyuk column. The latter may also act

in favor of the prefractionator arrangement, since "two–point" control (i.e. in both column ends) is easier to implement.

(4) The Petlyuk column is in general more favorable with respect to energy loads ("first law effects") than energy levels ("second law effects"). Since the Petlyuk column consumes all heat at the highest temperature (reboiler) and all cooling at the lowest temperature (bottoms), the utilities may be more expensive than for the prefractionator arrangement where some of the boilup and reflux is supplied at less "extreme" levels.

(5) For retrofit and revamping studies, where columns and heat exchangers often are available on cite, the prefractionator arrangement may have some advantages. This owes also to the possibility for using heat integration of the intermediate utility (prefractionator column), which is not possible for the fully integrated Petlyuk column. Hence if utility from some other process stream is available at the level required for the prefractionator column, the "overall" energy consumption may in fact be smaller than the Petlyuk column. One may also operate the two columns in the prefractionator arrangement under different pressure, so as to take advantage of different utility levels on a large scale.

(6) An issue that favors the Petlyuk column is that it may be implemented in a single shell using a dividing wall as suggested by Wright (1949). Thus one may also considerably reduce the capital costs and the literature indicates savings in the order of 30% (Smith 1995). However, for such dividing wall columns the aspects of operation and control may become even more crucial. Recent industrial practice however indicates that these are issue which may be resolved.

(7) Finally we give a comment on the claim by some authors (e.g. Carlberg and Westerberg (1989)) that the Petlyuk column is only favored when the temperature difference between the heat sources and sinks are large. Although this argument based on "second law effects" (levels) certainly applies, one should at the same time recognize that the "first law" savings (loads) for the Petlyuk column is the largest when the relative volatilities are small, i.e. the temperature differences are small. Hence it is important to always keep in mind this important trade off. However, for close boiling mixtures we also acknowledge that a very large number of stages is required for the Petlyuk column, so that the pressure drop should also be taken into account.

5.10 Discussion and Conclusions

In this paper we have proposed analytic expressions to obtain the minimum energy usage (V_{min}) for prefractionator arrangements. These expressions allows one to obtain V_{min} explicitly for any split of the intermediate component in the prefractionator. Furthermore we have addressed the issue of using the preferred separation as the initial split for multicomponent separations. We have shown that for sharp splits of ideal mixtures, the preferred separation yields the true overall V_{min}. An equally important

observation in terms of implications for practical operation, is that there may exist a (large) region of splits in the prefractionator for which V_{min} stays relatively constant. Interestingly we find that using the idea of the preferred separation (Stichlmair 1988) suggest operating the column at one end in this "constant" region, whereas the idea of balancing the main column (Triantafyllou and Smith 1992), suggest operation in the other end. In practical operation it is however usually best to use an intermediate value, because column operation is then relative insensitive to changes.

To verify the significance of the analytical results, we also studied the importance of using the preferred separation for columns with a finite number of stages and for non-sharp separations. For sharp splits we found good agreement between the analytical and numerical results. Results from numerical simulations also indicate that using direct coupling between column sections introduces a degree of flexibility in the column, which proves favorable in terms of operation. For the prefractionator arrangement we find that there is a region of recoveries for which the minimum energy usage stays relatively constant, i.e. there is a "flat region". For the Petlyuk column there is similarly a region where the minimum energy in fact stays constant. This constant region has been showed in the literature to hold for infinite columns and sharp splits, and in this paper we present numerical simulations that shows that it holds also for Petlyuk columns with a finite number of stages and non-sharp separations. Numerical results are also presented which indicate that the fractional savings of the Petlyuk column in fact increases as the purity of the intermediate product is decreased.

Based on the results presented in this paper, we find that in order to maintain operation in the vicinity of the optimum, it may for some cases suffice to use only "one-point control" in the prefractionator. This means that one may overpurify in one end of the prefractionator, and control the composition in the other end to keep this at its optimum value. For the Petlyuk column we may for instance fix the vapor split R_V and use the liquid split R_L to control either the heavy impurity in the top of the prefractionator or the light impurity in the bottom depending on whether the upper or lower feed controls. This finding is supported by simulations where we find that the energy surface is "flat" in certain regions, within which optimal operation should take place.

In order to project our results onto possible directions for future research, we believe that the results presented in this paper may be quite easily extended to multicomponent mixtures of more than three components. In particular we believe that the concepts of the preferred separation and balancing sidestream columns should prove to be very useful in the analysis of other complex distillation arrangements. We expect that using the concept of the preferred separation, which gives the optimal distribution of intermediate components for a pseudo-binary split (for the Petlyuk column it gives *one* of the optimal solutions), may be used to decompose a multicomponent separation to that of a sequence of pseudo-binary splits.

Nomenclature

A, B, C – Component indices

D – Notation for direct split
d – Distillate flow rate [kmol/min]
f – Parameter in minimum reflux expression, i.e. $f = 1 + z_B/100$
F – Feed flow rate [kmol/min]
I – Notation for indirect split
L – Reflux flow rate [kmol/min]
N – Number of theoretical stages
q – Feed enthalpy
R_L – Vapor split fraction in Petlyuk column
R_V – Liquid split fraction in Petlyuk column
S – Separation factor
t – Time [min]
V – Boilup from reboiler [kmol/min]
x_i – Liquid mole fraction of component i
x_i^P – Product composition of component i
y_i – Vapor mole fraction of component i
z_i – Mole fraction of component i in feed

Greek letters

α_{ij} – Relative volatility between components i and j
Δ – Deviation variable
ϵ – Upper bound on impurity mole fractions
λ – Lagrangian multiplier
∂ – Derivatives
ϕ_i^d – Fractional recovery of component i in distillate
ϕ^{pref} – Fractional recovery of component B for the preferred separation
ϕ^{bal} – Fractional recovery of component B for balanced main column
θ_i – ith root of Underwood equation

Sub– and superscripts

bal – Balanced column
$main$ – Main sidestream column in prefractionator arrangements
F – Feed stage
min – Minimum flow conditions for infinite number of stages
$pref$ – Preferred separation
P – Product

References

Carlberg, N. A. and A. W. Westerberg (1989). Temperature-Heat Diagrams for Complex Columns. 3. Underwood's Method for the Petlyuk Configuration. *Ind. Chem. Eng. Res.* **28**(9), 1386–1397.

Cerda, J. and A. Wersterberg (1981). Shortcut Methods for Complex Distillation Columns. 1. Minimum Reflux. *Ind. Chem. Eng. Process Des. Dev.* **20**(3), 546–557.

Fidkowski, Z. and L. Krolikowski (1986). Thermally Coupled system of Distillation Columns: Optimization Procedure. *AIChE Journal* **32**(4), 537–546.

Fidkowski, Z. and L. Krolikowski (1990). Energy Requirements of Nonconventional Distillation Systems. *AIChE Journal* **36**(8), 1275–1278.

Glinos, K. and M.F. Malone (1984). Minimum Reflux, Product Distribution, and Lumping Rules for Multicomponent Distillation. *Ind. Eng. Chem. Process Des. Dev.* pp. 764–768.

Glinos, K. and M.F. Malone (1988). Optimality Regions for Complex Column Alternatives in Distillation Systems. *Chem. Eng. Res. Des.* **66**(3), 229–240.

King, C. J. (1971). *Separation Processes*. McGraw-Hill Chemical Engineering Series. McGraw-Hill Book Company.

Morud, J. (1995). Studies on the Dynamics and Operation of Integrated Processes. PhD thesis. University of Trondheim. The Norwegian Institute of Technology. Norway.

Nikolaides, I. P. and M. F. Malone (1988). Approximate Design and Optimization of a Thermodynamically Coupled Distillation with Prefractionaton. *Ind. Chem. Eng. Res.* **27**(5), 811–818.

Petlyuk, F. B. and V. M. Platonov (1964). Thermodynamically Reversible Multicomponent Distillation. *Khim. Prom.* (10), 723.

Petlyuk, F. B., V. M. Platonov and D. M. Slavinskij (1965). Thermodynamically Optimal Method for Separating Multicomponent Mixtures. *Int. Chem. Eng.* **5**(3), 555–561.

Petlyuk, F. B., V. M. Platonov and V. S. Avetlyan (1966). Optimum Arrangements in the Fractionating Distillation of Multicomponent Mixtures. *Khim. Prom.* **42**(11), 865.

Smith, R. (1995). *Chemical Process Design*. Wiley.

Stichlmair, J. (1988). Distillation and Rectification. *Ullmann's Encyclopedia of Industrial Chemistry* **B3**, 4–1 – 4–94.

Stupin, W. J. (1970). The Separation of Multicomponent Mixtures in Thermally Coupled Distillation Systems. PhD thesis. University of Southern California, USA.

Triantafyllou, C. and R. Smith (1992). The Design and Optimization of Fully Thermally Coupled Distillation Columns. *Trans. Inst. Chem. Eng.* **70**(Part A), 118–132.

Underwood, A. J. V. (1948). Fractional Distillation of Multicomponent Mixtures. *Chem. Eng. Prog.* **44**(8), 603–614.

Wolff, E. A. and S. Skogestad (1995). Operation of Integrated Three–Product (Petlyuk) Distillation Columns. *Ind. Chem. Eng. Res.* **34**(6), 2094–2103.

Wright, R. O. (1949). U.S. Patent 2,471,134.

Appendix A Fractional Recoveries for the "Preferred" Separation

The underlying assumption in the expressions for minimum reflux presented by King (1971) and Stichlmair (1988), is the occurrence of a pinch at the feed point for *all* components in a multicomponent mixture. In the main body of the paper we showed how one may find expressions for cases where the feed is saturated liquid. We here show how to derive similar expressions for *saturated vapor feeds*.

A.1 Preferred separation for saturated liquid and vapor feeds

Assuming that all components pinch at the feed point under limiting flow conditions (i.e. minimum reflux), we find using the component balances around each stage that the minimum reflux ratio is given by

$$\left(\frac{L}{D}\right)_{min} = \frac{x_{Di} - y_{Fi}}{y_{Fi} - z_i} \tag{5.48}$$

This can easily be illustrated from McCabe–Thiele diagrams for each component. For a *saturated vapor feed* we have from (King 1971)

$$\left(\frac{V}{F}\right)_{min} = \frac{\alpha_{LH}\phi_L^d - \phi_H^d}{\alpha_{LH} - 1} \tag{5.49}$$

If we then equate expression (5.49) twice for the sharp split between components A and C ($\phi_A^d = 1$ and $\phi_C^d = 0$), and the corresponding split between A and B, we obtain

$$\frac{\alpha_{AC}}{\alpha_{AC} - 1} = \frac{\alpha_{AB} - \phi_B^d}{\alpha_{AB} - 1} \tag{5.50}$$

which gives

$$\phi_{vapor}^{pref} = \frac{\alpha_{AC} - \alpha_{AB}}{\alpha_{AC} - 1} \tag{5.51}$$

If we assume that all components pinch at the feed point also for *non-sharp* separations, we may use the formulas given above also for this case. For saturated liquid feeds and non-sharp separations we thus have (King 1971)

$$\left(\frac{L}{F}\right)_{min} = \frac{\phi_A^d - \alpha_{AB}\phi_B^d}{\alpha_{AB} - 1} = \frac{\phi_A^d - \alpha_{AC}\phi_C^d}{\alpha_{AC} - 1} \tag{5.52}$$

Given the recoveries of A and C, we may thus obtain the fractional recovery of B *exact* for the preferred separation also when the purities are not high, i.e.

$$\phi_{liquid}^{pref} = \frac{\phi_A^d\,(\alpha_{BC} - 1) + \alpha_{BC}\phi_C^d\,(\alpha_{AB} - 1)}{\alpha_{AC} - 1} \tag{5.53}$$

For vapor feeds use equation (5.49) and obtain

$$\phi_{vapor}^{pref} = \frac{\phi_A^d\,(\alpha_{AC} - \alpha_{AB}) + \phi_C^d\,(\alpha_{AB} - 1)}{\alpha_{AC} - 1} \tag{5.54}$$

These equations then reduce to (5.9) and (5.51) in the special case of sharp splits.

Chapter 6

Complex Distillation Arrangements: Extending the Petlyuk Ideas

Atle C. Christiansen, Sigurd Skogestad* and Kristian Lien

Department of Chemical Engineering
Norwegian University of Science and Technology, NTNU
N–7034 Trondheim Norway

Extended version of paper presented at
PSE'97 / ESCAPE–7, Trondheim, Norway, May 26-29, 1997
Proceedings p. 237-242

Abstract

The task of separating a multicomponent mixture into streams enriched in the respective components is commonly carried out in conventional distillation columns arranged in series. However, due to the scrutiny of tighter requirements for energy and cost efficiency, current research aims at alternative column arrangements that offer savings in both operational (energy) and capital costs. Among these we have the Petlyuk or dividing wall column, in which three components are separated in a single shell using only one reboiler and one condenser. In this paper we extend the Petlyuk ideas to separations of four components, although extensions to more components is straightforward. We provide a general definition of *Petlyuk arrangements* and discuss alternative structures from the literature. Following this overview we consider particular arrangements that allows for implementation in a *single shell* using dividing walls or vertical partitions.

*Author to whom correspondence should be addressed : Fax : +47 7359-4080, E-mail: skoge@chembio.ntnu.no

6.1 Introduction

Industrial distillation processes are commonly known to be highly energy–demanding operations. Recent surveys indicate that energy inputs to distillation columns account for roughly 3% of the *total* energy consumption in the U.S. (Ognisty 1995). For this reason there is ample scope for developing more energy efficient separation schemes. In order to reduce energy consumption at least two alternative approaches have been proposed both in the literature and by industrial practitioner. These approaches subscribe to either integrating conventional distillation arrangements, or to the design of new configurations. The former approach typically involves distillation columns arranged in series with energy integration between columns or other parts of the plant. Among the "new" configurations that offer both energy and capital savings we find the dividing wall column first proposed by Wright (1949). Beloved children are known by many names, and this arrangements is also known as the Petlyuk column, due to a theoretical study of Petlyuk *et al.* (1965), or as a *fully thermally coupled* column (Triantafyllou and Smith 1992). In order to provide a common framework for future work, we use the following definition:

> *A Petlyuk arrangement is a column arrangement separating three or more components using a single reboiler and a single condenser, in which any degree of separation (purity) can be obtained by increasing the number of stages (provided the reflux is above a certain minimum value and the separation is thermodynamically feasible).*

Use of this definition eliminates for example a conventional sidestream column from being considered as a Petlyuk arrangement, since these require infinite reflux to obtain a pure sidestream product (even with an infinite number of stages).

A schematic of the well known Petlyuk Column for separations of ternary mixtures ($n = 3$), is illustrated in Figure 6.1. We emphasize that the two representations are identical from a computational and thermodynamical point of view if we neglect heat transfer across the dividing wall. Although the Petlyuk arrangement shown in Figure 6.1 have been known for almost 50 years (Wright 1949), it has only quite recently gained interest also in industry. The Petlyuk column has nevertheless been the subject of several theoretical studies (see e.g. Petlyuk *et al.* (1965), Petlyuk *et al.* (1966), Fidkowski and Krolikowski (1986), Carlberg and Westerberg (1989), Kaibel (1987), Triantafyllou and Smith (1992) and Wolff and Skogestad (1995)). In the literature it is reported that for ternary mixtures ($n = 3$), the Petlyuk column requires typically 30% less energy input compared to conventional arrangements using simple columns in sequence. Due to the possibility of implementing the column in a single shell (dividing wall column), and savings of one reboiler and one condenser, the capital savings are also typically in the order of 30% (Smith 1995). The literature on Petlyuk arrangements for separating mixtures with more than three components is relatively scarce. Among the few contributions are some ideas presented by Kaibel (1987). However, neither detailed analysis nor computational results are presented.

The main contributions from this chapter lie in providing a systematic framework for analysis and design of Petlyuk arrangements for separations of mixtures with four

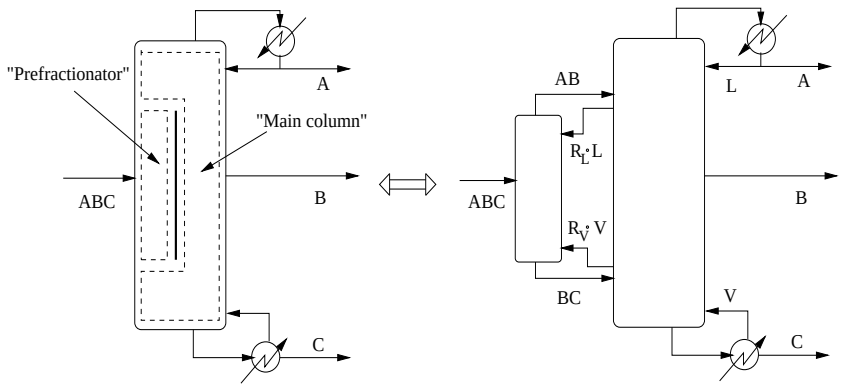

Figure 6.1: Petlyuk column for ternary separations. Left : Left : Dividing wall implementation. Right : Equivalent prefractionator arrangement.

or more components. Let n here denote the number of components in a mixture to be separated into its pure constituents. For a conventional scheme consisting of a sequence of *regular* columns, it is well known that for sharp separations a minimum of $2(n-1)$ sections with $(n-1)$ reboilers and $(n-1)$ condensers is required. Here a section denotes a part of the column from which no streams enter or leave.

In order to derive the "optimal" scheme from all possible sequences, various methods have been presented in the literature. The mathematical problem may be formulated as a MINLP–problem to be solved by some optimization–algorithm. However, for a large number of components, one in practice often fails to locate the global optimum due to non–convexities and computational issues. To overcome these limitations, heuristics and evolutionary strategies have been proposed to guide the engineer in choosing from the set of possible arrangements (e.g. Tedder and Rudd (1978) and Nishida *et al.* (1981)). Among the most important tasks when seeking to find the optimal column arrangement, is that of deriving a general *superstructure* which incorporates all other configurations as substructures. In this work we consider three different "superstructures" for Petlyuk arrangements proposed in the literature. These are based on the works of Sargent and Gaminibandara (1976), Agrawal (1996) and Kaibel (1987).

Before going into detailed analysis of different Petlyuk arrangements, we will elaborate on certain issues of fundamental importance. Firstly we address the issue of *sharp* splits, which is crucial in order to understand the achievable separations for binary and multicomponent distillation. We then briefly discuss some aspects related to the question of energy versus exergy.

6.2 Sharp Split Arrangements

It is common practice within theoretical studies on batch, continuous and complex distillation columns to infer the separation of a given mixture in terms of *sharp splits*.

For instance, Cerda and Wersterberg (1981) use the word *sharp* for the case where the recoveries of light and heavy key are *"close to one"*. However, the sharpness of the splits obviously depends on a number of factors such as the structure of the column, the number of stages, the reflux and the thermodynamic properties (e.g. relative volatility). In this paper we are mainly interested in the structure (arrangement) of the columns and we propose the following definition:

> A sharp split arrangement is an arrangement of columns in which any degree of separation (purity) can be obtained by increasing the number of stages (provided the internal refluxes are above certain minimum values and provided the separation is thermodynamically feasible).

A Petlyuk column is then a sharp split arrangement with a single condenser and a single reboiler. To clarify the above definition, we note that a special property of distillation columns is that any degree of separation (purity) can be achieved by increasing the number of stages. In order to illustrate this point, consider first the McCabe–Thiele diagrams in Figure 6.2. In the case of limiting flow conditions (min-

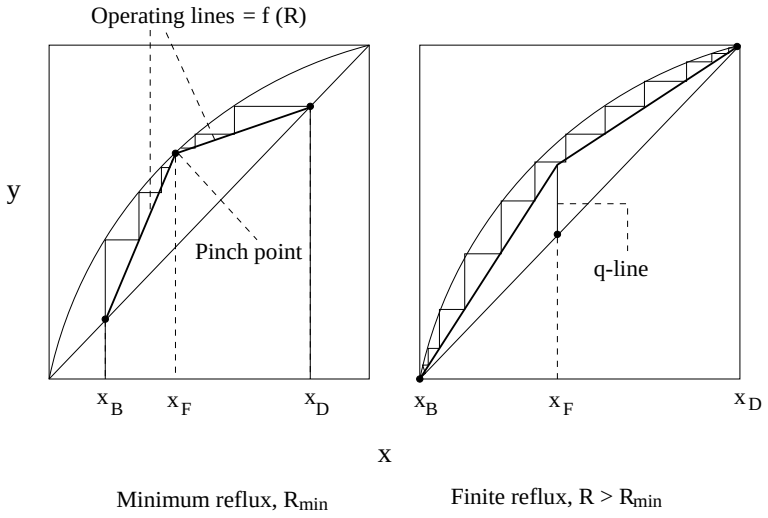

Figure 6.2: McCabe-Thiele diagrams for binary separations

imum reflux R_{min}), a pinch zone occurs in the vicinity of the feed point, requiring a large number of stages in this section. However, by increasing the number of stages, and allowing for a *finite* increase in R, we may in fact achieve any purity. This relation is also revealed if we consider the approximate expression for the *separation factor* as derived by Skogestad and Morari (1987) for a binary mixture with constant relative volatility α:

$$S \stackrel{\text{def}}{=} \frac{x_T/(1-x_T)}{x_B/(1-x_B)} \approx \alpha^N \frac{(L/V)_T^{N_T}}{(L/V)_B^{N_B}} \tag{6.1}$$

where T and B denote the top and bottom respectively. We see clearly that $S \to \infty$ when $N \to \infty$, whilst $S \to \alpha^N$ when $L \to 1$ (total reflux). The latter is the well known Fenske equation which yields the minimum number of stages N_{min} for a given separation. Before going into detailed analysis of particular Petlyuk arrangements and the issue of deriving superstructure, we briefly discuss the issue of reversibility and its impact on the energy consumption of distillation processes.

6.3 Reversible Distillation and Energy versus Exergy

In a thermodynamic sense distillation may be considered as the task of removing the entropy of mixing in the feed by providing exergy. Exergy is supplied by means of adding heat to the reboiler at a temperature T_R and removing (cooling) heat in the condenser at a temperature T_C. As stated by Westerberg (1985), one may thus crudely characterize a column as *"a device that degrades.... heat from T_R to T_C and thereby produces separation work"*. Another important issue is that the exergy required for a conventional distillation process is in general much larger than the amount needed for the limiting case of a *reversible separation*. There is thus "inherently" a certain amount of *lost work* due to by process irreversibilities in various forms that cause exergy losses, i.e. entropy production. A number of previous studies have been devoted to the task of exploring and analyzing such irreversibilities, based on concepts of *availability* (exergy) and thermodynamic lost work (see e.g. Gomez-Munoz and Seader (1985), Kaibel *et al.* (1990) and Ognisty (1995)). Among the most important irreversibilities are (large) temperature differences for heat transfer at separate stages, and irreversible mixing effects during mass transfer due to differences in chemical potential. Both sources, owing to lack of equilibrium, contributes to the *total* exergy loss which also includes lost work due to pressure drops and finite temperature differences in heat exchangers.

By reducing exergy losses caused by irreversibilities one may approach the theoretical limit of reversible separation. However, since reversibility requires an infinite number of trays and intermediate heaters *and* coolers at each stage, the capital costs obviously become infeasible from a practical point of view. However, the additional capital cost associated with a large number of trays and intermediate utilities is somewhat counteracted by two factors (see e.g. King (1971)). These are lesser degradation of heat supply (adding heat at lower temperatures and cooling at higher temperatures) and reduced tower diameter (less fluid flow towards column ends). Close boiling mixtures may be thought of as a "practical" example of potentially reversible splits, for which the composition changes from tray to tray are small. For such separations, the degradation of heat input is also lesser since the temperature difference between reboiler and condenser becomes small. However, since the number of stages required is very large, the pressure drop in such columns may become considerable. Next, we consider in more detail exergy losses caused by irreversible mass and heat transfer, thereby taking a partial account of why Petlyuk columns may prove to be superior to conventional processes.

6.3.1 Reversible Mixing

Even though reversible distillation is infeasible in practice, important insights are still gained by examining the impact of different sources of exergy losses. Although reversibility requires infinite columns and infinitely distributed heating and cooling, one of the requirements for reversibility as stressed by Petlyuk *et al.* (1965), concerns the actual split sequence for the multicomponent separation. This relates to one source of irreversibility which is discussed here.

For conventional arrangements where all of the intermediate components enter the downstream column from the top (indirect split scheme) or in the bottoms (direct split) of the upstream column, back-mixing of intermediate component always occur (Triantafyllou and Smith 1992). This phenomenon is explained if we consider for instance the direct sequence for a ternary separation. The composition of the intermediate component (B) will in this case increase below the feed location since the composition of the light component (A) decrease. However, further down the column the composition of the heavy component C increases, again causing a decrease in the composition of B. The argument is similar for the indirect sequence. For infinite columns there will thus be a pinch zone either at the lower or upper end of the column, where the composition of B passes through a maximum. However, for the Petlyuk column we have the special feature that the intermediate component distributes itself between the distillate and bottoms of the prefractionator column, and the only pinch zone will be at the feed location. Analyzing these conditions in some detail leads to the so called *easiest split* (Petlyuk *et al.* 1965) or the *preferred separation* (Stichlmair 1988), which gives the overall minimum energy usage for a ternary separation as discussed in chapter 5. For the Petlyuk column, back-mixing is in this case avoided, i.e. the composition of intermediate component increases towards the top and bottom without passing through a maximum. Taking the discussion of reversibility one step further, we discuss in the next section how Petlyuk arrangements may allow for distribution of utility in a simple and straightforward manner.

6.3.2 Distribution of Utility

An important source of thermodynamic inefficiency in Petlyuk arrangements, owes to the fact that reboiler duty must be supplied at the highest possible temperature, i.e. boiling point of the heavy component. Similarly, the condenser duty is added at the lowest column temperature. One may therefore find that energy integrated schemes with simple columns in some cases yield lower overall energy costs due to cheaper utilities at less extreme temperature levels (see e.g. Westerberg (1985), Smith (1995) or Annakou and Mizsey (1996)). For such *indirectly* coupled (heat integrated) schemes one may operate the columns under different pressures and thus vary the reboiler temperatures of the different columns independently. However, we emphasize that Petlyuk arrangements still require smaller heat *loads*. As noted by several authors there is thus a trade off between energy loads ("1st law heat") and levels ("2nd law heat"). This illustrates that the optimality conditions for the Petlyuk column versus heat integrated arrangements in general are case specific rather than general, in that it depends on the particular mixture to be separated, available energy inputs etc. As

a comment on this issue, we however stress that if energy is available at the level required for the reboiler, it is in general more efficient to supply all heat input to the reboiler rather than redistributing it. There are however some mixtures where this does not hold.

As for conventional distillation columns, it is possible to increase the thermodynamic efficiency in the Petlyuk column by distributing the energy input along the column. We already mentioned that Petlyuk arrangements offer the potential for large cost–savings when built in a single shell with vertical partitions. However, instead of using simply simple metal sheets for these partitions, as suggested by Wright (1949), Kaibel (1987) and Triantafyllou and Smith (1992), one may consider implementing these vertical partitions as say plate heat exchangers. One may thus distribute the heat input along the column, i.e. cooling at stages above and heating below the feed location. Such plate exchangers may be implemented in a straightforward fashion by allowing cooling duty (reflux) to flow from the condenser down to the feed plate, and boilup from the reboiler to the feed plate. Similar designs are in fact well known under the name of *dephlagmators*. We recognize that intermediate heat exchange increase the required number of stages, since the operating lines are moved closer to the equilibrium line. It thus represents a tradeoff between energy and capital costs. However, lowering the heat loads in the condenser and reboiler also reduce the fluid traffic towards the columns which results in in *narrower* columns (King 1971). Furthermore, for practical implementation the distributed heat exchange may take place only at certain designated locations along the column, chosen on the basis of the regions (stages) in which the largest exergy losses occur. We now return to the task of finding a suitable superstructure in order to find the "optimal" Petlyuk arrangement for a quaternary separation.

6.4 Superstructures for Petlyuk Arrangements

A simple way to compare the different column arrangements for the separation of a quaternary mixture $ABCD$ into its constituents, is provided by the network in Figure 6.3 (e.g. Agrawal (1996)). Using such networks yield convenient visualizations of the pseudo-binary splits that are carried out in the various sections. In this network, the feed represents a node, whereas each line connecting neighboring nodes represents a column section, i.e. a stripping or rectifying section. The intermediate nodes represent streams that are passed from one two–sectional unit to another. The column configuration corresponding to the network in Figure 6.3 consists of $n(n-1)$ sections ($= 12$ sections for $n = 4$). It is possible to eliminate some of the intermediate nodes in the network, thus decreasing the number of sections. However, we note that any structure with less than $n(n-1)$ sections, cannot produce only the *"preferred separation"*. This is explained by recalling the discussion for the preferred separation in chapter 5, where we stressed that only the components with the highest and the lowest boiling points should be separated in each section. For an $n-component$ mixture this requires the "maximum number" of $n(n-1)$ sections.

We first consider the superstructure proposed by Sargent and Gaminibandara (1976) consisting of $n(n-1)$ sections as shown in Figure 6.4. As indicated, the authors

also incorporate the option of additional heating and cooling in each column section. As the authors note, the number $n(n-1)$ actually represents the maximum number of sections in sharp split arrangements for an n–component separation, as all nodes in Figure 6.3 are included. According to the authors, this superstructure contained all

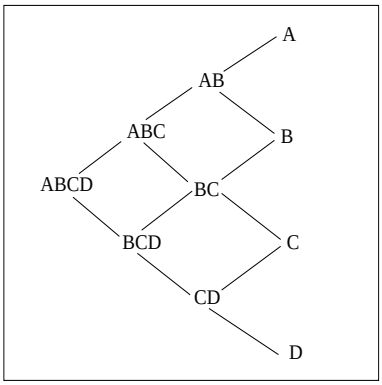

Figure 6.3: Network representation of possible separations involved in separating 4–component mixtures.

functionally possible column arrangements as substructures. However, as illustrated by Agrawal (1996), the proposed superstructure actually fails to do so (see e.g. Figure 6.6). This means that some potentially interesting column arrangements cannot be obtained by removing either column sections or flows from the superstructure.

In a recent article, Agrawal (1996) proposes an alternative superstructure for a certain subclass of Petlyuk arrangements. By considering arrangements with $n-2$ *satellite columns* in communication with a central distillation column, he arrives at the superstructure for quaternary separations shown in Figure 6.5. Agrawal claims that by using this superstructure in combination with a network representation, one may derive all previously proposed configurations giving "sharp splits". Again, this is however not quite true as we will illustrate by a much simpler structure proposed by Cahn *et al.* (1962) and later by Kaibel (1987). For the sake of argument we still appreciate that Agrawal's superstructure is more general than Sargent's arrangement, in the sense that fluid transfer may take place between *any* of the interconnected columns, and it includes Sargent's superstructure and also Kaibel's and Cahn's arrangements as substructures. We furthermore note that in Sargent's sequential structure, there is no direct fluid flow between the first and the last columns. This conceptual difference between the "superstructures' owes to the fact that Sargent considers $n-1$ interconnected distillation columns *in sequence*, whereas Agrawal's superstructure consists of $n-2$ *satellite columns* arranged around a central distillation column. Agrawal also argues that the *minimum* number of rectifying and stripping sections required for sharp splits using such *satellite arrangements*, is equal to $4n-6$ (10 sections for $n=4$). These may be obtained by deleting the BC, ABC or BCD node from the network in Figure 6.3. By deleting for example the BC node we obtain such a structure with 10 sections as shown in Figure 6.6. For $n>4$ the "minimum" number of sections may

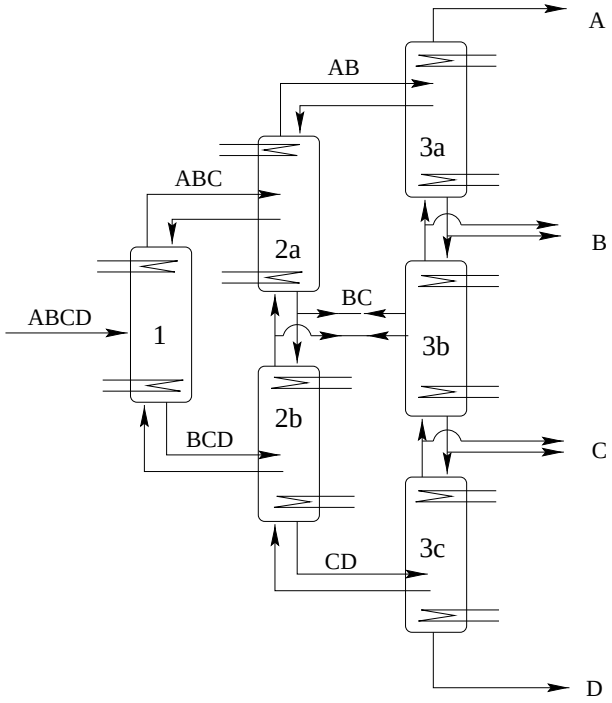

Figure 6.4: Sequence proposed by Sargent and Gaminibandara with $n(n-1) = 12$ sections for $n = 4$ (gives Petlyuk arrangement by deleting intermediate heaters and coolers)

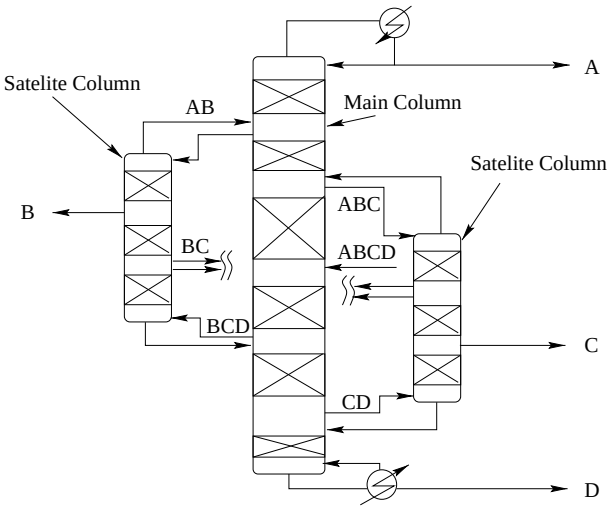

Figure 6.5: Satellite column arrangement proposed by Agrawal with $n(n-1) = 12$ sections for $n = 4$

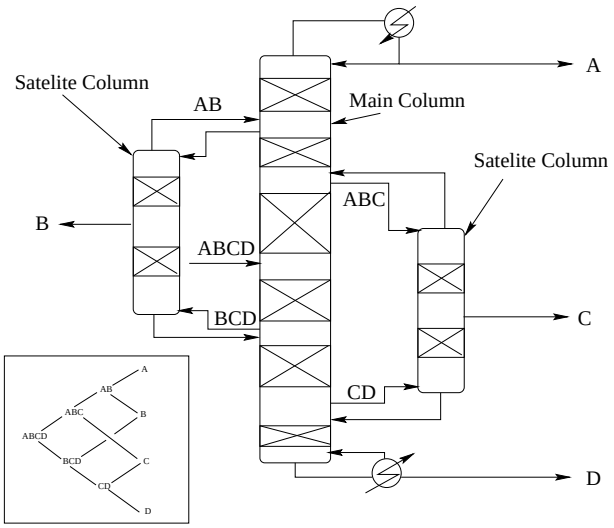

Figure 6.6: Agrawal's substructure with *"minimum"* number of sections, $4n-6 = 10$ sections for $n = 4$

thus become much smaller than $n(n-1)$ as suggested by Sargent and Gaminibandara (1976). However, we stress that $4n - 6$ in fact *does not* give the minimum number of sections for a Petlyuk or sharp split arrangement, as illustrated by considering the Kaibel column in Figure 6.7. Before analyzing the latter arrangement, we ask the reader to note that we later will demonstrate how the arrangements in Figures 6.4, 6.5 and 6.6 may be implemented in a single shell with two vertical partitions.

In the work of Kaibel (1987), columns consisting of *vertical partitions* are considered, based on the *dividing wall* column previously described by Wright (1949). Although Kaibel analyzes in detail only the case of $n = 3$, he also indicates interesting arrangements for $n \geq 4$. In Figure 6.7 we illustrate the simplest extension of the Petlyuk column, in which one simply adds another sidestream for the intermediate. The arrangement to the right is due to an early patent by Cahn *et al.* (1962) whereas the dividing wall column to the left was later proposed by Kaibel (1987). However, since only the latter considered the possibility of implementing columns in a single shell, we in the following denote this arrangement the *Kaibel* column.

The column in Figure 6.7 consists of 7 sections, which is considerably less than Agrawal's *"minimum"* number of 10. The reason for this "inconsistency" is that the Kaibel arrangement consists of only $n - 2 = 2$ columns, whereas Agrawal only considers satellite arrangements with $n - 1$ columns. In order to understand how the *Kaibel column* may result, and how pure products can be obtained in the sidestreams, we draw attention to the schematic in Figure 6.8. Comparing the network representations given in the bottom of Figure 6.8 with the network in Figure 6.3, we see that Kaibel's structure corresponds to eliminating the ABC, BCD and BC nodes, whereas one section is added between the B and C nodes. It is also easily derived from both Agrawal's and Sargent's superstructures.

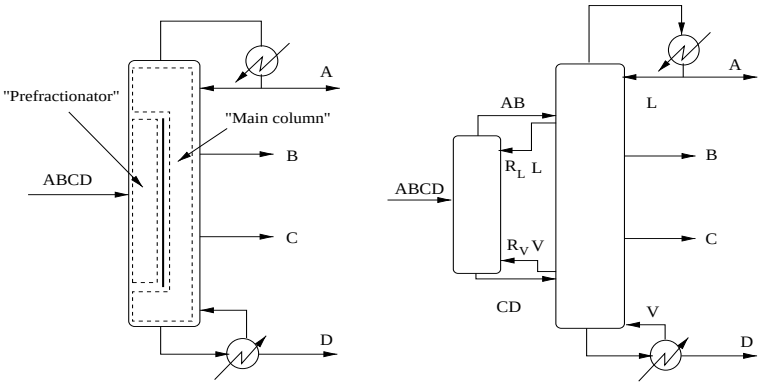

Figure 6.7: Arrangements with 7 sections proposed by Cahn *et. al.* (right) and Kaibel (left)

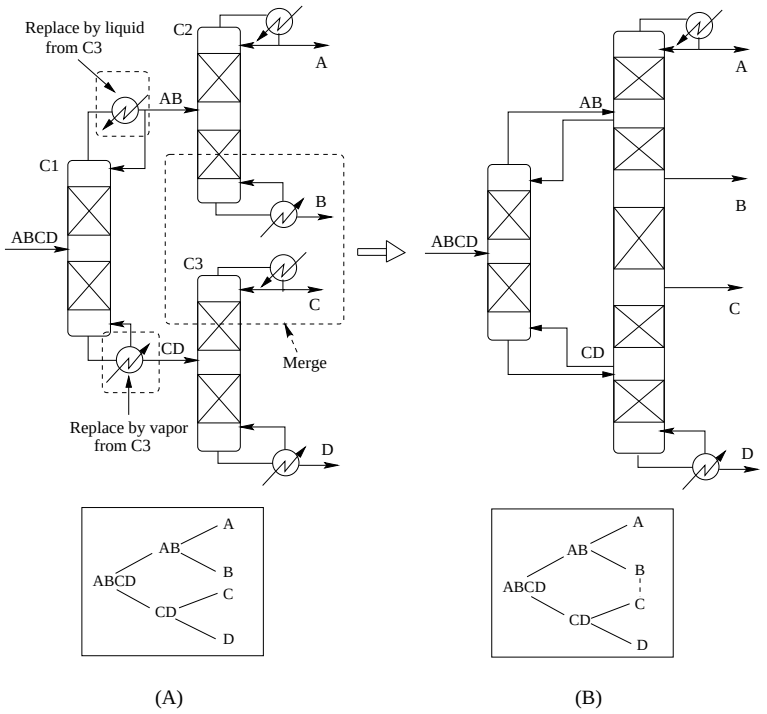

Figure 6.8: Steps towards the Kaibel column. (A) : conventional arrangement. (B) : arrangement after (1) merging columns $C2$ and $C3$ (2) adding an intermediate section and (3) taking boilup and reflux for $C1$ from $C2$ and $C3$.

Having considered some "superstructures" for Petlyuk arrangements, we now focus on how these may be implemented in single shells with dividing walls. In this work we consider arrangements in which we also allow for *communication points* between neighboring sections. In order to cope with some inadequacies of the conventional *dividing wall* columns, we also introduce some novel geometrical wall structures such as the $\vdash$ column and the *triangular* wall column.

6.5 Petlyuk Arrangements with One Dividing Wall

A benefit of a Petlyuk arrangement with a single reboiler and a single condenser is that it may be realized in a single shell with dividing walls, which possibly yields capital savings in addition. We first consider the simplest extension of the Petlyuk column, given in Figure 6.8, for the separation of a quaternary mixture $ABCD$ into its constituents.

Compared with the Petlyuk column in Figure 6.1 for ternary separations, we first acknowledge that the requirement for an *easiest split* is violated. The easiest split requires that only the components with the highest and the lowest boiling points should be separated at each step (see e.g. Petlyuk *et al.* (1965) or King (1971)), in this case requiring a first split between A and D in the prefractionator. However, for the *Kaibel* column we recognize that to obtain *pure* products, a sharp split between the intermediates B and C is required in the prefractionator. If any B enters the main column from the bottom of the prefractionator, some B necessarily leaves the main column with the sidestream where C is drawn off. Similarly, if any C enters in the vapor over the top, a certain fraction of C is withdrawn in the B–sidestream. Thus, one should bear in mind that *any* arrangement with less than $n(n-1)$ sections cannot produce the the easiest split, which most likely increases the required energy input.

Furthermore, we note that the section between the sidestreams in the *Kaibel column*, in fact has no designated separation task, as far as we require that only A and B should enter the main column from the top, and only C and D from the bottom. This leaves only the two binary separations of A/B and C/D for the main column. Ideally, this section should thus operate under *total reflux* with $L = V$, since we want no net transport between the pure B in the upper sidestream and the pure C in the lower side stream. However, B and C might undergo remixing, which in case represents a source of thermodynamic inefficiency. The impact of this remixing is however counteracted if the intermediate section is operated under total reflux and with a certain minimum number of stages (N_{min}^{BC}), where N_{min}^{BC} may be obtained from the well known Fenske equation which applies to any column or column section;

$$N_{min} = \frac{log\,(S_{LH})}{log\,(\alpha_{LH})}, \quad S_{LH} = \frac{x_{L,T}/x_{H,T}}{x_{L,B}/x_{H,B}} \tag{6.2}$$

Here S_{LH} denotes the separation factor, α_{LH} the relative volatility and $x_{L,T}$ and $x_{H,B}$ the purities of the light and heavy keys in the top (T) and bottoms (B) of the column or column section. In practice it may however be very difficult to obtain $L/V = 1$ in the intermediate section, which may prevent high purities of the sidestreams.

6.5.1 Introducing the ⊢ Column

In order to overcome these operational problems with the *Kaibel* column, we introduce a novel arrangement with a *horizontal* partition between the sidestream outlets for B and C, as illustrated in Figure 6.9. We stress that the two representations in Figure 6.9 are identical from a computational point of view, if heat transfer across the partitions is neglected. Providing a conceptual interpretation of the ⊢ column, we note that the

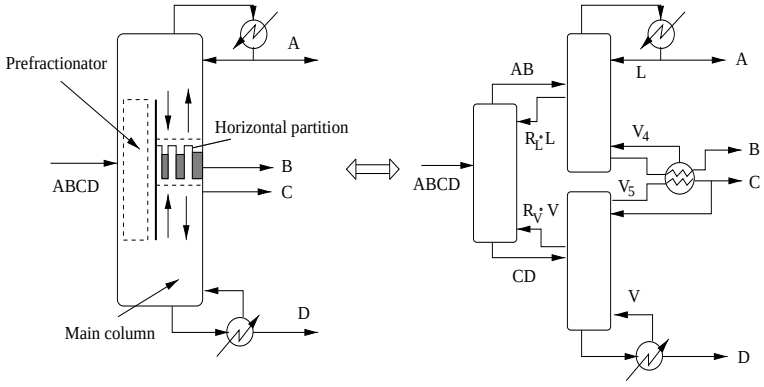

Figure 6.9: ⊢ column with vertical and horizontal partition for quaternary separations

prefractionator is linked via *direct* (thermal) coupling (Petlyuk idea), whereas there are two indirectly coupled (heat integrated) "simple" columns in which waste heat is utilized. Thus, according to our definition it is not a Petlyuk arrangement in a strict sense, for which only a single reboiler and a single condenser should be used. As illustrated in Figure 6.9, the heat exchange may occur either within the column shell (left Figure) or in an external heat exchanger (right Figure). In the former case the heat exchange may take place for example using a dephlagmator, inside which condensation continuously takes place on the hot side and evaporation on the cold side. The choice of heat exchange "unit", either internal or external, is obviously a matter of practicality as well as economy, depending for instance on the required heat transfer area.

If the ⊢ column is to be operated without using additional utilities, the vapor flows V_4 and V_5 in the two heat integrated "simple" columns are directly coupled. For instance, in the case of constant molar flows it is required that $V_4 = V_5$. Such a direct coupling may be desirable for a *balanced* separation, that is, in a column where the separation difficulty in terms of required boilups V_4 and V_5 are similar for the two columns. However, in general this strong coupling may be undesirable, and one may want to introduce additional heating or even cooling to eliminate the coupling between V_4 and V_5 (this disadvantage also applies to the Kaibel column). The single shell ⊢ column is in any case a compact and thus cost efficient arrangement, which should be considered whenever there is a sufficient difference in boiling points for the intermediate components. In case of limiting driving forces one might also consider using a heat pump to raise the temperature level of the available heat, or as mentioned

use additional utility. The ⊢ column should also be relatively easy to operate, and startup may for instance take place simply by running the column under total reflux until there is sufficient buildup of liquid on the cold side.

We appreciate that designs which have many of the same features as the ⊢ column have been considered by previous authors. In fact, there is an early patent by Seidel (1935), in which a two–column implementation of the ⊢ column is proposed. The author propose that the intermediate heat exchange, to provide condensation and evaporation, takes place in an internal heat exchanger (dephlagmator). Others have considered separation in the context of multi-effect distillation systems, e.g. King (1971) and Andrecovich and Westerberg (1985). The idea is here to split the feed mixture so as to enable heat exchange between two columns operated under different pressures. This is well known for the separation of ternary mixtures. Carlberg and Westerberg (1989*b*) also considered a column with a side stripper and side enricher to separate a quaternary mixture. As for the ⊢ column, this design has the advantage that it does not require heat exchange to take place between columns run at different pressures. If we assume "pure" intermediate components (sharp splits), the hot and cold flows are of different compositions, so that heat may be passed from the condenser to the reboiler provided there is a sufficient temperature driving force between the streams. However, no authors have to our knowledge considered a column implemented in a single shell with vertical and horizontal partitions. In an energy perspective the simplicity of building columns in a single shell in itself offers energy savings, since production of materials off course requires energy. Before extending the analysis to arrangements with two dividing walls, we give a brief analysis of the number of degrees of freedom (DOFs) available for operation.

6.5.2 Degrees of Freedom (DOFs) with One Dividing Wall

When analyzing the degrees of freedom for a given process, one should in the general case distinguish between degrees of freedom (DOF) for *design* and the DOFs for *control* (operation). In this paper we consider only the latter, hence we restrict ourselves to columns with fixed number of stages, feed location(s) and feed condition(s). These variables off course must be taken into account for optimization purposes, i.e. optimal design.

Assuming that the holdups and the pressure are controlled, conventional binary columns yield two potentially manipulated variables, e.g. reflux (L) and boilup (V). For columns with vertical partitions, we gain in general one DOF for each sidestream and two for each dividing wall (the vapor and liquid split). Hence, the following formula yields the number of operation DOFs for a column with n_S sidestreams and n_D dividing walls

$$DOF = 2 + n_S + 2n_D \tag{6.3}$$

For the Kaibel column we thus have 6 ($n_S = 2, n_D = 1$) potentially manipulated variables available for operation. However, for a sharp split we require that only small amounts of C should appear in the overhead from the prefractionator, and small amounts of B in the bottoms from the prefractionator. Thus we have already implicitly fixed two DOFs (e.g. liquid (R_L) and vapor splits (R_V)). If we want to achieve a

certain purity for *all* 4 products, it thus seems as though we have enough DOFs left. However, for energy efficient operation of the Kaibel column, it is as previously noted strongly desirable to balance the column such that total reflux ($L/V = 1$) is achieved in the middle section between the sidestreams. Hence, we need to use one DOF to meet this requirement during operation. We are therefore in fact short of DOFs if we wish to control all purities and at the same time keep the column in the vicinity of the energy minimum. This lack of DOFs is due to the above mentioned direct coupling between V_4 and V_5. One way of compensating for this lack of DOFs is to allow for *over-purification*, i.e. allow for higher purities of one side product. The lack of DOFs also applies to the $\vdash$ column which has only 5 DOFs, of which 2 must be used to achieve a sharp separation between B and C in the prefractionator. However, in this case we at least avoid the additional operational problem of achieving $L/V = 1$ in the intermediate section. Furthermore, it may be easier to use additional heating or cooling in the $\vdash$ column to compensate for the loss of DOFs. In the next section we extend the analysis to Petlyuk arrangements with two dividing walls.

6.6 Petlyuk Arrangements with Two Dividing Walls

A column arrangement which allows for potentially reversible splits in a single shell, is represented by the schematic in Figure 6.10. This arrangement is due to a superstructure consisting of three interconnected *regular* columns proposed by Sargent and Gaminibandara (1976). We emphasize that the two arrangements in Figure 6.4 are identical from a computational point of view if we neglect heat transfer across the dividing walls. The Petlyuk arrangement consists of $n(n-1) = 12$ sections, which in

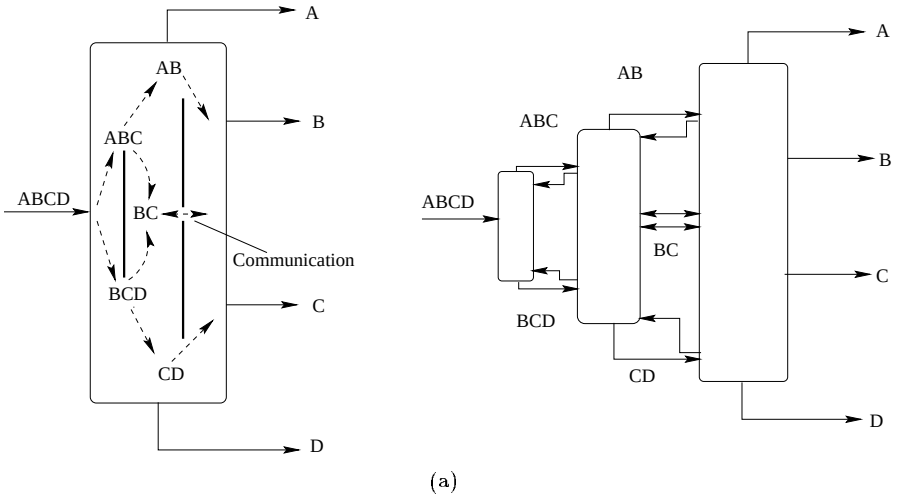

Figure 6.10: Petlyuk arrangement for Sargent's superstructure

fact is the *maximum* number for sharp splits of a four component mixture. This is

seen more clearly if we consider the network representation given in Figure 6.3. We recognize that since every possible node is present (see e.g. Agrawal (1996)), only the lightest and heaviest components are separated from the mixture in each section. Hence, due to potentially reversible splits we should expect this design to display better performance in terms of thermodynamic efficiency, thus requiring a lower energy input compared to the Kaibel and the $\vdash$ columns.

A dividing wall implementation of the *satellite arrangement* proposed by Agrawal (1996) is illustrated in Figure 6.11. The schematics In Figure illustrate both the satellite arrangement and the corresponding dividing wall implementation similar to Agrawal's superstructure. To compare with the sequential arrangement by Sargent, we note that both superstructures consists of $n-1$ interlinked columns and require the *maximum* number of sections for a sharp split, i.e. $n(n-1)$. However, as previously discussed we emphasize that Agrawal's arrangement allows for communication between any of the "columns" (i.e. main and satellite columns). If we examine the di-

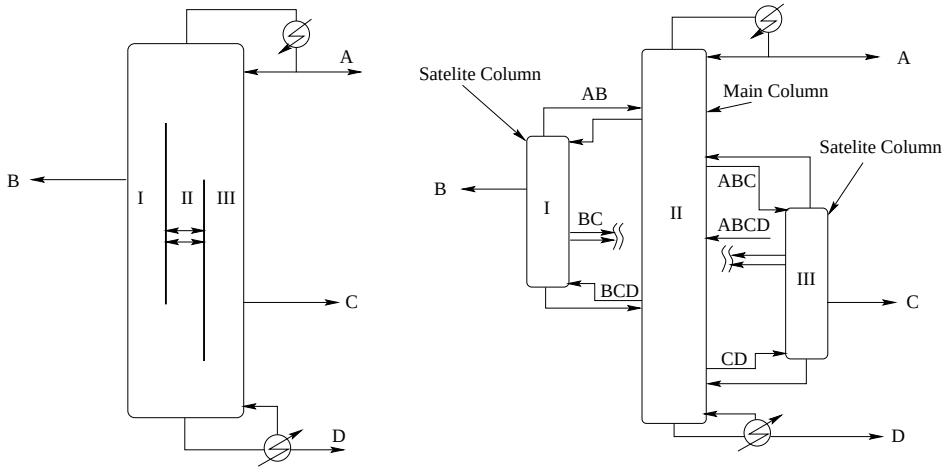

Figure 6.11: Petlyuk arrangements for for Agrawal's superstructure

viding wall arrangement in Figure 6.11 in some more detail, we recognize that further scrutiny is required in order to visualize the feed location and the transfer of the intermediate BC node. We first note that the feed may in general enter the column from any of the three parts I, II and III indicated in Figure 6.11. This is perhaps more clearly understood if we consider a view from above the column as demonstrated to the left in Figure 6.12. However, if there is to be any transfer of the BC node within the dividing wall column, we must enable communication between *any* of the three parts. This is indeed possible if we consider the *triangular* structure to the right in Figure 6.12, which allows for interconnections between any two neighboring *parts* of the column. Hence, we may in principle allow for communication between any two stages in the column arrangement. In the schematic to the right in Figure 6.12 we

have also indicated that one may implement a tube along the center section in order to allow for fluid transport between various sections. In practice this is achieved by withdrawing fluid from one stage and passing it to the appropriate stage in the corresponding section.

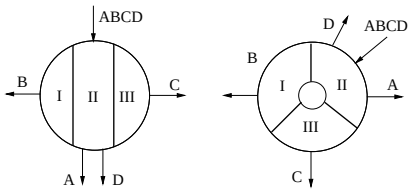

Figure 6.12: Top view of dividing wall implementation for Agrawal's superstructure

If we then compare these dividing wall implementations with the Satellite arrangements proposed by Agrawal (1996), the author argues that there are 3 different satellite arrangements corresponding to the "minimum" of 10 sections for a 4–component separation. If we consider the dividing wall implementation to the left in Figure 6.12, we find that it allows for only one possible arrangement with 10 sections, because no communication is allowed between parts I and III. However, by using the triangular structure one may realize any column arrangement corresponding to sequences of $(n-1)$ regular columns.

6.6.1 Degrees of Freedom (DOFs) with Two Dividing Walls

If we thus allow for the possibility of having liquid and vapor transport (communication) between certain stages on both sides of a wall, there are in fact four streams which may be redistributed (liquid and vapor on each side). Thus, we add yet another four degrees of freedom for each *communication point*. In Figure 6.13 we give an illustration of the additional liquid and vapor splits due to fluid transfer through the communication point. To avoid confusion in the proceeding discussion of columns with such communication points, we make the somewhat fictitious distinction between *dividing walls* for the overall structure and *vertical partitions*. Hence, we may have a column with two dividing walls and three partitions as illustrated by Figures 6.13. The total number of DOFs for a structure with n_C communication points is thus

$$DOF = 2 + n_S + 2n_D + 4n_C \tag{6.4}$$

For the Petlyuk arrangements in Figures 6.11 and 6.10 we thus have, according to equation (6.4), a total of $2+2+2*2+4=12$ DOFs for operation. However, based on physical insight we may conjecture that in the general case fluid should only be transported in the direction towards the final products, i.e. with $R_{L3} = R_{V3} = 0$ in Figure 6.13. The liquid and vapor splits in the middle partition (R_{L2} and R_{V2}) then constitutes an intermediate feed *to* the sidestream side. The *"feed condition"* thus depends on the relative amounts of R_{L2} and R_{V2}. The optimal feed condition

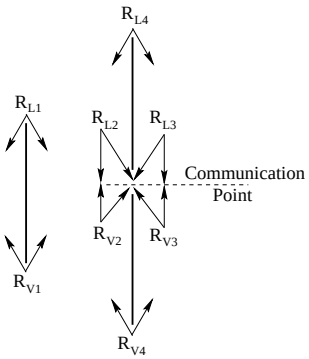

Figure 6.13: DOFs due to communication points

would in general be the subject of optimization, but for practical purposes it is much easier to transport only liquid across the partition (i.e. $R_{V2} = 0$). Taking the latter observations into account, 9 potential DOFs remain. As a comparison, the structure proposed by Kaibel yields only 6 DOFs.

6.7 Conclusions

In this paper we have extended the Petlyuk ideas to dividing wall columns that permit multicomponent separations within a single shell. In order to provide a common basis for this and future works, we proposed definitions of what is to be referred to as *Petlyuk arrangements* and *sharp split arrangements*. The importance of using these definitions is to eliminate for example sidestream columns from the class of Petlyuk arrangements. We then addressed different *superstructures* proposed in the literature for arrangements with $n - 1$ interconnected columns, and demonstrated how such arrangements may be implemented in a single shell with vertical partitions.

We briefly discussed the issue of reversibility, in terms of factors that contribute to exergy losses in conventional columns. From this we examined the extent to which Petlyuk arrangements allow for potentially reversible splits, which strongly influences the required energy input. A discussion on the large number of degrees of freedom for such column arrangements is also given in some detail. In this respect we suggested simple formulas for computing the number of DOFs for Petlyuk arrangements. For design and optimization purposes, we find that the number of DOFs may become excessive if all variables are set arbitrarily. An issue of great importance for future work thus rests in providing guidelines which implicitly reduce the set of DOFs.

Nomenclature

A, B, C, D – Component indices
F – Feed flow rate [kmol/min]
L – Reflux flow rate [kmol/min]

L_i – Liquid flow rate in section i
N_T – Number of theoretical stages in top section
N_B – Number of theoretical stages in bottom section
n – Number of components
n_C – Number of communication points
n_D – Number of dividing walls
n_S – Number of sidestreams
q – Feed enthalpy
R – External reflux ratio
R_L – Liquid split fraction
R_V – Vapor split fraction
S_{LH} – Separation factor between light L and heavy H component
V – Boilup from reboiler [kmol/min]
V_i – Vapor flow rate in section i [kmol/min]
$x_{H,B}$ – Liquid mole fraction of heavy component in the bottom
$x_{H,T}$ – Liquid mole fraction of heavy component in the top
$x_{L,B}$ – Liquid mole fraction of light component in the bottom
$x_{L,T}$ – Liquid mole fraction of light component in the top

Greek letters

α_{ij} – Relative volatility between components i and j

References

Agrawal, R. (1996). Synthesis of Distillation Column Configurations for a Multicomponent Separation. *Ind. Eng. Chem. Res.* **35**(4), 1059–1071.

Andrecovich, M. J. and A. W. Westerberg (1985). A Simple Synthesis Method Based on Utility Bounding for Heat-Integrated Distillation Sequences. *AIChE journal.*

Annakou, O. and Peter Mizsey (1996). Rigorous Comparative Study of Energy-Integrated Distillation Schemes. *Ind. Chem. Eng. Res.* **35**(6), 1877–1885.

Cahn, R. P., E. Di Micelli and A. G. Di Micelli (1962). Separation of Multicomponent Mixture in Single Tower – U.S. Patent 3,058,893.

Carlberg, N. A. and A. W. Westerberg (1989*a*). Temperature-Heat Diagrams for Complex Columns. 3. Underwood's Method for the Petlyuk Configuration. *Ind. Chem. Eng. Res.* **28**(9), 1386–1397.

Carlberg, N. A. and A. W. Westerberg (1989*b*). Temperature-Heat Diagrams for Complex Columns. 2. Underwood's Method for Side Strippers and Enrichers. *Ind. Chem. Eng. Res.* **28**(9), 1379–1386.

Cerda, J. and A. Wersterberg (1981). Shortcut Methods for Complex Distillation Columns. 1. Minimum Reflux. *Ind. Chem. Eng. Process Des. Dev.* **20**(3), 546–557.

Fidkowski, Z. and L. Krolikowski (1986). Thermally Coupled system of Distillation Columns: Optimization Procedure. *AIChE Journal* **32**(4), 537–546.

Gomez-Munoz, A. and J. D. Seader (1985). Synthesis of Distillation Trains by Thermodynamic Analysis. *Comp. Chem. Eng.* **9**(4), 311–341.

Kaibel, G. (1987). Distillation Columns with Vertical Partitions. *Chem. Eng. Technol.* **10**, 92–98.

Kaibel, G., E. Blass and J. Köhler (1990). Thermodynamics - Guideline for the Development of Distillation Column Arrangements. *Gas Separation and Purification* **4**, 109–114.

King, C. J. (1971). *Separation Processes*. McGraw-Hill Chemical Engineering Series. McGraw-Hill Book Company.

Nishida, N., G. Stephanopoulos and A. W. Westerberg (1981). A Review of Process Synthesis. *AIChE Journal* **27**(3), 321–351.

Ognisty, T. P. (1995). Analyze Distillation Columns With Thermodynamics. *Chem. Eng. Prog.* pp. 40–46.

Petlyuk, F. B., V. M. Platonov and D. M. Slavinskij (1965). Thermodynamically Optimal Method for Separating Multicomponent Mixtures. *Int. Chem. Eng.* **5**(3), 555–561.

Petlyuk, F. B., V. M. Platonov and V. S. Avetlyan (1966). Optimum Arrangements in the Fractionating Distillation of Multicomponent Mixtures. *Khim. Prom.* **42**(11), 865.

Sargent, R. W. H. and K. Gaminibandara (1976). Optimum Design of Plate Distillation Columns. In: *Optimization in Action* (L. W. C. Dixon, Ed.). pp. 267–314. Academic Press. London.

Seidel, M. (1935). German Imperial Patent No. 61503.

Skogestad, S. and M. Morari (1987). A Systematic Approach to Distillation Column Control. In I. Chem. E. Symposium Series, No. 104, A71-A86.

Smith, R. (1995). *Chemical Process Design*. Wiley.

Stichlmair, J. (1988). Distillation and Rectification. *Ullmann's Encyclopedia of Industrial Chemistry* **B3**, 4–1 – 4–94.

Tedder, D. W. and D. F. Rudd (1978). Parametric Studies in Industrial Distillation. *AIChE Journal* **24**(2), 303–315.

Triantafyllou, C. and R. Smith (1992). The Design and Optimization of Fully Thermally Coupled Distillation Columns. *Trans. Inst. Chem. Eng.* **70**(Part A), 118–132.

Westerberg, A.W. (1985). The Synthesis of Distillation-Based Separation Systems. *Comp. Chem. Eng.* **9**(5), 421.

Wolff, E. A. and S. Skogestad (1995). Operation of Integrated Three–Product (Petlyuk) Distillation Columns. *Ind. Chem. Eng. Res.* **34**(6), 2094–2103.

Wright, R. O. (1949). U.S. Patent 2,471,134.

Chapter 7

Optimization and Design of Generalized Petlyuk Arrangements

Atle C. Christiansen and Sigurd Skogestad*

Department of Chemical Engineering
Norwegian University of Science and Technology, NTNU
N–7034 Trondheim Norway

A preliminary version was presented at
Distillation & Absorption'97, Maastricht, The Netherlands, 8-10 Sept. 1997
Proceedings p. 745-756

Abstract

In this paper we consider generalized Petlyuk arrangements, where a feed mixture can be separated in four pure products in an integrated column with a single reboiler and a single condenser. We compare the energy consumption in optimized Petlyuk arrangements with that of optimized sequences of regular columns. The results are based on simulations using a simple yet detailed stage to stage model for the separation of ideal mixtures. To our knowledge this is the first detailed simulation study of such columns for quaternary mixtures. For the optimization we use a gradient projection method, in which optimization is embedded in a continuation scheme. The results indicate that the Petlyuk arrangements offer considerable energy savings, typically in the order of 40%, compared to conventional sequences of regular columns. The results also indicate that Petlyuk arrangements require a relatively large number of stages in order to exploit the full potential of energy savings. In order to characterize the optimal solutions, we also demonstrate in terms of a sensitivity analysis that feedback control of the internal splits is required for optimal operation.

*Author to whom correspondence should be addressed : Fax : +47 7359-4080, E-mail: skoge@chembio.ntnu.no

7.1 Introduction

A schematic of the well known Petlyuk (Petlyuk *et al.* 1965) column, or dividing wall column (Wright 1949), for the separation of ternary mixtures is illustrated in Figure 7.1. This complex column arrangement has received considerable attention in

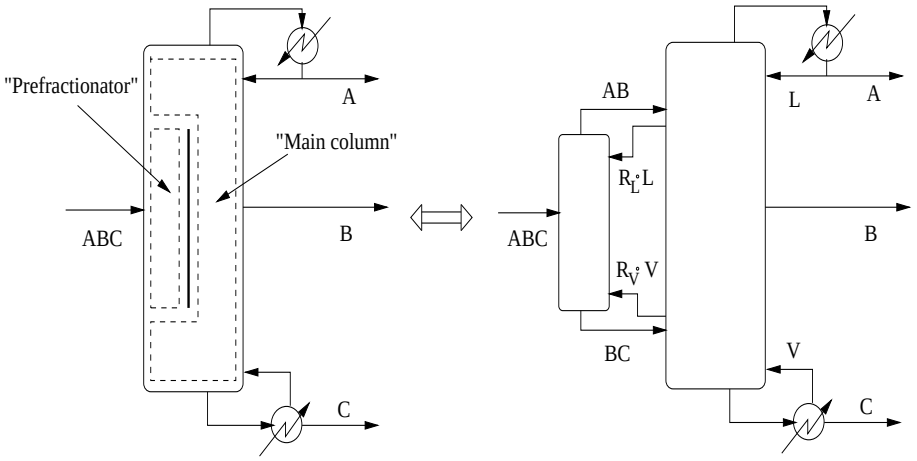

Figure 7.1: Petlyuk column for the separation of a ternary mixture. Left : Column with vertical partition. Right : Prefractionator arrangement

the literature, even though experimental work and studies on practical operation are practically non-existing. Some findings with important implications for operation and control were however discussed in chapter 5. Results from previous works indicate that savings in capital and energy costs are typically in the order of 30% compared to conventional arrangements with regular columns in sequence (e.g. Smith (1995)), although previous works by Fidkowski and Krolikowski (1986) and Glinos and Malone (1988) report that the maximum energy savings are as large as 50%. In this paper we extend the *Petlyuk ideas* to consider also Petlyuk arrangements for quaternary separations, for which we compare the energy consumption in optimized Petlyuk arrangements with that of optimized sequences of regular columns. There has been some discussion in the literature on the use of Petlyuk arrangements to separate four or more components, but no studies on the potential energy savings are available. The latter is the focal point in the proceeding discussion.

In the previous chapter we presented a framework for conceptual analysis and design of Petlyuk arrangements, for separating mixtures of four components, although extensions to more components is straightforward. We proposed a general definition of a Petlyuk arrangement (Christiansen *et al.* 1997), which is repeated here for convenience:

> *A Petlyuk arrangement is a column arrangement, separating three or more components using a single reboiler and a single condenser, in which any degree of separation (purity) can be obtained by increasing the number*

of stages (provided the reflux is above a certain minimum value and the separation is thermodynamically feasible).

The importance of using this definition is to eliminate for example conventional sidestream columns from the class of Petlyuk arrangements, since these require infinite reflux to obtain pure products (even with an infinite number of stages).

Based on this definition we considered two *"superstructures"* previously proposed in the literature and illustrated how these may be implemented in single shells using vertical partitions. In particular we considered the *sequential arrangement* proposed by Sargent and Gaminibandara (1976) and the *satellite arrangement* by Agrawal (1996), both corresponding to structures with $n-1$ interconnected columns. We also considered a simple structure proposed by Cahn *et al.* (1962) and later by Kaibel (1987). We also proposed a single wall implementation of an old patent by Seidel (1935), called the $\vdash$ column. The distinguishing feature of this design is that it also uses a *horizontal partition* to facilitate energy integration, so that remixing of already separated components is avoided. It is thus somewhat of a *hybrid* column arrangement, in that the prefractionator is directly coupled with the main column (Petlyuk idea) whereas the intermediate sections in the main column are indirectly coupled via heat integration (conventional approach). In the present paper we make further investigations of complex distillation arrangements, in which we compare the energy consumption of optimized petlyuk arrangements with that of sequences of regular columns.

An important issue when comparing different column arrangements is the use of an objective or cost function. In the literature it is generally agreed that the total vapor consumption (boilup) is the dominant variable when estimating the total cost (operation and capital) of distillation columns (e.g. Tedder and Rudd (1978), Fidkowski and Krolikowski (1986) and Glinos and Malone (1988)). In this paper we thus present numerical results for Petlyuk arrangements optimized with respect to the boilup consumption. The reader may note that we compare the energy consumption for these arrangements to optimized schemes of regular columns in sequence. Hence, we do not consider *heat integrated* columns, which would have extended the scope of this study. In order to consider heat integrated columns, one would in general also have to consider other characteristics such as different pressure levels, which influences the vapor liquid equilibrium, and the availability of utilities at different temperatures. We also note that a heat integrated scheme that are operated under different pressures, degrade heat over a larger temperature range than a sequence of regular columns, so that the temperature of the utilities must be increased (similar to the Petlyuk column). One should furthermore appreciate that the capital costs of heat integrated schemes are higher compared to conventional schemes, due to more complex instrumentation and piping. The underlying motivation for this work, is thus to provide *typical* measures of the potential energy savings with Petlyuk arrangements for simple models of ideal mixtures. A natural basis of comparison is hence to use a conventional structure with regular columns in sequence. However, we stress that in order to obtain the *optimal* arrangement for a specific separation, one should of course consider all *possible* structures, which also includes heat integrated schemes.

Numerical results presented in this work for quaternary mixtures indicate that

Petlyuk arrangements offer savings in the order of 40%. The optimization problems were solved using a gradient projection method embedded in a continuation scheme, which we found to be very efficient. This algorithm was described in chapter 3, and draws from the partly unpublished work by Morud (1995) and a previous work by the authors (Christiansen *et al.* 1996). Note that in the optimizations we do not include design parameters such as the distribution of the number of stages, which require using also integer variables. For the "global" optimization problem, such parameters should also be considered.

Before going into detailed analysis of Petlyuk arrangements for quaternary separations, we briefly revisit the Petlyuk column for ternary separations. The reason for this is the need to shed some light on some ambiguities related to under what conditions the "ordinary" Petlyuk columns offer the largest savings.

7.2 The Petlyuk Column Revisited

We first consider the separation of a ternary mixture in a "conventional" Petlyuk column. In order to account for the lower energy consumption of Petlyuk arrangements over conventional designs, there are two crucial aspects that one needs to recognize. Firstly we have the simple fact that separating agents (reflux and boilup) are generated at only two designated locations and thus reused throughout the system, whereas conventional arrangements require $2(n-1)$ condensers and reboilers. In a Petlyuk column the boilup and reflux for the prefractionator is thus supplied by *direct* thermal coupling with the main column as illustrated in Figure 7.1. Eliminating reboilers and condensers may thus in itself reduce the required energy input, but as noted by several authors (e.g. Westerberg (1985), Carlberg and Westerberg (1989), Smith (1995) and Agrawal *et al.* (1996)), one should also recognize the trade off between the energy levels and loads. This argument refers to the first and second law of thermodynamics, which emphasizes the trading between total energy *consumption* (first law) and energy *levels* (second law). Thus, even though Petlyuk arrangements may require smaller heat loads, this comes at the expense of adding all heat at the highest temperature (reboiler), and cooling at the lowest temperature (condenser). For this reason we may find that Petlyuk arrangements in some cases require a higher energy *cost*("first and second law heat"), even though the energy *consumption* is lower ("first law heat"). In a sense this makes the optimality conditions of Petlyuk arrangements case specific, in that it depends on the actual prizing of the available utilities (i.e. low pressure and high pressure steam).

The second important aspect is that Petlyuk arrangements offer means for decreasing the exergy losses caused by process irreversibilities such as irreversible mixing effects. Since the Petlyuk column allows for separations between components that are non-adjacent in terms volatilities, thus allowing for the the intermediate components to distribute over the top and the bottom in a bisectional column, *back-mixing* of the intermediate components is reduced (Triantafyllou and Smith 1992). Furthermore, by using direct (mass) coupling between column sections, exergy losses at column ends may also be eliminated.

In the literature it has been shown that the maximum energy saving for the Petlyuk

column is 50 % compared to the conventional direct and indirect sequences (Glinos and Malone 1988). The authors found that maximum savings occur when the feed composition of the intermediate component approaches zero, but that savings may be large also for large amounts of intermediate. However, it is also stated that Petlyuk columns yields the *largest* savings for large amounts of intermediate (e.g. Tedder and Rudd (1978), Fidkowski and Krolikowski (1986) and Annakou and Mizsey (1996)). In fact, the maximum savings of 50% are also obtained in the limiting case where the relative volatilities are small and the amount of intermediate is large.

An important issue when comparing the Petlyuk column to conventional arrangements, such as the direct and indirect split sequences, is whether to choose a *total* or a *partial* condenser. If the objective is to minimize the vapor requirement, it is clearly optimal to use a partial condenser for the indirect sequence, so that the feed to the second column is taken as vapor. This was a topic of discussion in chapter 3. In the literature it is for some reason often assumed that only total condensers are used, see e.g. the analysis of Glinos and Malone (1988), who found that the indirect sequence in general was favorable *only* for relatively small amounts of low boiler. However, if one instead use a partial condenser and thus a vapor feed to the downstream column, we showed in chapter 3 that the optimality region for the indirect sequence increases considerably. We now want to consider in some more detail how the potential savings depend on the amount of intermediate component.

The numerical results presented here are obtained from optimizations of relatively simple models assuming constant molar flows and constant relative volatility. We consider four different feed compositions where we have equal amounts of A and C in the feed, and we thus only need to give the feed composition of B, i.e. z_B. The relative volatility between the three components are 4:2:1 in all cases. We find that the indirect sequence is favorable for all cases when we use a partial condenser. The direct and indirect sequence are however equal in the limiting case where $z_B \to 1$, which is easily verified using Underwood's method or the analytical equations given by Stichlmair (1988). For the case studies we thus compare the energy efficiency to the indirect scheme. Since the number of stages also is important for the comparisons, we consider two columns with a total number of 60 and 90 stages (N_T) respectively. We assume an equal distribution of stages between the sections for the conventional scheme, whereas for the Petlyuk column we use a ratio of 1:2 for the number of stages in the prefractionator relative to the "main column, i.e. 20:40 for $N_T = 60$. The feed flow rate is $F = 1$ [kmol/min] and is fed to the middle stage in the prefractionator. Further details of the mathematical models are presented in the next section, when we extend the analysis to generalized Petlyuk arrangements for quaternary mixtures. In all cases the purity specifications for the products are 99% in the top (A) and the bottom (C) and 95% for the side product (B).

To provide some details from the optimizations, we give the optimized parameters and flows for different feed compositions and $N_T = 90$ in Table 7.1. Note here that $R_L = 0$ for $z_B = 0.80$. This means that there is in fact no reflux, and thus no separation effect in the top section of the prefractionator. Composition profiles for two of these cases are shown in Figure 7.2. As seen in the Figures, the prefractionator essentially carries out a split between A and C, so that the composition of B increases

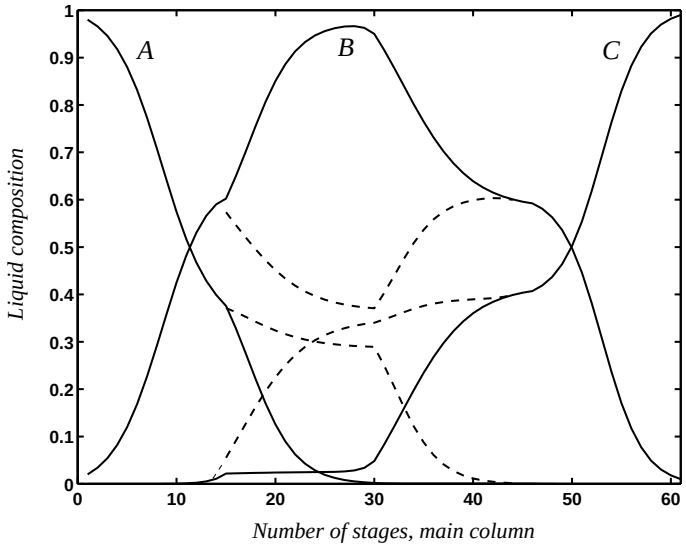

(a) $z_A = z_B = z_C = 0.33$

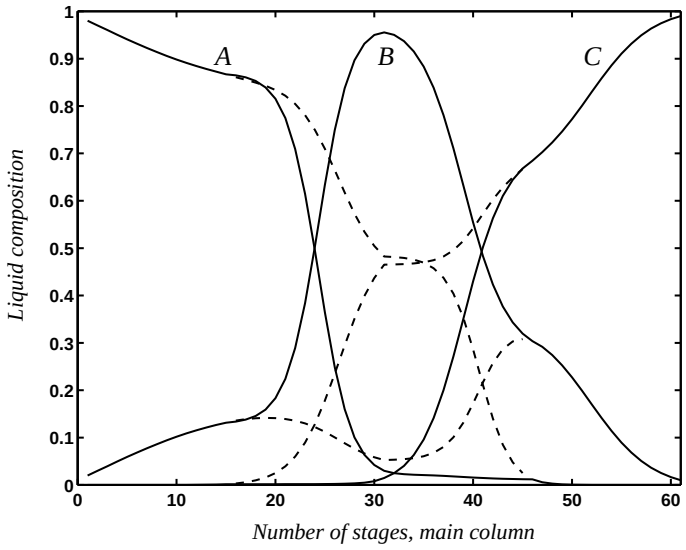

(b) $z_A = 0.475, z_B = 0.05, z_C = 0.475$

Figure 7.2: Composition profiles for optimized Petlyuk column. Solid line - main column, dashed line - prefractionator column.

Table 7.1: Optimized parameters and flows for Petlyuk column with $N_T = 90$ and $\alpha = 4 : 2 : 1$

Feed composition	V	L	S	R_L	R_V
$z_B = 0.05$	0.992	0.514	0.0426	0.700	0.853
$z_B = 0.20$	1.185	0.782	0.202	0.426	0.686
$z_B = 0.33$	1.311	0.975	0.344	0.359	0.641
$z_B = 0.80$	1.154	1.057	0.840	0	0.482

towards both ends of the prefractionator. A comparison of the Petlyuk column with the *indirect split* scheme for different number of stages is then given in Table 7.2. (We may note that the savings relative to the *direct split* scheme is even larger.) For a

Table 7.2: Energy savings with Petlyuk column relative to the indirect scheme for non-sharp splits with $\alpha = 4 : 2 : 1$.

Feed composition	$N_T = 60$	$N_T = 90$	$N_T = 180$
$z_B = 0.05$	$\Delta V = 23.9$ %	$\Delta V = 29.8$ %	$\Delta V = 30.5$ %
$z_B = 0.20$	$\Delta V = 26.2$ %	$\Delta V = 32.6$ %	$\Delta V = 33.4$ %
$z_B = 0.33$	$\Delta V = 26.9$ %	$\Delta V = 32.8$ %	$\Delta V = 33.8$ %
$z_B = 0.80$	$\Delta V = 31.3$ %	$\Delta V = 41.3$ %	$\Delta V = 44.7$ %

finite number of stages we thus find that the relative savings for the Petlyuk column increase as z_B *increases*, for the given α and equal amounts of A and C. We also see that the energy savings increase as we increase the number of stages. The reason is that Petlyuk columns require a large number of stages to achieve the overall minimum energy usage.

To compare also the overall minimum energy usage V_{min} for infinite columns ($N = \infty$), we use the analytical expressions for the Petlyuk column derived by Fidkowski and Krolikowski (1986) and Underwood's method for the conventional arrangements. We here consider *sharp splits* (product purities of 100%). In this case, where we also include results for the direct split, we find as shown in Table 7.3 that the savings are in fact largest when z_B is small and do not vary significantly with z_B for the given relative volatilities. This is in line with the conclusions given by Glinos and Malone (1988). By comparing the results in Tables 7.3 and 7.2, we find that if we

Table 7.3: Energy savings for sharp splits with $\alpha = 4 : 2 : 1$ in an infinite Petlyuk column, relative to direct and indirect schemes, respectively.

Feed composition	Indirect	Direct
$z_B = 0.05$	$\Delta V_{min} = 35.4$ %	$\Delta V_{min} = 40.5$ %
$z_B = 0.20$	$\Delta V_{min} = 33.3$ %	$\Delta V_{min} = 35.7$ %
$z_B = 0.33$	$\Delta V_{min} = 32.8$ %	$\Delta V_{min} = 34.1$ %
$z_B = 0.80$	$\Delta V_{min} = 33.0$ %	$\Delta V_{min} = 33.0$ %

reduce the purity of B the energy saving is largest when the amount of B is large, i.e.

$z_B = 0.80$. However, for sharp splits the savings are largest for small amounts of B. This in itself demonstrates that it is difficult to state clearly under what conditions Petlyuk columns give the largest savings. In general there are also a number of other parameters that will influence the optimality conditions. Note for consistency that we here compare the energy usage for sharp splits in infinite columns $N = \infty$ with non-sharp splits in a column with $N_T = 180$ which should be sufficiently large.

It may however not come as a surprise that prefractionator arrangements are particularly cost-efficient for non-sharp splits. As shown by Westerberg (1985) for a simple example, the energy usage of a conventional distillation process, where products are split into intermediate pure products and then remixed, may be several times higher than for a simple non-sharp column.

For sharp splits Glinos and Malone (1988) found that the maximum saving relative to the conventional sequences is 50 % for the case where $z_B \to 0$ and $z_A = (\alpha_{AB} - 1)/(\alpha_{AC} - 1)$. However, as discussed above, the authors did not consider the option of using vapor feeds for the indirect splits. If one instead consider vapor feeds, the maximum savings of 50 % apply only to the direct split. The saving for the indirect splits with a partial condenser is in in this case only 33%. We now proceed to discuss Petlyuk Arrangements for quaternary separations.

7.3 Petlyuk Arrangements for Quaternary Separations

We first consider the simplest extension of the Petlyuk column, given in Figure 7.3, for the separation of a quaternary mixture $ABCD$ into its constituents. The arrangement

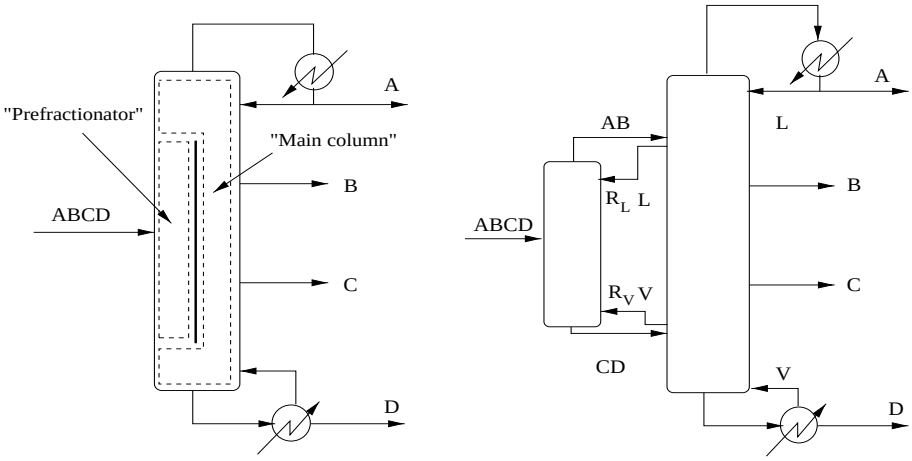

Figure 7.3: Petlyuk arrangement with one dividing wall for quaternary separations.

to the right is due to an early patent by Cahn *et al.* (1962) whereas the dividing wall column to the left was later proposed by Kaibel (1987). In the following we denote

these arrangements the *Kaibel* column. We emphasize that the two arrangements in figure 7.3 are identical from a computational and thermodynamical point of view if we neglect heat transfer across the dividing walls.

In the previous chapter we discussed on some of the benefits and drawbacks with such an arrangement. Among the important conclusions from this analysis was; (1) violation of the split sequence corresponding to the "preferred separation" scheme described in chapter 5; (2) total reflux operation of the intermediate section between the sidestreams is required for sharp splits and (3) lack of degrees of freedom (DOFs) for optimal operation. However, we also argued that the arrangement still should offer considerable savings in capital and energy costs for a wide range of separation tasks.

To overcome some of the operational problems with the *Kaibel* column, we then proposed an arrangement, called the ⊢ column, in which we suggested to use a *horizontal* partition in the main sidestream column to avoid remixing of the already separated intermediates. A schematic of the ⊢ column is illustrated in Figure 7.4. Even though the inherent problem of remixing in the Kaibel column is avoided, we

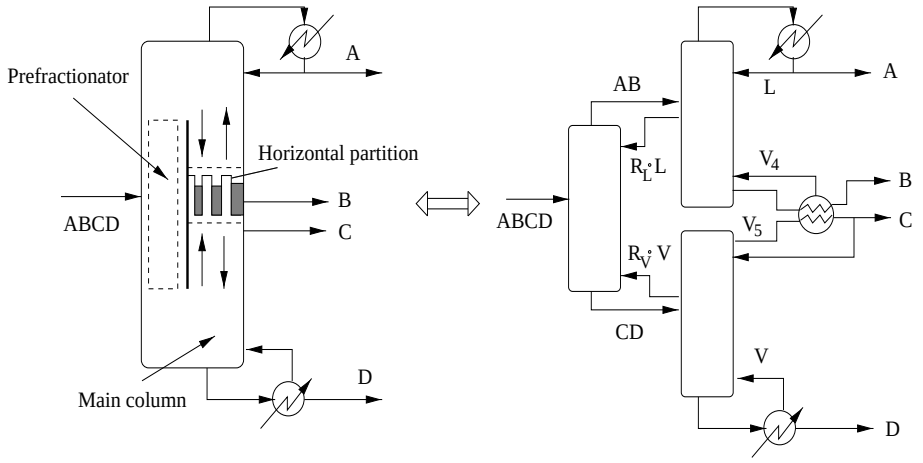

Figure 7.4: ⊢ column with vertical and horizontal partition for quaternary separations

showed that this arrangement also suffers from a lack of DOFs during operation. This may however be counteracted by using external utility for the required (intermediate) boilup and reflux.

In chapter 5 we discussed the issue of using the *preferred separation* for ternary mixtures, which refers a certain *easiest split* that requires the overall minimum usage in an infinite column. This preferred separation requires the "maximum number of sections" for sharp splits, which is equal to $n\,(n-1) = 6$ for ternary mixtures. If this particular sequence of *easiest splits* is optimal for any multicomponent separation, then the maximum number of $n\,(n-1)$ sections are required. In the last chapter we then proposed two dividing wall implementations that allows for this energetically "optimal" separation path. The two Petlyuk arrangements that we in this chapter

will use for optmization purposes are given in Figures 7.5 and 7.6. A distinguisihing

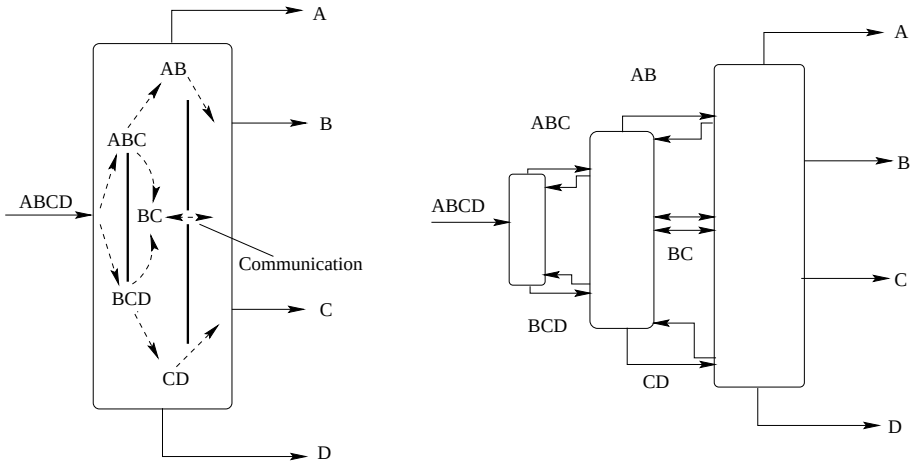

Figure 7.5: Petlyuk arrangement for Sargent's superstructure

feature of these arrangements is that only the lightest and heaviest components may be separated from the mixture in each section. For the ternary case we showed in chapter 5 that the minimum energy usage always correspond to this preferred separation. Since the arrangements proposed here allows for "preferred separations" also for quaternary mixtures, we expect these designs to require a lower energy input compared to the Kaibel and the $\vdash$ columns. In order to visualize how Agrawal's arrangement may be implemented within a single shell, we gave in the last chapter a geometric view of a *triangular* wall structure.

Before discussing aspects related to the optimizations, we briefly comment on the large number of DOFs available for the Petlyuk arrangements. For consistency we restate the formula presented in the previous chapter, giving the total number of DOFs for a Petlyuk arrangement with n_C communication points, n_S number of sidestreams and n_D dividing walls:

$$\text{DOFs} = 2 + n_S + 2n_D + 4n_C \tag{7.1}$$

According to equation (7.1) we thus have 6 DOFs for the Kaibel column and 12 DOFs for Sargent's and Agrawal's arrangements. Note that the $\vdash$ column, for which equation (7.1) does not apply, has only 5 DOFs. This owes to the fact that the $\vdash$ column is not to be considered as a Petlyuk arrangement according to our definition (no direct coupling and thus more than one reboiler and one condenser). In many cases, with this large number of DOFs, we face a rather difficult optimization task. We therefore discuss in the next section some simple strategies in which we use physical insight to provide good initial guesses.

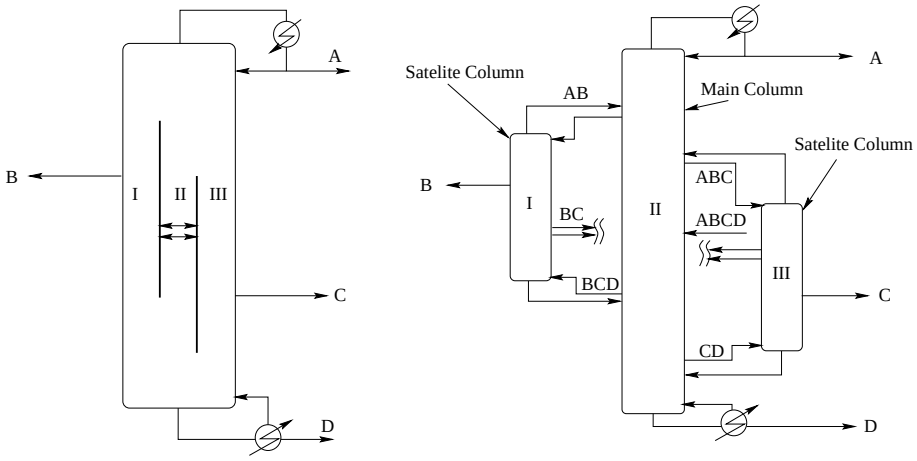

Figure 7.6: Petlyuk arrangement for Agrawal's superstructure

7.4 Guidelines for Optimization of Petlyuk Arrangements

In this work we minimize the energy consumption of Petlyuk Arrangements by equilibrium stage calculations. Such numerical simulations are in general rather time consuming since the problem size in general tend to be large, and simulations are indeed infeasible if it is desirable to compute the overall minimum energy usage V_{min}, which is obtained in inifite columns. For this reason there are a number of works in the literature on extending the set of Underwood equations (e.g. Underwood (1948)) to more complex columns. Fidkowski and Krolikowski (1986) showed by careful analysis how the Underwood equations apply to the Petlyuk column for ternary mixtures, and we showed in chapter 5 that their findings carry over also to finite columns. The Underwood equations were then used by Glinos and Malone (1988) to obtain optimality regions for the Petlyuk column. Carlberg and Westerberg (1989) extended the analysis of Fidkowski and Krolikowski (1986) to also include any number of middle components. However, for the Petlyuk arrangements considered in this work, where we consider separating a quaternary mixture into four pure products in a *directly* coupled column, there are to our knowledge no methods available at present to estimate V_{min}. We still recognize that it may be possible to extend the Underwood methods proposed by the previous authors to also include such columns.

For the optimizations we use a gradient projection algorithm embedded in a continuation scheme. This algorithm has proven to work very well for ill–conditioned problems that otherwise are difficult to solve. The features of the method were thoroughly discussed in chapter 3, but a brief description is given in Appendix A. Before considering the case studies, for which we have successfully applied the algorithm, we elaborate on some special features that may be exploited in the optimization of

Petlyuk arrangements. These are given in the form of general heuristics, but they also serve the purpose as a basis for an a posteriori analysis of the optimized arrangements.

7.4.1 Fluid transfer between communicating sections

For the Petlyuk arrangements in Figures 7.6 and 7.5, we note that component B is withdrawn above the communication point whereas component C is withdrawn below. In terms of the physics of the separation, we thus conjecture that the optimum should be to "lift" B up towards the outlet and conversely "push" C downwards from the communication point. For Agrawal's superstructure we thus argue that the communication of fluid between the sidestream sections should take place so that vapor is transferred primarily in the direction *from* the section where C is drawn off (column III), and *to* the section where B is withdrawn (column I). Conversely, one would expect that liquid should be transferred primarily in the direction from column I towards column III. However, we stress that the task of determining the optimal distribution of liquid and vapor is still left for optimization. The same argument applies in the also for Sargent's superstructure in Figure 7.5. In the latter case this guideline suggests that fluid should be transferred in the direction towards the product withdrawals.

7.4.2 Net fluxes in sidestream sections

If we consider the sections from which the intermediates B and C are withdrawn, we argue that one should in general avoid operating regimes where there is a net flux of intermediates across the stage where the sidestreams are withdrawn. The reason is that such a net flux inevitably leads to an internal recycle within the column, which most likely increases the energy requirements. Hence, above the sidestream stages, there should be a larger fraction of intermediates in the liquid, and conversely a larger fraction in the vapor below the outlet. If we denote the liquid and vapor flows of intermediates *a*bove the side-outlet by L_i^a, V_i^a and *b*elow by L_i^b, V_i^b, we pose the following *heuristic guideline* for the distribution of internal flows within the sidestream sections

$$L_i^a > V_i^a, \quad L_i^b < V_i^b \tag{7.2}$$

Condition (7.2) thus ensures that there is no net transport of intermediates across the outlets. We however stress that the optimum distribution of internal flows is still left for optimization.

7.4.3 Exploit symmetry for initial solutions

An important task in all aspects of steady state simulation, is that of providing good initial values. A "reasonable" initial guess (design) not only prevents convergence problems, but also strongly assists the task of locating the (global) optimal solution. The latter is of special importance when the number of optimization variables (DOFs) is large and when the process model is highly non–linear, for which most optimization algorithms yield at best a local optima.

When using mathematical models derived from first-principles, one is often able to make qualified judgements based on physical insight, regarding the operating regimes under which optimal solutions are likely to be found. For instance, if we consider the Petlyuk arrangement in figure 7.5, we recognize that there is a strong element of symmetry. By symmetry we here refer to a certain split sequence, for which the multicomponent separation may be decomposed to a set of pseodu-binary separations. This symmetry is nicely illustrated if we consider the distribution of components as given by the network representation in Figure 7.7. Thus we may consider as an initial candidate for the optimal design a column which preserves this element of symmetry. This path corresponds to separating in each bisectional column only the

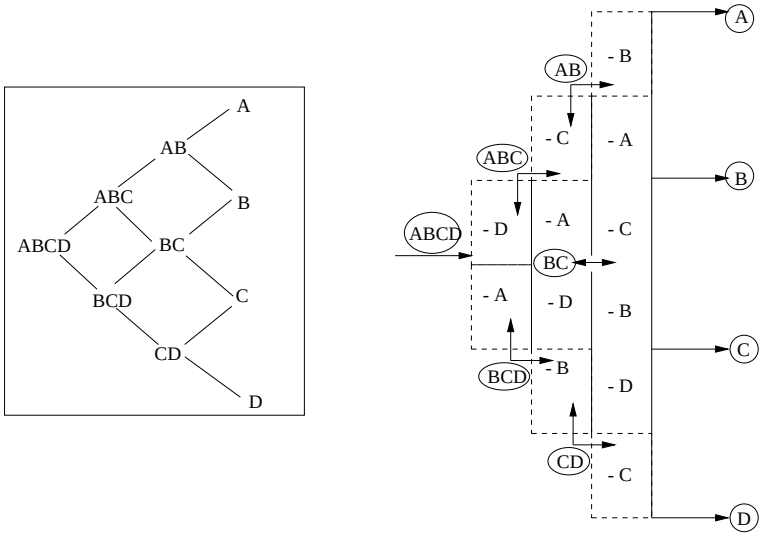

Figure 7.7: Symmetry illustrated by network representation and distribution of components

lightest and heaviest components, similar to the *"preferred separation"* for the ternary case discussed in chapter 5. The distillation process thus operates on pseodu-binary mixtures with extreme volatilities, for which a minimum of energy most likely is required.

As discussed above for the flow distribution within column sections, we proposed as another important guideline to avoid operating regimes in which there is a net flux of intermediate component B upwards above the upper sidestream outlet S_1, or conversely a net flux of C downwards below the outlet. Thus, if we use the notation given in figure 7.8, we may according to equation (7.2) require as a mimimum that $L_9 > V_9$ and $L_{10} < V_{10}$. The same argument also applies to component C, so we require that $L_{11} > V_{11}$ and $L_{12} < V_{12}$. Furthermore, if we aim for a design that also maintains the aspect of "symmetry", we may initially distribute the liquid flows immediately *above* the sidestream sections so that

$$L_i = V_i + \frac{S_i}{2} \tag{7.3}$$

and immediately *below* the side outlets so that

$$L_i = V_i - \frac{S_i}{2} \tag{7.4}$$

If only liquid is transferred through the communication point, the amount is thus simply given by $L' = S_1/2 + S_2/2$. As a general comment on this issue, we should note that by specifying a certain set of flows, we consume the same number of DOFs, and thereby reduce the set of optimization variables. To optimize Sargent's arrangement we use these arguments of symmetry to specify the flow rates in the initial solution. We then use dynamic simulation to obtain a steady state for the full model, i.e. for compositions on all stages. This solution then serves the purpose of an initial guess for the optimization algorithm.

7.5 Optimized Petlyuk Arrangements for Quaternary mixtures

In order to make it easier for the reader to comprehend the results from the optimizations, and to provide suficient details so that the results may be reproduced, we first present a "complete" example for illustrative purposes. The underlying motivation for the example is also to elaborate on some of the issues discussed in section 7.4. We use Sargent's and Agrawals superstructures for the example, and we present a comprehensive outline of the conceptual models. Note that similar but much simpler models apply to the Kaibel and $\vdash$ columns, so that detailed models are not given for these and we instead refer to Figures 7.3 and 7.4 for notation. We however give some details for the optimizations of these arrangements in a later section. The purpose of this introductory example is also to discuss certain characteristics of Petlyuk arrangements such as

- Vapor (R_V) and liquid (R_L) splits
- Column composition profiles
- Internal flow distribution

We provide values for the optimal parameters and discuss their siginifance. After presenting the details for this introductory example, we proceed to discuss other effects related to the trade off between the number of stages and the energy usage.

7.5.1 Mathematical models of Petlyuk arrangements

Schematics of Sargent's and Agrawal's superstructures are shown in Figures 7.8 and 7.9. Note that the vapor R_{Vj} and liquid R_{Lj} splits are defined so that they give the fractions *leaving* each section. We however refer to the set of equations in (7.5) and (7.8) for details. Note also that we illustrate here only the conceptual models, which are indedependent of the actual implementation, i.e. in a single shell or with $n-1$ interconnected columns. For convenience we refer to the arrangements in

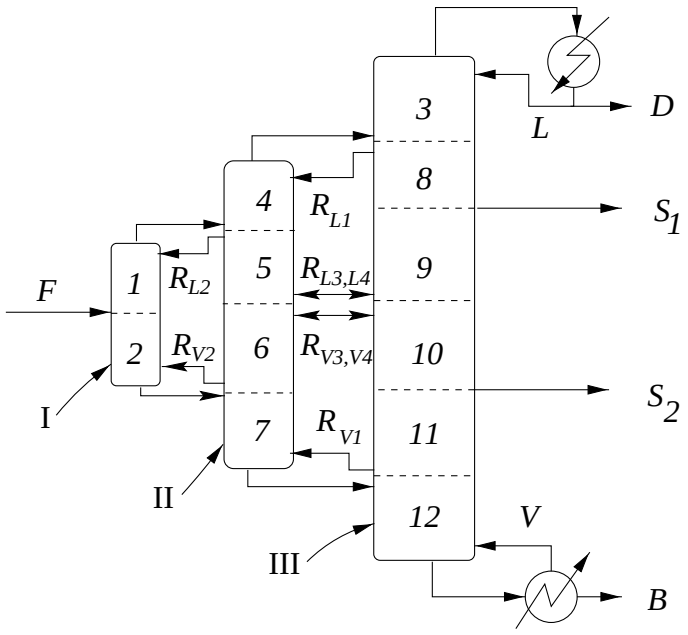

Figure 7.8: Schematic of Sargent's superstructure for introductory example

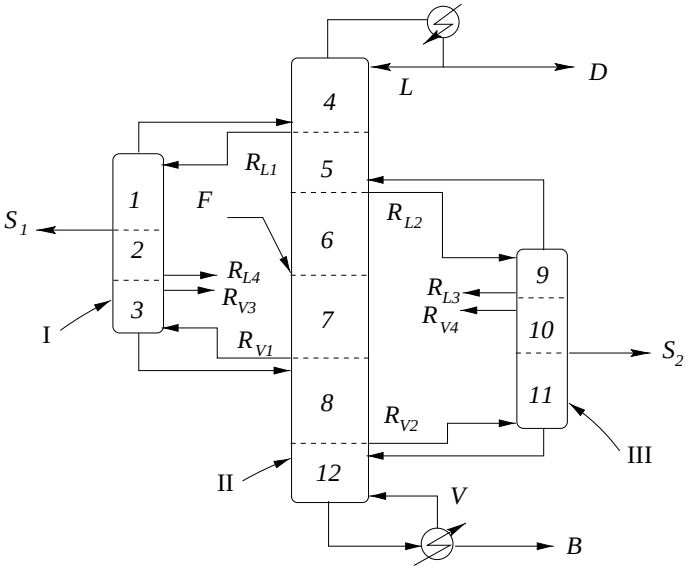

Figure 7.9: Schematic of Agrawal's's superstructure for introductory example

Figures 7.8 and 7.9 in terms of columns I, II and III. For Sargent's arrangement, the bisectional column I serves the purpose of a prefractionator, in which the task is to carry out a split between the light component A and heavy component D. The task for column II is then essentially to carry out the two ternary splits between A and C in the top, i.e. sections 4 and 5, and between B and D in the bottom, i.e. sections 6 and 7. Finally, pure products may be recovered in column III where the pseudo binary splits between the adjacent components occur. For Agrawal's arrangement, the prefractionation takes place in sections 6 and 7 immediately above and below the feed.

The conceptual models used for these arrangements are kept reasonably simple, since our objective is to discuss *typical* features such as the overall energy usage, and compare this with other arrangements. The model assumption are as follows

- Constant molar flows
- Constant relative volatilities
- Total condenser
- Products withdrawn as saturated liquids

We use a simple staged model, constituted by component mass balances, vapor liquid equilibria (VLE) and algebraic relations for the internal flows. The $n(n-1) = 12$ sections are enumerated from 1 to 12 as shown in Figures 7.8 and 7.9. Recall that a section denotes a part of the column from which no streams enter or leave. Using the number of each section as subscript for the flows *entering* each section, we may assign the distribution of flows within the column. For Sargent's superstructure the internal liquid L_j and vapor flows V_j are given by the set of equations in (7.5).

$$\begin{array}{ll}
L_1 = R_{L2} L_4 & V_1 = V_2 + R_F F \\
L_2 = L_1 + (1 - R_F) F & V_2 = R_{V2} V_7 \\
L_3 = L & V_3 = V_4 + V_8 \\
L_4 = (1 - R_{L1}) L_3 & V_4 = V_5 + V_1 \\
L_5 = (1 - R_{L2}) L_4 & V_5 = (1 - R_{V4}) V_6 + R_{V3} V_{10} \\
L_6 = (1 - R_{L3}) L_5 + R_{L4} L_9 & V_6 = (1 - R_{V2}) V_7 \\
L_7 = L_6 + L_2 & V_7 = (1 - R_{V1}) V_{12} \\
L_8 = R_{L1} L_3 & V_8 = V_9 \\
L_9 = L_8 - S_1 & V_9 = (1 - R_{V3}) V_{10} + R_{V4} V_6 \\
L_{10} = (1 - R_{L4}) L_9 + R_{L3} L_5 & V_{10} = V_{11} \\
L_{11} = L_{10} - S_2 & V_{11} = R_{V1} V_{12} \\
L_{12} = L_7 + L_{11} & V_{12} = V
\end{array} \tag{7.5}$$

Note that the vapor and liquid splits are implicitly defined by this set of equations. Here F is the molar feed flow rate and R_f the vapor fraction of the feed. Note that the split ratios are restricted to the region$[0, 1]$. In order to make sure that the overall mass balance is satisfied, we find by substitution

$$V_3 = V + R_F F \tag{7.6}$$

$$L_{12} = L + (1 - R_F) F \tag{7.7}$$

which yields the correct assignment. For Agrawal's satellite arrangement we similarly obtain

$$\begin{array}{ll} L_1 = R_{L1} L_4 & V_1 = V_2 \\ L_2 = L_1 - S_1 & V_2 = (1 - R_{V3})\, V_3 + R_{V4} V_{10} \\ L_3 = (1 - R_{L4})\, L_2 + R_{L3} L_9 & V_3 = R_{V1} V_8 \\ L_4 = L & V_4 = V_1 + V_5 \\ L_5 = (1 - R_{L1})\, L_4 & V_5 = V_6 + V_9 \\ L_6 = R_{L2} L_5 & V_6 = V_7 + R_F F \\ L_7 = L_6 + (1 - R_F)\, F & V_7 = (1 - R_{V1})\, V_8 \\ L_8 = L_3 + L_7 & V_8 = R_{V2} V_{12} \\ L_9 = (1 - R_{L2})\, L_5 & V_9 = R_{V3} V_3 + (1 - R_{V4})\, V_{10} \\ L_{10} = R_{L4} L_2 + (1 - R_{L3})\, L_9 & V_{10} = V_{11} \\ L_{11} = L_{10} - S_2 & V_{11} = (1 - R_{V2})\, V_{12} \\ L_{12} = L_8 + L_{11} & V_{12} = V \end{array} \tag{7.8}$$

The full models are then obtained by taking the component mass balances around each equilibrium stage i for all sections j, i.e.

$$L_j x_{c,i-1} - V_j y_{c,i} \quad = \quad L_j x_{c,i} - V_j y_{c,i+1} \tag{7.9}$$

where $x_{c,i}$ and $y_{c,i}$ are the liquid and vapor mole fractions of component c on stage i. The stage count i starts at the top stage within each section. The vapor mole fraction is given by the VLE

$$y_{c,i} = \frac{\alpha_c x_{c,i}}{\sum_{c=A,B,C,D} \alpha_c x_{c,i}} \tag{7.10}$$

The mole fractions are constrained by the sum equations

$$\sum_{c=A,B,C,D} y_{c,i} = 1, \qquad \sum_{c=A,B,C,D} x_{c,i} = 1 \tag{7.11}$$

The models then consist of $(NC - 1)\, N_T$ equations and we have 12 DOFs, see equation (7.1). 4 of the 12 DOFs are consumed to obtain the required product purities. This leaves us with 8 DOFs for the optimizations, i.e. all liquid and vapor splits. In the next section we give numerical results for the introductory example.

7.5.2 Introductory example

Process data for the introductory example considered in this section are given in Table 7.4. For the initial example we have chosen arrangements where the number of stages in the "main column", counting from the condenser to the reboiler is $N^H = 60$. For Sargent's structure we use the same number of stages within each section j, i.e $N_j = 10$. For Agrawal's arrangement we use a different distribution, in that the satellite columns have sections of 5, 10 and 15 stages respectively, so that there is an equal distribution above and below the sidestream outlets. The total number of stages is thus $N_T = 120$ for both arrangements, which yields a system of 364 nonlinear algebraic equations (with the product specifications) and 8 DOFs. Using

Table 7.4: Process data for introductory example

Feed flowrate	$F = 1.0$ [kmol/min]
Feed compositions	$z_A = z_D = z_B = z_C = 0.25$
Distillate purity	$x_A^s \geq 0.99$
Upper sidestream purity	$x_B^s \geq 0.95$
Lower sidestream purity	$x_C^s \geq 0.95$
Bottom purity	$x_D^s \geq 0.99$
Relative volatilities	$8 : 4 : 2 : 1$

the optimization procedure described in chapter 3 we obtained the optimized variables given in Table 7.5.

Note from the equations in (7.5) and (7.8) that the split ratios are defined somewhat differently for the two arrangements, which to some extent account for the differences. In order to analyze these results in some detail, we also comment on the heuristics discussed in section 7.4, regarding the net fluxes of intermediate components in the sidestream sections and the fluid transfer across the communication points.

Table 7.5: Optimized variables for introductory example

Variable	Sargent	Agrawal
V [kmol/min]	1.32	1.31
L [kmol/min]	1.07	1.06
S_1 [kmol/min]	0.259	0.259
S_2 [kmol/min]	0.253	0.254
R_{L1}	0.600	0.545
R_{L2}	0.327	0.292
R_{L3}	0.426	0
R_{L4}	0	0.606
R_{V1}	0.292	0.383
R_{V2}	0.586	0.676
R_{V3}	0	0
R_{V4}	0.256	0.184

Net fluxes in sidestream sections

We previously argued that one should avoid internal recycles of components, i.e. avoid net fluxes across the side outlets. In order to analyze these in detail we also need information from the composition profiles. These are displayed for both superstructures in Figures 7.10 and 7.11. For both columns we have given the profiles for all components in the *main column*. For the satellite columns in Agrawal's superstructure we only illustrate the profiles for the intermediate components, i.e. components B and C. For Sargent's arrangement we similarly give the profiles only for the intermediates in column II. Using the computed composition profiles, we may then compute the net fluxes for the intermediate components in the liquid and vapor phases across the

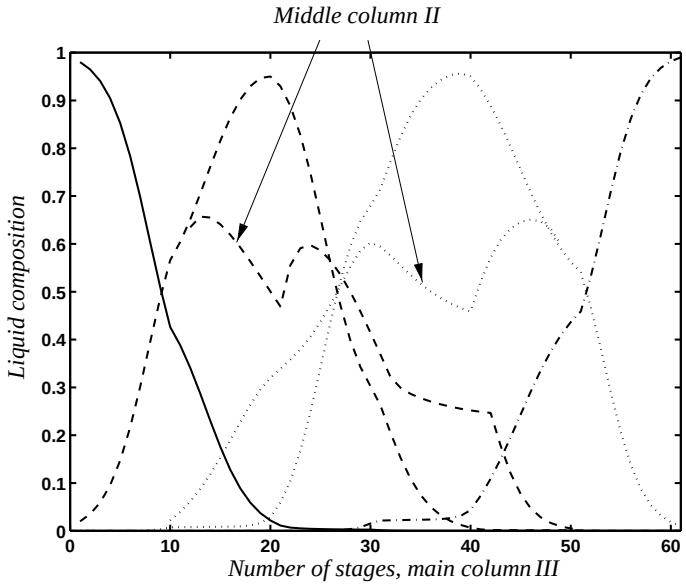

Figure 7.10: Composition profiles for main column in Sargent's superstructure. Solid line - component A, dashed line - component B, dotted line - component C and dashed-dotted line - component D.

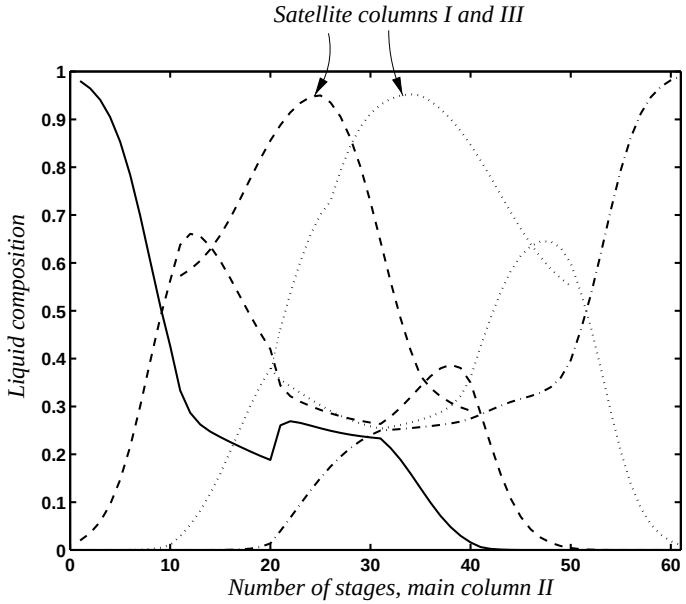

Figure 7.11: Composition profiles for main column in Agrawal's superstructure. Solid line - component A, dashed line - component B, dotted line - component C and dashed-dotted line - component D.

sidestream outlets. For simplicity we show results only for Sargent's arrangement, but similar results were also obtained for Agrawal's arrangement. The net fluxes for component B above and below the sidestream outlet in sections 8 and 9 are given by

$$J_B^8 = L_8 x_{B,i} - V_8 y_{B,i}, \quad i = 1 : N_8 \tag{7.12}$$

$$J_B^9 = V_9 y_{B,i} - L_9 x_{B,i}, \quad i = 1 : N_9 \tag{7.13}$$

where index i indicates stage i and N_8 and N_9 the number of stages in these sections. In Figure 7.12 we illustrate that there is indeed a net flux of component B downwards in section 8, and upwards in section 9. Hence there is no internal recycle of B in the top sections. The same was found for component C for the sections above and below the sidestream S_2, i.e. there is a net flux of C downwards in section 10 and a net flow of C upwards in section 11 (not shown here). It is also of some interest to examine

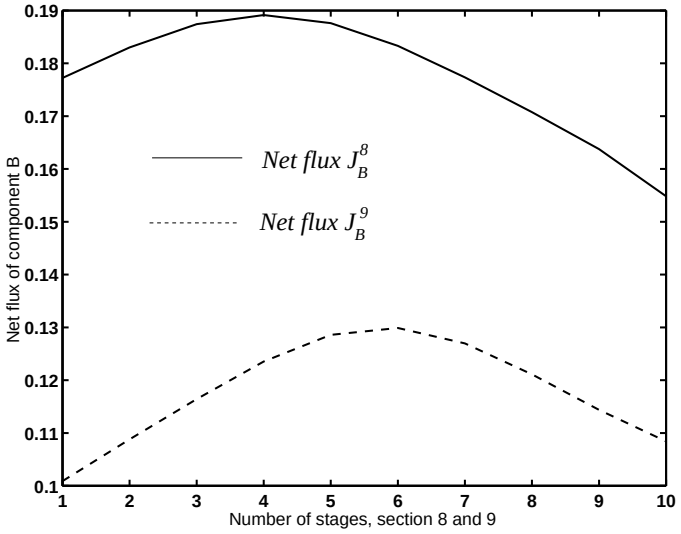

Figure 7.12: Net flux J_B of intermediate component B for optimized Sargent's superstructure. Solid line - net flux *downwards* in section 8 above sidestream S_1, dashed line - net flux *upwards* in section 9 below sidestream.

the internal reflux ratios L_j/V_j for the various sections. Figure 7.13 illustrates this for the main column in Sargent's arrangement. As expected we see from the Figure that L/V is less than one above a "feed" location, and larger than one below a "feed" location.

Fluid distribution between communicating sections

When analyzing the distribution of flows across the communication point, we previously argued for Agrawal's arrangement that it is probably optimal to have vapor primarily flowing from column III to column I, and liquid flowing in the reverse direction. As given by equation (7.8), the flows across the communication points are determined by the liquid and vapor splits R_{L3}, R_{L4}, R_{V3} and R_{V4}. From the data

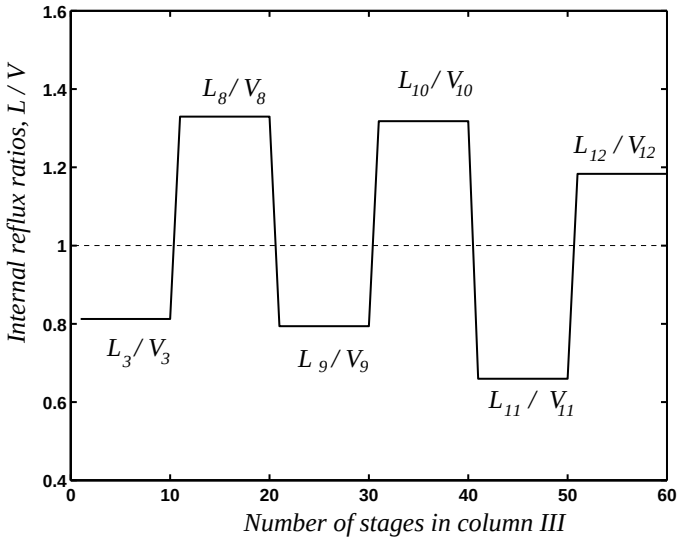

Figure 7.13: Internal reflux ratios for the sections in column III in Sargent's superstructure

in Table 7.5 we have that for Agrawal's superstructure, $R_{V3} = R_{L3} = 0$ at the optimum. With the definitions from the equations in (7.8), we find that that there is no liquid transport from column III to column I, and no vapor transport in the opposite direction. Our heuristics are thus confirmed for this case, which signifies that using physical insight is crucial in order to analyze and understand the optimal solutions for such complex columns. For Sargent's superstructure, we similarly find from the results in Table 7.5 that $R_{L4} = 0$ and $R_{V3} = 0$, so that there is no fluid transport from column III to column II. This implies that all transport takes place in the direction towards the product withdrawals. The only communication is thus liquid flowing from section 5 to section 10 ($R_{L3} = 0.426$) and vapor from section 6 to section 9 ($R_{V4} = 0.256$).

From the composition profiles in Figure we also find that the maximum composition of the intermediate B occurs *at* the stage from which sidestream S_1 is withdrawn, i.e. $x_B = 0.95$. This indicates that the optimal location has been found for $S1$. For the intermediate C, the maximum composition occurs above the sidestream S_2. This may indicate that it is optimal to move the sidestream to some stage above the chosen location. Re-optimizing the column with the same number of total stages, but using $N_{10} = 8$ and $N_{11} = 12$ (i.e. moving the sidestream two stages up the column), indeed lowers energy usage, although the savings are insignificant. However, we stress that the finding the optimal location requires a model in which we allow for withdrawals from any stage within these sections. Results for the latter are not presented here.

In order to comment on the split–sequences in the column and compare to the *easiest split*, we may consider the composition profiles in the prefractionator column I for Sargent's arrangement. The profile is given in Figure 7.14. From the profiles we find that the first split is essentially between the light A and heavy component D,

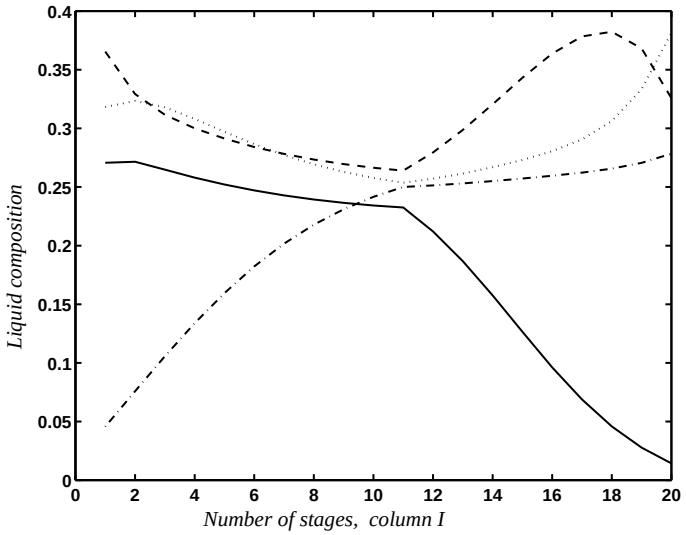

Figure 7.14: Composition profiles for column I in Sargent's superstructure. Solid line - component A, dashed line - component B, dotted line - component C and dashed-dotted line - component D.

whereas the intermediates B and C distributes between the top and bottom products. We may note that there is no sharp A/D split, which is not required since we do not require "pure" products.

After this introductory example, we now proceed to compare the energy efficiency to optimized sequences of regular columns. We also discuss some effects related to the trade off between the number of stages (capital cost) and the energy requirements. Results are also given for the Kaibel and $\vdash$ columns. Since we use the same conceptual model for all columns as was described for the introductory example, we leave out details for the models and give only the energy usage.

7.6 Comparing Optimized Petlyuk and Conventional Arrangements

In order to compare the performance of Petlyuk arrangements with conventional designs it might be disputed how one should select the number of stages. For the optimizations given in this work we have chosen to compare the arrangements on basis of the *total* number of stages, i.e. adding every stage in all sections. We denote this total number of stages by N_T, whereas we use the term N_H for the number of stages in the *main column* counting from the reboiler (bottom) to the condenser (top), i.e. the "column height". If we consider Agrawal's and Sargent's superstructures with 12 sections and 10 stages in each section, we thus have $N_T = 120$ and $N_H = 60$. A Petlyuk arrangement generally requires more stages (N_T) than a series of conventional

columns for a finite reflux ratio. However, as noted also by Wolff and Skogestad (1995), using N_T may be conservative when comparing the Petlyuk arrangements with conventional arrangements. To justify using N_H instead of N_T, one could also argue that the number of stages in sections on either side of a partition comes *for free* with respect to column height and diameter. This follows if we take into account that the internal flows, which more or less determine the size of the column internals, are distributed between the partitioned sections within the single shell. In any case, we indicate both N_H and N_T for the different arrangements for the numerical results.

For the case studies we use the same relative volatilities and purity specifications given in Table 7.4. We also consider mixtures with different feed compositions which we denote by mixtures a, b and c are given in Table 7.6

Table 7.6: Feed mixtures for case studies

Feed mixture a	$z_A = z_D = 0.4$, $z_B = z_C = 0.1$
Feed mixture b	$z_A = z_B = z_C = z_D = 0.25$
Feed mixture c	$z_A = z_D = 0.1$, $z_B = z_C = 0.4$

7.6.1 Infinite energy input – Minimum N

If we consider a conventional sidestream column we may compute the minimum number of stages N_{min} for a quaternary separation using the well known Fenske equation, i.e.

$$N_{min} = \frac{log\,(S_{LH})}{log\,(\alpha_{LH})}, \quad S_{LH} = \frac{x_{L,T}/x_{H,T}}{x_{L,B}/x_{H,B}} \tag{7.14}$$

where subscripts T and B denote the top and bottom products whereas L and H refer to the light and heavy keys, respectively. The sidestream column corresponds to an arrangement in which the stages for each bisectional column is stacked on top of each other (3 regular columns). We note that the results for N_{min} are the same as for the direct and indirect split schemes, since each section performs a given pseudo-binary separation. Recall in the following that we require purities of 99% for A and D and 95% for B and C. If we then assume that only adjacent components appear as impurities, and also an equal distribution of impurities in the intermediate products, we have for the impurities that $x_B^A = x_B^C = 0.025$, $x_C^B = x_C^D = 0.025$ and $x_A^D = x_D^C = 0.01$. Here the subscripts refer to the products and the superscript to impurities respectively. Using the Fenske equation (7.14) and relative volatilities between adjacent components of $\alpha_{ij} = 2$, we thus obtain

$$N_{min} = \frac{log(S_{AB})}{log(2)} + \frac{log(S_{BC})}{log(2)} + \frac{log(S_{CD})}{log(2)} = 34.3 \tag{7.15}$$

However, with the dividing wall column in Figure 7.6 the given separation is achieved in a column with only 6 stages in each section and 5 stages in the the top and bottoms section. This gives $N_H = 34$, which is less than N_{min}. We note for the sake

of consistency that the total number of stages is $N_T = 70$ in this case. The latter also illustrates that if we consider N_T instead of N_H, Petlyuk arrangements in general requires a larger N_{min} than conventional arrangements. This is simply due to the fact that a larger number of sections is required to produce sharp splits.

7.6.2 Minimum energy input – finite$N$. One dividing wall

We first consider the $\vdash$ and Kaibel columns which are the simplest simplest extension of the Petlyuk column. To enable comparisons between these columns, we need to specify the number of stages in the middle section between the sidestream outlets in the Kaibel column. As discussed above, this section should ideally act as a total reflux column for which it requires a certain minimum number of stages N_{min}^{BC} to avoid remixing of intermediates B and C (the $\vdash$ and Kaibel columns are almost identical if total reflux $L/V = 1$ is achieved in the intermediate section). With the given purity requirements, we may compute a "lower bound" for N_{min}^{BC} if we consider a separation in which only intermediates are present in the sidestreams, i.e. no light or heavy components. In this case equation (7.14) yields $N_{min}^{BC} = 8.5$. A more reasonable situation is to assume an even distribution of impurities as discussed in the last section, hence equal amounts of A and C in the B–sidestream and conversely equal amounts of B and D in the C–sidestream. In the latter case we have a pseudo-binary mixture of B and C for which $x_{L,T} = x_{H,B} = 0.95$ and $x_{L,B} = x_{H,T} = 0.025$. Using this we obtain $N_{min}^{BC} = 10.5$ from equation (7.14). Hence, if we use 11 stages in the middle section, we should obtain a purity slightly higher than 95% for the side streams.

We should emphasize that when comparing the $\vdash$ and the Kaibel columns, the difference (in cost) owes to either an additional (external) heat exchanger or an intermediate section (dephlagmator) within the column shell. For the simulations we have thus chosen to *exclude* the "extra" stages in the intermediate section for the Kaibel column, corresponding to the required N_{min}. In order to compare the performance with conventional designs we considered a 3–column arrangement which closely resembles the $\vdash$ and the Kaibel arrangement as shown in Figure 7.15. The main reason for choosing this particular design is that it yields the same values for both N_T and N_H. Note as previously discussed that for the optimizations we have 6 DOFs for the Kaibel column and 5 DOFs for the $\vdash$ column, out of which 4 are consumed for the product purities. Note in light of the discussion above, that for this particular example we used 15 stages in all sections of the Kaibel column, except for the intermediate section between the sidestreams where we used 9 stages. For the $\vdash$ column we use 15 stages in all of the 6 sections, i.e. $N_H = 60$, $N_T = 90$. Results from the optimizations for feed mixture a are shown in Table 7.7 and we refer to Figures 7.3 and 7.4 for notation.

Table 7.7: Optimized variables for the Kaibel and $\vdash$ columns with feed mixture a and $N_T = 90$

	V	L	S_1	S_2	R_L	R_V
Kaibel	1.167	0.764	0.096	0.098	0.39	0.68
$\vdash$	1.167	0.766	0.096	0.097	0.40	0.69

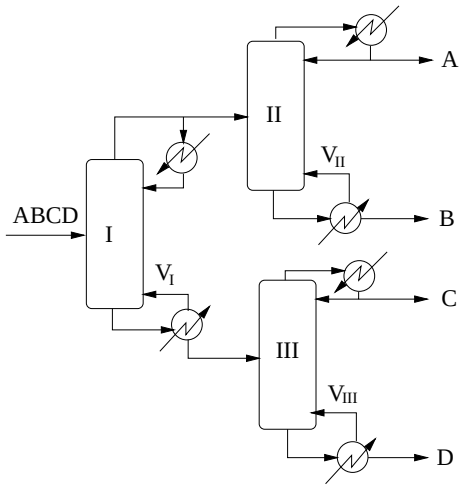

Figure 7.15: 3–column arrangement for quaternary separations

As expected the differences between the two columns are insignificant. As previously discussed the columns are equal when we have total reflux $L/V = 1$ in the intermediate section of the Kaibel column, whereas for the example we have $L/V = 0.99$. Composition profiles for the main columns of the Kaibel and $\vdash$ columns are given in Figure 7.16. Note for the $\vdash$ column that the product composition in the lower sidestream is equal to the *vapor* composition on the top stage. The vapor composition is in fact lower than the liquid composition (shown in the Figure) due to the presence of the lower boiling intermediate B. Recall that we require saturated liquid products, for which the vapor leaving the top stage is condensed through heat exchange with the sidestream from the bottom of the section above. The upper sidestream is also withdrawn as liquid.

The relative energy savings ΔV compared to the 3–column arrangement in Figure 7.15 are given for feed mixtures a and b in Table 7.8[1].

Table 7.8: Minimum energy inputs for arrangements with one vertical partition

	3–column arrangement	$\vdash$ and Kaibel[2]	Savings
$N_H = 60,\ N_T = 90$	$V^a = 1.96$	$V^a = 1.17$	$\Delta V^a = 40\%$
	$V^b = 2.31$	$V^b = 1.55$	$\Delta V^b = 33\%$

From the results we find that the $\vdash$ and Kaibel columns offer considerable energy savings in the order of $30-40\%$ compared to the 3–column arrangement. However, we should also emphasize that the arrangements are probably not well suited when $z_B \neq z_C$, for which case the main column is not balanced. We also note that among the other conventional arrangements (5 possible sequences for 4 components), results showed

[1] Superscripts refer to the feed mixture

[2] For the Kaibel column we must add N_{min}^{BC} stages in the intermediate section

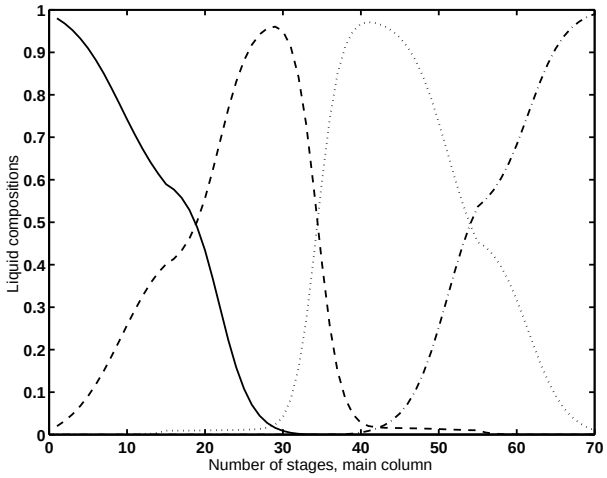

(a) Kaibel column

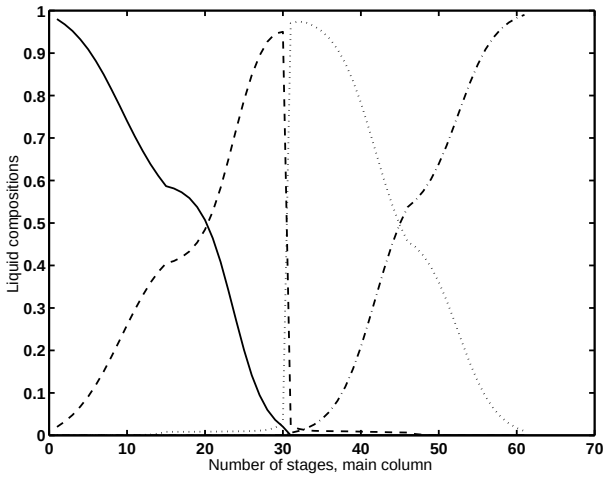

(b) $\vdash$ column

Figure 7.16: Composition profiles in the main columns for the Kaibel (a) and $\vdash$ column (b). Solid line - component A, dashed line - component B, dotted line - component C and dash–dotted line -component D

that the performance of the indirect split sequence (with vapor feed to subsequent columns) was similar to the 3–column arrangement whereas the direct split required a larger V for mixtures a and b.

7.6.3 Minimum energy input – finite$N$. Two dividing walls

We then proceed to compute energy savings for Petlyuk arrangements with the maximum number of $n(n-1)$ sections. To compare the energy efficiency of Sargent's and Agrawal's superstructure with a conventional sequence of regular columns, we have chosen the arrangement in Figure 7.17, denoted the "direct–indirect" scheme. Recalling the previous discussion of how one should choose the number of stages,

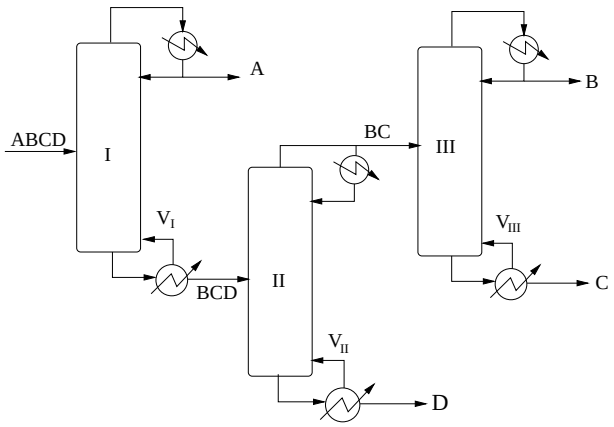

Figure 7.17: Conventional "direct-indirect" 3–column arrangement for quaternary separations

we mention that the main reason for choosing this particular arrangement, is the fact that it may yield the same values for both N_T and N_H as the Agrawal's arrangement. In Table 7.9 we give results in which we compare Agrawal's (satellite) and Sargent's (sequential) arrangements with the "Direct–indirect" scheme in Figure 7.17. ΔV denotes the fractional savings of the Agrawal arrangement relative to the "direct–indirect" scheme. Provided there is a sufficient number of stages we thus

Table 7.9: Minimum energy inputs for arrangements with two vertical partitions

	"Direct–indirect"	Sargent	Agrawal	Maximum savings
$N_H = 40$, $N_T = 80$	$V^a = 1.90$	$V^a = 1.69$	$V^a = 1.47$	$\Delta V^a = 23\%$
	$V^b = 2.45$	$V^b = 2.27$	$V^b = 2.11$	$\Delta V^b = 14\%$
$N_H = 60$, $N_T = 120$	$V^a = 1.75$	$V^a = 1.07$	$V^a = 1.06$	$\Delta V^a = 39\%$
	$V^b = 2.27$	$V^b = 1.32$	$V^b = 1.31$	$\Delta V^b = 42\%$
	$V^c = 2.58$	$V^c = 1.46$	$V^c = 1.40$	$\Delta V^c = 46\%$

find that relative savings are in the order of 40%. However, we clearly see that the

number of stages have a large impact on the. For $N_T = 80$ we find that Agrawal's arrangement is the better, whereas for Sargent's arrangement the savings are modest. The fact that the savings increase with N_T signifies that the conventional arrangement requires fewer stages to achieve the overall minimum V_{min} than the Petlyuk arrangements. We also mention that the two Petlyuk arrangements should give the same V_{min} when $N \to \infty$, since they use the same number of sections and thus allow for the same *easiest split* sequence. In order to examine how far the values in Table 7.9 are from the actual V_{min}, we examine in the next section more closely the relation between the number of stages and minimum energy input.

In order to compare the relative savings for Petlyuk arrangements with one and two dividing walls given in Tables 7.9 and 7.8, we stress that the Petlyuk arrangements are not strictly comparable in terms of N_T. This is firstly due to the $\vdash$ column not being a Petlyuk arrangement in a strict sense, since both direct and indirect thermal coupling takes place. Secondly, we previously pointed out the ambiguity in selecting the appropriate number of stages for comparisons. We have that the Kaibel column requires $N_T + N_{min}^{BC}$ and that the $\vdash$ column uses either an extra heat exchanger or an internal region to provide the required heat transfer area. Due to these reasons we have chosen different conventional schemes in Figures 7.15 and 7.17 for comparisons, since we aimed for conventional arrangements which may yield the same N_T *and* N_H as the Petlyuk arrangements. If we use the same N_H for the conventional arrangements , we find that the the "direct-indirect" scheme yields a larger N_T than the 3–column arrangement. Finally, we add that among the other *conventional* schemes, the direct split scheme required a considerably larger energy input than the "direct-indirect" scheme, whereas the indirect split (vapor feed to subsequent columns) with the same N_T was slightly better (i.e. in the order of 1 % lower V). However, we again stress that the direct and indirect splits with the same N_T requires a structure with larger N_H.

7.6.4 Minimum energy input - infinite N

In this section we want to obtain the overall minimum energy usage for a quaternary separation in a Petlyuk arrangement. We should mention that for Petlyuk columns separating a mixture into three products, there are methods proposed in the literature to obtain V_{min}, e.g. Fidkowski and Krolikowski (1986), Glinos and Malone (1988) and Carlberg and Westerberg (1989). The basis for these works are Underwood's method, which yields exact results for infinite columns. However, since no such method is available for the complex Petlyuk arrangements discussed here, we resort to numerical simulations. We pose the task of finding reliable shortcut methods for estimating the minimum energy input as an interesting and important problem for future work. Thus, we aim to find what is a "sufficiently" large number of stages so that only small reductions in V are possible by increasing this number. To do so we know that for conventional distillation columns, the relation between the number of stages N and the energy input V takes the shape of a hyperbolic function. This function reveal two distinguished asymptotes, where one gives N_{min} for the limiting case of infinite internal flows ($L, V = \infty$), whereas minimum boilup V_{min} is obtained for $N = \infty$.

Hence, by optimizing the Petlyuk arrangements with respect to V for an increasing number of stages, we will obtain a curve that asymptotically converges to the true V_{min}.

The relation between N_T and V for feed mixture a is given in figure 7.18. Note here that each point of the curve represents the minimized V for the given N_T. As

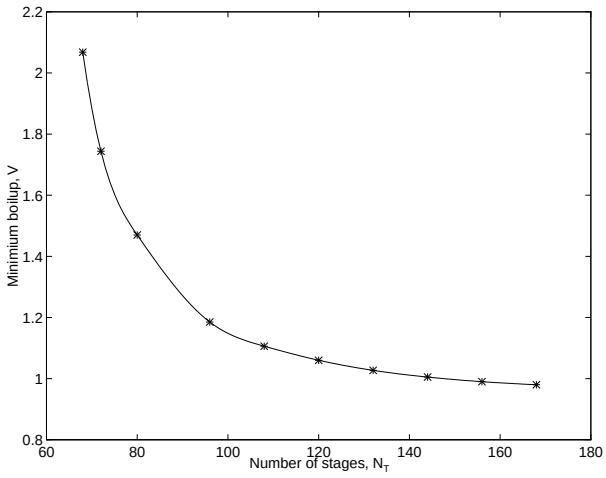

Figure 7.18: Trade–off between N_T and V for Agrawal's arrangement and feed mixture a

seen in the Figure, we find that with a relative volatility of $\alpha_{ij} = 2$, the hyperbolic curve approaches $V^a_{min} \approx 0.98$ as $N_T > 160$. We thus find that the value of 1.06 given in Table 7.9 is reasonably close to V^a_{min}. We furthermore find that V^a_{min} is in fact less than one. The energy usage is thus very low, for instance compared to the results for the *ternary* mixture given in Table 7.2. For the Petlyuk column with $N_H = 60$ and $N_T = 90$ (note that N_T is smaller but N_H the same) we found the lowest energy usage of $V = 0.99$, which was obtained for the feed mixture of $z_F = [0.475, 0.05, 0.475]$.

7.7 Sensitivity Analysis

In this section we show that additional and useful information may be extracted from the optimized solutions, by obtaining sensitivity functions derived from the augmented Lagrangian function. This is a very important issue when analyzing the energy efficiency of Petlyuk arrangements, since we may characterize the process behavior in the vicinity of optimum. Using information for the sensitivities provides crucial information for the steady state behavior, since we may quantify the deviations from the optimum when the process is subject to changes in the process parameters. The steady state properties of the Petlyuk column for ternary mixtures have previously been discussed by several authors (e.g. Chavez *et al.* (1986), Wolff and Skogestad (1995), Morud (1995) and Halvorsen and Skogestad (1997)). It is shown that Petlyuk arrangements may display complex nonlinear behavior, such as multiple steady

states (Chavez *et al.* 1986) and even *holes* within certain operating regions (Wolff and Skogestad (1995) and Morud (1995)). In the latter case it was found that by specifying one of the impurities impurity in the middle product, in addition to the three product purities, there may in fact not exist any steady state solution for the set of specifications. In practice this means that one should only control one composition in each product.

In a recent paper Halvorsen and Skogestad (1997) addressed certain issues related to optimizing control of Petlyuk columns using feedback mechanisms. The objective was to find suitable measurements and manipulated variables for optimal operation based on steady state arguments. The authors found that the energy surfaces are characterized by certain *"good"* and *"bad"* directions in the parameter space. This may not be surprising in light of the previous findings of Fidkowski and Krolikowski (1986), where it was shown that the energy surface for infinite columns in fact is *constant* within certain enclosed regions. The latter was also verified from simulations of "finite" columns in chapter 5 in this thesis. However, extracting such information is of great importance in order to understand under which operating regimes the energy consumption is relatively insensitive to changes in the parameters. Halvorsen and Skogestad (1997) obtained the "good" and "bad" directions by inspection of the solution surface which was computed the continuation scheme discussed in chapter 3 of this work. However, since the number of DOFs are much larger for the Petlyuk arrangements discussed here, it is not that straightforward to obtain information directly from the solution surfaces. For Agrawal's and Sargent's superstructure, there are 8 remaining DOFs giving a 8 dimensional energy surface.

What we seek here is thus some measure of the sensitivity for the objective function (boilup) with respect to changes in the manipulated variables. Since the first order derivatives vanish in the optimum, one must resort to second order information available from the Hessian matrix evaluated at the optimum. The approach used here to compute the Hessian is due to a procedure described by Morud (1995). The core element in this procedure is to approximate the solution surface in the vicinity of the optimum by a quadratic surface, i.e. a Taylor series expansion in which terms of third and higher order are eliminated.

7.7.1 Deriving sensitivity functions from Taylor series

Consider the optimization problem which may be posed as

$$\begin{aligned} &\min_{u} \Phi(z) \\ \text{s. t.} \quad &f(z) = 0 \end{aligned}$$

where $z = [x\ u]$ is an augmented vector of dependent variables (x) and inputs (u). In this context the constraints $f(z)$ are constituted by the steady state process model. The optimization problem is commonly solved by formulating the augmented **Lagrangian** objective function given by

$$\mathcal{L} = \Phi(z) + \lambda^T\ f(z), \quad z = [x\ u] \tag{7.16}$$

where λ denotes the vector of Lagrange multipliers. The optimum Φ^* is then found by solving the first order necessary conditions for an extremal point

$$\mathcal{L}_z = 0, \quad \mathcal{L}_\lambda = 0 \tag{7.17}$$

and subsequently check whether it is a minimum (e.g. use the *Kuhn–Tucker* conditions). However, since the process model is highly nonlinear and ill–conditioned, which commonly causes convergence problems, we have as previously discussed in this work chosen to approach the optimum in a stepwise manner by embedding the optimization in a continuation scheme. To refine the obtained solution we may subsequently apply a few Newton–Raphson iterations on the system

$$\hat{f}\,(z, \lambda^*) = \left\{ \begin{array}{c} f(z) \\ \mathcal{L}_z(z) \end{array} \right\} = 0 \tag{7.18}$$

The system given by (7.18) thus in general constitutes a non-singular system in z and λ, which may be solved using any standard numerical method. However, since the optimum $\hat{z}$ in our case is already known, we have an over-determined system of equations from which we in fact may obtain the optimal Lagrangian multipliers λ^*. We may thus compute the multipliers λ^* in a least squares sense using the first order optimality condition. For this purpose we need to evaluate the pseudo–inverse of the Jacobian $f_z^\dagger$ so that

$$\lambda^* = -(f_z^T)^\dagger \Phi_z^T \tag{7.19}$$

The (non-square) Jacobian $f(z)_z$ may be derived numerically using finite difference formulas. We may also mention that in our case Φ_z is simply a unit vector (i.e. linear in z), since V is one of the system variables z. The computed λ^* may, as is well known from optimization theory, be interpreted as shadow prices. Hence, by considering the equations in $f(z)$ which corresponds to *specifications*[2] constraints, one in fact has a measure of the sensitivity in the objective function towards incremental changes in these specifications. For instance, if f_n denotes a purity specification, then a change of ϵ in the purity yields a change in the objective function (V) by

$$\delta V = \epsilon \lambda_n \tag{7.20}$$

Note that the specification f_n should enter linearly with coefficient 1. After finding the optimal multipliers, we may then proceed to compute the sensitivity function for the objective function subject to changes in the inputs u at the nominal optimum.

To provide the sensitivity functions we have used an analogy to a previous work of Morud (1995), in which a procedure based on Taylor series expansions was proposed. The details of the Taylor series expansion is shown in Appendix B, but we strongly encourage the interested reader to also elaborate on the work of Morud (1995). According to the Taylor series expansion at the optimum, we find that *small* perturbations in u impose changes in the minimum boilup V_0 given by

$$\delta V = V - V_0 = \frac{1}{2} \delta u^T \mathcal{L}_{uu} \delta u \tag{7.21}$$

[2] We emphasize that multipliers (λ) corresponding to equations in $f(z)$ that constitutes for instance mass-balances or VLE, does not give meaningful interpretations as shadow prices

where the Hessian of the objective function V with respect to the inputs (u) is given by

$$\mathcal{L}_{uu} = M^T \mathcal{L}_{zz} M \tag{7.22}$$

Here M is a matrix representing a linear approximation of the process model $f(x,u)$, i.e.

$$\delta z = \begin{bmatrix} \delta x \\ \delta u \end{bmatrix} = \begin{bmatrix} -f_x^{-1} f_u \\ I \end{bmatrix} \delta u = M \delta u \tag{7.23}$$

where I is an identity matrix with same dimensions as u. The reason for why we may substitute simply a *first order* process model, is shown in Appendix B where λ is used to eliminate first order terms in the Taylor series expansion of the objective function. The Hessian of the Lagrangian $\mathcal{L}_{zz}$ may be obtained numerically from finite (second order) perturbations of the Lagrangian function (7.16) at the nominal optimum. The second order information available in the Hessian may be utilized for several purposes. In the next section we examine the directionality of $\mathcal{L}_{zz}$, in order to obtain knowledge of the directions in which the objective function displays large/small sensitivities.

7.7.2 Sensitivity to changes in inputs

In this section we consider the effect of changes in the inputs on the energy usage. Using the available information from the Hessian at the optimum $\mathcal{L}_{uu}$, we may characterize the optimal solution by computing for instance a singular value decomposition (SVD) of $\mathcal{L}_{uu}$. Using the SVD we have *local* information of the directions in parameter space in which the objective function is the most (high gain) and least (low gain) sensitive with respect to changes in u. We here denote the SVD by

$$\mathcal{L}_{uu} = U \Sigma V^H \tag{7.24}$$

in which the diagonal matrix Σ takes as non–zero elements the singular values σ_i and the matrices U and V constitutes the *output* and *input* directions. Since the Hessian matrix is symmetric, the output and input directions are identical, i.e. $U = V^H$. For the analysis we may thus consider only the input directions. In order to enable a numerical comparison between the different inputs u_i, one should in general introduce scaling $\hat{u} = Du$, where D is an appropriate diagonal matrix. However, in our particular case scaling is not necessary since u contains only vapor and liquid splits, and are thus "inherently" scaled within the range $[0,1]$.

To ensure that we are reasonably close to the overall V_{min}, and to keep the problem size small for numerical convenience we consider a numerical example of Agrawal's superstructure with $N_H = 42$ and $N_T = 84$ and a mixture with relative volatilities $\alpha_{ij} = 3$ and feed composition $z_f = [0.4, 0.1, 0.1, 0.4]$. Increasing α has similar impact on the separation as increasing the number of stages. We refer to Figure 7.9 for notation. For this column, numerical simulations revealed that one of the vapor splits R_{V3} exceeded the allowable region $[0,1]$ at the optimum, and is thus not considered in the sensitivity analysis. From the remaining 11 DOFs, 4 inputs (L, S_1, S_2, V) are

consumed to achieve the purity constraints, which leaves us with 7 DOFs (internal splits) after consuming 4 DOFs for purity control, i.e.

$$u = [R_{L1}, R_{V1}, R_{L2}, R_{V2}, R_{L3}, R_{L4}, R_{V4}]^T \tag{7.25}$$

Taking an SVD of the Hessian $\mathcal{L}_{uu}$ we obtain the singular values:

$$\Sigma = \text{diag}[69.4,\ 6.2,\ 1.1,\ 0.32,\ 5.6e^{-2},\ 2.4e^{-3},\ 3.7e^{-4}] \tag{7.26}$$

The condition number, which gives the ratio of the largest to the smallest singular value, is in this case very large ($\gamma = 1.87e^5$), which illustrates that the system is very ill–conditioned. The largest and smallest singular values correspond to the high $\overline{u}$ and low gain $\underline{u}$ directions, given by the first and last columns of U. For the example these were found to be

$$\overline{u} = [0.386,\ 6.87e^{-3},\ -0.156,\ 0.832,\ -0.104,\ 0.352,\ -1.94e^{-2}]^T \tag{7.27}$$

$$\underline{u} = [0.342,\ 2.07e^{-2},\ 0.608,\ -4.53e^{-5},\ 0.618,\ 9.61e^{-2},\ 0.350]^T \tag{7.28}$$

We thus find that the parameters which have the largest impact, as given by the high gain direction, are the vapor split in the bottom R_{V2} and the liquid split in the top R_{L1}. Giving a physical interpretation of the results, we argue that these findings are as expected. This is based on the simple fact that R_{V2} and R_{L1} in fact determine the distribution of liquid and vapor in *all* sections within the column, whereas the other inputs only affect smaller "subsystems" (sections) of the column. This is also reflected by analyzing the low gain direction in which only small changes in R_{V2}.

To characterize the behavior of the Petlyuk arrangements we first consider the *open loop* effect of perturbations in the internal splits on the product compositions. The inputs (flows) used to keep the product purities at their set–points are thus kept at the nominal (optimum) values. In Figure 7.19 we show the results from a nonlinear dynamic simulation which illustrate the open loop effect of a 10 % perturbation in the high gain direction ($\overline{u}$) on the product compositions. The actual perturbation corresponds to a 10 % *increase* in the nominal value of R_{V2}, which according to the the SVD decomposition is the parameter with the largest impact. We see that the impact is detrimental, as the purity of the intermediate component C drops from 0.95 to 0.86. From simulations we also found as expected that perturbations in the low gain directions had almost insignificant effects on the purities (results are not displayed). The results clearly demonstrate that one needs feedback control to keep the product purities at their set-points, although partial control may be sufficient.

We then consider the *closed loop* effect of perturbations in the parameters on the energy consumption, i.e. the external flows are now consumed for purity control. In figure 7.20 we illustrate the impact of changes in the liquid and vapor splits on the boilup to feed ratio V/F along the high $\overline{u}$ (solid line) and low gain $\underline{u}$ direction (stapled line). As seen from the Figure, we find that the fitting of a quadratic objective function in the vicinity of the optimum is reasonable. Furthermore we note as expected that the boilup changes very little in the low gain direction, whereas perturbations in the high gain direction has a much larger impact. This demonstrates that for practical operation, one needs some kind of monitoring and feedback control of the internal

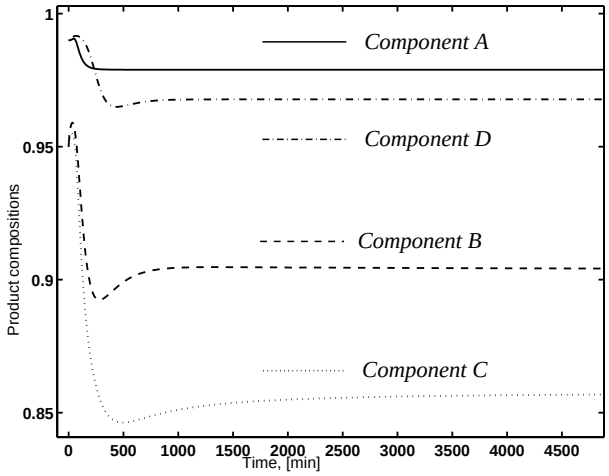

Figure 7.19: Open loop simulations for 10 % perturbation in high gain direction for the internal splits R_{Lj} and R_{Vj}, for intermediate purities of B and C, i.e $x_B^s = x_C^s = 0.95$.

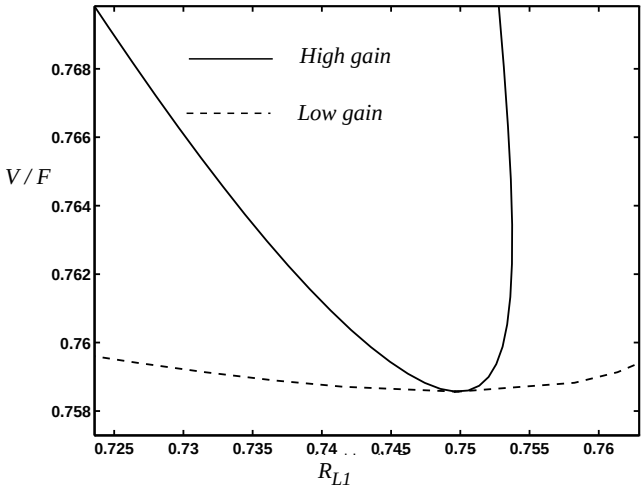

Figure 7.20: Closed loop sensitivities in high and low gain directions for intermediate purities of B and C, i.e $x_B^s = x_C^s = 0.95$.

splits in order to maintain operation in the vicinity of the energy minimum. These results further emphasize the need for monitoring of the process parameters and an appropriate feedback control structure, in order to maintain operation in the vicinity of the optimum. The issue of optimizing control is for this reason of great interest. In a recent work by Halvorsen and Skogestad (1997) some steps are taken in this direction for the ternary Petlyuk column. The authors addressed issues such as identifying key variables that are available for on line measurements and finding appropriate manipulated inputs for optimal operation.

7.7.3 Sensitivity to changes in output specifications

We here consider the effect of the output (purity) specifications on the energy consumption. In the nominal optimum we may also obtain vital information by computing the *shadow prices* (Lagrange multipliers λ^*), with respect to the purity specifications. For the purity constraints $x_A^s = 0.99$, $x_B^s = x_C^s = 0.95$ and $x_D^s = 0.99$, the optimal Lagrange multipliers was found to be

$$\lambda^{*T} = [0.158,\ -0.0028,\ 0.403,\ 2.75] \tag{7.29}$$

This means that if we decrease the purity specification in the bottoms product (x_D^s) from 0.99 to say 0.985, the Lagrange multiplier indicates that the boilup should be reduced by the amount $0.005 \cdot 2.75 = 1.38 \cdot 10^{-2}$. In order to verify the numerical results, we performed additional numerical simulations in which we used the new set-point $x_D^s = 0.985$. From the optimizations we found that the reduction in V was equal to $1.15 \cdot 10^{-2}$, i.e. only slightly lower than the predicted value. For the intermediate C, the prediction using the multipliers in fact came out even better. The optimal multiplier $\lambda^*_{y_C^s} = 0.403$ implies that increasing x_C^s by 1% to 0.96 requires a boilup of $V = 0.7626$. From numerical optimizations we obtained the actual value of $V = 0.7622$. Taking into account that the Hessian only provides local information, and that the changes in set-points are in the order of 0.5 and 1.0%, we take the results as a proof of the usefulness of our analysis. For smaller deviations from the nominal optimum, the Hessian off course provides even more accurate results. We again stress that using information from the Hessian matrix presupposes that the solution surface may indeed be approximated by a quadratic surface in the vicinity of the optimum.

Analyzing the above results in some more detail, one should note that the results are obtained from a design in which we have not considered the optimal distribution of stages within the different sections. This may in fact partly explain why the shadow prices for the intermediate product (B) is much lower than for the top and bottoms. If we examine the composition profiles given in Figure 7.21 (a), we find that the maximum compositions of the intermediates does not occur at the stage from which the sidestreams are withdrawn. This indicates that the location of the sidestream outlet is suboptimal. Furthermore, using an analogy, this also means that there is some "slack" with respect to the separation occurring in these sidestream sections. Compared to the profiles for the light and heavy product, we find that the maximum compositions indeed occur at the top (light) and bottom (heavy) stages. Hence, it seems reasonable that the shadow prices is larger for the top and bottom products.

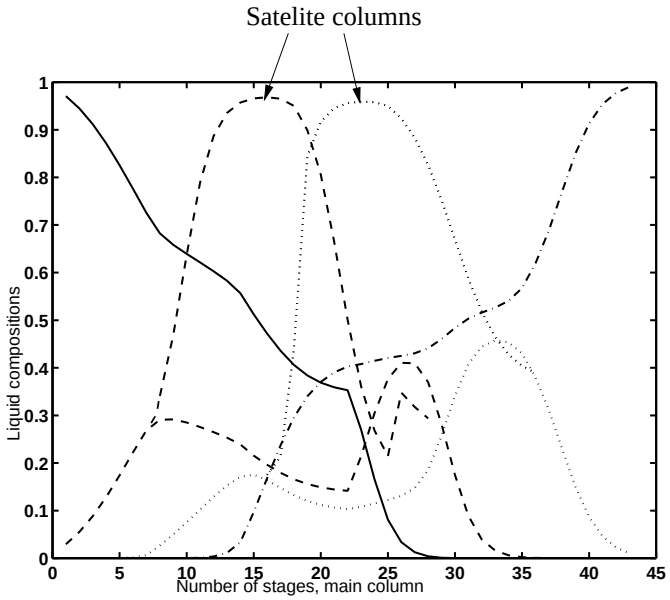

(a) $x^s_A = x^s_D = 0.99$, $x^s_B = x^s_C = 0.95$

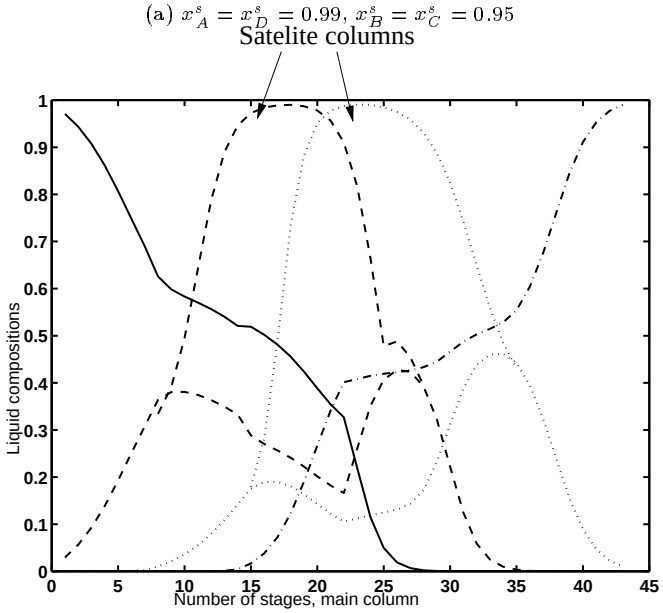

(b) $x^s_i = 0.99$

Figure 7.21: Composition profiles for Agrawal's satellite arrangement. Solid line - light component A, dashed line - intermediate component B, dotted line - intermediate component C and dash-dotted line heavy component D.

To investigate this issue further, we considered the same column where we increased the product purities of the intermediates so that *all* purities are $x_i^s = 0.99$. As one may expect we then found that the *shadow prices* was in the same order of magnitude for all product specifications, i.e.

$$\lambda^{*T} = [1.16,\ 1.21,\ 3.32,\ 2.17] \tag{7.30}$$

This to some extent justifies the previous argument, and at the same time illustrates that if one requires the same product purities, yielding a *balanced* column (relative volatilities are equal; $\alpha_{ij} = 3$)), the sensitivities towards changes in purity requirements are in the same order for all products. The minimum boilup was in this case $V^* = 0.799$ compared to $V = 0.759$ with $x_B^s = x_C^s = 0.95$. Since high purity distillation is known to be highly nonlinear, we also expect sensitivities to be larger in this case. The sensitivities for perturbations in the strong direction is indeed more strongly pronounced for both the closed loop (steady state) and open loop (dynamic) simulations as shown in Figure 7.22. In Figure 7.22 (b) we also note the considerable difference between the strong (solid line) and the weak directions (stapled). From the open loop simulations we find that the purity of intermediate B in this drops from 0.99 to 0.87, whereas the top and bottoms changes relatively less.

7.8 Discussion and Conclusions

In this paper we have considered using Petlyuk arrangements for the separation of quaternary mixtures, and demonstrated how such arrangements may be implemented in a single shell using dividing walls. Numerical results for a few example problems indicate that the fractional savings compared to conventional schemes typically are in the order of 40%. However, we emphasize that the results are only tentative, in the sense that savings may be even larger (or smaller) for other mixtures. Our results also demonstrate that Petlyuk arrangements require a larger number of stages compared to conventional designs to achieve the minimum boilup.

Since Petlyuk arrangements give a large number of DOFs at steady state, and the conceptual models commonly display highly nonlinear behavior, the task of computing the optimal solution is indeed a very difficult one. In fact, even finding a steady state solution requires robust and reliable numerical algorithms. In this work we used numerical integration of a *dynamic* model to obtain an initial steady state solution. The optimized solutions were then computed from a *steady state* model by continuation in the subspace spanned by the DOFs. Furthermore, due to the size and complexity of the problems (typically $3N_T$ number of equations and up to 12 DOFs), there is no way of guaranteeing that a global optimum has been obtained using the method proposed in this work. However, based on an a posteriori analysis of the numerical results, in which we studied characteristics such as the composition profiles, the internal distribution of components, the presence internal recycles etc., it seems likely that the results are at least close to the global optimum.

Furthermore, we stress that the Petlyuk arrangements have only been optimized with respect to the degrees of freedom available for *operation*. For a column with a

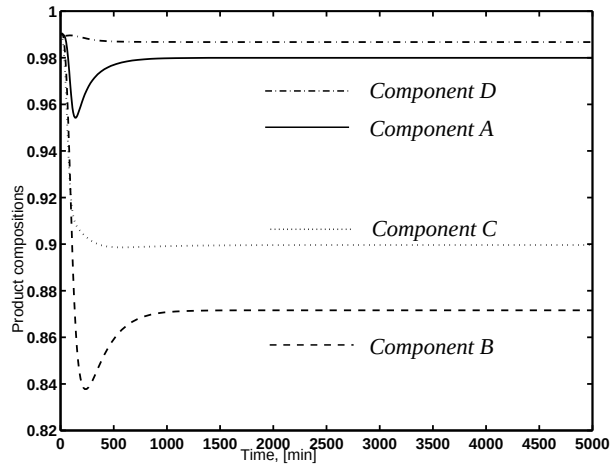

(a) Open loop

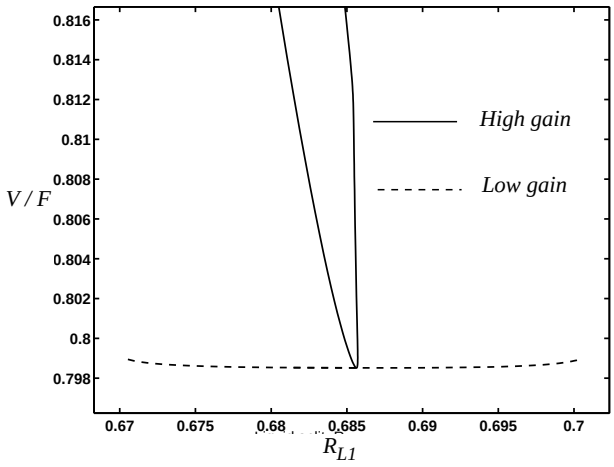

(b) Closed loop

Figure 7.22: Open (a) and closed loop (b) simulations for perturbations in strong and weak directions for high purities $x_i^s = 0.99$

given structure (i.e number of sections and total number of stages), we stress that additional savings are possible if one also takes into account discrete *design* parameters such as the distribution of stages between the different sections and the feed– and side–stream locations. Still, the main contribution from our work is to demonstrate that there is a large potential for extending the Petlyuk ideas to separations of four or more components. Future work is needed to investigate for what mixtures Petlyuk arrangements yield the largest potential savings.

Acknowledgments. Contributions and valuable comments from John Morud are gratefully acknowledged.

Nomenclature

A, B, C, D – Component indices
F – Feed flow rate [kmol/min]
J_B^i – Net flux of component B in section i
L – Reflux flow rate [kmol/min]
L_i – Liquid flow rate in section i
M – Matrix representing a linearized model
N_H – Number of theoretical stages in main column
N_T – Total number of theoretical stages in column arrangement
N_i – Number of theoretical stages in section i
n_C – Number of communication points
n_D – Number of dividing walls
n_S – Number of sidestreams
q – Feed enthalpy
R_L – Liquid split fraction
R_V – Vapor split fraction
S_i – Side stream flow rate [kmol/min]
S_{LH} – Separation factor between light L and heavy H component
U – Matrix of output singular vectors
u – Vector of input variables
$\overline{u}$ – High gain input direction
$\underline{u}$ – Low gain input direction
V^H – Matrix of input singular vectors
V – Boilup from reboiler [kmol/min]
V_i – Vapor flow rate in section i [kmol/min]
x – Vector of (state) variables
$x_{c,i}$ – Liquid mole fraction of component c on stage i
x_c^s – Product specification for component c
$y_{c,i}$ – Vapor mole fraction of component c on stage i
z – Augmented vector of variables and parameters
z_i – Mole fraction of component i in feed

Greek letters

α_{ij} – Relative volatility between components i and j

λ – Lagrangian multiplier

∂ – Derivatives

Φ – Objective function

$\sum$ – Matrix of singular values

Calligraphic

$\mathcal{L}$ – Lagrangian objective function

References

Agrawal, R. (1996). Synthesis of Distillation Column Configurations for a Multicomponent Separation. *Ind. Eng. Chem. Res.* **35**(4), 1059–1071.

Agrawal, R., Z. T. Fidkowski and J. Xu (1996). Prefractionation to Reduce Energy Consumption in Distillation Without Changing Utility Temperatures. *AIChE Journal* **42**(8), 2119–2127.

Annakou, O. and Peter Mizsey (1996). Rigorous Comparative Study of Energy-Integrated Distillation Schemes. *Ind. Chem. Eng. Res.* **35**(6), 1877–1885.

Cahn, R. P., E. Di Micelli and A. G. Di Micelli (1962). Separation of Multicomponent Mixture in Single Tower – U.S. Patent 3,058,893.

Carlberg, N. A. and A. W. Westerberg (1989). Temperature-Heat Diagrams for Complex Columns. 3. Underwood's Method for the Petlyuk Configuration. *Ind. Chem. Eng. Res.* **28**(9), 1386–1397.

Chavez, C. R., J. D. Seader and T. L. Wayburn (1986). Multiple Steady–State Solutions for Interlinked Separation Systems. *Ind. Eng. Chem* **25**, 566–576.

Christiansen, A. C., J. Morud and S. Skogestad (1996). A Comparative Analysis of Numerical Methods for Solving Systems of Nonlinear Algebraic Equations. In: *Proceedings of the 38th SIMS Simulation Conference* (T. Iversen, Ed.). SIMS. pp. 217–230.

Christiansen, A. C., S. Skogestad and K. Lien (1997). Complex Distillation Arrangements : Extending the Petlyuk Ideas. *Comp. Chem. Engng.* **21**(Suppl.), S237–S242.

Fidkowski, Z. and L. Krolikowski (1986). Thermally Coupled system of Distillation Columns: Optimization Procedure. *AIChE Journal* **32**(4), 537–546.

Glinos, K. and M.F. Malone (1988). Optimality Regions for Complex Column Alternatives in Distillation Systems. *Chem. Eng. Res. Des.* **66**(3), 229–240.

Halvorsen, I. J. and S. Skogestad (1997). Optimizing Control of Petlyuk Distillation: Understanding the Steady-State Behavior . In: *Proceedings for PSE'7/ESCAPE-7*. Pergamon. pp. S249–S254.

Kaibel, G. (1987). Distillation Columns with Vertical Partitions. *Chem. Eng. Technol.* **10**, 92–98.

Morud, J. (1995). Studies on the Dynamics and Operation of Integrated Processes. PhD thesis. University of Trondheim. The Norwegian Institute of Technology. Norway.

Petlyuk, F. B., V. M. Platonov and D. M. Slavinskij (1965). Thermodynamically Optimal Method for Separating Multicomponent Mixtures. *Int. Chem. Eng.* **5**(3), 555–561.

Sargent, R. W. H. and K. Gaminibandara (1976). Optimum Design of Plate Distillation Columns. In: *Optimization in Action* (L. W. C. Dixon, Ed.). pp. 267–314. Academic Press. London.

Seidel, M. (1935). German Imperial Patent No. 61503.

Smith, R. (1995). *Chemical Process Design*. Wiley.

Stichlmair, J. (1988). Distillation and Rectification. *Ullmann's Encyclopedia of Industrial Chemistry* **B3**, 4–1 – 4–94.

Tedder, D. W. and D. F. Rudd (1978). Parametric Studies in Industrial Distillation. *AIChE Journal* **24**(2), 303–315.

Triantafyllou, C. and R. Smith (1992). The Design and Optimization of Fully Thermally Coupled Distillation Columns. *Trans. Inst. Chem. Eng.* **70**(Part A), 118–132.

Underwood, A. J. V. (1948). Fractional Distillation of Multicomponent Mixtures. *Chem. Eng. Prog.* **44**(8), 603–614.

Westerberg, A.W. (1985). The Synthesis of Distillation-Based Separation Systems. *Comp. Chem. Eng.* **9**(5), 421.

Wolff, E. A. and S. Skogestad (1995). Operation of Integrated Three–Product (Petlyuk) Distillation Columns. *Ind. Chem. Eng. Res.* **34**(6), 2094–2103.

Wright, R. O. (1949). U.S. Patent 2,471,134.

Appendix A Optimization by Continuation

The optimization algorithm we have used in this work was described in chapter 3, and we therefore give only a brief summary of the principles, referring to chapter 3 for details. The task we consider here is thus to optimize any steady state model of a Petlyuk arrangement, constituted by a system of NAE's which we denote by

$$g(x, y, u) = 0 \tag{7.31}$$

Here x are the states (compositions), y the outputs (purities) and u a set of variables which we are free to specify, i.e. control variables (flows) and system parameters (vapor and liquid splits). The purpose of optimization is thus to minimize the energy input (boilup), i.e.

$$\min_u V\ (x, y, u) \tag{7.32}$$

subject to the steady state model (7.31) and constraints on the purities. Given an initial solution, the purpose is thus to traverse the path to the optimum by continuation in which search directions are defined according to a local linearization.

Appendix B Derivation of sensitivities from Taylor series expansion

This appendix draws from a work by Morud (1995) for which the objective was to derive a Taylor series expansion of the *loss function*, referring to the loss by not

compensating for disturbances at a nominal optimum. This appendix is thus an analogy to the latter work, in which the purpose is to use the Lagrangian multipliers to eliminate the first order terms in the objective function. Using this "trick" we may use a first order *process model* to provide an expression for the sensitivity function (Hessian) towards perturbations in the optimization parameters at a *precomputed* optimum. For convenience we first repeat the optimization problem in which V denotes the objective function, i.e. the boilup

$$\min_u V\ (z) \tag{7.33}$$

$$\text{s. t.}\quad f(z) = 0 \tag{7.34}$$

Commonly the optimum is found by solving the augmented system of equations constituted by the original process model and the first order necessary conditions for the Lagrangian $\mathcal{L}$, i.e.

$$\mathcal{L}_\lambda = f(z) = 0; \quad \mathcal{L}_z = V_z + \lambda^T f_z = 0 \tag{7.35}$$

where subscript z refers to partial derivatives with respect to z. This constitutes a non-singular system of nonlinear algebraic equations in the augmented vector of variables z and the Lagrange multipliers λ, which may be solved using any numerical algorithm. However, in our case the optimum solution is already found (by continuation), and we thus have an over-determined system of equations for determining λ.

The "trick" is in this case to use λ in order to obtain the Taylor series expansion for the objective function $V(z)$. The derivation of the Taylor series expansion requires that all functions (i.e. V and f) is expanded to the same order. However, in our case V is linear in z (the boilup V is one of the system variables) so that the second order term vanishes, hence we obtain the following Taylor series

$$f_i(z) = f_{i0} + \frac{\partial f_i}{\partial z}\delta z + \frac{1}{2}\delta z^T \frac{\partial^2 f_i}{\partial z^2}\delta z + \mathcal{O}(\delta z^3) \tag{7.36}$$

$$V(z) = V_0 + \frac{\partial V}{\partial z}\delta z + \frac{1}{2}\delta z^T \frac{\partial^2 V}{\partial z^2}\delta z + \mathcal{O}(\delta z^3) \tag{7.37}$$

After multiplying equation (7.36) by λ_i, summing up all f_i and finally adding equation (7.37) we obtain

$$\begin{aligned} V(z) &\equiv V(z) + 0 = V(z) + \lambda^T f(z) \\ &= (V_0 + \lambda^T f_0) + (V_z + \lambda f_z)\,\delta z + \frac{1}{2}\delta z^T \left(V_{zz} + \lambda^T f_{zz}\right)\delta z + \mathcal{O}\left(\delta z^3\right) \end{aligned} \tag{7.38}$$

Since $f(z) = 0$, we have only added terms equal to zero to the objective function. The underlying purpose for doing this derivation now emerges. Since the second term $\mathcal{L}_z = V_z + \lambda^T f_z$ is equal to zero at the optimum, we may rewrite equation (7.38) and obtain

$$V(z) = (V_0 + \lambda^T f_0) + \frac{1}{2}\delta z^T \left(V_{zz} + \lambda^t f_{zz}\right)\delta z + \mathcal{O}(\delta z^3) \tag{7.39}$$

We have thus used the process model to eliminate the first order terms in the Taylor series expansion of $V(z)$. Hence, if we use a second order process model, the second order terms will vanish since they are multiplied by zero. It is thus sufficient to use simply a 1st order model for z, i.e.

$$f(x,u) \approx f_x \delta x + f_u \delta u = 0 \tag{7.40}$$

so that

$$\delta z = \begin{bmatrix} \delta x \\ \delta u \end{bmatrix} = \begin{bmatrix} -f_x^{-1} f_u \\ I \end{bmatrix} \delta u = M \delta u \tag{7.41}$$

where I is an identity matrix with same dimensions as u. The overall error using a first order model will then still be of order 3, i.e. $\mathcal{O}(\delta z^3)$, so that the Taylor series expansion of $V(z)$ is still accurate to the 2nd order. Introducing the 1st order model (7.41) into equation (7.39) we obtain

$$V(z) = \left(V_0 + \lambda^T f_0\right) + \frac{1}{2} \delta u^T \left(M^T \mathcal{L}_{zz} M\right) \delta u + \mathcal{O}(\delta z^3) \tag{7.42}$$

Using that $f_0 = 0$, we finally obtain the following expression for $V(z)$ in the vicinity of the optimal solution

$$\delta V = V(z) - V_0 = \frac{1}{2} \delta u^T \left(M^T \mathcal{L}_{zz} M\right) \delta u + \mathcal{O}(\delta z^3) \tag{7.43}$$

However, if the first order term $V_z + \lambda^T f_z$ had not been eliminated, one would have to use a second order process model.

Chapter 8

Parametric Sensitivity in Batch Distillation

Atle C. Christiansen, Elling W. Jacobsen[‡*], John D. Perkins[‡] and Sigurd Skogestad[†]

†Department of Chemical Engineering
University of Trondheim - NTH
N-7034 Trondheim, Norway

‡Center for Process Systems Engineering,
Imperial College of Science and Technology
London SW7 2BY, UK

A preliminary version was presented at
AIChE annual meeting Miami, Nov. 1995, Paper 184d

Abstract

The paper addresses parametric sensitivity in batch distillation processes. By considering the effect of small changes in the operating parameters, e.g., initial conditions, we show that even ideal binary columns may display highly sensitive regions of operation. Through analysis of a general model we determine operating conditions that favor parametric sensitivity and show that parametric sensitivity in general will be most severe in columns operated with reflux or internal reflux ratio as a manipulated input. We also consider the impact of different operating policies, for which we analyze columns operated with constant reflux-ratio and constant distillate composition, respectively. The analytical results are verified through numerical computations for several case studies

*Corresponding author. Present address: S3 – Automatic Control, Royal Institute of Technology – KTH, S–100 44 Stockholm, Sweden, E-mail: jacobsen@s3.kth.se

8.1 Introduction

Batch distillation has become of increasing importance in industry during the last decades. In academia, this is reflected in the large number of articles that have appeared on the optimization of batch distillation operations (see e.g. Sørensen (1994) or Diwekar (1995)). Somewhat surprisingly, however, the fundamental dynamic behavior of batch distillation columns has received relatively little attention in the literature. In particular, few studies attempt to establish qualitative results regarding the dynamic behavior of batch distillation columns. Doherty and Perkins (1978) consider the dynamics of simple distillation with a focus on the behavior close to singular points of the residue map. Singular points here refer to stationary states of the residue curve, i.e., end points of the state trajectory. They show that such points occur only for pure components or azeotropes, and that they are either (unstable) saddles or stable nodes. Dongen and Doherty (1985) attempt to extend these results to multistage batch distillation columns with reflux, and discuss how batch trajectories may be predicted from residue curve maps in the case of azeotropic mixtures. More recently, Davidyan *et al.* (1994) consider the dynamic behavior of batch columns with a middle vessel, and show that such columns have additional singular points which are neither pure components nor azeotropes. These additional singular points are always saddles or unstable nodes, and occur due to additional degrees of freedom compared to conventional columns.

In this paper we study the sensitivity of state trajectories in batch distillation to small changes, or uncertainties, in the operating conditions. If small changes in some parameter, e.g., the initial concentration, produces large changes in the state trajectory, then the system is said to exhibit *parametric sensitivity* (Bilous and Amundson 1956). Understanding the extent and causes of such behavior is important, not the least because operating policies usually are implemented in an open-loop fashion (e.g., Macchietto and Mujtaba (1992)). Thus, there is usually no feedback correction if key outputs diverge from the desired trajectories, and the existence of parametric sensitivity may cause the end-product to deviate significantly from the specifications. It is the aim of this paper to answer whether parametric sensitivity may exist in batch distillation and, if so, which operating conditions that favor such sensitivity.

The paper is organized as follows. First, we introduce the reader to batch distillation and common ways of operating batch columns. We then discuss the analysis of parametric sensitivity for general dynamical systems and critically review some of the criteria employed in studies of parametric sensitivity in batch reactors. The analysis of parametric sensitivity in batch distillation is divided into two parts. We first analyze a model with the common assumption that the control variables, e.g., reflux, are specified in molar units. However, in practice, the control variables are more likely to be specified on a mass or volume basis, and we therefore proceed to analyze this case. Finally, we discuss some practical implications of the derived results and present a complete example for illustration.

8.2 Batch Distillation

Conventional batch distillation columns are usually operated as batch rectifiers or, in some cases, as batch strippers. More recently one has also started looking at alternative designs (see e.g. Hasebe *et al.* (1992),Hasebe *et al.* (1995), Davidyan *et al.* (1994) or Skogestad *et al.* (1997)). In this work, however, we limit ourselves to binary separations in rectifying columns as illustrated in the schematic in Figure 8.1. A typical rectifying column consists of a heated vessel (reboiler) where the liquid

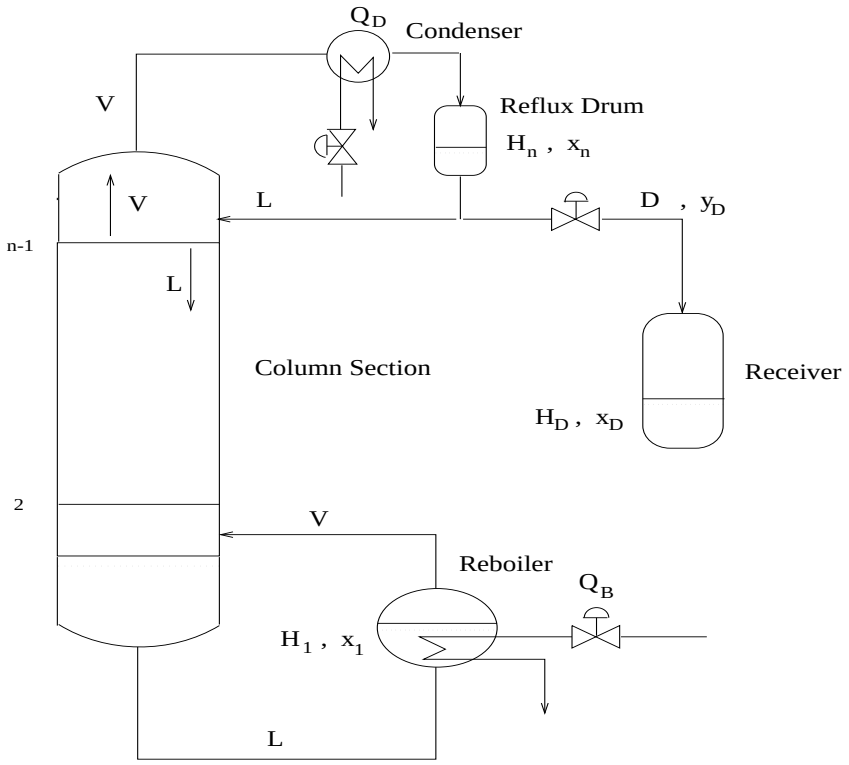

Figure 8.1: Rectifying batch distillation column.

is vaporized, the rectifying section with plates or packed material, the condenser (total or partial) where the vapor leaving the column is condensed, a reflux drum which collects the condensed vapor and one or more receivers (accumulators) where the distillate is collected. Some of the condensed vapor is normally returned to the column (reflux) in order to improve the separation.

Operating policies. Typically, after filling the reboiler with the batch charge, the column is run under total reflux until steady state or to a state where the distillate composition reaches a desired purity. Distillate is then continuously withdrawn ac-

cording to the chosen operating policy, and different cuts are obtained by switching to alternate receivers. The operation is usually performed according to one of the following policies

(1) Constant reflux or reflux ratio, in which case the distillate composition continuously changes as the batch proceeds.

(2) Constant distillate composition, in which case the reflux, or reflux ratio, is continuously changed. Typically, the input profile is computed off-line and then implemented in an open-loop fashion.

(3) Optimal reflux ratio, in which case the input profile is determined by solving an optimization problem, usually off-line. There exist a vast literature on determining the optimal policy in batch distillation, and typical optimization criteria involves amount of distillate of a given purity and distillation time (see e.g. Sørensen (1994), Mujtaba (1989) or Kerkhof and Vissers (1978)).

In all the above policies, it is common practice to assume the boilup V fixed for all times.

In this work we will focus on operating policies (1) and (2). Operating policy (3) is less generic since it depends on the specific optimization criteria chosen. However, since this policy typically involves reflux profiles somewhere in between those of policies (1) and (2), we expect the results derived to be relevant also for this case.

Control configurations. Having determined an operating policy, e.g., in terms of reflux, there are several ways in which the policy may be implemented in practice, depending mainly on the chosen *control configuration*. With a control configuration we understand the manipulated inputs that are available after the level and pressure control system has been configured. For instance, if condenser level is controlled using distillate flow D and pressure is controlled using condensation rate V_T, then reflux L and boilup V are left as free inputs for manipulation, and the configuration is accordingly labeled the *LV-configuration*. Note that it is also possible to use different *combinations* of flows as manipulated variables, e.g. L/D or L/V. Here L/D is the *external reflux ratio* and L/V is the *internal reflux ratio*. For batch distillation columns, the most common configurations are probably the LV-, $(L/V)V$ and $(L/D)V$-configurations. We stress that any given operating policy may be implemented using *any* control configuration through the use of simple transformations. For instance, with the LV–configuration, one may transform a computed policy in terms of reflux ratio L/V into a policy in terms of reflux L.

Specification of flows. In model based studies of distillation column operations, it is usually assumed that all flows, i.e., manipulated variables, may be specified on a molar rate basis, i.e., in [kmol/min]. The main reason for this is probably that it is the molar flows that naturally enters in the model of a distillation column. However, in practice, liquid flows are more likely to be specified on a mass or volume rate basis (Jacobsen and Skogestad 1991). At a first glance this may seem like a trivial difference. However, as shown by Jacobsen and Skogestad (1991), the use of mass or

volume flows may have a significant impact on the behavior of continuous distillation columns. As they show, a column operating with mass or volume flows may display multiple steady states and unstable operating points where a model with molar flows would predict unique and stable solutions. The reason is that the transformation between mass or volume flows and molar flows is nonlinear due to the composition dependence, and may become singular under certain conditions. Based on these results one might expect that the use of mass or volume flows may have a significant impact also on the dynamics of batch distillation columns. Thus, having first analyzed the case with molar flows, we proceed to analyze the effect of using mass flows on parametric sensitivity. The rationale behind analyzing both cases is that we thereby obtain insight into the importance of the choice of units for flows in models of batch distillation units.

Dynamic Model. In this work we analyze a general dynamic model of a binary batch distillation column. The modeling assumptions we employ are

- Binary separation.
- Ideal VLE.
- Theoretical trays.
- Total condenser.
- Constant molar overflow.
- Negligible holdup on the plates and in the condenser.

With these assumptions we obtain a model with only two states, one for reboiler composition and one for reboiler holdup. Such a low order model is convenient for deriving analytical results. However, in order to verify the analytical results we employ simulations with more rigorous models, e.g., including tray holdups.

Material and component balances over the entire column yields the dynamic model

$$\frac{dH_B}{dt} = L - V \tag{8.1}$$

$$\frac{dx_B}{dt} = \frac{L - V}{H_B}(y_D - x_B) \tag{8.2}$$

where H_B is the reboiler holdup and x_B and y_D denote the fraction of light component in the reboiler liquid and distillate flow, respectively. Based on the assumption of negligible tray and condenser holdups, the tray compositions are given by the algebraic equations

$$L(x_{i+1} - x_i) + V(y_{i-1} - y_i) = 0 \; ; \quad i = 2, N \tag{8.3}$$

from which y_D may be computed given L, V and x_B.

For the case of constant relative volatility, α, the vapor composition is given by the VLE equation

$$y_i = \frac{\alpha x_i}{1 + (\alpha - 1)x_i} \tag{8.4}$$

Given this simple two–state model, our objective is to provide insight as to whether batch distillation columns may exhibit parametric sensitivity, and if so, to investigate under what operating conditions sensitivity is likely to be most severe.

8.3 Analysis of Parametric Sensitivity

The analysis of parametric sensitivity involves the analysis of dynamical systems described by ordinary or partial differential equations. We here restrict ourselves to systems described by ordinary differential equations on the general form

$$\begin{gathered} \dot{\mathbf{x}} = f\left(\mathbf{x}, \xi(t), t\right), \quad \mathbf{x}\left(0\right) = \mathbf{x}_0 \\ \mathbf{x} \in \mathcal{R}^n, \xi \in \mathcal{R}^p, f : \mathcal{R}^n \times \mathcal{R}^p \mapsto \mathcal{R}^n \end{gathered} \tag{8.5}$$

where $\mathbf{x}$ denotes the vector of state variables and ξ are the parameters including the control inputs. The solution of (8.5) is conveniently denoted by

$$\mathbf{x}\left(t\right) = \phi\left(t, \xi(t), \mathbf{x_0}\right) \tag{8.6}$$

A sufficient condition for the existence and uniqueness of $\phi\left(t, \xi(t), \mathbf{x}_0\right)$ is that the function f and its first-order derivatives $\partial f/\partial x$ are continuous on the domain considered (see e.g Sansone and Conti (1964)). These conditions are met for any realistic model of a batch distillation process with homogeneous mixtures.

In the analysis of parametric sensitivity we are interested in the sensitivity of a nominal solution $x^*(t) = \phi(t, \xi^*, x_0^*)$ to small perturbations $\delta\xi$ and δx_0 in the parameters ξ and initial conditions x_0, respectively. In the linear approximation, the perturbation $\delta x(t)$ of the nominal trajectory is given by solving the *linear time–varying* (LTV) differential equation

$$\dot{\delta\mathbf{x}} = A(t)\delta\mathbf{x} + B(t)\delta\xi; \quad \delta\mathbf{x}\left(0\right) = \delta\mathbf{x}_0 \tag{8.7}$$

with $A(t) = \partial f/\partial x$ and $B(t) = \partial f/\partial\xi$ evaluated along the nominal trajectory $x^*(t)$. If $||\delta x(t)||$ in some sense becomes large for some t and small $||\delta\xi||$ or $||\delta x_0||$, the system is said to exhibit parametric sensitivity (e.g., Bilous and Amundson (1956), Vajda and Rabitz (1992) and Vajda and Rabitz (1993)). Thus, the definition of parametric sensitivity is qualitative rather than quantitative.

Since, in the general case, an analytical solution does not exist for (8.7), the *sensitivity functions* $\delta x(t)/\delta\xi$ and $\delta x(t)/\delta x_0$ must be computed numerically for specific examples. The sensitivity function for perturbations in the initial state x_0 is given by the solution of the first variational equation

$$\dot{\delta\mathbf{x}} = A(t)\delta\mathbf{x}; \quad \delta\mathbf{x}\left(0\right) = \delta\mathbf{x}_0 \tag{8.8}$$

A general solution is given by

$$\delta \mathbf{x}(t) = \phi\,(t, t_0)\,\delta \mathbf{x}_0 \tag{8.9}$$

Here the *transition matrix* $\phi(t, t_0)$ is given by

$$\phi\,(t, t_0) = \mathbf{F}(t, t_0)\mathbf{F}(t_0, t_0)^{-1} \tag{8.10}$$

where $\mathbf{F}\,(t, t_0)$ is a solution of the matrix differential equation

$$\dot{\mathbf{F}}\,(t) = A\,(t)\,\mathbf{F}(t, t_0) \tag{8.11}$$

with the initial condition $\mathbf{F}\,(t_0, t_0)$ being any non-singular matrix.

Using the transition matrix, one may also compute the sensitivity function for perturbations in the parameters ξ

$$\delta \mathbf{x}(t) = \int_{t_0}^{t} \phi(t, \tau) B(\tau) \delta\xi\, d\tau \tag{8.12}$$

Thus, sensitivity to changes in the parameters is directly related to the sensitivity to changes in the initial conditions. We will in this work therefore focus on sensitivity to initial conditions, which depend on the properties of the Jacobian $A(t)$ only.

It is sometimes assumed that the transition matrix $\phi(t, t_0)$ may be approximated by the matrix exponential of the *integral* of A (e.g.,Bilous and Amundson (1956), Douglas (1972)), i.e.,

$$exp\left[\int_{t_0}^{t} A(\tau) d\tau\right] \tag{8.13}$$

However, the *integral solution* (8.13) is correct only if the Jacobian matrices $A(t_1)$ and $A(t_2)$ commute, i.e. $A(t_1)A(t_2) = A(t_2)A(t_1)\ \forall t_1, t_2$. This is a rather severe requirement which, except for in the scalar case, is rarely satisfied for time–varying systems (see e.g. Wiberg (1972)). By comparing the solution of (8.13) with the transition matrix for a number of examples, we find that the integral solution may produce large errors, and thus contradictive results for the sensitivity functions.

An important issue in the present work is to determine under which operating conditions parametric sensitivity is favored in batch distillation. Although some insight may be gained from numerical case studies, it is hard to draw general conclusions based on specific examples. Hence, instead of resorting to numerous and time consuming simulations, we will consider simple indicators of parametric sensitivity that may be evaluated analytically. Computation of sensitivity functions for specific examples will be performed only in order to partly confirm the analytical results.

Eigenvalues as indicators of sensitivity. By considering the linear system (8.7), we recognize that one particular situation in which to expect parametric sensitivity, is when the nominal trajectory is locally unstable, i.e., when the perturbation $\delta x(t)$ grows exponentially on some time-interval for small perturbations δx_0. If the Jacobian $A(t)$ is constant, the existence of at least one RHP eigenvalue, i.e., with positive real

part, provides a necessary and sufficient condition for local instability. However, in studies of parametric sensitivity, $A(t)$ is generally time–varying. In this case an eigenvalue analysis can not be used to determine neither necessary nor sufficient conditions for local instability, as is erroneously claimed in some studies of parametric sensitivity in chemical reactors (e.g., Vajda and Rabitz (1992) and Vajda and Rabitz (1993)). The only exception is for scalar systems, where the eigenvalue plays a similar role as in time-invariant systems. For time-varying systems with more than one state, the sensitivity functions may decay for all times despite the existence of RHP eigenvalues (Sansone and Conti 1964). Similarly, it is known that systems with only LHP eigenvalues for all times may have exponentially growing sensitivity functions (Wiberg 1972). It is important, however, to note that all such examples involve systems in which the elements of $A(t)$ vary rapidly. Indeed, if the derivatives of the elements of $A(t)$ are bounded below some limit, then stability of (8.7) may be decided based on consideration of the eigenvalues (Rosenbrock 1963). Thus, it seems reasonable to assume that the existence of RHP eigenvalues in $A(t)$ usually will serve as a strong *indicator* of parametric sensitivity.

Sufficient conditions for sensitivity. All existing necessary and sufficient conditions for the stability, or equivalently instability, of (8.7) require the knowledge of the transition matrix (8.10), which in general must be computed numerically (Willems 1970). However, a number of sufficient conditions for stability and instability, based on properties of the Jacobian $A(t)$, are available. Most of these are potentially highly conservative (Willems 1970). However, a sufficient condition for instability of (8.7) is (Willems 1970)

$$\lim_{t\to\infty} \int_{t_0}^{t} trA(\tau)d\tau = \infty \tag{8.14}$$

This condition is based on the relation

$$det[\phi(t,t_0)] = exp\left[\int_{t_0}^{t} trA(\tau)d\tau\right] \tag{8.15}$$

Thus, if a perturbation in some or all of the system states is introduced at t_0, a positive trace of the Jacobian for $t > t_0$ acts as a sufficient condition for local growth of some or all of the sensitivity functions on some time interval $t > t_0$. Note that the trace of a matrix equal the sum of its eigenvalues, i.e.,

$$trA = \sum_{i=1}^{n} \lambda_i \tag{8.16}$$

and that a positive trace therefore always implies at least one eigenvalue with a positive real part, while the opposite is not necessarily true.

In conclusion, it is not possible to derive exact analytical conditions for the existence of parametric sensitivity in general dynamical systems. However, strong indicators of parametric sensitivity, which may be evaluated analytically, include the eigenvalues and the trace of the Jacobian $A(t)$. We have in this work chosen to base our analysis on these indicators.

8.4 Parametric Sensitivity in Batch Distillation

8.4.1 LV–, $(L/V)V$– and $(L/D)V$–configurations

In this section we make the common assumption that all flows may be fixed on a molar rate basis and analyze the LV–, $(L/V)V$– and $(L/D)V$– configurations. These are all common control configurations in batch distillation practice. Since the transformation between the different configurations are independent of the states, under the assumption of molar rate inputs, the parametric sensitivity is independent of the specific choice of configuration. We therefore refer only to the LV–configuration below.

Analytical Treatment. As a first step in the analysis of parametric sensitivity we linearize the model (8.1) – (8.2) along some nominal trajectory to obtain a LTV model in terms of the perturbed state $\delta x(t)$

$$\dot{\delta x} = A(t)\delta x(t) + B(t)\delta\xi(t) \tag{8.17}$$

With the LV-configuration, the Jacobian is given by

$$A^{LV}(t) = \begin{bmatrix} 0 & 0 \\ \frac{V-L}{H_B^2}(y_D - x_B) & \frac{V-L}{H_B}\left(1 - \left(\frac{\partial y_D}{\partial x_B}\right)_L\right) \end{bmatrix} \tag{8.18}$$

The input matrix $B^{LV}(t)$ will depend on the specific parameters considered. However, as noted previously, the existence of parametric sensitivity or, equivalently, exponential growth of $\delta x(t)$, depends on properties of the Jacobian $A(t)$ only. The properties of the parameter matrix $B(t)$ will only affect the extent of the potential sensitivity. We therefore restrict our analysis to consider properties of the Jacobian $A^{LV}(t)$ only.

In order to determine the possible existence of parametric sensitivity we consider the eigenvalues and the trace of the Jacobian $A^{LV}(t)$. Recall that eigenvalues with a positive real part serves as an indicator of parametric sensitivity while a positive trace of $A^{LV}(t)$ is a sufficient condition for local growth of at least one sensitivity function. The eigenvalues of $A^{LV}(t)$ (8.18) are given by

$$\lambda_1^{LV}(t) = 0\ ; \qquad \lambda_2^{LV}(t) = \frac{V-L}{H_B}\left(1 - \left(\frac{\partial y_D}{\partial x_B}\right)_L\right) \tag{8.19}$$

Thus, one eigenvalue is zero for all times, which is explained by the integrating nature of the holdup H_B. Furthermore, the structure of the Jacobian (8.18) reveals that the eigenvalue λ_2^{LV} affects the composition x_B only. The trace of $A^{LV}(t)$ is given by

$$trA^{LV}(t) = \lambda_1^{LV}(t) + \lambda_2^{LV}(t) = \lambda_2^{LV}(t) \tag{8.20}$$

In this case a positive eigenvalue $\lambda_2^{LV}(t)$ is hence a *sufficient* condition for local exponential growth of the sensitivity function for x_B.

Since $(V - L) \geq 0$ at all times, we derive from (8.19) the necessary and sufficient condition for a positive eigenvalue λ_2^{LV}

$$\lambda_2^{LV} > 0 \text{ iff } \left(\frac{\partial y_D}{\partial x_B}\right)_L < 1 \tag{8.21}$$

In order to understand under which operating conditions (8.21) is satisfied, we derive below expressions for the partial derivative $(\partial y_D/\partial x_B)_L$.

Simple distillation. We first consider the simplest case with only a single equilibrium stage, the reboiler, and no reflux, i.e., *simple distillation*. For this case we have

$$\frac{y_D/(1-y_D)}{x_B/(1-x_B)} = \alpha \tag{8.22}$$

where α is the relative volatility. Differentiation of (8.22) with respect to x_B, assuming α constant, yields

$$\left(\frac{\partial y_D}{\partial x_B}\right)_L = \frac{\alpha}{(1+(\alpha-1)x_B)^2} = \frac{y_D(1-y_D)}{x_B(1-x_B)} \tag{8.23}$$

and the condition for a positive eigenvalue (8.21) becomes

$$x_B > \frac{1}{\sqrt{\alpha}+1} \tag{8.24}$$

or, equivalently,

$$y_D > 1 - x_B \tag{8.25}$$

From (8.19) we have that the positive eigenvalue is largest when $(\partial y_D/\partial x_B)_L$ is small. Based on (8.23) and (8.24) we thus conclude that, in the case of simple distillation, parametric sensitivity is most likely to occur when the reboiler is rich in light component and the relative volatility is large, or equivalently, when the distillate is of high purity relative to the reboiler composition.

In order to illustrate the results derived above we show in Figure 8.2 numerical results for a simple distillation process of a mixture with relative volatility $\alpha = 10$, boilup $V = 1.0$ $[kmol/min]$, initial holdup $H_{B0} = 100$ and initial composition $x_{B0} = 0.75$.

As expected, the largest eigenvalue is positive during the first period of the batch, i.e., for $t \in [0, 74.4]$ min, corresponding to the period for which $x_B > 1/(\sqrt{10}+1) = 0.24$, or equivalently, $y_D > 0.76$. We also see that the positive eigenvalue grows over some time interval, despite the fact that $(\partial y_D/\partial x_B)_L$ increases as y_D and x_B decreases. This is explained by the fact that the holdup H_B is steadily decreasing, thereby increasing the magnitude of the eigenvalue according to (8.19). From Figure 8.2 we also see that the sensitivity $\partial x_B/\partial x_{B0}$ increases over the time interval where the eigenvalue is positive. However, the peak of the sensitivity is moderate with a value of approximately 2.4. The interpretation of the sensitivity function is that a perturbation of 0.01 in the initial concentration x_{B0} will increase to a maximum deviation of 0.024 in $x_B(t)$.

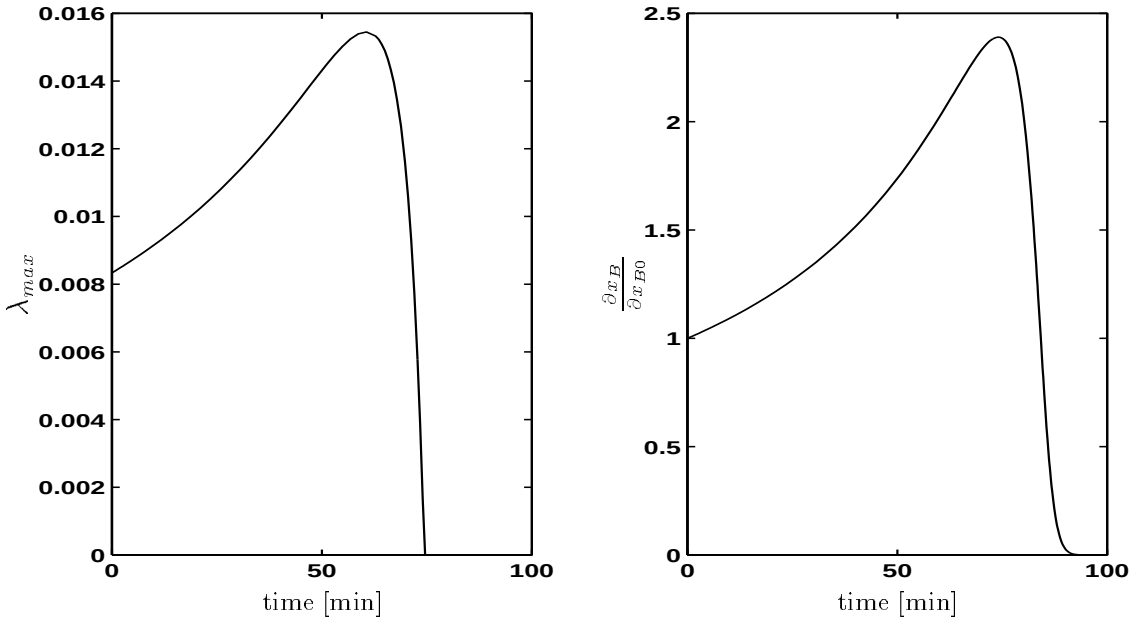

Figure 8.2: Maximum eigenvalue of Jacobian $A(t)$ and sensitivity function for x_B for simple distillation column.

Multistage Columns. We next turn to multistage columns with reflux. For this case the *Separation factor*

$$S = \frac{y_D/(1-y_D)}{x_B/(1-x_B)} \tag{8.26}$$

plays much the same role as the relative volatility α in the single stage case. The separation factor S usually varies only slightly with varying operating conditions and may thus be assumed constant under small perturbations in x_B. Differentiating (8.26) with respect to x_B, assuming S constant, yields

$$\left(\frac{\partial y_D}{\partial x_B}\right)_L = \frac{y_D(1-y_D)}{x_B(1-x_B)} \tag{8.27}$$

[The exact expression when S is not constant is

$$\left(\frac{\partial y_D}{\partial x_B}\right)_L = \frac{y_D(1-y_D)}{x_B(1-x_B)}\left[1 + \frac{x_B(1-y_D)}{y_D}\left(\frac{\partial S}{\partial x_B}\right)_L\right] \tag{8.28}$$

and we see that the contribution from $(\partial S/\partial x_B)_L$ becomes negligible when either the reboiler or the distillate is of high purity, i.e., $x_B \approx 0$ or $y_D \approx 1$.]. From (8.19) and (8.27) we get that the largest eigenvalue is positive when

$$x_B > \frac{1}{\sqrt{S}+1} \quad \Leftrightarrow \quad y_D > 1 - x_B \tag{8.29}$$

Thus, like for the case of simple distillation, we conclude that parametric sensitivity is likely to be most severe under the following conditions

- The reboiler is rich in light component, i.e., during the first period of the batch.
- The separation factor is large.

  or, equivalently, when

- The distillate is of high purity relative to the reboiler composition.

The main difference between simple distillation and multistage distillation is that the compositions, and hence the gain $(\partial y_D/\partial x_B)_L$ according to (8.27), may change more drastically in the latter case. In particular, for sharp separations with a constant reflux policy, the distillate composition y_D is typically close to 1 until the reboiler is almost depleted in light component, in which y_D abruptly drops to almost 0. If we denote the time when y_D starts to drop by t^*, we may use the following approximations for the maximum eigenvalue (8.19)

$$\begin{array}{lllll} t < t^*: & y_D \simeq 1 & \Rightarrow & \partial y_D/\partial x_B \simeq 0 & \Rightarrow \quad \lambda_2^{LV} \simeq (V-L)/H_B \\ t > t^*: & y_D \simeq 0 & \Rightarrow & \partial y_D/\partial x_B > 1 & \Rightarrow \quad \lambda_2^{LV} < 0 \end{array} \tag{8.30}$$

Thus, for sharp separations with the constant reflux policy, one should expect parametric sensitivity to exist throughout almost the whole period in which the light product is drawn off.

For separations with a constant distillate composition policy, it is seen from (8.27) that the gain $(\partial y_D/\partial x_B)_L$ decreases with an increasing y_D and thus the maximum eigenvalue (8.19) will expectedly be larger for higher purity separations. The criterion $y_D > 1-x_B$ for a positive eigenvalue is also likely to be satisfied for a larger fraction of the distillation time for higher purity separations. Thus, parametric sensitivity should increase with increasing distillate purity for separations according to the constant distillate composition policy.

Note from the expression for the eigenvalue $\lambda_2^{LV}(t)$ (8.19) that the magnitude of the positive eigenvalue will depend on the size of the distillate flow $D = V-L$ and reboiler holdup H_B. The effect of increasing D and decreasing H_B is to increase the magnitude of the eigenvalue. Thus, it might appear that parametric sensitivity depends strongly on the size of D and the initial holdup H_{B0}. However, this is somewhat misleading since an increase in D, or a decrease in H_{B0}, in general will reduce the time for which the distillate is of high purity and thus the time for which a positive eigenvalue exist. In the examples below we introduce a scaled eigenvalue which essentially is independent of D and H_{B0}.

Numerical Examples In order to verify the analytical results derived above, we consider here some numerical examples. Data for the base case column we consider are given in Table 8.1. Two different levels of separation are considered, one with intermediate purity of the final collected distillate, $x_{Ds} = 0.95$, and one with relatively

Table 8.1: Data for *base case* column

Number of trays :	$N = 8$ + total condenser
Molar Boilup :	$V = 5.0\ [kmol/min]$
Relative volatility :	$\alpha = 4$
Molar weight of light component :	$M_1 = 20\ [kg/kmol]$
Molar weight of heavy component :	$M_2 = 40\ [kg/kmol]$
Initial composition in reboiler :	$x_{B0} = 0.5$
Initial amount in reboiler :	$H_{B0} = 100\ kmol$
Final amount of collected distillate:	$H_{Ds} = 50\ kmol$
Final collected distillate composition:	$x_{Ds} = 0.95$ / $x_{Ds} = 0.99$

high purity, $x_{Ds} = 0.99$. In both cases the final amount of collected distillate is specified to be $H_{Ds} = 50\ kmol$. We first consider operation according to the constant reflux policy, i.e., constant L, after which we present results for the constant distillate composition policy using a precomputed reflux profile $L(t)$.

Since the length of the production period, t_{final}, will vary significantly from case to case, we introduce a dimensionless time $\tau = t/t_{final}$ in order to facilitate comparisons of the results. The eigenvalues are scaled accordingly so that $\bar{\lambda} = \lambda\ t_{final}$.

Constant Reflux Policy. The distillate composition profiles for the two separations, corresponding to $x_{Ds} = 0.95$ ($L = 3.433\ kmol/min$, $t_{final} = 31.91\ min$) and $x_{Ds} = 0.99$ ($L = 4.616\ kmol/min$, $t_{final} = 130.21\ min$), respectively, are shown in Figure 8.3. From the figure we see that in both cases the distillate composition stays close to 1 for a prolonged period of time before dropping down to a relatively low value. The transition from high purity to low purity distillate is seen to be more abrupt for the high-purity separation as discussed for sharp separations above.

The maximum (scaled) eigenvalue $\bar{\lambda}_{max}$ for the two cases are shown in Figure 8.3 and we see that in both cases the eigenvalue is positive during the period for which the distillate has high purity, i.e., where y_D is close to 1. This is as expected from the analysis above. From (8.19) we have that the maximum scaled eigenvalue during the period when $y_D \approx 1$ is

$$\bar{\lambda}_{max}(\tau) \approx \frac{D(\tau)}{H_B(\tau)} t_{final} = \frac{H_{Ds}}{H_B(\tau)} \tag{8.31}$$

Thus, the scaled eigenvalue is the same for both separations initially and increases with time due to the decrease in $H_B(\tau)$. The eigenvalue peaks at a larger value for the higher purity separation, $x_{Ds} = 0.99$, due to the fact that the distillate purity stays close to 1 for a larger fraction of the production period.

The sensitivity functions $\partial x_B/\partial x_{B0}$ are also shown in Figure 8.3, and we see that the sensitivity functions grow during the period for which there exist a positive eigenvalue. Since the higher purity separation, $x_{Ds} = 0.99$, has a larger eigenvalue for a longer period of time, the sensitivity function peaks at a higher value for this case. The size of the sensitivity functions are, however, moderate in both cases with a peak of

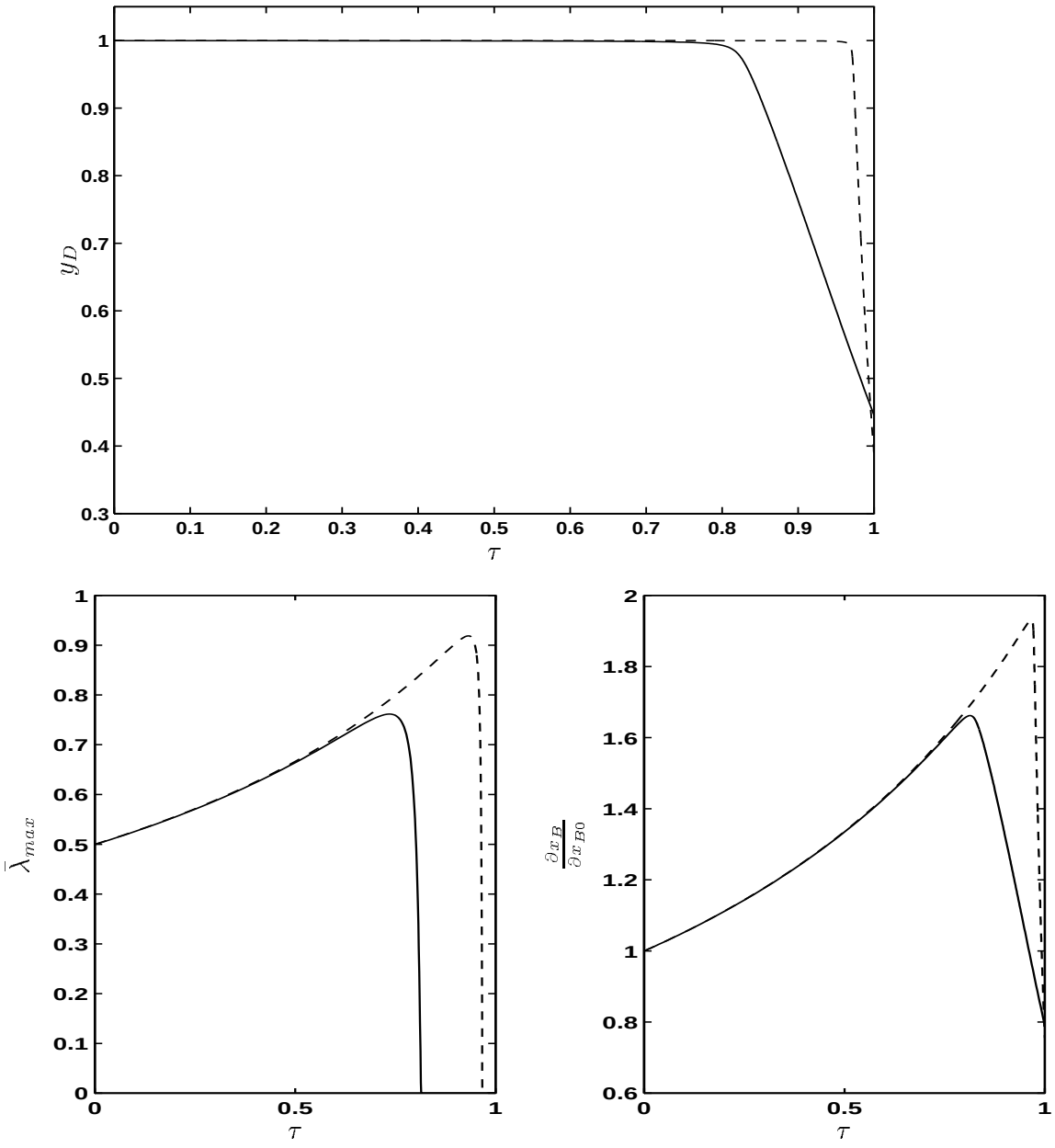

Figure 8.3: Distillate composition profiles and corresponding maximum scaled eigenvalues and sensitivity functions for columns in Table 8.1 with constant reflux policy. Solid line - $x_{Ds} = 0.95$, dashed line - $x_{Ds} = 0.99$.

approximately 1.65 and 1.95, respectively.

We next consider the effect of changing the initial concentration x_{B0} and the relative volatility α, respectively, on the parametric sensitivity. In both cases we consider the separation corresponding to $x_{Ds} = 0.99$. The final amount of collected distillate is specified as $H_{Ds} = H_{B0}x_{B0}$, i.e., the recovery is the same in all cases. In the first case we increase α from 4 to 8, while in the second case we increase x_{B0} from 0.5 to 0.75. The resulting distillate composition profiles are shown together with the base case profile in Figure 8.4. As seen from the Figure, the profile $y_D(\tau)$ is almost unaffected by the changes in α and x_{B0}. This is explained by the fact that, in each case, the area under the profile $y_D(\tau)$ should equal $x_{Ds} = 0.99$, and since all separations are sharp, the profiles become almost identical. The effect on the eigenvalues may therefore be derived from (8.31). Since changing α has no effect on H_{Ds} and $H_B(\tau)$, the maximum scaled eigenvalue, and hence the sensitivity, is almost unaffected. This is confirmed by the numerical results in Figure 8.4, i.e., the maximum scaled eigenvalues and sensitivity function for $\alpha = 4$ and $\alpha = 8$ are almost indistinguishable. The main effect of increasing α, with x_{Ds} and H_{Ds} given, is to decrease the required distillation time t_{final}. The main effect of increasing x_{B0} is to increase H_{Ds} while simultaneously decreasing $H_B(\tau)$, thus increasing the magnitude of the positive eigenvalue according to (8.31). Note that decreasing $H_B(\tau)$ is a result of the scaling and thus applies only to this case, where have $H_B(\tau) = H_B(0) + \tau(H_B(1) - H_B(0))$. In the nominal case we thus have $H_B(1) = H_B(0) - H_B(0)x_B(0)$ so that $\partial H_B/\partial tau = -H_{B0}x_{B0}$. This is confirmed by the numerical results in Figure 8.4.

Constant Distillate Composition Policy. We next consider operation corresponding to a constant distillate composition y_D, in which the required reflux profile $L(t)$ is assumed to be implemented in open loop. Figure 8.5 shows the maximum eigenvalue and sensitivity function for the separations corresponding to $x_{Ds} = 0.95$ ($t_{final} = 21.96$) and $x_{Ds} = 0.99$ ($t_{final} = 30.36$), respectively. From the figure we see that positive eigenvalues are displayed in both cases. As expected from the analysis above, the higher purity separation has a larger eigenvalue which furthermore is positive for a larger fraction of the production period, resulting in a larger sensitivity. By comparing the results for constant y_D with those for constant L, we see that the eigenvalues are positive for a shorter period of the batch and furthermore have smaller magnitudes. This results in a smaller sensitivity for the case with constant y_D compared to the case with constant L.

In conclusion, we have shown both by analytical results and numerical simulations that batch distillation columns with flows specified on a molar rate basis may display parametric sensitivity. The sensitivity is most likely to occur when the distillate is of high purity and the reboiler is rich in light component. The sensitivities found in the numerical examples may appear small and insignificant. However, note that we, in order to illustrate the presence of parametric sensitivity and its dependence on operating conditions, have restricted ourselves to consider the sensitivity of the absolute reboiler composition to changes in initial conditions only. In practice, the sensitivity relative to the absolute purity, e.g., $\partial x_B/x_B$, will be more relevant. Furthermore, sensitivities of other key variables like the accumulated distillate composition x_D will

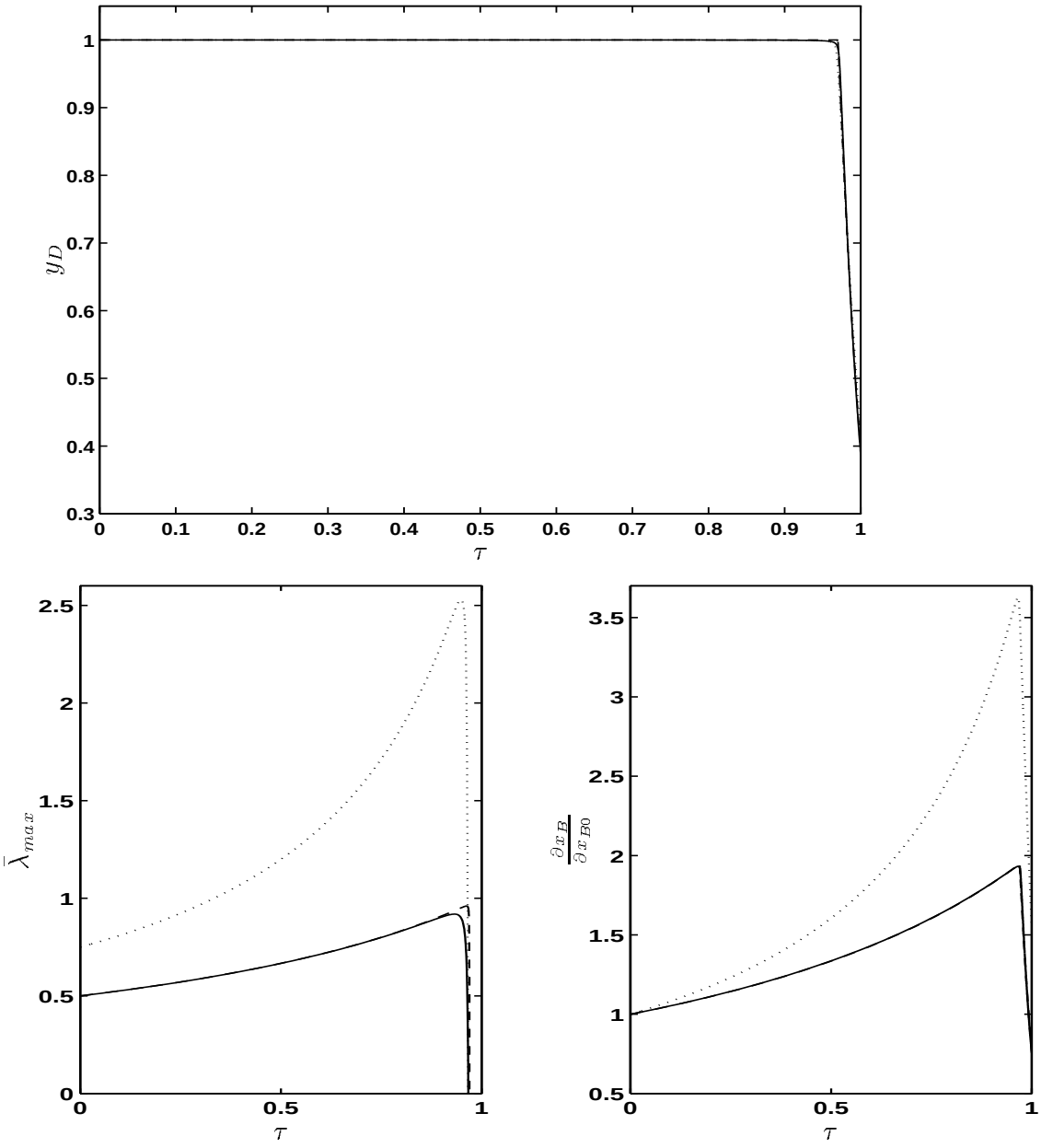

Figure 8.4: Effect of changes in relative volatility α and initial composition x_{B0} for separation with $x_{Ds} = 0.99$ and constant reflux policy. Solid line - nominal, dashed line - $\alpha = 8$, dotted line - $x_{B0} = 0.75$.

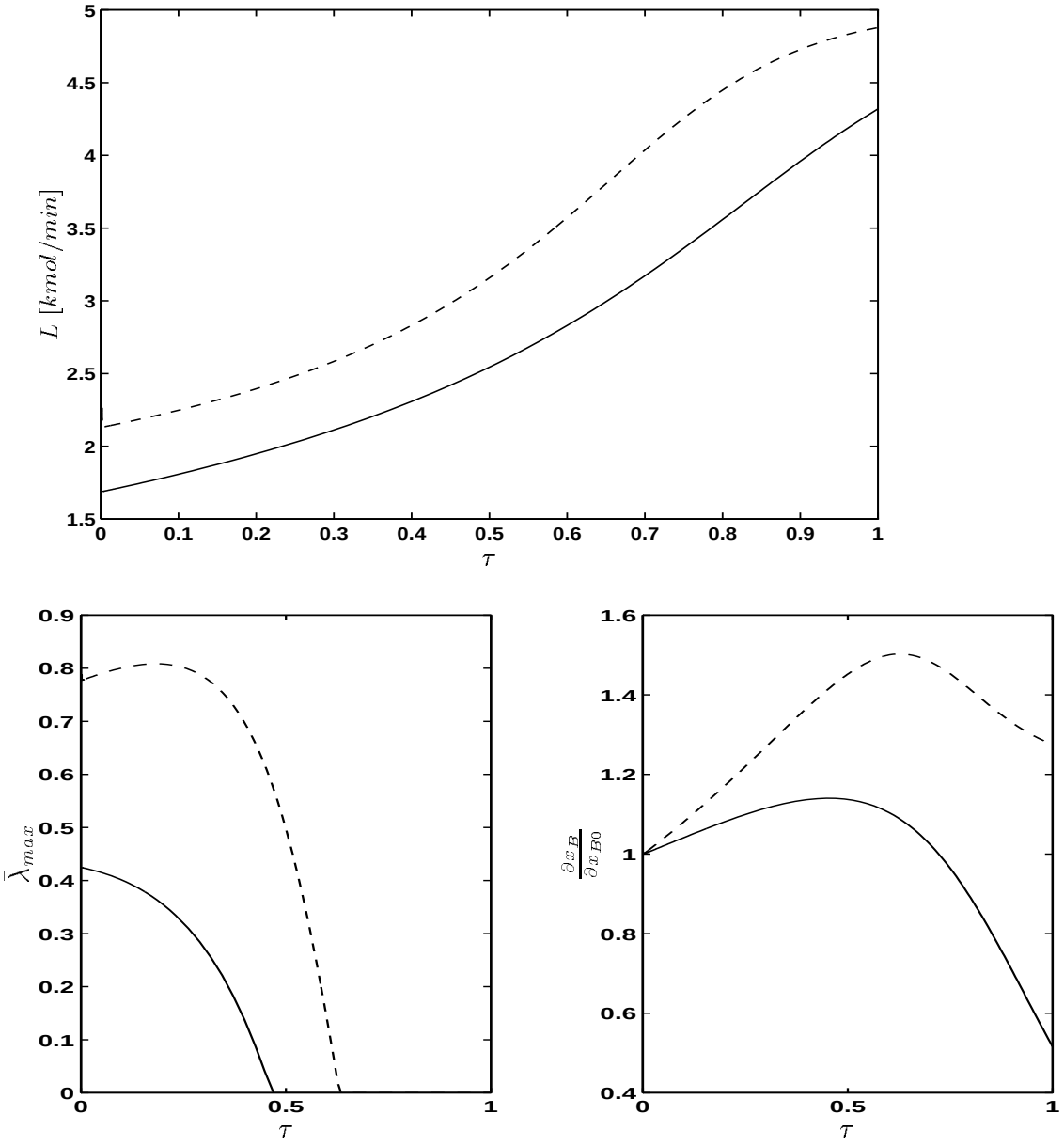

Figure 8.5: Reflux profiles and corresponding maximum scaled eigenvalues and sensitivity functions for columns in Table 8.1 with constant distillate composition policy. Solid line - $x_{Ds} = 0.95$, dashed line - $x_{Ds} = 0.99$.

be of interest. In a detailed case study at the end of the paper we consider the sensitivity of all key variables to changes in several key operating parameters and show that the sensitivity in practice may become severe.

8.4.2 L_wV– and $(L_w/V)V$—configurations

We here consider the case where the *liquid* flows are given on a mass rate basis, i.e., L_w and D_w in $[kg/min]$[1], which applies to most industrial batch columns (Jacobsen and Skogestad 1991). We assume, however, that the boilup V may be fixed on a molar rate basis. This is a reasonable assumption since the boilup usually is determined by fixing the heat input Q_B, which corresponds to fixing V if we assume the heat of vaporization to be independent of composition (Jacobsen and Skogestad 1991). Note that the choice of units for the flows has no implications for the $(L_w/D_w)V$-configuration when there is a total condenser and the distillate flow D_w and reflux L_w are given in the same units. Thus, in most cases the results presented above for the case of molar flow units applies also to the $(L_w/D_w)V$-configuration, i.e., operation with *external reflux ratio* as an independent input. We furthermore note that there is no difference between the $(Lw/V)V$- and L_wV-configuration since we assume boilup V fixed, that is, fixing L_w/V corresponds to fixing L_w. Thus, in the following we refer to the L_wV–configuration only.

Analytical treatment. The dynamic model with the L_wV-configuration is the same as for the LV-configuration, i.e., (8.1) and (8.2). However, since we now specify the reflux on a mass basis, the molar reflux L becomes dependent on the distillate composition according to the transformation

$$L = \frac{L_w}{M}, \quad M = y_D M_1 + (1 - y_D) M_2 \tag{8.32}$$

Here M_1 and M_2 denote the molecular weight of the most volatile and least volatile component, respectively. Note that the transformation is nonlinear and introduces a feedback from the distillate composition y_D to the molar reflux L. The feedback is positive when $M_2 > M_1$, i.e., when the least volatile component has the larger molecular weight, which applies to most mixtures. Due to the nonlinear positive feedback effect one might expect the transformation (8.32) to have a significant impact on the parametric sensitivity of batch distillation columns.

The Jacobian of the dynamic model (8.1), (8.2) and (8.32) linearized about a nominal trajectory becomes

$$A^{L_wV}(t) = \begin{bmatrix} 0 & \left(\frac{\partial L}{\partial x_B}\right)_{L_w} \\ \frac{V-L}{H_B^2}(y_D - x_B) & \frac{(V-L)\left(1-\left(\frac{\partial y_D}{\partial x_B}\right)_{L_w}\right) - \left(\frac{\partial L}{\partial x_B}\right)_{L_w}(x_B - y_D)}{H_B} \end{bmatrix} \tag{8.33}$$

[1] Similar results are obtained if we instead consider volumetric flows

Here

$$\left(\frac{\partial L}{\partial x_B}\right)_{L_w} = L\frac{M_2 - M_1}{M}\left(\frac{\partial y_D}{\partial x_B}\right)_{L_w} \tag{8.34}$$

and

$$\left(\frac{\partial y_D}{\partial x_B}\right)_{L_w} = \frac{\left(\frac{\partial y_D}{\partial x_B}\right)_L}{1 - L\frac{M_2 - M_1}{M}\left(\frac{\partial y_D}{\partial L}\right)_{x_B}} \tag{8.35}$$

Note from (8.33) that, since the molar flows now depend on the compositions through (8.32), the holdup is no longer a pure integrator and hence parametric sensitivity will affect holdup as well as composition. The expressions for the eigenvalues and trace of the Jacobian become significantly more involved in this case compared to those obtained for the LV-configuration. In order to obtain some insight into the effect of using mass flows on parametric sensitivity we will therefore first consider a one-stage column before proceeding to the multistage case.

One-Stage Column with Reflux. We consider a one-stage column with reflux. Obviously, such a column would never be operated in practice since the reflux has no effect on separation and therefore simply wastes energy. Nevertheless, we consider it here to illustrate the effect of using mass flows on parametric sensitivity.

The fact that reflux has no effect on separation implies that $(\partial y_D/\partial L)_{x_B} = 0$ in (8.35), and hence $(\partial y_D/\partial x_B)_{L_w} = (\partial y_D/\partial x_B)_L$. The Jacobian (8.33) thus becomes

$$A^{L_w V}(t) = \begin{bmatrix} 0 & L\frac{M_2 - M_1}{M}\left(\frac{\partial y_D}{\partial x_B}\right)_L \\ \frac{V-L}{H_B^2}(y_D - x_B) & \frac{(V-L)\left(1-\left(\frac{\partial y_D}{\partial x_B}\right)_L\right) + L\frac{M_2-M_1}{M}\left(\frac{\partial y_D}{\partial x_B}\right)_L (y_D - x_B)}{H_B} \end{bmatrix} \tag{8.36}$$

Since the analytical expressions for the eigenvalues become rather complicated, we make use of the fact that the eigenvalues for a 2×2 matrix may be expressed in terms of the trace and determinant according to

$$\lambda_{1,2} = \frac{trA \pm \sqrt{(trA)^2 - 4detA}}{2} \tag{8.37}$$

We easily deduce from (8.37) that $A(t)$ has at least one RHP eigenvalue when $detA < 0$ and/or $trA > 0$.

We first consider under which conditions the determinant of $A^{L_w V}(t)$ is negative, in which the Jacobian has a single positive eigenvalue. From (8.36) we derive

$$detA^{L_w V}(t) = -\frac{V - L}{H_B^2}(y_D - x_B)L\frac{M_2 - M_1}{M}\left(\frac{\partial y_D}{\partial x_B}\right)_L \tag{8.38}$$

From (8.38) it is easily deduced that, provided $M_2 > M_1$, i.e., the least volatile component has the larger molecular weight, $detA^{L_w V}(t)$ is negative at all times. Thus, with mass reflux and $M_2 > M_1$, the one-stage column displays one RHP eigenvalue, and thus potential parametric sensitivity, throughout the production period.

We next consider the trace of $A^{L_wV}(t)$, which from (8.36) becomes

$$trA^{L_wV}(t) = \frac{1}{H_B}\left[(V-L)\left(1-\left(\frac{\partial y_D}{\partial x_B}\right)_L\right) + L\frac{M_2-M_1}{M}\left(\frac{\partial y_D}{\partial x_B}\right)_L (y_D - x_B)\right] \tag{8.39}$$

Comparing (8.39) with the expression for the trace of $A(t)$ for the LV-configuration (8.20) we see that we may write

$$trA^{L_wV} = trA^{LV} + L\frac{y_D - x_B}{H_B}\frac{M_2-M_1}{M}\left(\frac{\partial y_D}{\partial x_B}\right)_L \tag{8.40}$$

Thus, trA^{L_wV} is always larger than trA^{LV} if $M_2 > M_1$, implying that we should expect larger sensitivity with the L_wV-configuration than with the LV-configuration.

We next consider operating conditions that favor parametric sensitivity with the L_wV-configuration. From (8.38) and (8.40) it is seen that increasing L while keeping $(L-V)$ constant, i.e., increasing the internal flows, increases trA^{L_wV} while decreasing $detA^{L_wV}$, which implies that the magnitude of the positive eigenvalue increases. Increasing the difference in molecular weights, i.e., increasing M_2/M_1, is seen to have the same effect. Thus, increasing the internal flows and the difference in molecular weights should generally increase the parametric sensitivity throughout the production period. The other parameters in (8.38) and (8.40) will vary significantly during the production period. The gain $(\partial y_D/\partial x_B)_L$ is typically close to 0 initially and thus $trA^{L_wV} \approx trA^{LV}$ and $detA^{L_wV} \approx detA^{LV} = 0$, i.e., the effect of using mass flows is typically negligible during the first period of the batch. However, as the batch proceeds, and x_B decreases, $(\partial y_D/\partial x_B)$ increases according to (8.23). As this gain exceeds 1 at some point, i.e., when $y_D = 1 - x_B$, trA^{LV} becomes negative and the effect of using mass reflux becomes significant as seen from (8.38) and (8.40). The size of this effect is proportional to the difference in purity between top and bottom $(y_D - x_B)$, which reaches a maximum for some intermediate purity in the top. Thus, we conclude that parametric sensitivity with the L_wV-configuration is likely to be most severe under the following conditions

- Large internal flows, i.e., large L/V.
- Large difference in molecular weights, i.e., large M_2/M_1.
- Similar purities in the top and bottom, i.e., $y_D \approx 1 - x_B$.

We illustrate the results above through numerical computations of a one-stage distillation column with $\alpha = 10$, $x_{B0} = 0.75$, $H_{B0} = 100.0\ kmol$, $M_1 = 20.0\ kg/kmol$ and $M_2 = 40.0\ kg/kmol$. We first consider fixing the boilup at $V = 5.0\ kmol/min$ and the mass reflux at $L_w = 82.58\ kg/min$, corresponding to an initial distillate flow rate $D(0) = 1.0\ kmol/min$. The resulting maximum eigenvalue $\bar{\lambda}_{max}$ and sensitivity function $\partial x_B/\partial x_{B0}$ are shown together with the corresponding results for the LV-configuration with $L = 4.0\ kmol/min$ $(D = 1.0\ kmol/min)$, in Figure 8.6. From the figure we see that, initially, the difference between the LV- and L_wV-

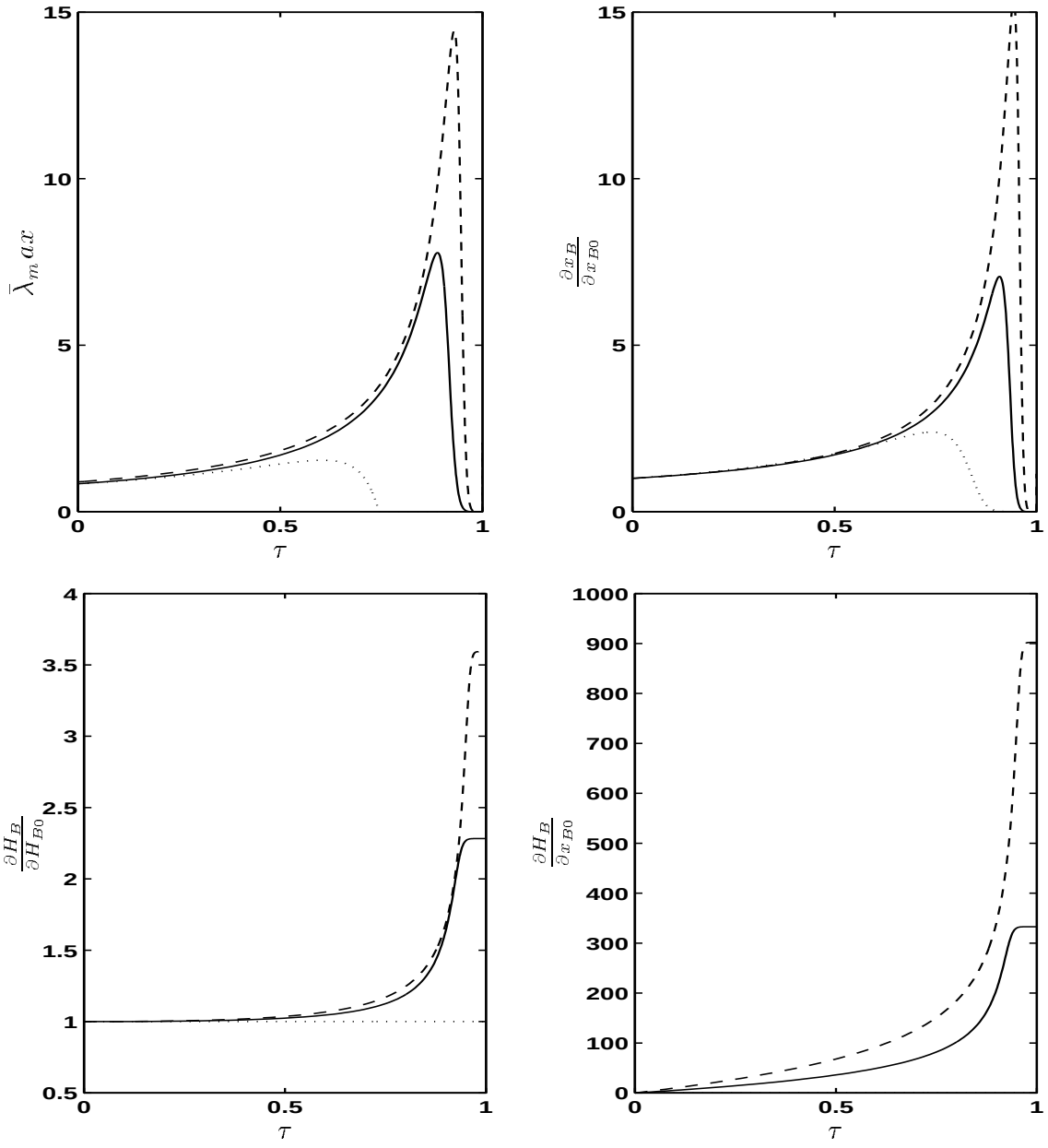

Figure 8.6: Maximum scaled eigenvalue and sensitivity functions for batch distillation column with L_wV-configuration. Solid line - $V = 5.0\ kmol/min$, dashed line - $V = 10.0\ kmol/min$, dotted line - LV-configuration.

configurations in terms of the maximum eigenvalue is small. However, at the point where the maximum eigenvalue for the LV-configuration drops to zero, the eigenvalue for the L_wV-configuration starts to grow almost exponentially and hence peaks at a considerably larger value. The larger eigenvalue for the L_wV-configuration implies a larger sensitivity for x_B as may be seen from Figure 8.6.

In order to illustrate the effect of the internal flows on parametric sensitivity, we also show results for the case where the boilup is increased to $V = 10\ kmol/min$ and $L_w = 185.8\ kg/min$, again corresponding to $D(0) = 1.0\ kmol/min$. As seen from Figure 8.6, the effect of increasing the internal flows is to increase the maximum eigenvalue λ_{max} and the sensitivity function $\partial x_B/\partial x_{B0}$.

As noted above, with the L_wV-configuration, parametric sensitivity will affect also the holdup $H_B(t)$. To illustrate this we show the sensitivity functions $\delta H_B/\delta x_{B0}$ and $\delta H_B/\delta H_{B0}$ in Figure 8.6. As seen from the figure, the sensitivity functions increase during the period for which the maximum eigenvalue is positive. However, somewhat surprisingly, the sensitivity functions do not decrease when the maximum eigenvalue becomes negative. This is understood by the fact that the sensitivity for $H_B(t)$ is given by the differential equation

$$\frac{d(\partial H_B)}{dt} = L\frac{M_2 - M_1}{M}\left(\frac{\partial y_D}{\partial x_B}\right)_L \partial x_B(t) \tag{8.41}$$

Here the coefficient on the right hand side is always positive when $M_2 > M_1$, and since $\partial x_B(t)$ never changes sign, $d(\partial H_B)/dt$ has the same sign for all t. From Figure 8.6 it is seen that the peak of $\partial H_B/\partial x_{B0}$ is about 900 with $V = 10\ kmol/min$, which corresponds to a maximum deviation of 9.0 $kmol$ in $H_B(t)$ for a perturbation of 0.01 in x_{B0}.

Multistage Columns. For the LV-configuration we found that the results for the one-stage column carried almost directly over to the multistage case, and that the main difference was that the gain $(\partial y_D/\partial x_B)_L$ varies significantly more over the production period in the multistage case. Similar arguments apply to the L_wV-configuration, i.e., the main difference between the one-stage case and the multistage case is found in the gain $(\partial y_D/\partial x_B)_{L_w}$. For the multistage case this gain is given by (8.35), i.e.,

$$\left(\frac{\partial y_D}{\partial x_B}\right)_{L_w} = \frac{\left(\frac{\partial y_D}{\partial x_B}\right)_L}{1 - L\frac{M_2 - M_1}{M}\left(\frac{\partial y_D}{\partial L}\right)_{x_B}} \tag{8.42}$$

Here

$$\left(\frac{\partial y_D}{\partial L}\right)_{x_B} = y_D(1 - y_D)\left(\frac{\partial lnS}{\partial L}\right)_{x_B} \tag{8.43}$$

From (8.43) it is seen that $(\partial y_D/\partial L)_{x_B}$ is close to zero when $y_D \approx 1$ or $y_D \approx 0$ and thus reaches a maximum for some intermediate y_D. From (8.42) it is seen that the variation in $(\partial y_D/\partial L)_{x_B}$ will amplify the variation in $(\partial y_D/\partial x_B)_L$ such that $(\partial y_D/\partial x_B)_{L_w}$ generally will have a significantly larger variation. In fact, as seen

from (8.42), the gain may even become infinite, or singular, if

$$\left(\frac{\partial y_D}{\partial L}\right)_{x_B} = \frac{M}{L(M_2 - M_1)} \tag{8.44}$$

In fact, we find that this condition is fulfilled at some point for most separations we have considered, in which the final collected distillate is of intermediate or high purity. Around a singularity, the gain $(\partial y_D/\partial x_B)_{L_w}$, and hence the gain $(\partial L/\partial x_B)_{L_w}$ according to (8.34), changes sign through $\pm\infty$. From (8.33) we see that this implies that $detA^{L_wV}$ and trA^{L_wV} changes sign through $\pm\infty$. Thus, close to a point at which (8.44) is fulfilled, we will have at least one eigenvalue at infinity. From a linear point of view, this suggests that we can have "infinite" parametric sensitivity in a multistage column operated with the L_wV-configuration. However, this only serves as an indicator that a linear analysis no longer is sufficient and that we need to consider nonlinear aspects. Indeed, the singularities in the Jacobian elements implies that the right-hand side of the differential equations (8.1)-(8.2) are discontinuous, and hence the sufficient condition for uniqueness of the trajectory $(H_B(t), x_B(t))$, as discussed previously, is violated. Thus, we need to consider whether the nominal trajectory still is unique when (8.44) is fulfilled.

We consider first the case in which the column is operated according to the constant reflux policy, i.e., constant L_w. In this case, the fact that $(\partial y_D/\partial x_B)_{L_w}$ and $(\partial L/\partial x_B)_{L_w}$ changes sign through $\pm\infty$ implies that we will have at least two solutions for L and y_D for a given x_B in some neighborhood of the singular point. This is illustrated in Figure 8.7 for the base-case separation $x_{Ds} = 0.95$ in Table 8.1, achieved with $L_w = 83.8\ kg/min$. As seen from the figure, there are two singular points and hence there exist three solutions in terms of y_D and L for $x_B(t)$ in the range 0.071 to 0.104. However, since the start of the batch corresponds to $x_B(0) = 0.5$, for which only the upper solution branch exist, and $dx_B/dt < 0$ for all times, $y_D(t)$ and $L(t)$ will simply jump from the upper to the lower solution branch as the singular point at $x_B = 0.071$ is reached. Thus, the trajectory is unique despite the singularity in the Jacobian elements. We might therefore expect that the sensitivity close to the singular point will be large, although it will not be infinite as suggested by the linear analysis above. One might also consider the possibility of starting the product drawoff in an operating region where multiple solutions are displayed, i.e. the initial distillate composition $y_D(0)$ may have mutliple solutions. However, if one assumes that start up commences from a state of total reflux until equilibrium is reached (as considered here), we have that $y_D(0) = \alpha^N x_B(0)$ so that no multiplicity arise.

Consider next the case in which the column is operated with a pre-computed reflux profile $L_w(t)$ according to a constant distillate composition policy. Also in this case will a singularity in $(\partial y_D/\partial x_B)_{L_w}$ and $(\partial L/\partial x_B)_{L_w}$ imply that at least two solutions exist in terms of y_D and L for a given x_B close to the singular point. However, in this case the nominal solution has $y_D(t)$ constant, and hence there will be no discontinuous jump along the nominal trajectory. Instead, the singularity will in this case imply that at least two solutions in terms of $y_D(t)$ and $L(t)$, and hence $x_B(t)$, branch out from the singular point. This is illustrated in Figure 8.8 for the base-case

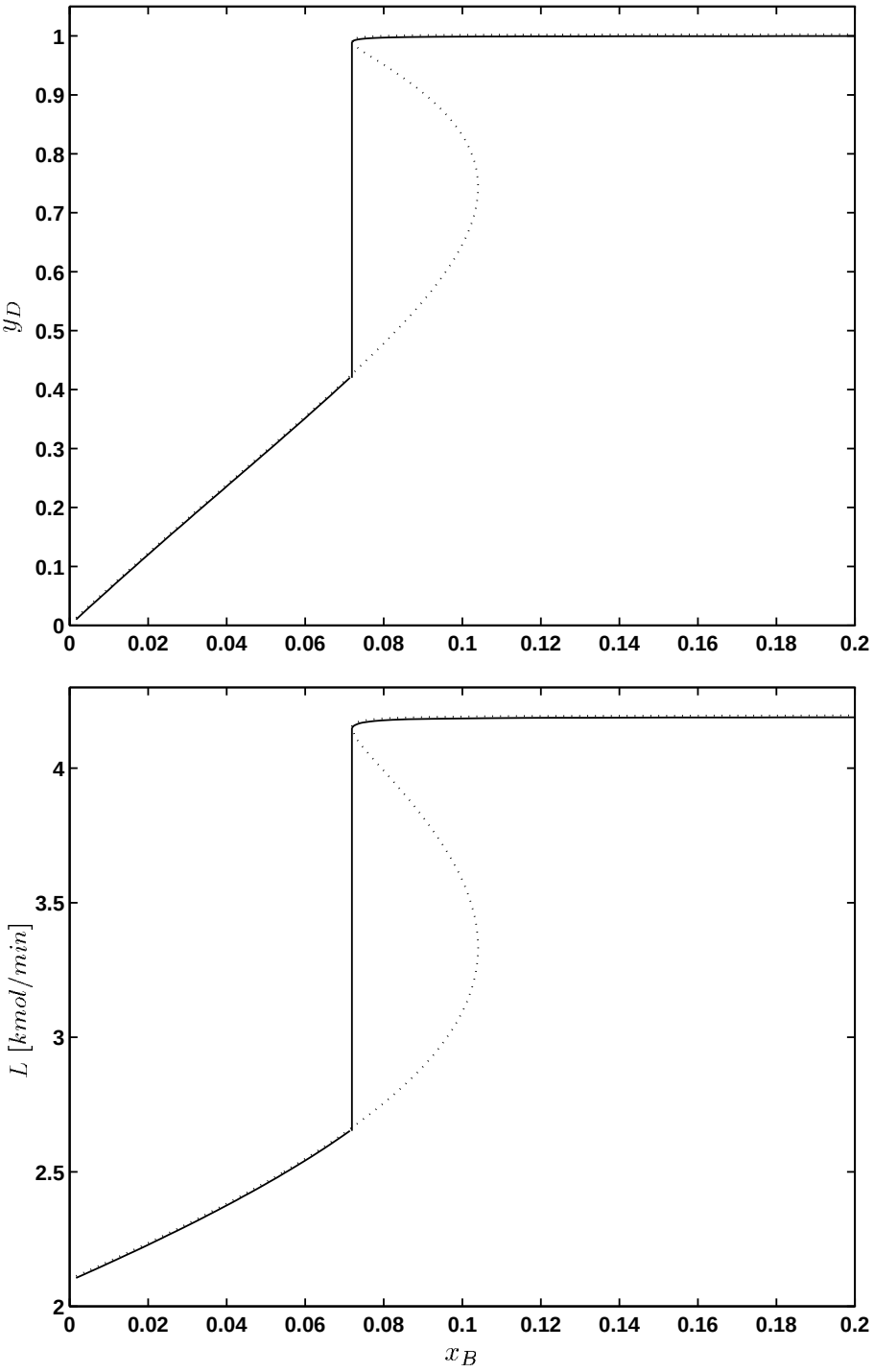

Figure 8.7: Distillate composition y_D and reflux L as a function of reboiler composition x_B for batch column in Table 8.1 with $x_{Ds} = 0.95$ and constant reflux L_w policy. Dotted line shows possible solution, solid line shows nominal trajectory.

separation $x_{Ds} = 0.95$ in Table 8.1. As seen from the figure, for a given reflux profile $L_w(t)$, there exist three possible solutions in terms of $y_D(t)$ and $L(t)$. The upper solution $y_{D1}(t)$ is continuous but has a discontinuous first derivative with respect to time at the singular point. The lower solution $y_{D2}(t)$ is discontinuous at the singular point. The actual solution will follow the upper solution for an infinitesimal positive perturbation in x_{B0}, while it will follow the lower solution for an infinitesimal negative perturbation in x_{B0}. In this case we can therefore talk about an "infinite" sensitivity because an infinitesimal perturbation to the system will yield a finite perturbation in the state variables at times after the singular point is passed. We should furthermore comment that although there may be multiple solutions, these will not be realized unless a perturbation is applied, i.e. the solutions will remain at the upper branch up to the singular point. Thus, in order to perturb the solution from the upper to the lower branch at an earlier point, one would have to introduce perturbations in another parameter, e.g. L_w, V or α. It is possible to compute the required extent of such perturbations, but as we comment next this is not of great interest since the singularities will not occur if we include holdup on the stages.

The results presented above may appear somewhat surprising in light of the statement, made earlier in this paper, that any realistic model of a batch distillation column will yield a unique trajectory. However, note that the singularity found above appears in the algebraic equations (8.3)-(8.4) relating y_D, L and x_B. These algebraic equations results from the assumption of negligible holdup on all trays including the condenser. Indeed, when holdup is included in the model, a singularity is no longer possible. In light of this one may be attempted to conclude that the results presented above are artificial and of little relevance to real columns. However, it is reasonable to suspect that a large sensitivity in the model neglecting holdups indicates a large sensitivity also in a model including holdup. Indeed, we show in Figure 8.9 results for the base-case separation $x_{Ds} = 0.95$ with the constant distillate composition policy and a holdup of $M_i = 0.1$ *kmol* on all trays including the condenser. In this case there are no singularities along the trajectory and the nominal solution $y_D(t) = 0.95$ is therefore unique. However, as seen from the figure, a perturbation of only 0.1% in x_{B0} has a large effect on the solution. Furthermore, a negative perturbation yields a trajectory which approaches the lower solution of the model neglecting holdup, while a positive perturbation yields a trajectory which approaches the upper solution.

Note that similar results to those obtained for the base-case separation with $x_{Ds} = 0.95$ are obtained for the base-case separation with $x_{Ds} = 0.99$. We do not present more detailed results for the base-case separations in Table 8.1 here, since the presence of singularities along the nominal trajectories imply that a linear analysis becomes meaningless. Rather, we present in the last section detailed results for the case where holdup is included on all trays.

In conclusion, we find that columns operated with the L_wV-configuration usually will display a larger sensitivity than models with the assumption of molar inputs, i.e., LV-configuration. The sensitivity will generally increase with increasing internal flows and increasing difference in molecular weight. Furthermore, the sensitivity is

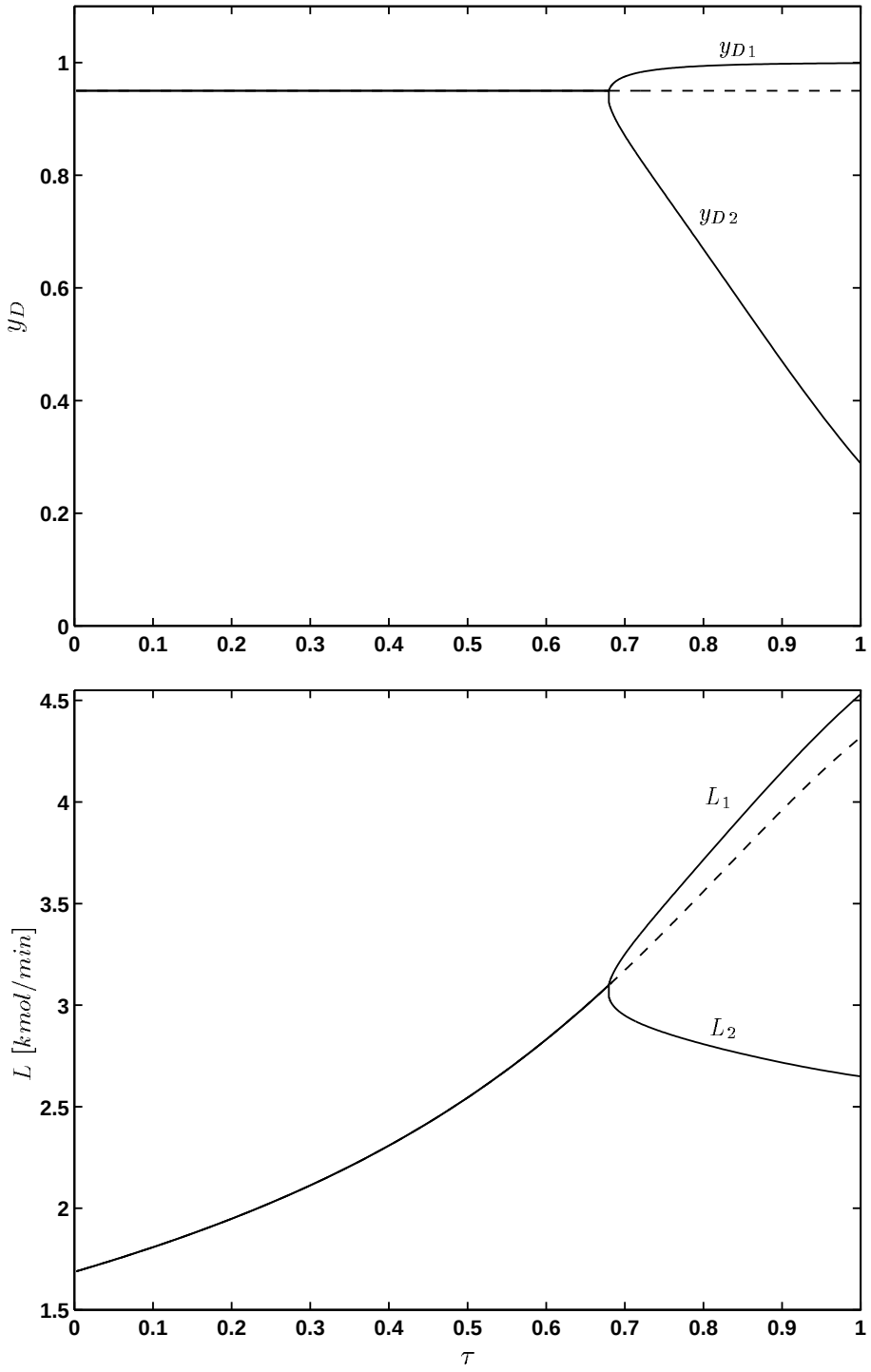

Figure 8.8: Profiles for distillate composition y_D and reflux L for batch column in Table 8.1 with $x_{Ds} = 0.95$ and constant distillate composition policy using L_wV-configuration. Dashed line shows nominal solution, solid lines show solutions resulting from infinitesimal positive and negative perturbations in x_{B0}.

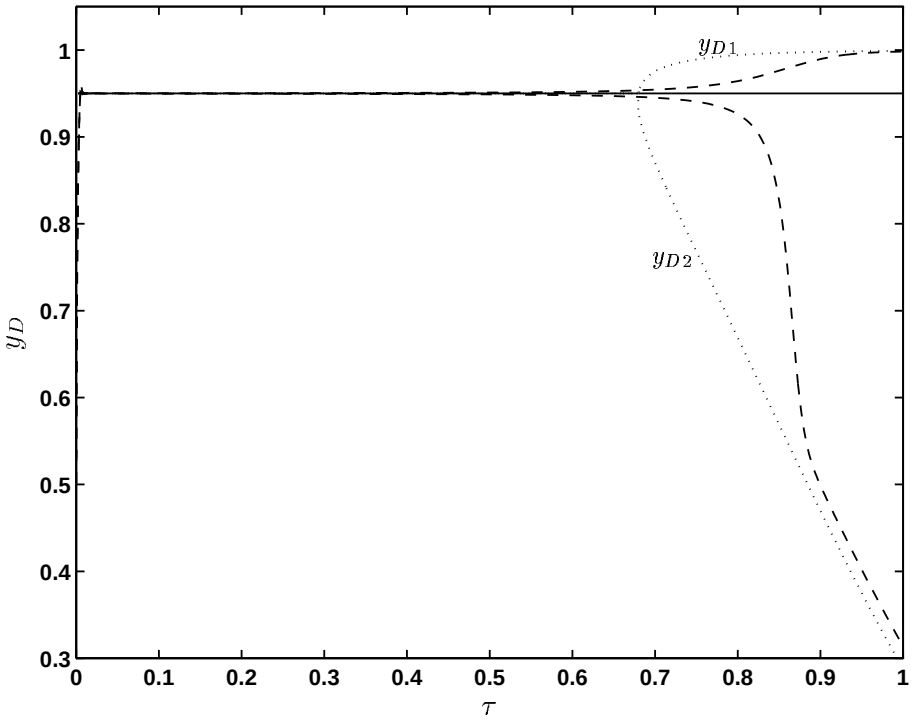

Figure 8.9: Profiles for distillate composition y_D for batch column in Table 8.1 with $x_{Ds} = 0.95$ and constant distillate composition policy using L_wV-configuration. Dashed lines shows solutions with holdup $M_i = 0.1\ kmol$ on all trays and a perturbation of $\pm 0.1\%$ in x_{B0}, dotted lines shows solutions with negligible tray holdups.

likely to be most severe when the distillate and reboiler has similar purities.

8.4.3 Other Configurations

Among other possible configurations we may consider the D_wV configuration. By following the treatment of the L_wV-configuration above, we find that conditions for RHP eigenvalues become opposite to those for the L_wV-configuration, i.e., the effect of mass flows reduces the sensitivity if $M_2 > M_1$. This result compares well to similar results on multiplicity for the continuous case (Jacobsen and Skogestad (1991) and Jacobsen and Skogestad (1994)), where it is found that multiplicity with the D_wV configuration is unlikely. Sensitivity with the L_wV configuration may therefore be significantly reduced by switching the condenser level control from using distillate flow D_w to using reflux L_w.

8.5 Implications for Operation of Batch Columns

We present here a detailed numerical analysis of parametric sensitivity for the base-case separation in Table 8.1 with $x_{Ds} = 0.99$. Whilst we previously have neglected holdup on all trays, we here include a holdup of $M_i = 0.1\ kmol$ on each tray, including the condenser. The feed mixture is then assumed to distribute over the column, so that the tray holdups prior to total reflux operation have the same initial composition as the reboiler holdup.

8.5.1 Constant Reflux Policy

We consider operation both with constant molar reflux $L = 4.383\ kmol/min$, i.e., LV-configuration, and constant mass reflux $L_w = 92.15\ kg/min$, i.e., L_wV-configuration. In both cases we assume that the column is run under total reflux until equilibrium. The initial time $t = 0$ is taken to be the time at which distillate draw-off commences.

The first difference to note between the two configurations is that the required time for the separation is $t_{final} = 81.0\ min$ with constant L and $t_{final} = 125.2\ min$ with constant L_w. This implies a 55% increase in distillation time and approximately 58% increase in utility usage [computed as $\int_0^{t_{final}}(L+V)dt$] with the L_wV-configuration compared to the LV-configuration. This is not surprising since the optimal way of operating batch columns typically involves increasing the molar reflux L as the batch proceeds, while operation with a constant mass reflux L_w implies that the molar reflux L decreases as the batch proceeds and y_D decreases.

Rather than computing the linear sensitivity functions, we present here the actual sensitivities resulting from nonlinear simulations with perturbations in the initial composition x_{B0} and in the boilup V, respectively. We stress that the sensitivity functions, e.g. $\partial x_B/\partial x_{B0}$, are obtained from solving the (linearized) first variational

equation and thus do not depend on the size of the perturbation, i.e. they are independent of scaling. For the nonlinear case this is however not the case, and the nonlinear sensitivities, e.g. $\delta x_B/\delta x_{B0}$ depend on the magnitude of the perturbation. Figure 8.10 shows the resulting sensitivities for x_B and x_D for a 1% perturbation in x_{B0} and V, respectively. Note that we apply a negative perturbation in x_{B0} and a positive perturbation in V, implying that y_D decreases in both cases. As seen from Figure 8.10, the sensitivity functions for x_B increase during most of the production period, corresponding to the period in which the distillate is of high purity. The nonlinear sensitivities $\delta x_B/\delta V$ are seen to increase over the same horizon where $\delta x_B/\delta x_{B0}$ increase, illustrating the fact that the presence of sensitivity at large is independent of which parameter we consider. We also see that, as the sensitivities for the LV-configuration start to decrease, i.e., when $y_D \approx 1 - x_B$, the sensitivity functions for the L_wV-configuration increase further for a short period of time. However, since the separation is sharp, y_D drops quickly towards 0 after the point where $y_D \approx 1 - x_B$, and the difference between the two configurations therefore becomes small.

Also note that the nonlinear sensitivity $\delta x_B/\delta x_{B0}$ for the LV-configuration with holdup on all trays in Figure 8.10 is similar to the corresponding linear sensitivity without holdup in Figure 8.3. Thus, the presence of holdup does only have a slight effect on the parametric sensitivity in this case.

The sensitivity for the accumulated distillate composition x_D in Figure 8.10 is close to 0 for most of the production period, which is explained by the fact that $x_D \approx 1$ during the period for which $y_D \approx 1$. However, as y_D starts to drop, and hence the sensitivity functions for x_B decrease with the LV-configuration, the sensitivity for x_D is seen to increase. This is explained by the fact that the accumulated distillate composition is given by

$$x_D(t) = \int_0^t D(\tau) y_D(\tau) d\tau / H_D(t) \tag{8.45}$$

Thus, the sensitivity of x_D depends on the integrated sensitivity of the distillate composition y_D. The sensitivity of y_D is given by

$$\delta y_D = \left(\frac{\partial y_D}{\partial x_B}\right) \delta x_B \tag{8.46}$$

and hence is close to zero as long as $(\partial y_D/\partial x_B) \approx 0$ and becomes significant only when $(\partial y_D/\partial x_B)$ and δx_B are both large. This occurs where the sensitivity ∂x_B reaches a maximum with the LV-configuration, i.e., when $y_D \approx 1 - x_B$. Thus, the sensitivity for x_D will start to increase approximately where the sensitivity for x_B with the LV-configuration starts to decrease.

In practice, the final sensitivities of the product qualities and amounts will be of most interest. The product qualities are best represented in terms of the fraction of impurities, i.e., x_B and $1 - x_D$. We therefore introduce the scaled variables

$$\Delta(1 - x_D) = \frac{\delta(1 - x_D)}{1 - x_D^*} 100\% \; ; \quad \Delta x_B = \frac{\delta x_B}{x_B^*} 100\% \tag{8.47}$$

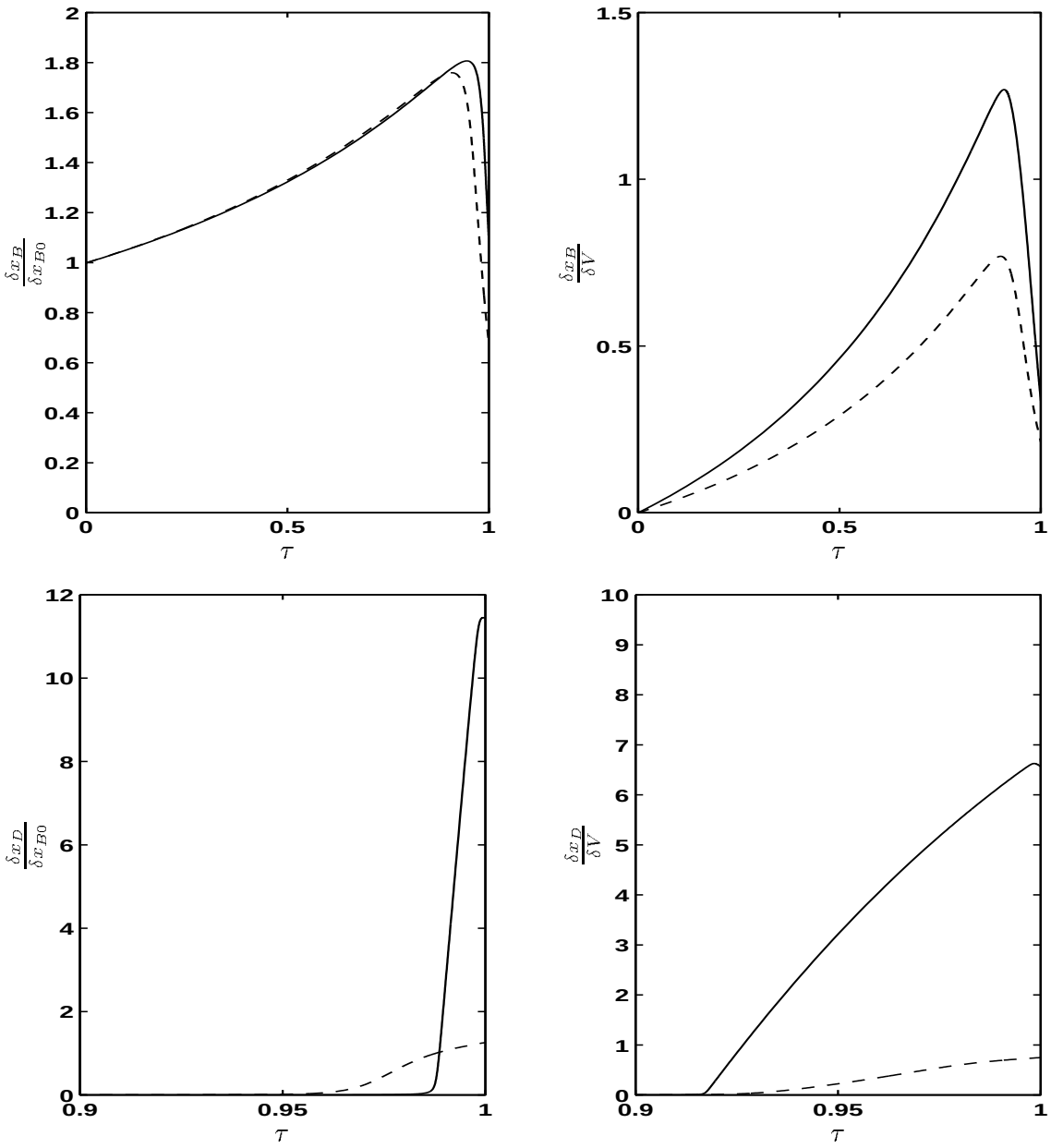

Figure 8.10: Nonlinear sensitivities for base-case column with $x_{Ds} = 0.99$ and constant reflux policy. The sensitivities correspond to perturbations of 1% in x_{B0} and V. Solid line - L_wV-configuration, dashed line - LV-configuration. Note the different time-scales in the upper and lower figures.

where superscript $*$ denotes nominal values. Thus, the scaled variables gives the percentage deviation in fraction of impurities. Similarly, we consider the scaled accumulator holdup

$$\Delta H_D = \frac{\delta H_D}{H_D^*} 100\% \tag{8.48}$$

The final sensitivities will in general depend also on the chosen *operating strategy*, i.e., the decision regarding when to stop the distillation of a given cut. We here consider the following strategies

1. Stop at a given time, t_{final}.
2. Stop at a given size of the cut, H_{Ds}.
3. Stop at a given temperature on tray i, T_{is}.

The motivation behind the last strategy is that composition measurements in the accumulator usually are unavailable, or are significantly delayed, while essentially delay free temperature measurements usually are available at a number of trays.

Tables 8.2 and 8.3 show the final sensitivities in terms of Δx_B, $\Delta(1-x_D)$ and ΔH_D for the different operating strategies above. For the strategy in which the distillation is stopped at a given tray temperature we have chosen the temperature on the tray below the condenser, i.e., tray 8, as the reference.

Table 8.2: Scaled sensitivities for 1 % perturbation in x_{B0} with constant reflux policy.

LV/L_wV	t_{final}	H_{Ds}	T_{8s}
Δx_B	20.4 / 31.3	20.4 / 5.01	0.13 / 0.36
$\Delta(1-x_D)$	62.9 / 571	63.0 / 90.8	2.41 / 2.79
ΔH_D	0 / 5.7	0 / 0	1.01 / 1.01

Table 8.3: Scaled sensitivities for 1 % perturbation in V with constant reflux policy.

LV/L_wV	t_{final}	H_{Ds}	T_{8s}
Δx_B	64.5 / 97.4	85.5 / 98.5	8.81 / 6.0
$\Delta(1-x_D)$	373.7 / 3283	88.3 / 97.6	17.2 / 167.2
ΔH_D	8.10 / 58.4	0 / 0	2.77 / 5.60

The results in Tables 8.2 and 8.3 clearly demonstrate that small changes in the initial conditions, or some other parameter, may have a severe effect on the final product. Note that a 100% change in $\Delta(1-x_D)$ corresponds to the final accumulator composition changing from $x_D = 0.99$ to $x_D = 0.98$. From the tables, the final sensitivities are

seen to depend strongly on the chosen operating strategy. Stopping at a given time generally yields the largest sensitivities, while stopping at a given tray temperature yields the smallest sensitivities. For the latter strategy, a 1% change in V yields a 17% change in $1 - x_D$ with the LV-configuration and a 167% change with the L_wV-configuration. Thus, the L_wV configuration has a severe final sensitivity even with the least sensitive operating strategy.

8.5.2 Constant Distillate Composition Policy

We consider here operation with a pre-computed reflux profile aimed at keeping the distillate composition y_D constant. We assume that the column is run under total reflux until y_D reaches the desired value, i.e., $y_D = 0.99$, and that $t = 0$ is taken to be time where product draw off commences. The total time required for the separation is in this case $t_{final} = 30.4\ min$ for both configurations Thus, as expected, the constant distillate composition policy is superior over the constant reflux policy in terms of time and energy usage.

The sensitivity functions for x_B and x_D for 1% perturbations in x_{B0} and V, respectively, are shown in Figure 8.11. The corresponding final scaled sensitivities are given in Tables 8.4 and 8.5. Note that we in this case has chosen the temperature in the reboiler T_1 as a stopping criterion. The reason for this is that for the constant reflux (L) policy, the temperature in the top (T_8) will be the most sensitive when y_D decreases. However for the constant y_D policy, the temperatures in the top are naturally rather constant, so that the largest variation occur near the bottom of the column.

Table 8.4: Scaled sensitivities for 1 % perturbation in x_{B0} and constant distillate composition policy.

LV/L_wV	t_{final}	H_{Ds}	T_{1s}
Δx_B	23.5 / 66.2	23.5 / 503	0 / 0
$\Delta(1 - x_D)$	46.1 / 2811	46.1 / 554	44.5 / 2181
ΔH_D	0 / 40.5	0 / 0	0.27 / 28.3

Table 8.5: Scaled sensitivities for 1 % perturbation in V and constant distillate composition policy.

LV/L_wV	t_{final}	H_{Ds}	T_{1s}
Δx_B	37.1 / 79.3	163.2 / 658	0 / 0
$\Delta(1 - x_D)$	198 / 3121	124 / 617	178 / 2337
ΔH_D	3.03 / 48.5	0 / 0	2.40 / 32.3

As seen from Figure 8.11 and Tables 8.4 and 8.5, the sensitivities are, as expected,

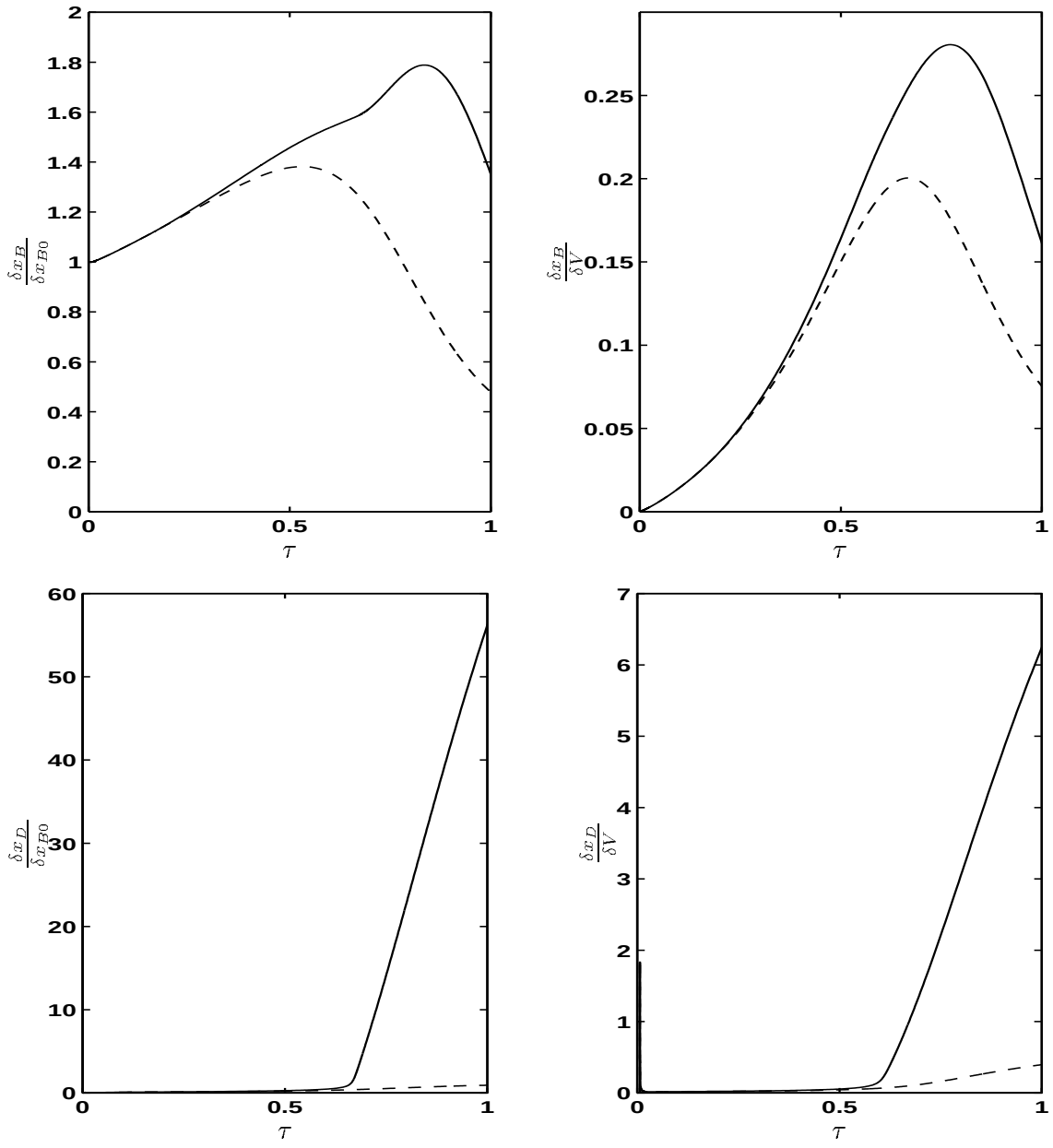

Figure 8.11: Nonlinear sensitivities for base-case column with $x_{Ds} = 0.99$ and constant distillate composition policy. The sensitivities correspond to perturbations of 1% in x_{B0} and V. Solid line - L_wV-configuration, dashed line - LV-configuration.

also in this case significantly larger with the L_wV-configuration than with the LV-configuration. By comparing the results in Table 8.4 and 8.5 with the results in Tables 8.2 and 8.3 for the constant reflux policy, we see that the scaled sensitivities generally are larger with the constant distillate composition policy. In particular, the constant distillate composition policy with the L_wV-configuration is seen to display an exceedingly large sensitivity. For this case, the least sensitive strategy is to stop the cut at a given accumulator holdup H_{Ds}. However, even with this strategy, we see that a 1% change in x_{B0} results in a final change of 554% in $1 - x_D$, i.e., the final accumulator composition becomes $x_D = 0.935$ instead of the desired $x_{Ds} = 0.99$. The corresponding change with the LV-configuration is "only" 46%, i.e., the final $x_D = 0.985$ after the perturbation in x_{B0}.

To illustrate the severe sensitivity with the L_wV-configuration, we show in Figure 8.12 the nominal trajectories $x_D(t)$ and $H_D(t)$ together with the trajectories resulting from a 1% perturbation in x_{B0}. As seen from the figure, the trajectories start to diverge rapidly around $\tau = 0.65$. This corresponds to the point where the underlying model neglecting holdups predicts a singularity according to (8.44). Thus, the the corresponding model with neglected holdup displays multiple trajectories for a given reflux profile $L_w(t)$, and as we anticipated above, this implies a large sensitivity also in the column including holdups.

8.6 Discussion

Model Assumptions. The analytical results derived in this paper are obtained from simplified models. Among the model assumptions we expect the effects of negligible or constant column holdup and constant molar flows (CMF) to be the most severe with respect to the applicability of our conclusions. Furthermore it is often argued that assuming CMF represents a limitation to the usefulness of the model for batch distillation columns (see e.g. Huckaba and Danly (1960) and Distefano (1968)). As a general remark we however stress that since the main objective of this work is to derive conditions that favor parametric sensitivity, emphasis is at large put on the the qualitative, rather than the quantitative results, and as such our conclusions are expected to be highly relevant in practice. Some discussion on the effect of column holdups on dynamic behavior is however included, partly since we included holdups in our final example.

Effect of Column Holdup. In order to derive our *two–state model*, we neglected holdups on all trays and in the condenser. The holdups basically have two dominant effects on system behavior, one which affects the transient behavior and the other being a *steady state* effect due to total reflux conditions. The dynamic effect, referred to as the *flywheel phenomenon* (see e.g. Rose and Welshans (1940) or R. L. Pigford and Garrahan (1951)), arises since holdup makes the changes in compositions occur more slowly due to its capacitive nature. Column holdup thus exerts an inertia effect which slows the dynamic response down, in the sense that changes in for example the reboiler heat duty do not have an immediate effect on the distillate compositions. The

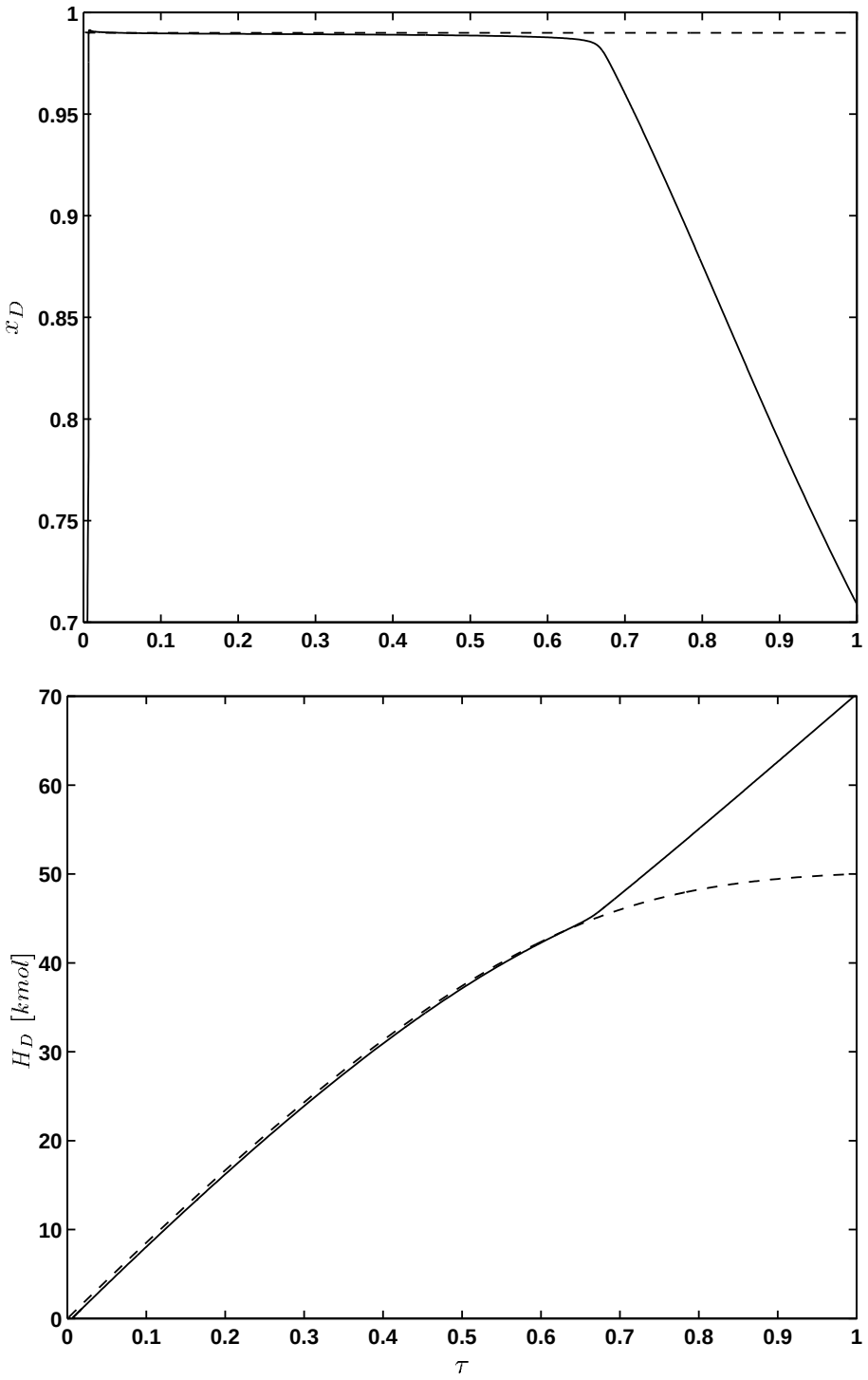

Figure 8.12: Profiles for accumulated distillate composition x_D and accumulator holdup H_D for base-case column with $x_{Ds} = 0.99$ and constant distillate composition policy using L_wV-configuration. Dashed line - nominal solution, solid line - solution after 1% perturbation in x_{B0}.

results in this paper conveniently illustrate this effect, in that singularities which may occur for columns where the holdups are neglected, do not occur when the holdups are included. Hence, the "infinite" sensitivity due to discontinuous trajectories apply only for columns with negligible holdups. The static influence of column holdup was considered by R. L. Pigford and Garrahan (1951), who found that increasing holdup in general increased the size of the intermediate cut, i.e. the distillate which is withdrawn immediately after y_D starts to drop. However, for sharp separations the effect of increasing holdups was an initial *decrease* in the intermediate cut, followed by an increase when the holdups exceeded certain limits. Since the size of the intermediate cut is shown to have a significant influence on PS, the overall impact of holdup on system behavior is somewhat ambiguous.

One should also be aware that there is a connection between column holdups and reflux ratio which may have a strong impact on for instance parametric sensitivity. If the column is operated at a high initial reflux ratio, the distillation of a cut takes relatively long time, and small perturbations may have a large effect on the accumulated distillate composition since rather small amounts of product is removed per time–unit. If, however, the reflux ratio and thus the required batch time is small, changes in the reboiler will not affect the accumulated distillate to the same extent, due to the flywheel phenomenon. Since there are several, and somewhat opposing effects of column holdup, which depend on both design and operating policies, it is difficult to draw general conclusions with respect to the overall effect on system behavior.

Energy balance. For continuous columns Jacobsen and Skogestad (1991) showed that including the energy balance may give rise to multiplicity even for molar flows, i.e. the LV–configuration due to interactions between the flows and compositions. The energy balance was thus shown to have the same impact as the transformation between mass and molar flows. Since we have demonstrated that the conditions for instabilities and multiplicity for continuous columns, at large carry over to batch distillation, we expect that including the energy balance will have a similar (large) impact also for batch columns, i.e. for *parametric sensitivity.*

Multicomponent mixtures. We have in this work restricted ourselves to binary mixtures. However, we believe that the results presented here in general may also apply to multicomponent mixtures, since one may treat the distillation of each cut as essentially separating a pseudo–binary mixture. This is the case at least if there is sufficient difference in relative volatilities, so that one essentially withdraws one component at the time in the distillate.

Feedback Control. A summary of the existing literature on closed loop control in batch distillation was recently given by Sørensen (1994). Since reliable and fast composition measurements are available only in rare cases, the use of temperature measurements to estimate on–line compositions has been suggested. By appropriate use of feedback control, combined with suitable on–line measurements, it should be possible to prevent the drastic effects of parametric sensitivity, and thus avoid costly re–distillation due to deterioration of product compositions.

8.7 Conclusions

We have in this paper addressed the issue of parametric sensitivity in batch distillation columns. We find that ideal binary batch columns may exhibit parametric sensitivity (PS), i.e. nominal trajectories are locally unstable. Evidence for such sensitivity are given through a mathematical analysis of a general model. We find that a linear analysis in most cases is useful, and we demonstrate that right half plane (RHP) eigenvalues of the Jacobian usually occur in the regions where parametric sensitivity is exhibited, i.e. RHP eigenvalues serve as strong *indicators* of sensitivity. Based on the eigenvalue analysis we derive analytical results that indicate under which operating conditions sensitivity is likely. These findings are then verified by dynamic simulations of simple models, and an example column where we also include holdups. Conditions that favor PS were found to be (*i*) large relative volatilities, (*ii*) large differences in molar weights and (*iii*) large internal flows.

Interestingly we find that the linear analysis in some cases predicts that the nominal trajectories of the state variables are not unique, i.e. singularities may arise along the trajectory. This indicates that the sensitivities become infinite at the singularities. However, this occurs only when the holdups on the trays are neglected, so that perturbations in the bottoms have an immediate effect on the top composition. When holdups are included the singularities no longer arise, but as shown the sensitivity may still be very large.

In order to address the implications for operation we also demonstrate that the choice of *control configuration* and *operating strategy* has a large impact on the sensitivity. Among the control configurations considered in terms of finding the optimal *operating policy*, we found that operating the column with the D_wV configuration is the best in terms of sensitivity. The most sensitive configuration was found to be columns operated with a constant distillate composition and a precomputed L_w–profile, i.e. L_wV–configuration. PS was furthermore shown to have greatest effect on columns operated with a final time policy.

Nomenclature

A – Jacobian matrix
$detA$ – Determinant of the Jacobian matrix
trA – Trace of the Jacobian matrix
B – Coefficient matrix for input variables
D – Distillate flow rate (kmole/min)
$\mathbf{F}$ – Matrix solution of first variational equation
H_B – Molar holdup of reboiler (kmole)
H_D – Molar holdup in accumulator (kmole)
L – Reflux flow rate (kmole/min)
M – Molar weight, usually of distillate stream (kg/kmol)

M_1 – Molar weight of more volatile component (kg/kmole)
M_2 – Molar weight of less volatile component (kg/kmole)
N – Number of theoretical stages
Q_B – Heat input to reboiler (kJ/min)
Q_D – Heat removal in condenser (kJ/min)
S – Separation factor
t_{final} – Final time for distillation of a cut
V – Boilup from reboiler (kmole/min)
x_B – Liquid mole fraction of more volatile component in reboiler
x_D – Liquid mole fraction of more volatile component in collected distillate
x_i – Liquid mole fraction of more volatile component on stage i distillate
y_D – Vapor mole fraction of more volatile component in distillate stream
y_i – Vapor mole fraction of more volatile component on stage i

Greek letters

α – Relative volatility
β – Variable of scalar time varying system
δ – Nonlinear sensitivies, e.g. $\delta x_B/\ x_{B0}$
Δ – Scaled deviation variables, i.e. Δx_B
λ_i – ith eigenvalue of the Jacobian matrix
$\bar{\lambda}$ – Scaled eigenvalue
∂ – Sensitivity functions, e.g. $\partial x_B/\partial x_{B0}$
ϕ – Transition matrix
τ – Dimensionless time $\tau = t/t_{final}$
ξ – Vector of parameters and control inputs

Subscripts

s – Set points for operating strategies
w – Mass flows in (kg/min)
0 – Initial conditions

References

Bilous, O. and N. R. Amundson (1956). Chemical reactor stability. *AIChE Journal*.

Davidyan, A. G., V. N. Kiva, G. A. Meski and M. Morari (1994). Batch distillation in a column with a middle vessel. *Chem. Eng. Sci.* **49**(18), 3033–3051.

Distefano, G. P. (1968). Mathematical modeling and numerical integration of multicomponent batch distillation equations. *AIChE Journal* **14**(1), 190–200.

Diwekar, U. M. (1995). *Batch Distillation. Simulation, Design and Control*. Taylor & FRancis.

Doherty, M. F. and J. D. Perkins (1978). On the dynamics of distillation processes - i. the simple distillation of multicomponent non–reacting, homogeneous liquid mixtures. *Chem. Eng. Sci.* **33**, 281–301.

Dongen, D. B. Van and M. F. Doherty (1985). On the dynamics of distillation processes – vi. batch distillation.. *Chem. Eng. Sci.* **40**(11), 2087–93.

Douglas, J. M. (1972). *Process Dynamics and Control, Volume 1 Analysis of Dynamic Systems*. Prentice-Hall Inc.

Hasebe, S., B. Abdul Aziz, I. Hashimoto and T. Watanabe (1992). Optimal design and operation of complex batch distillation columns. In: *Preprint of the IFAC Workshop on Interaction between Process Design and Process Control*. London.

Hasebe, S., T. Kurooka and I. Hashimoto (1995). Comparison of the separation performances of a multi–effect batch distillation system and a continuous distillation system. In: *Proc. IFAC–symposium DYCORD'95*. Denmark.

Huckaba, C. E. and D. E. Danly (1960). Calculation procedures for binary batch rectification. *AIChE Journal* **6**(2), 335–343.

Jacobsen, E. W. and S. Skogestad (1991). Multiple steady–states in ideal two–product distillation. *AIChE J.* **37**(4), 499.

Jacobsen, E. W. and S. Skogestad (1994). Instability of distillation columns. *AIChE J.* **40**(9), 1466–1478.

Kerkhof, L. H. J. and H. J. M. Vissers (1978). On the profit of optimum control in batch distillation. *Chem. Eng. Sci.* **33**, 961–970.

Macchietto, S. and I.M. Mujtaba (1992). Design of operating policies for batch distillation. In: *Proceedings of NATO ASI on Batch Processing Engineering, Antalya, Turkey.*

Mujtaba, I. M. (1989). Optimal Operating Policies in Batch Distillation. PhD thesis. Imperial College, University of London.

R. L. Pigford, J.B. Tepe and C. J. Garrahan (1951). Effect of column holdup in batch distillation. *Ind. Eng. Chem.* **43**(11), 2592–2602.

Rose, A. and L. M. Welshans (1940). Sharpness of separation in batch fractionation. *Ind. Eng. Chem.* **32**(5), 668–676.

Rosenbrock, H. H. (1963). The stability of linear time-dependent control systems. *J, Electron, Contr.* **15**, 73–80.

Sansone, G. and R. Conti (1964). *Non–Linear Differential Conditions*. Pergamon Press, Oxford.

Skogestad, S., B. Wittgens and R. Litto (1997). Multivessel Batch Distillation. *AIChE Journal* **43**(4), 971–978.

Sørensen, E. (1994). Studies on Optimal Operation and Control of Batch Distillation Columns. PhD thesis. University of Trondheim, The Norwegian Institute of Technology.

Vajda, S. and H. Rabitz (1992). Parametric sensitivity and self–similarity in thermal explosion theory. *Chem. Eng. Sci.* **47**(5), 1063–1078.

Vajda, S. and H. Rabitz (1993). Generalized parametric sensitivity : Application to a cstr. *Chem. Eng. Sci.* **48**(13), 2453–2461.

Wiberg, D. M. (1972). *State Space and Linear Systems*. Mcgraw Hill book company.

Willems, J. L. (1970). *Stability Theory of Dynamical Systems*. Nelson, London.

Chapter 9

Postscript

The motivation for this work is to enhance the understanding of issues related to operation and design of integrated distillation arrangements. The growing interest for considering such column arrangements stems from the scrutiny of tighter operational constraints as well as environmental requirements for increasing the energy efficiency. It is well documented in the literature that operation of conventional (industrial) distillation columns require large amounts of energy, In this work we perforce discuss issues related to design, simulation, optimization and operation of complex distillation arrangements. The main contributions from this thesis may be summarized as below

9.1 Conclusions

Chapter 2 discusses numerical methods to obtain initial solutions to a system of nonlinear algebraic equations (NAEs). By initial we here understand solutions for which all the degrees of freedom (e.g.system parameters) are specified, so that the task is to solve a square system of NAE's. We briefly discuss how one may find *constrained* solutions using feedback control when a dynamic model is available. The main part of the paper concerns different features of *homotopy–continuation* methods, and in particular we discuss situations in which the solution path becomes unbounded for which convergence problems are encountered. We propose simple strategies to deal with asymptotic behavior, based on simple transformations of the variables that display asymptotic behavior or the variable space to align the asymptotes and the coordinate axes. We however emphasize that these strategies are rather simple, and are not in their present state well suited for large systems. In the latter case one should instead use other more sophisticated methods proposed in the literature, for instance methods that use other homotopies that are restricted to certain domains in the variable space. We then introduced a novel *tear and grid method* based on conventional techniques of partitioning and precedence ordering. However, on top of this we propose to

make a grid of the tear variables to obtain partitions that are easier to solve. We thus avoid iterating on the teared functions in order to converge the system of NAEs. However, depending on the form of the non-teared functions, iterations are still required in the general case for the reduced partitions. In some special cases, for instance when the proper choice of tear variables reduce the remaining partitions to sets of linear equations, *explicit* solution schemes result.

Chapter 3 extends the scope of using numerical methods to solve systems of NAEs, where we now want to explore solutions in the parameter space, i.e. solve the system of NAE for a range of parameter values. We considered different implementations of a parameter continuation scheme, where we found that the most efficient was to use a secant predictor and apply Broyden's method to solve an augmented system of equations. Using Broyden's method allows one to use rank one updates of the Jacobian along the continuation path, so that expensive re-evaluations of this matrix are avoided. We also demonstrated that the *tear and grid* method may be used to solve non-square NAE's. The main advantages when using these methods are that they are easy to implement and still rather robust. The extent of "book–keeping" is kept reasonably low by using an augmented vector of (state) variables and parameters, so that we do not distinguish between those in the solution procedure. However, we recognize that both methods falls within the class of NP–hard problems, in that the computational complexity typically increases exponentially with the problem size. But for certain class of *sparse* problems, such as the conceptual design of distillation columns, the methods are very useful. The continuation method is also well suited for ill-conditioned problems, since one always stays close to the feasible solutions along the path. We also demonstrate how one may embed steady state optimization in such a continuation scheme.

Chapter 4 Whereas we in chapters 2 and 3 consider numerical methods for (exact) solutions of NAEs, for instance a conceptual model of a distillation column, we in this chapter propose an explicit *shortcut* method to obtain the minimum energy usage for multicomponent distillation. This method is based on certain simplifying assumptions regarding the distribution of non-key components. Although the method is only approximate, and may yield relatively large errors compared to exact methods such as Underwood's method, they may be used to extract valuable *qualitative* information that are not otherwise available. This is in fact the main contribution of the method, for which we argue that shortcut methods should be used to obtain insight that are not otherwise available, for instance using rigorous simulations. We use the method to obtain expressions for the potential energy savings of prefractionator arrangements, relative to conventional arrangements with regular columns in sequence. Another important contribution is that we elaborate on the optimality conditions for different column arrangements for ternary split. Although this is a well known problem, and an exhaustive amount of works are found in the literature, we find that many of these are based on the limiting assumption of using only total condensers and thus liquid feeds to downstream columns. In fact we show that using partial

condensers and thus vapor feeds to downstream columns, dramatically alters the picture of the optimality regions for the direct and indirect split scheme. Whereas the literature seems to indicate that the direct split is usually superior, we find in fact that the indirect split with a partial condenser is optimal for the majority of mixtures for ternary separations.

Chapter 5 In this chapter we consider *prefractionator arrangements* for the separation of ternary mixtures, with particular emphasis on the concept of the preferred separation. For a prefractionator arrangement, we show in terms of analytical results and numerical simulations, that the preferred separation always require the smallest energy usage. However, in terms of practical operation we find that it is usually not optimal to operate the column at this operating point. This is due to the finding that there is usually (at least for sharp splits) a "flat" operating region, in which the energy usage is relatively insensitive to changes in the operating parameters. Towards the ends of this region, "enclosed" by parameters for the preferred separation and a "balanced" main column, the energy usage is more sensitive. In terms of control we find that one may fix the boilup at the optimal value, and use the reflux for one-point control in the prefractionator. For practical operation we demonstrate that one should control the composition in the top or the bottom of the prefractionator, depending on whether the preferred separation or the balanced column requires the largest recovery of intermediate in the distillate. For the Petlyuk column we find that there is a similar region where the energy usage in fact remains *constant*, so that operation may take place within the region without any increase in the energy usage. We thus demonstrate that results in the literature, for infinite columns and sharp splits, carry over also to columns with a finite number of stages and non-sharp splits.

Chapter 6 Whereas chapter 5 consider using the Petlyuk column for ternary separations, we here extend the *Petlyuk ideas* to include also integrated columns for the separation of quaternary mixtures. We present a conceptual analysis, in which we propose definitions of Petlyuk and sharp split arrangements. A brief discussion of reversibility and how this relates to Petlyuk arrangements is also given. We then discuss the issue of finding appropriate superstructures, and show how these may be implemented in a single shell using vertical partitions. We give a discussion of the large number of degrees of freedom (DOFs) available for such design, and propose simple formulas to obtain these.

Chapter 7 We here proceed the discussion from chapter 6, and compare the energy usage of optimized Petlyuk arrangements with that of conventional arrangements of regular columns in sequence. We discuss certain aspects related to providing good initial guesses for the optimizations, which also serve the purpose of an a posteriori analysis of the optimized arrangements. For the examples considered, we find that using Petlyuk arrangements for quaternary separations typically offer savings in the order of 40%. In order to characterize the optimal solutions, we show how one may derive sensitivity functions for the energy usage. To obtain these we use the process model in order to eliminate the first order

terms in the Taylor series expansion of the energy usage. From a singular value decomposition of the Hessian matrix, evaluated at the optimum, we then obtain the *high* and *low* gain directions for changes in the parameter space, i.e. the directions in which the energy usage is the most and least sensitive to such changes. From these results we conclude that feedback control is required to maintain operation in vicinity of the optimal solution.

Chapter 8 then makes a slight diversion from the preceding analysis in chapters 2-7. Here we consider the fundamental dynamic behavior of batch distillation columns. Through analysis of a general model, we find that ideal binary batch columns may exhibit severe *parametric sensitivity* (PS), i.e. operation may become very sensitive to changes in some parameter. From a linear analysis, where we neglect column holdups, we derive analytical results that indicate under what conditions PS is favored. We find that the conditions that favor PS corresponds to those that cause multiplicities and instabilities for continuous columns, e.g. large internal flows and large differences in molar weights. In order to address the implications for operation, we also consider the influence of the choice of control configuration and operating policy on PS. In general we find that sensitivities are largest for columns operated with either constant or a pre-computed profile for the mass reflux, i.e. L_wV–configuration, and a final time policy. The impact of PS on important quality parameters, such as the composition and amount of collected distillate, are finally illustrated in terms of an example column where we also include column holdups.

9.2 Directions For Future Work

Some of the issues addressed in this thesis still resides on a conceptual level. We therefore suggest the following topics to be investigated in future works:

- **Optimal split sequences for multicomponent mixtures**. In this work we have derived approximate expressions to obtain the minimum energy usage for prefractionator arrangements, although detailed analysis are only carried out for the ternary case. An issue of great import in this respect is to extend the analysis of the *preferred separation* to the general case of multicomponent mixtures. Since the preferred separation deals with a certain optimal split sequence, for which the separation task may be decomposed to a sequence of pseudo–binary splits, there is ample scope for a comprehensive analysis also for more components. The analytical results derived in this thesis for prefractionator arrangements should be extended also to other multicomponent mixtures. In particular one may examine to what extent the findings from the ternary case given in chapter 5, carry over to the optimized Petlyuk arrangements for quaternary mixtures considered in chapters 6 and 7. One should furthermore elaborate on the impact of non-sharp separations in Petlyuk arrangements, in particular since results presented in this thesis indicate that the energy sav-

ings for Petlyuk arrangements increase with decreasing product purity of the intermediate component.

- **Optimal operation of Prefractionator arrangements**. We have addressed issues related to the optimal operation of prefractionator arrangements, including also the Petlyuk column. Among the important findings are that there exist enclosed regions in which the energy usage is "flat" (prefractionator) or constant (Petlyuk). For the Petlyuk column this is previously shown in the literature to hold for infinite columns and sharp splits, but we showed that it also applies to columns with a finite number of stages. We further showed that one may extract information from these findings that are important for aspects of on–line control. However, since we only considered the steady state properties, it is crucial in terms of operation to also analyze the dynamic behavior. Due to the highly non–linear behavior and strong element of coupling, Petlyuk arrangements should provide interesting and challenging examples for studies on controllability analysis and controller design. Preliminary results indicate the need for tight composition control and on–line control of the system parameters, i.e. the internal splits. We therefore pose the issue of optimizing control, which deals with how one should maintain optimal operation through the use of feedback mechanisms, as one of the promising and important tasks for future work. Current research at our institute aims at a greater understanding of this concept.

- **Rigorous modeling of Petlyuk arrangements**. Most of the work on Petlyuk columns found in the literature, draws from studies of simplified conceptual models. This is also the case for the results presented in this thesis. Although industrial practice seems to be taking up, there is still an apparent lack of understanding of practical issues and understanding of "real" operating columns. In order to promote industrial applications, and enhance the present understanding, we suggest that future work should study also rigorous models with non-ideal thermodynamics. One should thus assess other features with strong impacts on design and energy efficiency. Even though most investigations of non–ideal and azeotropic distillation up to this date have relied on time-consuming simulations, more recent trends indicate that reliable short-cut methods are emerging also for non-ideal mixtures. Recent developments in the area of minimum energy calculations, aims towards avoiding simulations and directly calculating the pinch points. Another important feature is that Petlyuk arrangements indeed should provide strong candidates for the separation of azeotropic mixtures. The reason for this lies in the finding that the largest relative energy savings of the Petlyuk columns arise when the relative volatilities approach one, which is the case for azeotropic mixtures. Other possible aspects to be covered are examining the effect of including the energy balance as well as incorporating liquid and pressure dynamics in the models.